

**Development of
a new platform technology for plant
Cytochrome P450 fusions**

Julia Schüchel

PhD Thesis

University of York

Department of Biology

January 2012

Abstract

To date more than 15000 Cytochromes P450 have been identified and named so far, with one third belonging to the plant kingdom. This is a key biochemical resource, providing a wealth of biocatalysts covering a diverse range of chemistries. Characterisation, however, has been greatly hindered by the poor solubility of many P450s, a result of the membrane anchoring region common to all plant P450s. Fusions of plant P450 heme domains to an appropriate reductase without the hydrophobic membrane anchor could provide the basis for developing robust, soluble plant enzyme systems for substrate screens to discover novel activities that are also of benefit to industry.

In this project, the two predominantly expressed Arabidopsis reductases ATR1 and ATR2 have been cloned, without the membrane anchor, and expressed in *Escherichia coli*. These two truncated enzymes have been purified and assessed for activity with ATR2 found to be more active than ATR1. ATR2 was chosen for engineering into a novel plant P450 reductase vector platform for high throughput applications, whereby the P450s can be easily and quickly swapped using ligation independent cloning techniques. Four different plant P450s (CYP93C1, CYP73A5, CYP82E4 and CYP81D8) were selected to validate this technology, and activity for the fusions of CYP93C1 (Isoflavone synthase I from *Glycine max*) and CYP73A5 (cinnamate-4-hydroxylase from Arabidopsis) with ATR2 have been shown. The presence of CYP73A5 fused to ATR2 was verified through purification and further studies showed that it has to be membrane associated for activity.

Additionally, CYP93C1 and CYP73A5 were also fused with the bacterial RhF reductase from *Rhodococcus* sp. and expressed in *E. coli* and compared to the plant P450 – plant reductase fusion protein. These novel plant-bacterial fusion P450 systems are the first example of active plant P450s fused to a reductase from a bacterium.

This platform technology will provide the possibility for characterisation studies of eukaryotic P450s with unknown function and the discovery of new activities.

Abstract	2
List of Tables	8
List of Figures	9
Acknowledgements	14
Author's Declaration	15
1 Introduction	16
1.1 Biotransformations in Industry	16
1.2 Cytochromes P450	17
1.2.1 History and Nomenclature of Cytochromes P450	17
1.2.2 Structure and Function of Cytochromes P450	22
1.2.3 Reaction Mechanism	25
1.2.4 Cytochromes P450 reactions	27
1.2.5 Interactions between Cytochromes P450 and reductases	28
1.2.6 Cytochrome P450 Fusion Systems	29
1.3 Applications of Cytochromes P450 in biocatalysis	33
1.3.1 Hydroxylation	33
1.3.2 Oxidation	35
1.4 Plant Cytochromes P450	37
1.4.1 Cytochromes P450s in <i>Arabidopsis thaliana</i>	37
1.4.2 Fusions of plant Cytochromes P450	43
1.5 Recombinant Expression Systems	47
1.5.1 Expression of P450s in <i>Escherichia coli</i>	48
1.5.2 Expression in Yeast	48
1.6 Aim of the project	50
2 Materials and Methods	51
2.1 Reagents and consumables	51
2.2 Media, strains and plasmids	52
2.2.1 Bacterial media	52
2.2.2 Bacterial strains	53
2.2.3 Plasmids for gene cloning and enzyme expression	55
2.3 Preparation of chemically competent <i>Escherichia coli</i> cells .	58
2.4 Plant media, growth conditions and strains	59
2.5 Plasmid DNA preparation	60
2.6 Purification of DNA fragments	60
2.7 Detection of the mRNA transcript	60
2.7.1 RNA extraction from <i>Escherichia coli</i>	60

2.7.2	RNA extraction from plant tissue	61
2.7.3	Reverse transcription from plant mRNA to cDNA	62
2.8	Traditional cloning method.....	62
2.8.1	Designing primers for truncated P450 and reductase genes	62
2.8.2	Polymerase chain reaction (PCR)	62
2.8.3	Preparation of PCR products for cloning	63
2.8.4	Transformation of plasmid DNA into chemically competent Escherichia coli cells	63
2.8.5	Screening transformants for recombinant genes by PCR	64
2.8.6	Restriction endonuclease digest of DNA.....	64
2.8.7	Dephosphorylation of DNA 5' end of the vector.....	64
2.8.8	DNA ligation reaction.....	65
2.8.9	DNA sequencing and analysis.....	65
2.9	Ligation independent cloning method	66
2.10	Protein expression and purification	67
2.10.1	Expression in Escherichia coli	67
2.10.2	Solubilisation buffers.....	68
2.10.3	Cell lysis by sonication	70
2.10.4	Protein purification in a batch process.....	71
2.10.5	Protein purification in a continuous process	71
2.11	Agarose gel electrophoresis.....	72
2.12	Protein detection	72
2.13	Sodium dodecyl sulphate-polyacrylamide gel electrophoresis (SDS-PAGE)	72
2.13.1	SDS PAGE with the Bio-Rad system	72
2.13.2	SDS PAGE with the RunBlue system from Expedeon.....	73
2.14	Western blot analysis.....	73
2.14.1	Protein detection with anti-poly Histidine peroxidase conjugate.....	73
2.14.2	Protein detection with alkaline phosphatase conjugate	74
2.15	Protein characterisation	75
2.15.1	Characterisation of the P450 reductases	75
2.15.1.1	Spectrophotometric characterisation	75
2.15.1.2	Activity assay with cytochrome c.....	75
2.15.1.3	Temperature and pH optima of ATR1tr and ATR2tr	76
2.15.1.4	Stability test of ATR2tr in different buffers	77
2.15.1.5	Kinetic studies of the reductases.....	77
2.15.2	Protein identification by MALDI-MS analysis.....	78
2.15.3	P450 enzyme activity assays	78
2.15.3.1	Activity assay for CYP71D15 with limonene	78

2.15.3.2	Activity assay for CYP81D8 and CYP81D11 with methyl-tolyl-suphide.....	79
2.15.3.3	Isoflavone synthase activity assay	80
2.15.3.4	Cinnamate-4-hydroxylase (CYP73A5) activity assay.....	81
2.15.3.5	Activity assay for CYP82E4.....	82
2.15.3.6	Activity assay for CYP81D8 with TNT and aminodinitrotoluenes.....	83
2.15.3.7	Activity assay for CYP81D8 with 7-ethoxycoumarin.....	84
3	Chapter: Expression of Cytochromes P450.....	86
3.1	Introduction.....	86
3.2	Objectives.....	90
3.3	Materials and Methods.....	90
3.3.1	Analysis of CYP73D15 PM2-2 construct.....	90
3.3.2	Materials and Methods for P450 expression in <i>Escherichia coli</i>	92
3.3.2.1	Isolation and cloning of the plant P450s.....	92
3.3.3	Expression of PM2-2 in <i>Escherichia coli</i>	92
3.3.4	Materials and Methods for P450 expression in yeast.....	93
3.3.4.1	Media	93
3.3.4.2	Transformation and expression in yeast	94
3.3.4.3	Yeast microsome preparation	95
3.4	Results	95
3.4.1	P450 amino acid sequence analysis.....	95
3.4.2	Analysis of CYP71D15 PM2-2.....	99
3.4.3	P450 cloning into the LIC-vector	100
3.4.4	P450 expression in <i>Escherichia coli</i>	101
3.4.5	Activity assay for 81D8tr, 81D11tr and CYP71D15 PM2-2	105
3.4.6	P450 expression in yeast.....	106
3.5	Discussion.....	108
3.5.1	P450s expressed in <i>Escherichia coli</i>	108
3.5.2	P450s expressed in <i>Saccharomyces cerevisiae</i>	110
4	Expression, purification and characterisation of truncated, soluble <i>Arabidopsis</i> Cytochrome P450 reductases.....	111
4.1	Introduction.....	111
4.2	Objectives.....	116
4.3	Results	116
4.3.1	Primer design for the N-terminal membrane anchor truncated ATR1 and ATR2.....	116

4.3.2	Cloning of ATR1tr and ATR2tr	118
4.3.3	Expression of ATR1tr and ATR2tr in Escherichia coli	118
4.3.4	Solubilisation of overexpressed ATR1tr	120
4.3.5	Purification of ATR1tr and ATR2tr in solubilisation buffer 18A	121
4.3.6	Characterisation of Arabidopsis P450 reductase ATR2tr	123
4.3.6.1	Activity assay with cytochrome c	123
4.3.6.2	Temperature and pH optima of ATR1tr and ATR2tr	126
4.3.6.3	Kinetic studies of the reductases ATR1tr and ATR2tr	128
4.3.6.4	Spectrophotometric characterisation of ATR2tr.....	131
4.3.6.5	Activity test of purified ATR2tr in buffer A and B	132
4.3.6.6	Stability test of ATR2tr in different buffers	133
4.4	Discussion	134
5	Development of the ATR2tr-LIC platform	137
5.1	Introduction	137
5.2	Objectives	140
5.3	Methods	141
5.3.1.1	Developing the platform technology of plant P450-ATR2tr fusions	141
5.3.2	Cloning of P450s into lamATR2tr- and licATR2tr-vector	142
5.3.2.1	Primer design	142
5.3.2.2	Cloning strategy	144
5.3.3	Expression and activity assays of the novel plant fusions	144
5.4	Results	145
5.4.1	Developing the platform technology for plant P450-ATR2tr fusions	145
5.4.1.1	Designing the linker region between P450 and reductase	145
5.4.2	Cloning of ATR2tr into the LIC-vector	146
5.4.3	Cloning of P450 inserts into lamATR2tr and licATR2tr	147
5.4.4	Expression and activity assays of the novel plant fusions	147
5.4.4.1	IFS-ATR2tr fusions	147
5.4.4.2	CYP73A5tr-ATR2tr fusions	152
5.4.4.3	CYP82E4tr-ATR2tr fusions	157
5.4.4.4	CYP81D8tr-ATR2tr fusions	160
5.5	Discussion	162
6	Comparison of plant Cytochromes P450 fused to different reductases	167
6.1	Introduction	167

6.2 Objectives	167
6.3 Methods	168
6.3.1 Expression of IFS-fusions	168
6.3.1.1 Expression conditions of IFS-CPR.....	168
6.3.1.2 Optimised conditions for the expression of the IFS-RhF fusion.....	169
6.4 Results	170
6.4.1 IFS fusions	170
6.4.1.1 Expression of IFS-CPR.....	170
6.4.1.2 Expression of IFS-RhF	172
6.4.1.3 Comparison of the IFS fusions in their growing cell cultures ...	176
6.4.1.4 Detection of IFS fusion enzymes.....	177
6.4.1.5 Purification of IFS-RhF	180
6.4.2 CYP73A5tr fusions	180
6.5 Discussion	183
7 Final Discussion	188
Appendix A	194
Appendix B	203
Abbreviations	214
References	218

List of Tables

Table 1.1: Arabidopsis P450s with known function	39
Table 1.2: Plant fusion P450s heterologously expressed in <i>E. coli</i>	45
Table 2.1: List of <i>E. coli</i> strains used for cloning and recombinant expression in this project.....	54
Table 2.2: Plasmids for gene cloning and enzyme expression.....	55
Table 2.3: List of primers used for sequencing.....	65
Table 2.4: Protocol for T4 polymerase treatment	67
Table 2.5: List of solubilisations buffer adapted from Lindwall <i>et al.</i> 2000 ³⁴⁷	69
Table 2.6: Buffers used for analyzing the pH optima of ATR1tr and ATR2tr	76
Table 2.7: HPLC program for the separation of methyl-tolyl-sulphide and its oxidised derivates.....	80
Table 2.8: HPLC program for the separation cinnamic acid and coumaric acid at 1 ml/min	82
Table 3.1: <i>Saccharomyces cerevisiae</i> strains used in this work.....	86
Table 3.2: P450s upregulated after TNT treatment from microarray data ³⁶³	87
Table 3.3: Primer used for sequence analysis of CYP71D15 PM2-2.....	91
Table 3.4: Primer used for PCR amplification of the truncated versions of CYP81D8 and CYP81D11.....	92
Table 3.5: Scheme of the test expression of the Arabidopsis P450s in the Lic-vector using different <i>E. coli</i> strains and media.....	102
Table 4.1: Kinetic data for ATR1tr and ATR2tr (calculated by the program GraFit).....	129
Table 5.1: Primer sequences for cloning ATR2tr into the LIC-vector	141
Table 5.2: List of P450s used for the creation of artificial plant fusions with the reductase ATR2tr	143
Table 5.3: Primer sequences for cloning P450 inserts into ATR2tr-LIC-vector	144
Table 5.4: List of chemical compounds considered to use as internal standard optimising the extraction method for the two flavonoids naringenin and genistein	148
Table 7.1: List of P450-reductase fusion constructs created in this project and their tested substrates.....	190

List of Figures

Figure 1.1: Original figure of the carbon monoxide difference spectra present in rat liver microsomes (from Klingenberg 1958 ¹⁸).....	18
Figure 1.2: Scientific articles published on National Center for Biotechnology Information (23th January 2012)	19
Figure 1.3: Schematic distribution of cytochromes P450 among the different kingdoms	19
Figure 1.4: Nomenclature of P450s	20
Figure 1.5: Schematic organisation of A the plant cytochrome and B the bacteria P450 systems.....	21
Figure 1.6: Ribbon diagram of Arabidopsis allene oxide synthase (CYP74A1) crystal structure	22
Figure 1.7: Topographic map showing the secondary elements represented for the CYP102 and commonly found among P450 enzymes.....	23
Figure 1.8: Ribbon diagram catalytic P450 centre with the 5-coordinated cysteine	24
Figure 1.9: Reaction cycle of a P450 hydroxylation.....	26
Figure 1.10: Variety of reaction types catalysed by cytochromes P450.....	28
Figure 1.11: Schematic arrangement of natural P450-reductase fusion systems..	31
Figure 1.12: <i>O</i> -dealkylation of 7-ethoxycoumarin to 7-hydroxycoumarin by P450-RhF.....	32
Figure 1.13: Hydroxylation of camphor by P450cam (<i>Pseudomonas putida</i>) to 5- <i>exo</i> -hydroxycamphor or P450camr (<i>Rhodococcus</i> sp.) to 6- <i>endo</i> -hydroxycamphor	33
Figure 1.14: Hydroxylation of progesterone to deoxycorticosterone by CYP21A2	34
Figure 1.15: Hydroxylation of 6- <i>oxo</i> -campestanol to cathasterone by Arabidopsis CYP90B1	35
Figure 1.16: P450 dependent heteroatom-oxidations of tertiary amines to N-oxides and thioether to sulfoxides or sulfones.....	35
Figure 1.17: P450 catalysed oxidation of 3-methylpyridine to pyridine-3-carboxylic acid	36
Figure 1.18: P450 catalysed epoxidation of an alkene.....	36
Figure 1.19: Phylogenetic tree of all cytochromes P450 from Arabidopsis ¹⁸²	38
Figure 1.20: 14 α -demethylation of obtusifoliol by plant CYP51	43
Figure 1.21: Conversion of the flavanones liquiritigenin and naringenin to the isoflavones daidzein and genistein, respectively, by the P450 isoflavone synthase I.....	46
Figure 1.22: Reaction mechanism of the conversion of naringenin to genistein by the P450 isoflavone synthase I.....	47
Figure 2.1: Vector map for pTrcHis2/ <i>lacZ</i>	56
Figure 2.2: Vector map of LIC-vector	57

Figure 2.3: pYeDP60 shuttle vector map with an origin of replication for <i>E. coli</i> and yeast.....	58
Figure 2.4: Schematic procedure for ligation independent cloning.....	66
Figure 2.5: LIC-vector after T4 /dTTP treatment	67
Figure 2.6: <i>E. coli</i> Rosetta 2 (DE3) cells A before and B after sonication	70
Figure 2.7: GC-MS program for analysing limonene and its hydroxylated products	79
Figure 2.8: HPLC chromatogram for the separation of nicotine and nornicotine	83
Figure 3.1: Chemical structure of 2,4,6-trinitrotoluene (TNT).....	87
Figure 3.2: Occurrence of CYP81D8 and CYP81D11 in the development of Arabidopsis	88
Figure 3.3: Regiospecific hydroxylation of (-)-4S-limonene to (-)-trans-isopiperitenol within the biosynthesis of (-)-menthol.....	89
Figure 3.4: N-terminal modification of CYP71D15 creating construct PM2-2 ³⁶⁷	90
Figure 3.5: Vector map for pCWori+.....	91
Figure 3.6: Analysis of the CYP81D8 amino acid sequence	96
Figure 3.7: Analysis of the CYP81D11 amino acid sequence	97
Figure 3.8: Analysis of the CYP71D15 amino acid sequence	98
Figure 3.9: Analysis of CYP71D15 PM2-2 in pCWori+-vector after digestion ..	99
Figure 3.10: Analysis of PCR products for native CYP81D8 (8nat), N-truncated CYP81D8 (8tr), native CYP81D11 (11nat) and N-truncated CYP81D11 (11tr).....	100
Figure 3.11: Analysis of crude extract of JM109 cells after expression of CYP71D15 PM2-2 (57 kDa).....	101
Figure 3.12: SDS PAGE analysis of crude extract from <i>E. coli</i> Rosetta 2 cells expressing 81D8tr (54 kDa) in LB medium with and without induction ...	102
Figure 3.13: SDS PAGE analysis of crude extract from <i>E. coli</i> Rosetta 2 cells expressing 81D11tr (53 kDa) in LB medium with and without induction .	103
Figure 3.14: SDS PAGE analysis of protein fractions containing 81D8tr and 81D11tr after purification on Ni-resin material	103
Figure 3.15: SDS PAGE analysis of protein fractions containing 81D8tr and 81D11tr after purification on Ni-resin material	104
Figure 3.16: SDS PAGE analysis of protein fractions containing CYP71D15 PM2-2 and empty vector control after purification on Ni-resin material.....	104
Figure 3.17: Analysis of plant P450s after purification on Ni-resin material.....	105
Figure 3.18: HPLC chromatogram of the methyl-tolyl-sulphide assay	106
Figure 3.19: CO difference spectrum of the microsoms for XplA heme from <i>Rhodococcus</i> sp. and CYP71D15 from peppermint	107
Figure 3.20: CO difference spectrum of the microsomes and the supernatant after the ultracentrifugation for CYP81A11 from Arabidopsis and CYP71D15 from peppermint.....	107
Figure 3.21: SDS PAGE analysis of yeast microsomes containing CYP81D11(57 kDa) and CYP71D15 PM2-2 (57 kDa).....	108

Figure 4.1: Phylogenetic tree of eukaryotic cytochrome P450 reductases	113
Figure 4.2: Amino acid sequence alignment between the CPR from <i>C. roseus</i> and the two Arabidopsis reductases ATR1 and ATR2 modified from Mizutani and Otha 1998 ³⁹¹	114
Figure 4.3: Expression levels of the three Arabidopsis cytochrome P450 reductases ATR1, ATR2 and ATR3 during the plant life cycle	115
Figure 4.4: Amino acid sequence analysis of ATR1 N-terminus.	117
Figure 4.5: Cell growth (OD ₆₀₀) after induction of ATR1tr in <i>E. coli</i> Rosetta 2 grown in LB medium	118
Figure 4.6: Analysis of crude extract by SDS PAGE	119
Figure 4.7: SDS PAGE analysis of ATR1tr (72kDa) during Ni-affinity purification	120
Figure 4.8: Protein concentration of the soluble total protein after overexpression in <i>E. coli</i> Rosetta 2 (DE3) using different solubilisation buffers 0-30.....	120
Figure 4.9: SDS PAGE analysis of the total soluble protein using solubilisation buffer 0-30. Red box show the overexpressed ATR1tr (72 kDa)	121
Figure 4.10: Analysis of ATR1tr after sonication in different solubilisation buffers	121
Figure 4.11: SDS PAGE Analysis of the purification of A) ATR1tr (72 kDa), B) ATR2tr (71 kDa) and C) negative control (empty vector expressed in <i>E. coli</i> Rosetta 2 (DE3))	122
Figure 4.12: ATR1tr and ATR2tr activity dependence on the cofactor NADH and NADPH.....	123
Figure 4.13: Cytochrome c conversion by different reductases in presence of the cofactor NADPH.....	124
Figure 4.14: Cytochrome c conversion by different reductases in presence of the cofactor NADPH.....	125
Figure 4.15: Temperature optimum for ATR1tr (1 mg/ml) and ATR2tr (0.01 mg/ml).....	126
Figure 4.16: Activity of 100 µg/ml ATR1tr and 1 µg/ml ATR2tr in 300 mM Britton Robinson buffer (1:1:1 mixture of boric acid, phosphoric acid and acetic acid) at different pH values.....	127
Figure 4.17: Activity of 1 µg/ml ATR2tr in diverse buffers covering different pH values.....	127
Figure 4.18: Stability of the cofactor NADPH at different pH values.....	128
Figure 4.19: Michaelis-Menten blots by GraFit for A) ATR1tr by Michaelis-Menten equation and B) ATR1tr by equation for substrate inhibition and C) ATR2tr by Michaelis-Menten equation	129
Figure 4.20: Cornish-Bowden blot for A) ATR1tr and B) ATR2tr	130
Figure 4.21: UV/Vis spectra of purified recombinant ATR2tr and negative control	131
Figure 4.22: UV/Vis spectra of 10 µM FMN and 10 µM FAD in 50 mM potassium phosphate buffer pH 7.5.....	131
Figure 4.23: Michaelis-Menten-diagram of purified ATR2tr	132

Figure 4.24: Stability of ATR2tr over time in A) buffer A (50 mM potassium phosphate buffer pH 7.5) and B) buffer B (30 mM potassium phosphate pH 7.8, 20 % glycerol, 0.1 mM EDTA, 2.0 μ M FMN)	133
Figure 5.1: Phenylpropanoid pathway showing the key role of the two P450s IFS (CYP93C) and C4H (CYP73A5) used in this project.....	138
Figure 5.2: Arrangement of IFS-CPR fusion construct	139
Figure 5.3: N-demethylation of nicotine to nornicotine by CYP82E4 from <i>Nicotiana tabacum</i>	139
Figure 5.4: Schematic construction of the P450-ATR2tr fusion containing the lam-linker	145
Figure 5.5: Analysis of positive transformants for the presence of the lam-ATR2tr in the LIC-vector	146
Figure 5.6: Analysis of positive transformants for the presence of the P450 73A5tr	147
Figure 5.7: HPLC analysis of the flavonoids biochanine A, genistein and naringenin.....	148
Figure 5.8: HPLC analysis of the flavonoids scopoletin, naringenin and genistein	149
Figure 5.9: Activity of <i>Glycine max</i> IFS fused to Arabidopsis ATR2tr	150
Figure 5.10: A) SDS-PAGE and B) western blot analysis (anti ATR2-antibodies) of <i>Glycine max</i> IFS fused to Arabidopsis ATR2tr	151
Figure 5.11: Activity of Arabidopsis P450 73A5tr fused to Arabidopsis ATR2tr in different media	152
Figure 5.12: Activity of Arabidopsis P450 73A5tr fused to Arabidopsis ATR2tr in M9 medium	153
Figure 5.13: Conversion of cinnamic acid to coumaric acid by artificial plant fusions containing Arabidopsis P450 73A5tr and Arabidopsis ATR2tr in a resting cell assay	154
Figure 5.14: SDS-PAGE and western blot analysis (anti His-antibody) of Arabidopsis P450 73A5tr fused to Arabidopsis ATR2tr	155
Figure 5.15: Cinnamate-4-hydroxylase activity in different fractions of the purification of 73A3tr-lamATR2tr.....	155
Figure 5.16: Cinnamate-4-hydroxylase activity of 73A3tr-lamATR2tr in different fractions after expression in <i>E. coli</i>	156
Figure 5.17: SDS-PAGE and western blot analysis of Arabidopsis P450 73A5tr fused to Arabidopsis ATR2tr as soluble and insoluble protein.....	156
Figure 5.18: Nicotine removal in a resting cell assay	157
Figure 5.19: HPLC analysis (reversed-phase column) of the crude cell extract for nicotine and nornicotine.....	158
Figure 5.20: HPLC analysis (chiral column) of the crude cell extract for nicotine and nornicotine.....	159
Figure 5.21: SDS-PAGE and western blot analysis of <i>Nicotiana tabacum</i> P450 82E4tr fused to Arabidopsis ATR2tr	159
Figure 5.22: TNT removal in a resting cell assay over time.....	160
Figure 5.23: Resting cell assay using 7-ethoxycoumarin as substrate.....	161

Figure 5.24: SDS-PAGE and western blot analysis of Arabidopsis P450 81D8tr fused to Arabidopsis ATR2tr	161
Figure 6.1: Flow scheme of the protocol for the expression of IFS-CPR fusion construct according to Leonard and Koffas ³⁰⁶	169
Figure 6.2: Observation of the cell growth of E. coli JM109 and Rosettas 2 during the expression of IFS-CPR.....	170
Figure 6.3: Activity of <i>Glycine max</i> IFS fused to <i>Catharanthus roseus</i> CPR when expressed with E. coli JM109 and Rosetta 2 cells.	171
Figure 6.4: Activity of <i>Glycine max</i> IFS fused to <i>Rhodococcus</i> sp. RhF reductase	172
Figure 6.5: Conversion of naringenin to genistein by IFS-RhF and IFS-CPR in a growing cell assay at 20 °C.....	173
Figure 6.6: Conversion of naringenin to genistein by IFS-RhF and IFS-CPR in a growing cell assay at 15 °C.....	174
Figure 6.7: Observation of the optical density during the expression of IFS-CPR and IFS-RhF at 20 °C in M9 medium	175
Figure 6.8: Conversion of naringenin to genistein in a resting cell assay.....	175
Figure 6.9: Production of genistein by IFS fusions in a growing cell assay.....	176
Figure 6.10: SDS-PAGE and western blot analysis of <i>Glycine max</i> IFS fused to <i>Catharanthus roseus</i> CPR and to <i>Rhodococcus</i> sp. RhF reductase in the soluble and insoluble fraction	177
Figure 6.11: SDS-PAGE and western blot analysis of <i>Glycine max</i> IFS fused to the RhF reductase from <i>Rhodococcus</i> sp. in total, soluble and insoluble protein fraction	178
Figure 6.12: SDS-PAGE and western blot analysis of <i>Glycine max</i> IFS fused to Arabidopsis reductase ATR2tr in total, soluble and insoluble protein fraction	178
Figure 6.13: Reverse transcription PCR for IFS-RhF.....	179
Figure 6.14: SDS-PAGE and western blot analysis of <i>Glycine max</i> IFS fused to <i>Rhodococcus</i> sp. RhF reductase after purification with Ni-affinity chromatography.....	180
Figure 6.15: Cinnamate-4-hydroxylase activity of Arabidopsis P450 73A5tr fused to Arabidopsis ATR2tr in a resting cell assay.....	181
Figure 6.16: SDS-PAGE and western blot analysis of Arabidopsis P450 73A5tr fused Arabidopsis ATR2tr or to <i>Rhodococcus</i> sp. RhF reductase in the soluble protein fraction	182
Figure 6.17: SDS-PAGE and western blot analysis of Arabidopsis P450 73A5tr fused Arabidopsis ATR2tr or to <i>Rhodococcus</i> sp. RhF reductase in the insoluble protein fraction	183
Figure 7.1: Schematic organisation of artificial A) plant-plant fusions (P450-ATR2tr) and B) plant bacterial (P450-RhF) fusions.....	193

Acknowledgements

At this point, I would like to say thank you to everyone who has helped me along the way to my PhD.

In particular, I would like to thank Prof. Neil C. Bruce and Dr. Gideon Grogan for great supervision, motivation and the opportunity for traveling around the world to attend the international P450 conferences, and for reminding me that plant P450s are a great challenge.

Thanks to Prof. Ian Graham and Dr. Gavin Thomas for the helpful advice at the training committee meetings.

Special thanks to all the members of the Bruce Group, especially Dr. Rosamond Jackson, Dr. Elizabeth Rylott, Dr. Astrid Lorenz and Dr. Joseph Bennett. Their kind help and endless support has helped me become a good lab member, an innovative report writer and creative presenter. Margaret, Helen, Chong, Andy, Will, Florian, Federico, Hazel, Mariya, Emily and Dana, I am grateful for the inspiring work environment and an unforgettable time here in York. Thank you very much!

Thanks to Prof. Mattheos Koffas for providing the IFS-CPR fusion, to Prof. Rodney Croteau for the CYP71D15 PM2-2 and Prof. Danièle Werck-Reichhart for the *Saccharomyces cerevisiae* strains WAT11 and WAT21, as well as for the plasmids pYeDP60-CYP89A9 and pYeDP60-CYP81D11.

Thanks also to the Centre of Excellence for Biocatalysis, Biotransformations and Biocatalytic Manufacture (CoEBio3) for their kind sponsorship.

Ganz lieb möchte ich mich auch bei meiner Familie und meinen Freunden bedanken. Durch eure Unterstützung habt ihr alle einen großen Anteil am Gelingen dieser Arbeit!

Meinem geliebten Ehemann, bestem Freund und größtem Kritiker Martin möchte ich für seine Liebe, Motivation und unermüdliche Unterstützung in all meinen Entscheidungen danken.

Author's Declaration

I declare that I am the sole author of the work in this thesis and that it is original except where indicated by special reference in the text. No part of this degree has been submitted for any other degree to any other institution.

1 Introduction

1.1 Biotransformations in Industry

The amazing world of biotechnology was started by humans more than a thousand years ago by producing alcohol and vinegar by fermentation without even knowing about the presence of microorganisms. Later, living cells, such as yeast, bacteria, filamentous fungi and plants were deliberately used to improve the stability and taste of food. Industrial biotechnology, also called “white” biotechnology, is a relatively new definition and means the fabrication of products by using microorganisms or enzymes by reducing energy and waste for the creation of a more environmentally beneficial process.¹ Over the last fifty years, many useful ‘biotransformation’ reactions have been identified and applied in industrial chemistry for processes including the hydrolysis and synthesis of ester and amide bonds, the hydrolysis of nitriles, the asymmetric reduction of prochiral ketones and the formation of chiral amines. Biotransformations have the advantage of converting substrates under relatively mild reaction conditions (neutral pH, room temperature, less activation energy) in comparison to conventional harsh chemical reactions. Moreover, enzymes are stereo- and regioselective and to recreate this selectivity is often a major challenge for synthetic and pharmaceutical chemistry using chemicatalysis. Therefore, enzymes are commercially important and often provide a more environmental friendly way for the synthesis of chemical compounds.

One particularly valuable class of enzymes are the oxygenase enzymes, which catalyse the introduction of oxygen into nonfunctionalised carbon skeletons. Oxygenations using conventional abiotic chemistry are energy consuming, often require either expensive catalysts and/or toxic reagents and are often neither regio- nor stereoselective. Hence there is now a substantial research effort into the discovery and application of enzymes that catalyse oxygenation reactions², which has included peroxidases³, flavin dependent monooxygenases⁴, and heme-containing enzymes known as cytochromes P450. Amongst these enzymes exist biocatalysts capable of the hydroxylation of C-H bonds, heteroatoms such as

nitrogen and sulphur and many other useful enzymes that are distinguished by their ability to catalyse their reactions with high chemo, regio- and stereo-selectivity.

1.2 Cytochromes P450

Cytochromes P450 (P450s) belong to the enzyme class monooxygenases, which has the Enzyme Commission number (numeral classification of enzymes based on the reaction type⁵) E.C.1.14.-.-. These heme-containing proteins are found in all kingdoms of life including humans, plants, insects, fungi, bacteria and also in viruses.⁶ In eukaryotes, they are mostly integral membrane bound, whereas prokaryotic P450 systems are more likely soluble and located in the cytoplasm.

P450s require auxiliary reductases for the activation of molecular oxygen for their different reactions. These reductases transfer two electrons in single steps from the cofactor NAD(P)H to the heme of the P450.

1.2.1 History and Nomenclature of Cytochromes P450

Ronald W. Estabrook, one of the pioneers in P450 research, published a summary of the outstanding research in the discovery of the cytochromes P450 in 2003.⁷ It all began in 1949 with Betty and Jim Miller and their graduate student Gerald C. Mueller, who performed *in vitro* studies on the metabolism of methylated aminoazo dyes in rat liver homogenates, to understand the degradation of the carcinogen 4-dimethylaminoazobenzene.^{8,9} Later, Jim Gillette and Julius Axelrod paved the way for a better understanding of the drug (acetanilide) metabolism, which also gave important momentum to the discovery of the P450s.¹⁰ The latter worked on the demethylation of ephedrine and showed that NADPH and oxygen are necessary for the reaction in rabbit liver microsomes.¹¹ Axelrod obtained the Nobel Prize in Physiology and Medicine (1970) together with Sir Bernard Katz and Ulf von Euler “*for their discoveries concerning the humoral transmitters in the nerve terminals and the mechanism for their storage, release and inactivation*”¹². Bernard B. Brodie, group leader of Jim Gillette and Julius Axelrod, published a classic paper on the hydroxylation of acetanilide and demethylation of monomethyl-4-aminoantipyrine in rabbit liver microsomes in

1955.¹³ The research in the area of the steroid hormone metabolism also contributed to the discovery of P450s, responsible for the C21 hydroxylation of progesterone in microsomes from the bovine adrenal cortex (Figure 1.14).¹⁴ Ryan and Engel showed in their studies the reversible inhibition of carbon monoxide by light for the first time.¹⁴ This observation led later to the discovery of P450 function as an oxidase using molecular oxygen and NADPH for their reactions.^{15,16} A breakthrough in P450 research – built on the knowledge and techniques found on cytochrome b₅ by Britton Chance and G. Ron Williams¹⁷ – was the detection of a shift from 413 nm to 450 nm in the carbon monoxide-bound form of an unknown pigment from rat liver by Martin Klingenberg in 1958 (Figure 1.1).¹⁸

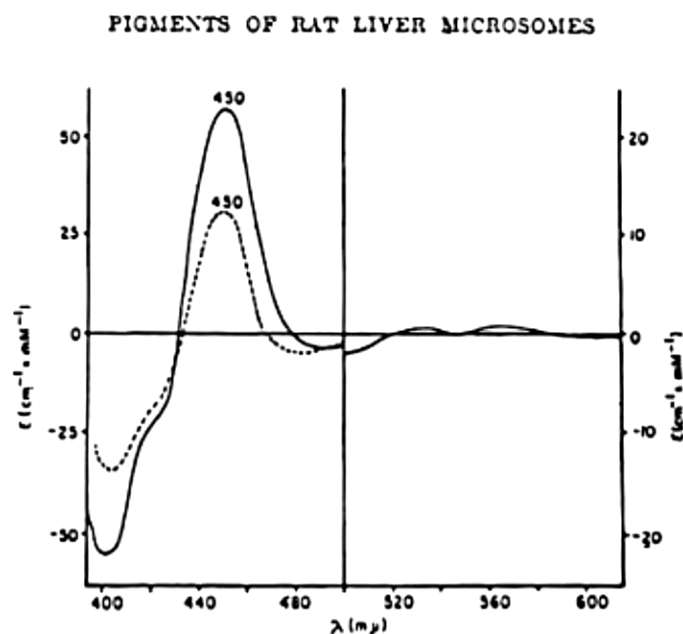


FIG. 3. Carbon monoxide difference spectra of rat liver microsomes. The millimolar extinction coefficients refer to the cytochrome b₅ present in the microsomes. ----- Curve A: Carbon monoxide with DPNH reduction. ——— Curve B: Carbon monoxide with dithionite reduction.

Figure 1.1: Original figure of the carbon monoxide difference spectra present in rat liver microsomes (from Klingenberg 1958¹⁸)

Enzymes of the superfamily cytochrome P450 received their name from Omura and Sato, who identified them as heme proteins in 1962.¹⁹ The P stands for “pigment” and the 450 for the characteristic absorption maximum at 450 nm (Soret peak) of the carbon monoxide bound form. This characteristic was also used to investigate a quantitative method for the detection of cytochromes

P450.^{20,21} From this time on, there was a steady increase in the numbers of P450 publications in each year (Figure 1.2). Since 2010, the National Center for Biotechnology Information (NCBI, <http://www.ncbi.nlm.nih.gov/>) has shown that more than 2000 papers on P450s have been published each year.

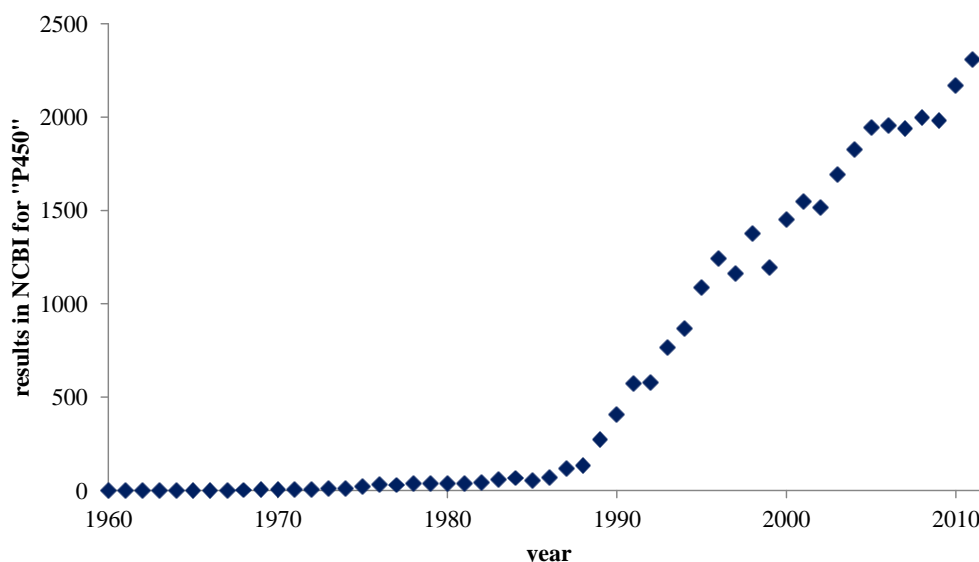


Figure 1.2: Scientific articles published on National Center for Biotechnology Information (23th January 2012)

Today, there are more than 15000 P450 genes identified (Figure 1.3).

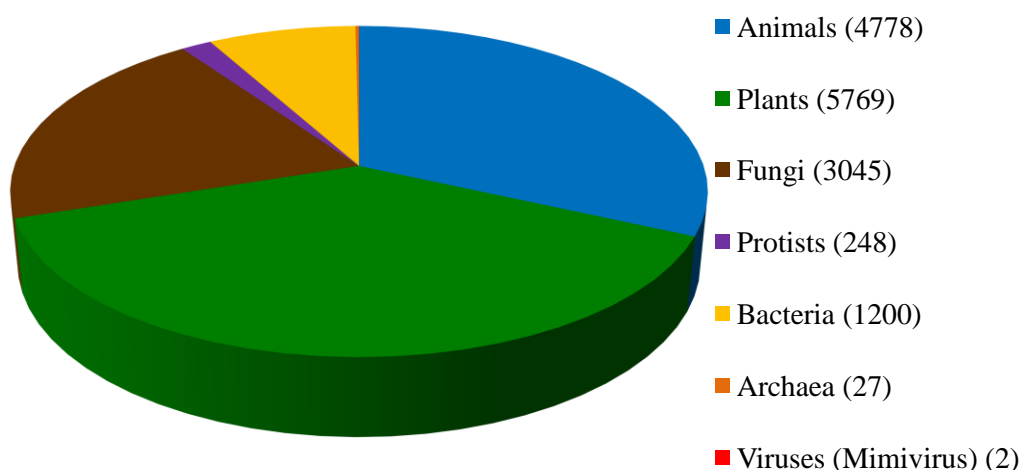


Figure 1.3: Schematic distribution of cytochromes P450 among the different kingdoms

One third of all known P450s belong to the plant kingdom and the P450 content in angiosperm genomes can reach up to 1%, whereas the typical vertebrate genome

contains less than 100 (e. g. humans with 57 and *Drosophila melanogaster* with 90 P450 genes).^{22,23} A few bacteria, such as the Gram-negative *Escherichia coli* were found to have no P450 gene sequence.²⁴

The first classification of 154 different genes of the P450 family from mammals, such as human, bovine, and rat as well as from yeast and bacteria (P450cam from *Pseudomonas putida*) was in 1991.^{25,26} Proteins sharing at least 40% of their amino acid sequence are classified into the same family and are assigned with the designation CYP for **cytochrome P450** followed by a number (Figure 1.4) by Nebert and coworkers. The plant genes start at CYP71 through to CYP99 and continue again from CYP701-999.⁶ Sequences of the same enzyme family members with a similarity of more than 55% in their amino acid sequence were arranged into subfamilies such as CYP71A and CYP71B.^{27,28} There are some exceptions, especially in plants, where the classification is based on phylogenetic data and the organisation of the genes.²³ The last number in the CYP name is unique to a single P450. Discoveries of new P450s resulted sometimes in modification of already named P450s. To monitor this, David Nelson (member of the Cytochrome P450 nomenclature committee) created a webpage with all identified P450s (<http://drnelson.uthsc.edu/CytochromeP450.html>).

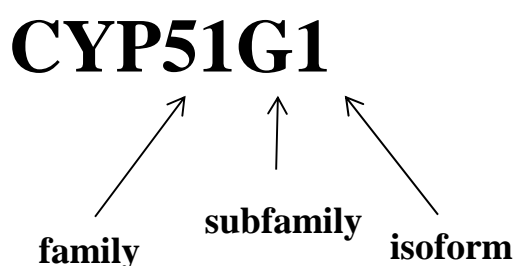


Figure 1.4: Nomenclature of P450s

P450 and reductase form the P450 system and they are grouped in three main types.

The members of the eukaryotic P450 superfamily are associated with the membrane of the endoplasmatic reticulum and so called ‘microsomes type’²⁴. This system has a single flavin adenine dinucleotide / flavin mononucleotide (FAD/FMN) as the reductase with a flavoprotein P450 (Figure 1.5A). Both are synthesised by membrane-bound ribosomes and then anchored by an uncleavable

hydrophobic N-terminus (with around 20 amino acids of the N-terminus²⁹) into the membrane.³⁰⁻³²

The second type ('mitochondrial type'²⁴), uniquely found in animals but not in plants or fungi, consists of a P450 bound to the inner mitochondria membrane³³ and a soluble FAD-containing flavoprotein with a ferredoxin-type iron-sulphur protein.^{34,35} However, some P450s have been reported to be present at the outer chloroplastic membrane, e. g. the Arabidopsis CYP74^{36,37}, CYP86B1³⁸ and CYP701A3³⁹ as well as an unnamed putative chloroplast P450 (AF107765)⁶ from *Prunus dulcis* (almond).

The third type are the prokaryotic P450s ('bacterial type'²⁴), where the P450 and the reductase parts are located solubly in the cytosol. Bacterial systems mostly utilise a ferredoxin reductase (FdR) combined with a ferredoxin (Fdx) as reductase part (Figure 1.5B) and generally use NADH as an electron donor.

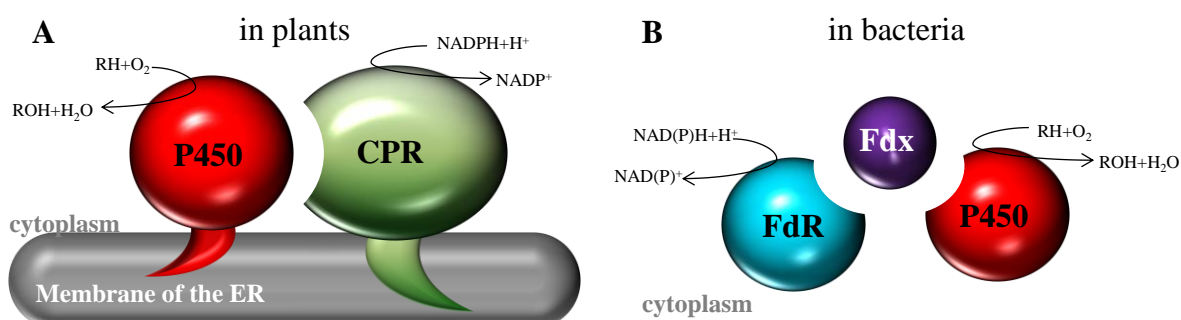


Figure 1.5: Schematic organisation of A the plant cytochrome and B the bacteria P450 systems

The substrates for cytochromes P450 are mostly hydrophobic organic compounds.²⁴ P450s have different functions and are involved in the biosynthesis of endogenous molecules as well as in the metabolism of many pharmaceuticals and xenobiotics. Across the kingdoms, P450s take part in a diverse range of processes: in prokaryotes, they participate in the assembly of antibiotics, in the catabolism of different carbon sources and in the metabolism of fatty acids.²⁸ By contrast in eukaryotes, P450s are involved in the biosynthesis of membrane sterols. In animals, they are part of the biosynthesis of signal molecules and steroid hormones as well as vitamin D₃.²⁸ In fungi, they carry out important roles in the synthesis of mycotoxins and in the metabolism of lipids, which are used as carbon

source.⁴⁰ Furthermore, in plants, they are found in the biosynthesis and catabolism of hormones and secondary plant compounds.⁴¹

1.2.2 Structure and Function of Cytochromes P450

P450s between the different families share low sequence identity (often less than 20%). However their structural organisation shows a strong conserved topology and three-dimensional fold.⁴²⁻⁴⁴ The number of crystal structures known for P450s is increasing rapidly since the first structure, of CYP101A1 (P450cam) from *Pseudomonas putida* was determined.^{42,43} Today, there are more than 70 crystal structures of P450s available on the Research Collaboratory for Structural Bioinformatics (RCSB) webpage (<http://www.rcsb.org>, 09/12/2011). The only solved crystal structure so far for Arabidopsis P450s is the allene oxide synthase (CYP74A1, Figure 1.6).⁴⁵

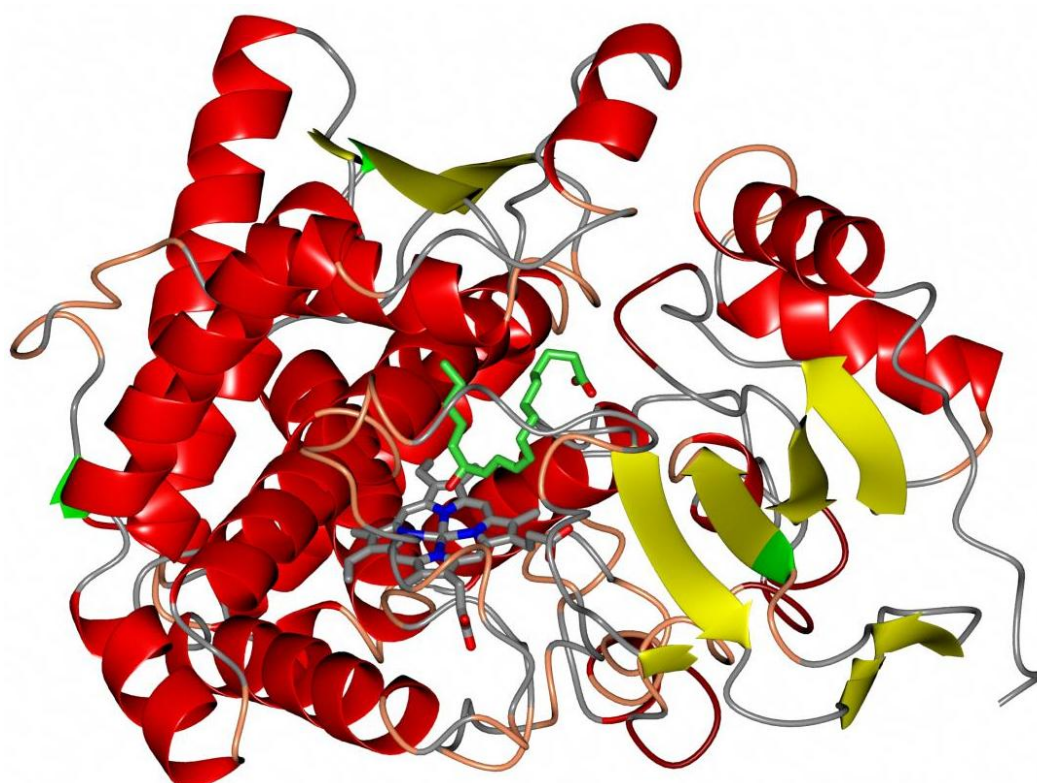


Figure 1.6: Ribbon diagram of Arabidopsis allene oxide synthase (CYP74A1) crystal structure
heme in grey, fatty acid substrate in green

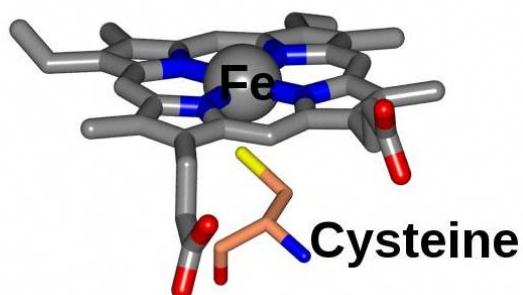


Figure 1.8: Ribbon diagram catalytic P450 centre with the 5-coordinated cysteine heme in grey, nitrogens in blue, oxygens in red, sulphur in yellow, Cysteine carbon skeleton in orange

The hydrophobic heme iron environment (β -bulge segment) is a very conserved region, where the cysteine residue is stabilised by hydrogen bonds from peptide NH-groups assisting the regulation of the redox potential of the heme.⁴⁹⁻⁵¹ A similar structure was also found in other enzyme groups such as nitric oxide synthase (NOS)⁵² and chloroperoxidase (CPO)⁵³.

Six substrate recognition sites (SRS) were identified by Gotoh using bioinformatics as dynamic protein regions opening and closing the substrate channel: SRS1 is on the B' helix, SRS2 and 3 are regions of the F- and G-helices, SRS4 is situated on the I-helix, SRS5 is the β 4 hairpin and SRS6 the K-helix β 1 connecting part.^{54,55}

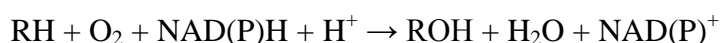
Eukaryotic P450 have usually a longer hydrophobic N-terminus of 25-50 residues for the association with a membrane and the amino acid sequence is depended of the membrane target and not essential for the P450 function as shown for many human P450s.⁵⁶⁻⁵⁹

Plant P450s often form metabolons with other proteins – a non-covalent complex of multiple enzymes of a metabolic pathway. A substrate can be directly transferred into a product without producing high concentration of intermediates.⁶⁰ One example for this phenomenon is the formation of a metabolon containing CYP79A1, CYP71E1, P450 reductase and the glycosyltransferase UGT85B1, which catalysis the reaction from tyrosine to dhurrin (a cyanogenic glucoside).⁶¹

1.2.3 Reaction Mechanism

P450s are classified by their sequence similarity and not by their reaction type as most other enzymes. P450s show a wealth of reactions such as the cleavage of C-C-single bonds, C-N-double bonds, hydroxylations, sulfoxidations, epoxidations, deaminations, dehalogenations, peroxidations or N-oxide-reductions^{62,63} with more than thousands of accepted substrates.⁶⁴ The ability to perform so many reactions may be due to the properties of the iron atom, which is able to change between different oxidation states.⁶⁵

The theory of the catalytic cycle of monooxygenases was developed in analogy with the reaction cycle of peroxidases, as P450s also use peroxide for monooxygenations.^{66,67} They require one oxygen and two electrons, which were usually donated in two single steps from the cofactor NAD(P)H to activate the oxygen, for the reduction of the heme iron²⁸:



At the start of the cycle the iron of the P450 has the oxidation state of +III and the sixth coordination centre is occupied by a molecule of water (Figure 1.9). The water ligand is displaced when a substrate is bound to the enzyme (1). As a result of this increase of the redox potential from a low spin state ($S = 1/2$) to high spin ($S = 5/2$), the enzyme can be reduced to P450-Fe(+II) by a single electron from the redox partner nicotinamide adenine dinucleotide (phosphate) (NAD(P)H) and the reductase (2).^{68,69} The result is a five times coordinate high-spin complex, which can bind different ligands such as molecular oxygen, carbon monoxide or cyanide (3). The oxygen-bound enzyme is similar to the superoxide-Fe(+III)-complex and is one of the detectable intermediates. The product of the following reduction through a single electron derived from the redox partners NAD(P)H and reductase (4) builds an unstable peroxy complex. After a protonation of the distal oxygen (5), it becomes a hydroperoxy intermediate (Compound 0), from which a water molecule is released after another protonation (6). The resulting product (Compound I) is unstable and was not isolated and characterised until recently (Rittle and Green 2010⁷⁰). Compound I is a high valent iron-oxo-complex with coordinated active oxygen responsible for the substrate conversion.^{70,71} Finally, the oxygen is transferred to the substrate (7) and a water molecule is initiated (8) so that the oxidised product and the initial state are formed.⁷²⁻⁷⁶

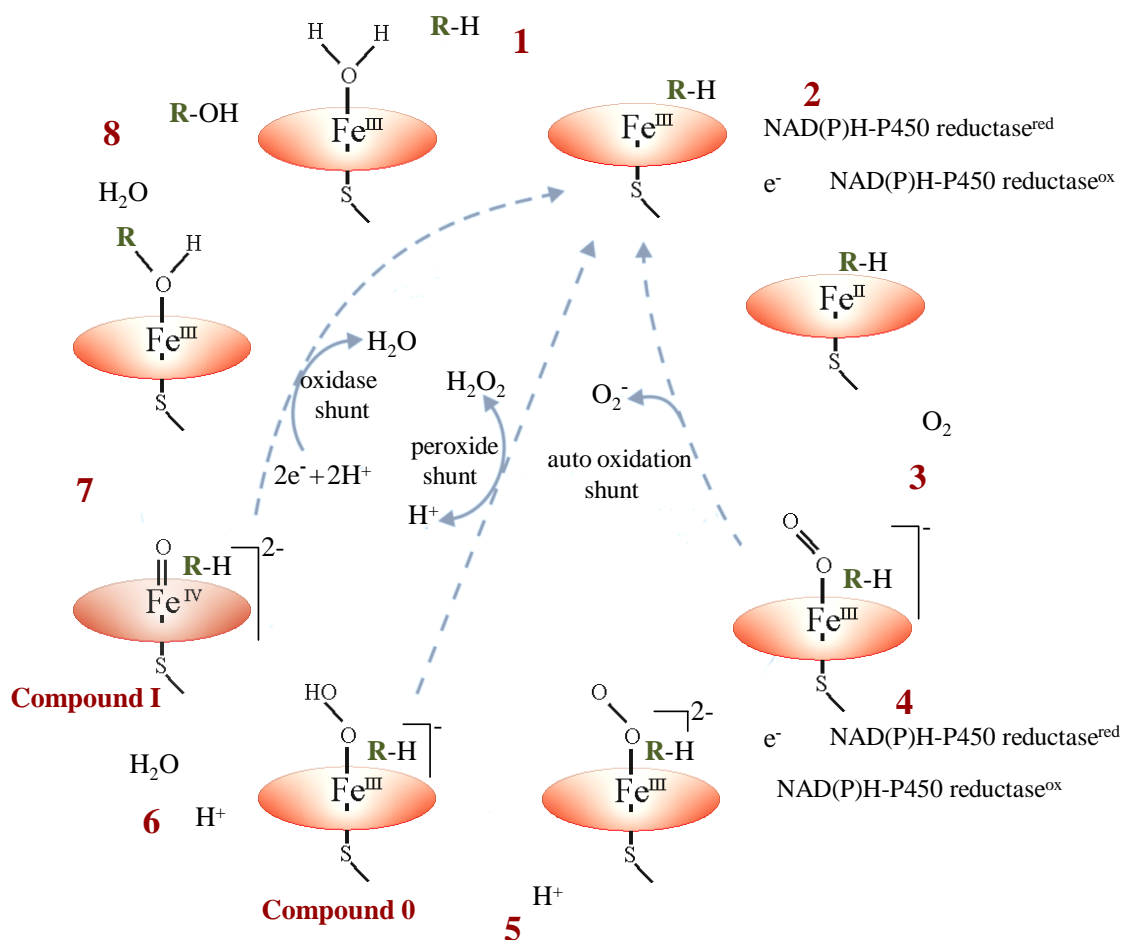


Figure 1.9: Reaction cycle of a P450 hydroxylation

(1) substrate binding, (2) reduction of the iron by NAD(P)H and reductase, (3) oxygen inserting, (4) reduction by NAD(P)H and reductase, (5) first protonation, (6) second protonation by formation of water, (7) substrate oxidation and (8) substrate release

The steps of the catalytic cycle are dependent on the substrate, electrons and protons. This avoids a consumption of reduction equivalents without oxygenation of the substrate, preventing futile cycling and stopping production of toxic superoxides. However, there are three major reactions (called “uncoupling”), which abort the catalytic cycle: The first is the autooxidation of the superoxide- $\text{Fe}(+\text{III})$ -complex by forming superoxide radicals. The second uncoupling, known as the peroxide shunt, separates hydrogen peroxide from the hydroperoxo intermediate. Some P450s use a short cut for their oxygenation reactions by introducing the oxygen from hydrogen peroxide into the substrate and using the peroxide shunt backwards, for example in fatty acid hydroxylation by CYP152A1 from *Bacillus subtilis* and CYP152B1 from *Sphingomonas paucimobilis*.⁷⁷ The third reaction is called oxidase shunt, where the active oxygen species

(Compound I) is protonated and reduced again by the dissociation of water instead of an insertion of the oxygen into the substrate.

1.2.4 Cytochromes P450 reactions

P450s provide a great variety of different regio- and stereospecific reactions, which make them interesting for industrial biocatalysis. Almost all P450s depend on a partner reductase and equimolar amounts of cofactors (NAD(P)H), which is a disadvantage when using these enzymes due to the increase in expense, however this problem can be avoided by performing whole cell experiments. The regeneration of NAD(P)H is also possible. For example, P450 BM3 (native fusion of a P450 and a reductase from *Bacillus megaterium*) can be coexpressed together with a glucose dehydrogenase. Glucose dehydrogenase converts glucose to gluconolactone in the process reducing NAD(P)⁺ to NAD(P)H, which is then used for the conversion of indole to indoxyl by P450 BM3. Indoxyl can dimerise to indigo, which is an important textile dye.⁷⁸

Using the knowledge of computer modeling, genomics and proteomics, P450s have been applied in industry for the investigation of new drugs, medicine or xenobiotics.^{79,80}

P450s with their wide range of substrate specificity catalyse key steps in many different pathways: In humans, they are mainly responsible for drug detoxification⁸¹⁻⁸³, in plants, for the activation or degradation of xenobiotics⁸⁴ as well as for the biosynthesis of biochemical compounds⁸⁵ and in bacteria, for the biodegradation of carbon sources^{41,86,87}.

The variety of reactions catalysed by P450s extends from hydroxylation and oxidation, which are the most common P450 reactions, to alkylation, dealkylation, epoxidation, demethylation, aryl migration and many more (Figure 1.10). P450s catalysing hydroxylations, oxidations and epoxidations are an important alternative for industry, because chemical problems such as the use of chlorinated solvents and heavy metals as part of the catalyst are removed.⁸⁸

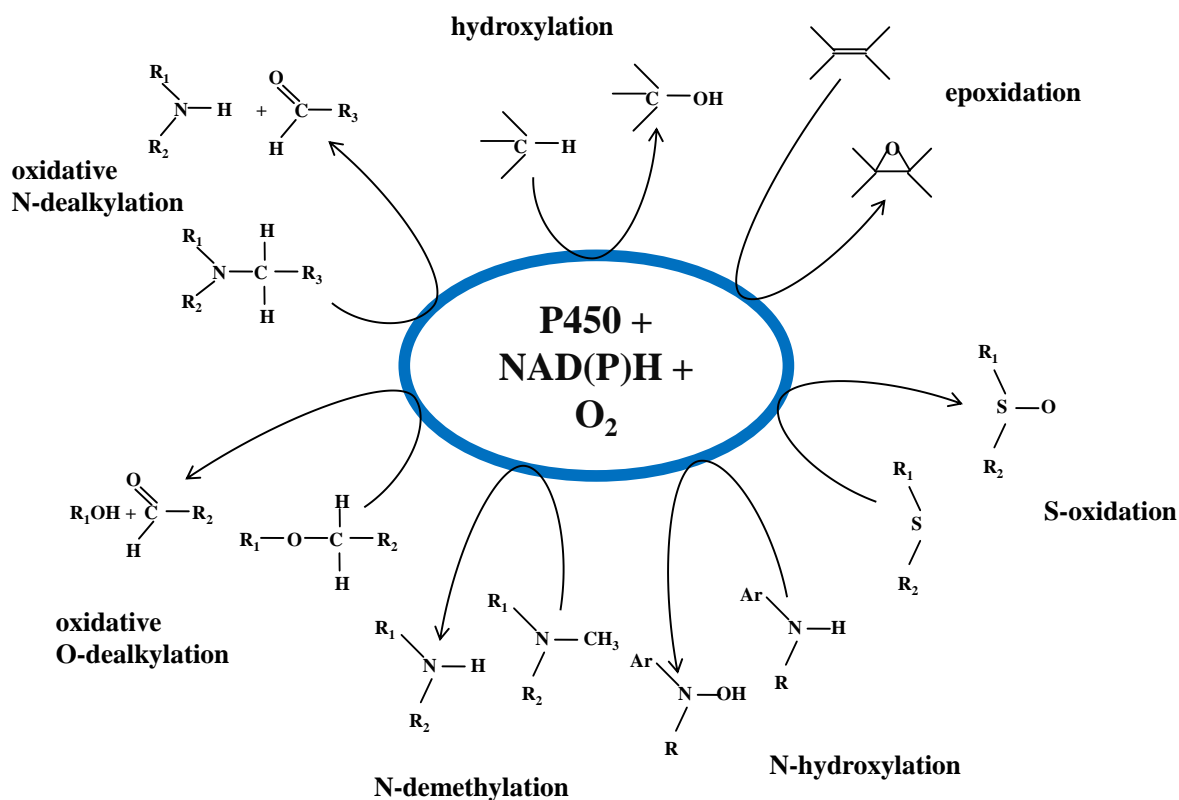


Figure 1.10: Variety of reaction types catalysed by cytochromes P450

1.2.5 Interactions between Cytochromes P450 and reductases

Early studies of mammalian P450s and their reductases indicated the formation of a complex consisting of one P450 and one reductase molecule.⁸⁹⁻⁹³ Different research groups were studying the different P450 systems to understand the electron transfer between reductase and P450. In the microsomal P450 system, where the P450 and the reductase are both membrane associated, the electron transfer was reported to happen by random collision between P450 and reductase on the membrane⁹⁴ or by a transient complex formation of the P450 and the reductase^{92,95,96}. Additionally, it was noticed that hydrophobic regions on the protein surface, such as the F-G loop, interact also with the membrane.^{97,98}

The number of mitochondrial P450 genes in animals is much smaller than for microsomal P450s. For example, seven mitochondrial P450s out of 57 are present in humans.³⁵ Mitochondrial P450s lack the hydrophobic membrane anchor and therefore their association with the inner mitochondria membrane is weak compared to the membrane anchored microsomal P450s. The hydrophobic F-G loop (e. g. positions 219-237 for CYP27A1) is thought to be responsible for the

interaction between P450 and the inner mitochondrial membrane.^{99,100} The reductase part of the mitochondrial system contains two parts: the adrenodoxin and the adrenodoxin reductase and both interact via electrostatic interactions. Adrenodoxin, a soluble Fe_2S_2 protein with high affinity to P450s, and the adrenodoxin reductase, are associated with the inner mitochondria membrane which enables the electron transfer between NADPH, reductase and P450.¹⁰¹⁻¹⁰⁵

It was also demonstrated that mitochondrial and microsomal P450s and reductases can be interchangeable. A mitochondrial P450 was artificially anchored to the endoplasmic reticulum and shown to be supported by a microsomal reductase system as well as a microsomal P450 by the mitochondrial reductase.^{104,106,107}

Bacterial P450 systems are soluble due to the fact that they are missing the hydrophobic membrane anchor. They are NAD(P)H dependent and consist usually of a P450, a ferredoxin and a ferredoxin reductase (Figure 1.5B). The genes for the bacterial P450 system are encoded on the chromosome or on plasmids, however, some bacteria such as *E. coli* have no P450.

There is one example, where the reductase is not required for the P450 reaction: androstenedione (4-androstene-3-17-dione) is hydroxylated *in vitro* by a P450 from rat liver in presence of NADPH and sodium periodate (NaIO_4)¹⁰⁸. Another exception is the soluble P450nor (nitric oxide reductase, CYP55A1) from *Fusarium oxysporum*, which uses electrons directly from the cofactor NADH for the reduction of nitric oxide (NO) to nitrous oxide (N_2O).¹⁰⁹ Homologous of P450nor have been found in *Cylindrocarpon tonkinense*¹¹⁰, *Trichosporom cutaneum*^{111,112} and *Histoplasma capsulatum*¹¹³ possibly as a result of horizontal gene transfer¹¹⁴.

1.2.6 Cytochrome P450 Fusion Systems

As the P450 reaction is typically dependent on the presence of single electrons derived from P450 reductases, co-expression is necessary to obtain effective P450 activity in recombinant systems.¹¹⁵⁻¹¹⁸ In Nature, the difficulty associated with using two separate enzymes is avoided by producing fusion P450-reductase enzymes, where usually the C-terminus of the P450 is fused to the N-terminus of the reductase. This phenomenon has only been found naturally to occur in bacteria and fungi so far.

The first self sufficient P450, where no additional enzymes are necessary, was the P450 BM3 (CYP102A1) from *B. megaterium* reported in 1986.¹¹⁹ The P450 (C-terminal) region of P450 BM3 is fused naturally into a single polypeptide chain to the cytochrome P450 reductase containing a FAD and a FMN. It has shown one of the highest turnover rates of all P450s, with about 17000 min⁻¹ (when arachidonic acid is oxygenated¹²⁰), thus it is an extremely effective biocatalyst and this improved efficiency is one possible evolutionary reason for the fusion of P450 and reductase.¹¹⁹⁻¹²² A second advantage may be that the regulation of a P450 fusion system is easier than regulating expression of the proteins separately.¹²³ However, the electron transfer between the three fusion domains of P450 BM3 has been shown to be mostly intermolecular by forming a dimer.^{124,125} Several homologues of P450 BM3 from different bacteria have been identified by sequencing, such as CYP102A2 and CYP102A3 from *Bacillus subtilis*¹²⁶, and the fusion proteins have been cloned and recombinantly expressed in a active form in *E. coli*.¹²⁷⁻¹²⁹

The P450 BM3 belongs to the P450-diflavin reductase (CPR) fusion systems (Figure 1.11A) and showed significant homology to mammalian P450s and mammalian P450 reductases.¹³⁰ This fusion type was imitated for the development of the first artificial fusion in 1987 containing the rat CYP1A1 and an NADPH cytochrome P450 reductase (from rat liver) expressed in *Saccharomyces cerevisiae*.¹¹⁶

Further examples of natural fusion P450s type P450 BM3 are the fungal fatty acid hydroxylase P450foxy (CYP505) from *Fusarium oxysporum* and the Fum6p from *Fusarium verticillioides* (NCBI: *Gibberella moniliformis*).¹³¹⁻¹³³

Fungi have usually various P450s and one or multiple separate corresponding reductase. Additionally, putative fungal P450-CPR fusions have been found in all filamentous ascomycetes except *Coccidioides immitis* by analysing fungal genomes.¹³⁴

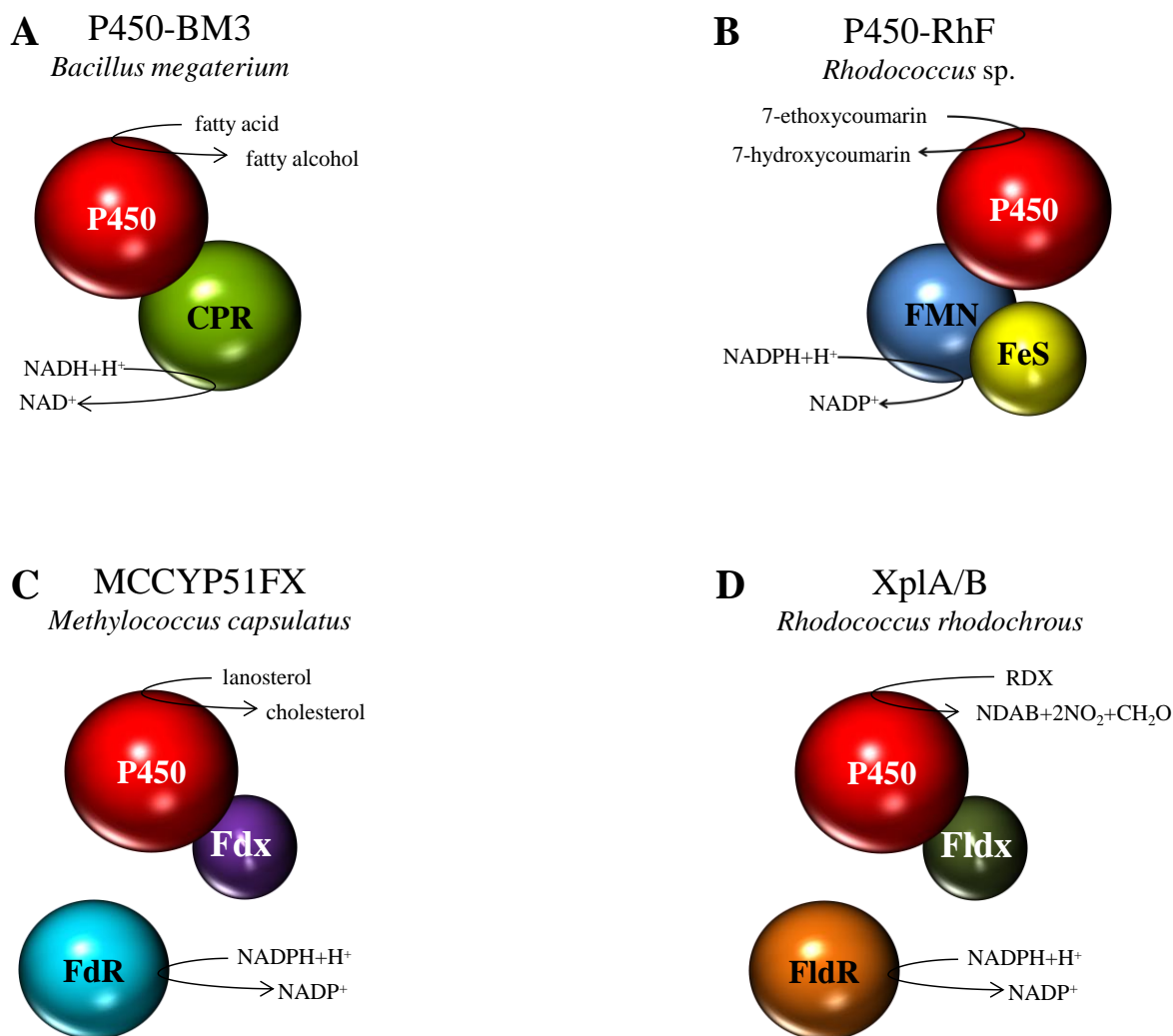


Figure 1.11: Schematic arrangement of natural P450-reductase fusion systems

A P450 BM3, a P450-diflavin reductase (CPR) fusion; **B** P450-RhF, a P450-phthalate dioxygenase reductase-like fusion; **C** MCCYP51FX, a P450-ferredoxin (Fdx) fusion with separate ferredoxin reductase (FdR) and **D** XplA/B, a P450-flavodoxin (Fldx) fusion with separate flavodoxin reductase XplB. Fusions are represented by overlapping spheres.

Through PCR-based screens another type of prokaryotic P450 fusion was found, where the P450 N-terminus was fused to a Phthalate Family Oxygenase Reductase (PFOR) containing an FMN and an iron-sulphur (2Fe-2S). One example belonging to this fusion type is the P450-RhF (CYP116B2) from *Rhodococcus* sp. (Figure 1.11B).¹³⁵ The native substrate of this P450 fusion is not known, however it can catalyse the *O*-dealkylation of 7-ethoxycoumarin (Figure 1.12).^{136,137}

1.3 Applications of Cytochromes P450 in biocatalysis

In the last few years, research in cytochromes P450 has expanded to include engineering of the biocatalysts for various applications. This has been reviewed in recent papers (Gillam 2008¹⁴⁸, Hlavica 2009¹⁴⁹, Grogan 2011¹⁵⁰, O'Reilly *et al.* 2011¹⁵¹). For example, the self-sufficient P450 BM3 was modified at its substrate access channel with site-directed mutagenesis to increase the activity up to 40 fold towards the polycyclic aromatic hydrocarbons phenanthrene, fluoranthrene and pyrene.¹⁵²

1.3.1 Hydroxylation

The regio- and stereoselective oxidative activation of a C-H bond is a challenging problem for synthetic organic chemistry.¹⁵³⁻¹⁵⁵ Enzymes, especially P450s, are an environmental friendly solution for hydroxylations with high selectivity.

P450-catalysed hydroxylation occurs by an activation of a C-H bond followed by the insertion of an oxygen atom and finally the formation of the corresponding alcohol. The first solubly expressed P450 derived from *Rhizobium* with azo-reductase activity was published in 1967.¹⁵⁶ One year later, another solubly expressed P450, the methylene hydroxylase (P450_{cam}) converting camphor to 5-*exo*-hydroxycamphor from *Pseudomonas putida* was reported (Figure 1.13).¹⁵⁷ Another organism, *Rhodococcus* sp. NCIMB 9784, is also able to use camphor as only carbon source. The P450 responsible for this metabolic activity is called P450camr, hydroxylating camphor to 6-*endo*-hydroxycamphor.¹⁵⁸

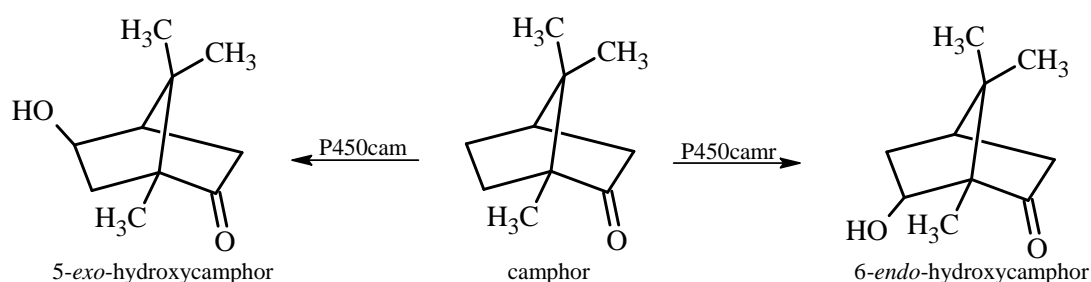


Figure 1.13: Hydroxylation of camphor by P450cam (*Pseudomonas putida*) to 5-*exo*-hydroxycamphor or P450camr (*Rhodococcus* sp.) to 6-*endo*-hydroxycamphor

Generally, bacteria use P450 hydroxylations as the first steps of the biodegradation of carbon sources, for example the degradation of cineole by

*Citrobacter braakii*¹⁵⁹, or for the biosynthesis of secondary metabolites, such as antibiotic or neurotoxine by *Streptomyces* sp.¹⁶⁰⁻¹⁶². Another prokaryotic P450, the CYP153A6 from *Mycobacterium* sp. HXN-1500 hydroxylates alkanes with a chain-length between C6 and C11 to primary alkanols with a large regioselectivity of over 95%.¹⁶³

The alkane hydroxylase of the CYP153 family from *Mycobacterium* sp. catalyses the conversion of limonene to perillyl alcohol, an anticancer drug. The hydroxylase can be recombinantly expressed in *Pseudomonas putida* in large bioreactors to produce sufficient enzyme for pharmaceutical applications.¹⁶⁴

One of the first discovered P450 with hydroxylation activity was the human CYP21A2, which converts progesterone to deoxycorticosterone (Figure 1.14).¹⁴

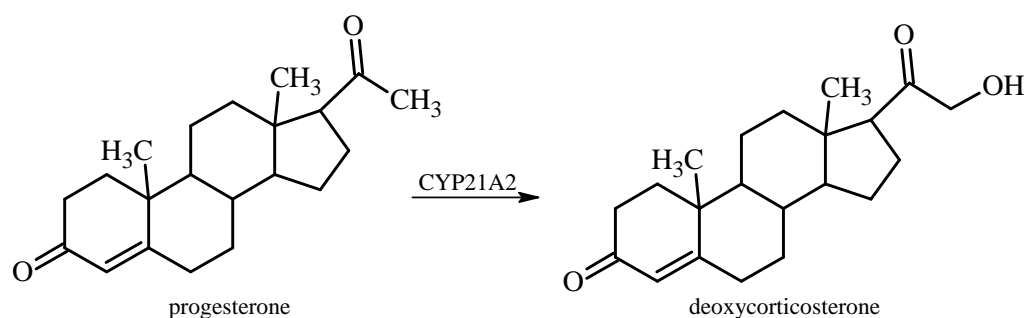


Figure 1.14: Hydroxylation of progesterone to deoxycorticosterone by CYP21A2

Other human P450s have been shown to be involved in steroid metabolism such as CYP2A19, which hydroxylates progesterone to 21-hydroxyprogesterone as the main product forming 16 α - and 17 α -hydroxyprogesterone as minor products. Furthermore, it was shown that CYP2A19 converted testosterone to androstenedione with low amounts of 2 β -, 6 β - and 16 β -hydroxy testosterones.¹⁶⁵

In the plant *Arabidopsis thaliana*, different cytochromes catalyse hydroxylations involved in different biosyntheses. One of the first P450s examined was the Arabidopsis cinnamic acid 4-hydroxylase (CYP73A5), which is involved with the 3'-hydroxylase (CYP98A3) and the 5-hydroxylase (CYP84A1) in the phenylpropanoid pathway and the biosynthesis of lignin¹⁶⁶⁻¹⁶⁸.

The metabolism of brassinolide involves a 22 α -hydroxylase CYP90B1 called DWF4 catalysing the conversion of 6-*oxo*-campestanol to cathasterone^{169,170}

(Figure 1.15) and the 23 α -hydroxylase CYP90A1 called *cpd* for 6-*oxo*-cathasterone^{171,172}. On the other hand, P450s, for example the 26-hydroxylase CYP72B1, also take part in the degradation of brassinolide¹⁷³.

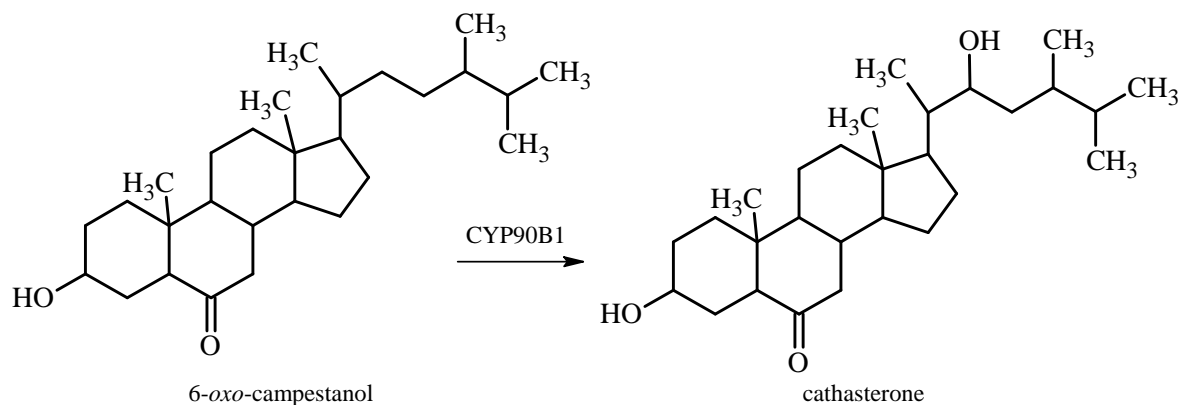


Figure 1.15: Hydroxylation of 6-*oxo*-campestanol to cathasterone by Arabidopsis CYP90B1

1.3.2 Oxidation

P450s are monooxygenases and oxidise the substrate following the equation:



Oxidases, dioxygenases and peroxidases catalyse similar reactions, however P450s are special, because they are able to introduce oxygen into double bonds, allylic positions and also non-activated C-H bonds.¹⁷⁴

Another typical P450 catalysed reaction is the oxidation of heteroatoms, for example nitrogen in tertiary amines to *N*-oxides or sulphur in thioethers to sulfoxides and sulfones (Figure 1.16).

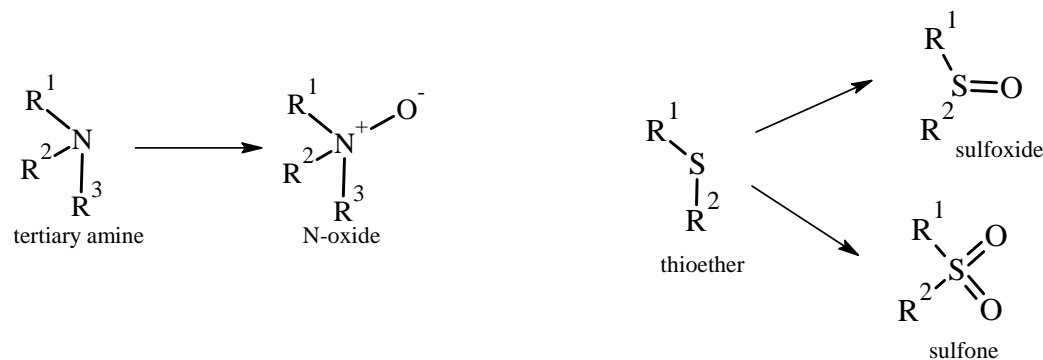


Figure 1.16: P450 dependent heteroatom-oxidations of tertiary amines to *N*-oxides and thioether to sulfoxides or sulfones

An enzymatic oxidation of methyl groups on aromatic heterocycles, such as pyridines, to the corresponding monocarboxylic acids was investigated by fermentation of *Pseudomonas putida* on industrial scale by Lonza AG (Figure 1.17).¹⁷⁵ Pyridine-3-carboxylic acid (niacin) is the water-soluble vitamin B3 used in animal feed supplementation and medicine.^{176,177}

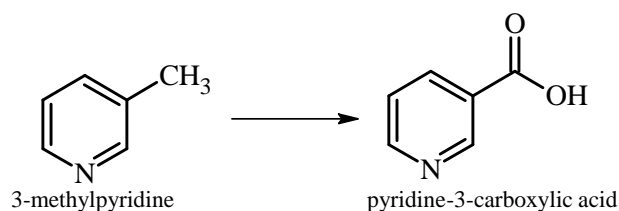


Figure 1.17: P450 catalysed oxidation of 3-methylpyridine to pyridine-3-carboxylic acid

P450s catalyse also the epoxidation of double bonds, for example the *Arabidopsis thaliana* (*Arabidopsis*) CYP77A4 can epoxidise unsaturated C18 fatty acids.¹⁷⁸ Epoxidations result in very reactive versatile epoxide species by transferring the P450 ferryl-oxygen to the alkene, which builds a radical intermediate followed by the epoxide formation (Figure 1.18).

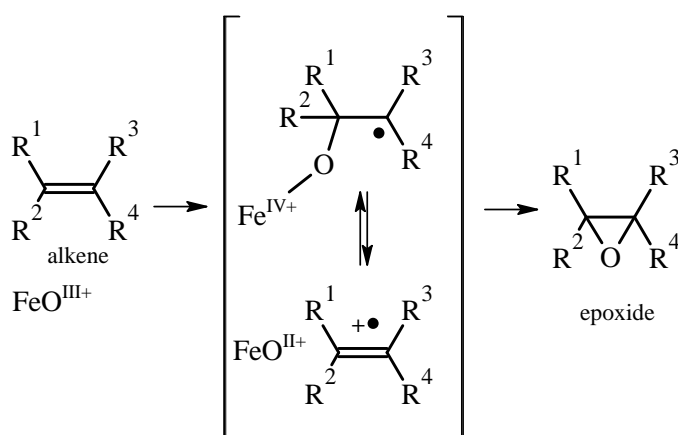


Figure 1.18: P450 catalysed epoxidation of an alkene

Epoxide can easily react with complex macromolecules useful for the synthesis of polymers¹⁷⁹ and pharmaceuticals⁸³ for industrial applications.

1.4 Plant Cytochromes P450

1.4.1 Cytochromes P450s in *Arabidopsis thaliana*

Arabidopsis is a much used model plant in biology, because of its fast growth cycle (48 days until the first silique¹⁸⁰) and ease of transformation. The whole genome is sequenced, and it is known that this plant has over 25000 genes, which code proteins from 11000 families.¹⁸¹ *Arabidopsis* has 244 P450 genes and 28 pseudogenes¹⁸² and represents a fantastic opportunity for a high number of different biocatalysts to be discovered.

The phylogenetic tree (adapted from Bak *et al.* 2011¹⁸², Figure 1.19) shows the evolutionary relationships between the different P450s in *Arabidopsis*.

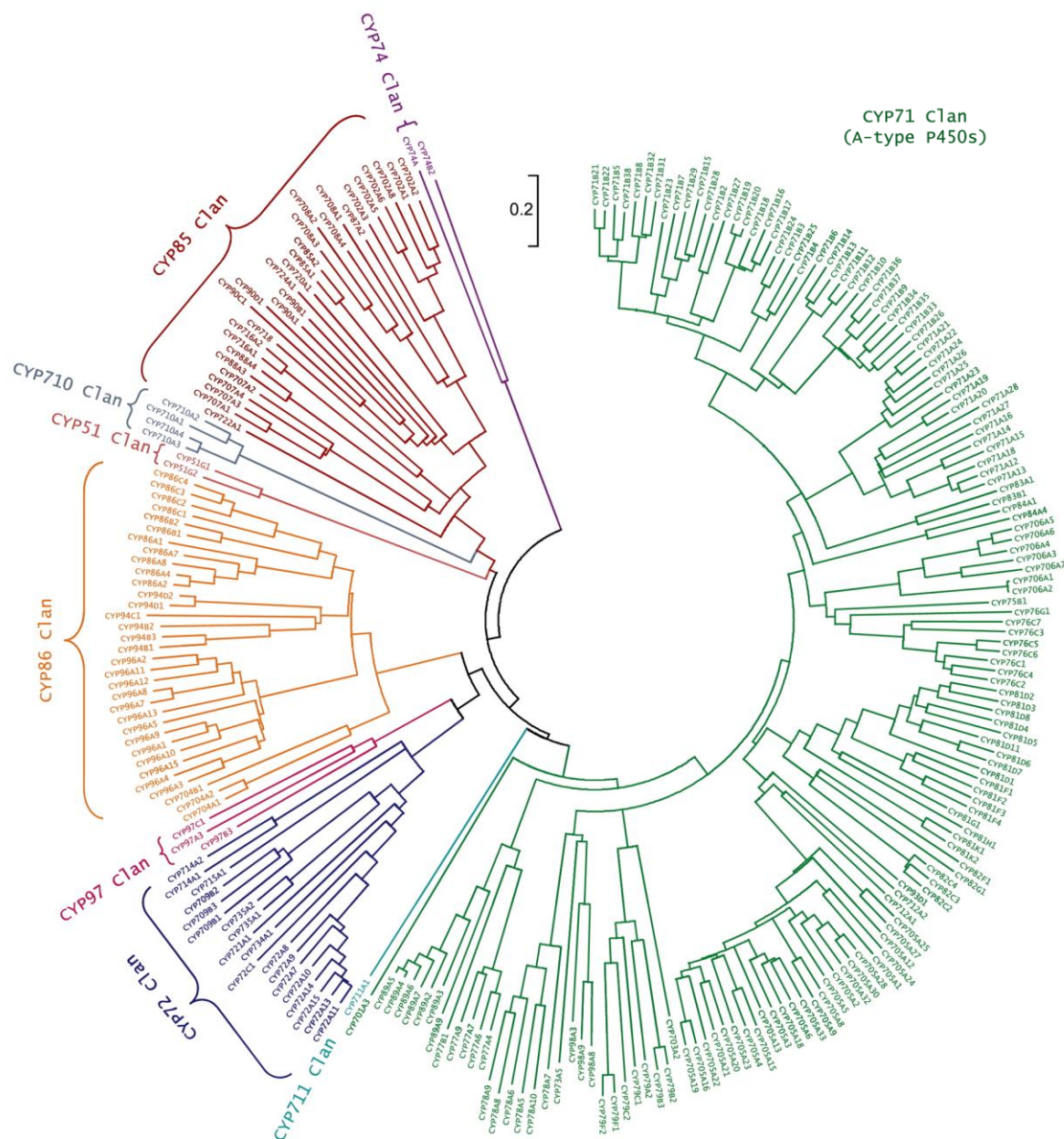


Figure 1.19: Phylogenetic tree of all cytochromes P450 from Arabidopsis¹⁸²

The 67 Arabidopsis P450s with known function are listed in Table 1.1. They are mainly involved in secondary metabolism, such as in the biosynthesis of hormones, pigments, flavours and for the production of complex macromolecules such as cutin, lignin and suberin or for defense compounds. Approximately 20 P450 contain a rich N-terminal Serine-Threonine sequence indicating a chloroplast signal.³⁸

Table 1.1: Arabidopsis P450s with known function

P450 (gene locus)	reaction	pathway	references
51G1 (At1g11680)	obtusifoliol 14 α -demethylase	sterols/steroids	183,184
71A12 (At2g30750)	hydroxylation and N-demethylation of pyrazoxyfen	metabolism of herbicide pyrazoxyfen, camalexin biosynthesis in roots	185,186
71A13 (At2g307700)	dehydration of indole acetaldoxime to indole-3-acetonitrile	camalexin biosynthesis	187
71B7 (At1g13110)	deethylation of 7-ethoxycoumarin (with cumene hydroperoxide as electron donor)		188
71B15 (At3g26830)	conversion of s-dihydrocamalexin acid to camalexin	camalexin	189,190
73A5 (At2g30490)	4-hydroxylation of <i>t</i> -cinnamic acid to <i>p</i> -coumaric acid; hydroxylation of cinnamic acid analogs	phenylpropanoid pathway, lignin biosynthesis	166,191,192
74A1 (At5g42650)	allene oxide synthase for linoleic acid hydroperoxide and linolenic acid hydroperoxide	jasmonate acid biosynthesis	37,45,193-196
74B2 (At4g15440)	hydroperoxide lyase for linoleic acid hydroperoxide and linolenic acid hydroperoxide	oxylipin pathway, jasmonate biosynthesis	197-199
75B1 (At5g07990)	3 ⁺ -hydroxylation of narigenin and dihydrokaempferol	phenylpropanoid pathway, flavonoid biosynthesis	200
76C1 (At2g45560)	10-hydroxylation of geraniol	terpenoid indole alkaloid biosynthesis	201
77A4 (At5g04660)	epoxidation of unsaturated C ₁₈ fatty acids (oleic, linoleic, α -linolenic acid)	fatty acid metabolism	178
77A6 (At3g10570)	in-chain 10-hydroxylation of 16-hydroxypalmitate	cutin biosynthesis	202
79A2 (At5g05260)	conversion of phenylalanine to oxime	benzylglucosinolate biosynthesis	203
79B2 (At4g39950)	conversion of tryptophan and tryptophan analogs to oxime	indole glucosinolate biosynthesis, camalexin biosynthesis, auxin biosynthesis	204-209
79B3 (At2g22330)	conversion of tryptophan and tryptophan analogs to oxime	indole glucosinolate biosynthesis, camalexin biosynthesis, auxin biosynthesis	204-209
79F1 (At1g16410)	N-hydroxylation of homo- to tetrahydro-methionine ($n = 3$ to 6) (short-chain methionine derivatives to their aldoximes)	biosynthesis of aliphatic glucosinolates	210-213

P450 (gene locus)	reaction	pathway	references
79F2 (At1g16400)	N-hydroxylation of long chain penta and hexahomomethionine to their aldoxime	biosynthesis of aliphatic glucosinolates	211-213
81F2 (At5g57220)	4-hydroxylation of indole-3-ylmethyl to 4-hydroxy-indole-3-ylmethyl glucosinolate	indole glucosinolate biosynthesis	214-216
81F4 (At4g37410)	putative P450	possibly involved in the indole glucosinolate biosynthesis	217
82C2 (At4g31970)	5-hydroxylation of 8-methoxypsoralen to 5-hydroxy-8-methoxypsoralen	metabolism of tryptophan-derived secondary metabolites, possibly involved in jasmonic acid induced indole glucosinolates	218,219
82C4 (At4g31940)	5-hydroxylation of 8-methoxypsoralen to 5-hydroxy-8-methoxypsoralen	Fe deficiency response, possibly through an IDE1-like mediated pathway	218,220
82G1 (At3g25180)	(<i>E,E</i>)-geranylinalool and the sesquiterpenoid (<i>E</i>)-nerolidol into the acyclic volatile C ₁₆ -homoterpene 4,8, 12-trimethylthdeca-1,3,7, 11-tetraene (TMTT) and the C ₁₁ -homoterpene 4,8-dimethyl-1,3,7-nonathene (DMNT), respectively		221
83A1 (At4g13770)	oxidation of methionine-derived oximes oxidation of p-hydroxyphenyl-acetaldoxime, indole-3-acetaldoxime, conversion of aldoximes to thiohydroximates	biosynthesis of aliphatic glucosinolate	222-224
83B1 (At4g31500)	oxidation of indole-3-acetaldoxime	biosynthesis of indole glucosinolate	222,223,225
84A1 (At4g36220)	5-hydroxylation of coniferaldehyde, coniferyl alcohol and ferulic acid	phenylpropanoid pathway, biosynthesis of lignin	167,226,227
84A4 (At5g04330)	putative ferulate-5-hydroxylase		228,229
85A1 (At5g38970)	C6-oxidase for 6-deoxycastasterone to castasterone, other steroids conversion of castasterone to brassinolide	biosynthesis of brassinolide	230-234
85A2 (At3g30180)	C6-oxidase for 6-deoxycastasterone to castasterone, other steroids conversion of castasterone to brassinolide	biosynthesis of brassinolide	230-233,235,236
86A1 (At5g58860)	ω -hydroxylation of saturated and unsaturated	fatty acid metabolism, biosynthesis of cutin,	237-240

P450 (gene locus)	reaction	pathway	references
	C12 to C20 fatty acids	biosynthesis of suberin	
86A2 (At4g00360)	ω -hydroxylation of saturated and unsaturated C12 to C18 fatty acids	fatty acid metabolism, biosynthesis of cutin	238,241,242
86A4 (At1g01600)	ω -hydroxylation of saturated and unsaturated C12 to C18 fatty acids	fatty acid metabolism, biosynthesis of cutin	202,238,242,243
86A7 (At1g63710)	ω -hydroxylation of lauric acid	fatty acid metabolism, biosynthesis of cutin	238,242
86A8 (At2g45970)	ω -hydroxylation of saturated and unsaturated C12 to C18 fatty acids	fatty acid metabolism, biosynthesis of cutin	238,242,244
86B1 (At5g23190)	ω -hydroxylation for long chain fatty acid (C22 and C24)	biosynthesis of suberin, fatty acid metabolism, polyester monomer biosynthesis	38,245
86C3 (At1g13140)	hydroxylation of fatty acids (C12, C14, C14:1, C16)	fatty acid metabolism	246
88A3 (At1g05160)	oxidation of <i>ent</i> -kaurenoic acid to gibberillin A12 in three steps	biosynthesis of gibberellins	39,247
88A4 (At2g32440)	oxidation of <i>ent</i> -kaurenoic acid to gibberillin A12 in three steps	biosynthesis of gibberellins	39,247
90A1 (At5g05690)	23 α -hydroxylation of steroids	biosynthesis of brassinolide	171,172,248,249
90B1 (At3g50660)	22 α -hydroxylation of C27, C28, C29 sterols	biosynthesis of brassinolide	169,249-251
90C1 (At4g36380)	C23-hydroxylation of sterols (typhasterol to castasterone)	biosynthesis of brassinolide	252-255
90D1 (At3g13730)	C23-hydroxylation of sterols	biosynthesis of brassinolide	253-255
94B3 (At3g48520)	12-hydroxylation of jasmonoyl-L-isoleucine	oxidative catabolism of jasmonate, jasmonate mediated signaling pathway	256,257
94C1 (At2g27690)	ω -hydroxylation of saturated and unsaturated C12 to C18 fatty acids and hydroxylation of ω -hydroxy fatty acid into dicarboxylic fatty acid	fatty acid metabolism	240,258
96A15 (At1g57750)	hydroxylation of midchain alkane to alcohols and second hydroxylation to ketone	biosynthesis of wax	259
97A3 (At1g31800)	β -hydroxylation of carotene	carotenoid metabolism	260,261
97B3 (At4g15110)	β -hydroxylation of β -carotene to zeaxanthin via β -cryptoxanthin	carotenoid metabolism	262
97C1 (At3g53130)	ϵ -hydroxylation of β , ϵ -carotene	carotenoid metabolism	260,263
98A3 (At2g40890)	3-hydroxylation of <i>p</i> -coumarate to caffeic acid	phenylpropanoid pathway, biosynthesis of lignin	168,264-267

P450 (gene locus)	reaction	pathway	references
	and 3-hydroxylation of coumaroyl-esters (shikimate and quinate esters)	monomers and soluble phenolics	
98A8 (At1g74540)	<i>meta</i> -hydroxylation of the three triferuloylspermidine phenolic rings, oxygenation of resveratrol	alternative phenolic pathway, pollen development	268,269
98A9 (At1g74550)	<i>meta</i> -hydroxylation of the three triferuloylspermidine phenolic rings, oxygenation of resveratrol	alternative phenolic pathway, pollen development	268,269
701A3 (At5g25900)	oxidation of <i>ent</i> -kaurene to <i>ent</i> -kaurenoic acid in three steps	biosynthesis of gibberellin	39,270-273
703A2 (At1g01280)	in-chain monohydroxylation of saturated fatty acids (C10-C16)	biosynthesis of sporopollenin, pollen development	274
704B1 (At1g69500)	ω -hydroxylation of saturated, unsaturated and epoxy C16 and C18 fatty acids	biosynthesis of sporopollenin, pollen development	275,276
705A5 (At5g47990)	conversion of thaliandiol to desaturated thaliandiol	thalianol metabolic pathway	277
707A1 (At4g19230)	8-hydroxylation of abscisic acid	abscisic acid catabolism	278-280
707A2 (At2g29090)	8-hydroxylation of abscisic acid	abscisic acid catabolism	278-281
707A3 (At5g45340)	8-hydroxylation of abscisic acid	abscisic acid catabolism	278,279,281-286
707A4 (At3g19270)	8-hydroxylation of abscisic acid	abscisic acid catabolism	278,279
708A2 (At5g48000)	hydroxylation of thalianol to thaliandiol	thalianol metabolic pathway	277
710A1 (At2g34500)	C22-desaturation of β -sitosterol to stigmasterol	biosynthesis of sterols	287-289
710A2 (At2g34490)	C22-desaturation of β -sitosterol and 24- <i>epi</i> -campesterol to stigmasterol and brassicasterol	biosynthesis of sterols	287
710A4 (At2g28860)	C22-desaturation of β -sitosterol to stigmasterol	biosynthesis of sterols	288
714A1 (At5g24910)	C13-hydroxylation of <i>ent</i> -kaurenoic acid to steviol	gibberillin catabolism	277,290
724A1 (At5g14400)	22 α -hydroxylation of brassinosteroid	biosynthesis of brassinolide	291
734A1 (At2g26710) initially classified as CYP72B	C26-hydroxylation of brassinolide and castasterone	brassinolide catabolism	173,292,293
735A1 (At5g38450)	<i>trans</i> -hydroxylation of isopentenyladenine, tri/di/monophosphates	biosynthesis of zeatin, cytokinin metabolism	294
735A2 (At1g67110)	<i>trans</i> -hydroxylation of isopentenyladenine, tri/di/monophosphates	biosynthesis of zeatin, cytokinin metabolism	294

The CYP51 is the most conserved P450 family across all kingdoms and counts as an eukaryotic P450 of prokaryotic origin.²⁹⁵ CYP51 is involved in the biosynthesis of sterols, e. g. cholesterol in animals²⁹⁶, obtusifoliol in plants^{183,184} and ergosterol in fungi²⁹⁷ by catalysing 14 α -demethylation (Figure 1.20).

In plants, the methyl group of carbon number 14 is hydroxylated to 14 α -carboxyalcohol and then converted to 14 α -carboxyaldehyde. In the last step a double bond is introduced by an oxidative deformylation with separation of formic acid.²⁹⁸

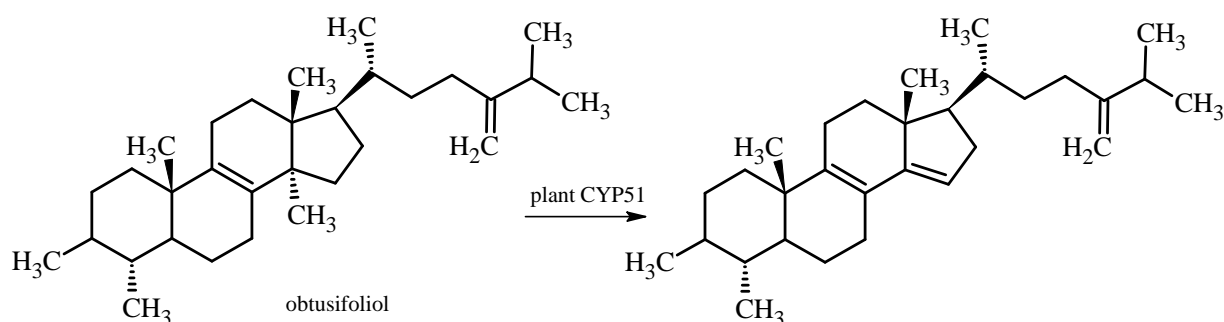


Figure 1.20: 14 α -demethylation of obtusifoliol by plant CYP51

75% of the *Arabidopsis* P450s are still with unknown function, which shows that there is a greater research potential for finding new metabolic pathways and reactions in plants.

1.4.2 Fusions of plant Cytochromes P450

In Nature there exists no native plant P450 fusion so far. There are now a few examples where plant P450s (C-terminus) fused to plant P450 reductase have been expressed as active enzymes in *E. coli* (Table 1.2). The first artificial plant fusion contained the cinnamate-4-hydroxylase (CYP73A4) and the P450 reductase (both enzymes from *C. roseus*, Madagascar periwinkle) and was engineered by Prof. Schröder's research group in 1995.²⁹⁹ They found activity in the insoluble protein fraction after expression in *E. coli*. A few years later, they determined that a fusion of a P450 and the reductase from two different plants (*Petunia hybrida* CYP75 fused to *C. roseus* reductases) resulted in 50% lower specific activity than when the two enzymes are both from *C. roseus*.³⁰⁰ Moreover, they demonstrated that their strategy is an alternative technique for expression of

functional plant P450s and engineered another two fusions of CYP71D12 (tabersonine-16-hydroxylase from *C. roseus*) and CYP72A1 (secologanin synthase from *C. roseus*) fused to the reductase of *C. roseus*.^{301,302} Tabersonine-16-hydroxylase catalyses the first reaction in the pathway of vinblastine and vincristine, both bisindoles that are important for the pharmaceutical industry where they are used as treatments for leukaemia.^{301,303} Secologanin synthase converts loganin to secologanin, which is a precursor of terpenoid indole alkaloids in various plants important for development of drugs in cancer treatment.^{302,304}

Another artificial plant fusion made of CYP71B1 from *Thlaspi arvensae* (field penny cress) and the *C. roseus* reductases was found to be active for the conversion of benzo(a)pyrene to 3-hydroxybenzo(a)pyrene in the membrane fraction after expression in *E. coli*.³⁰⁵

Table 1.2: Plant fusion P450s heterologously expressed in *E. coli*

P450	P450 from	Reductase from	linker sequence (amino acid)	Reference
CYP71B1	<i>Thlaspi arvensae</i> (field penny cress)	<i>Catharanthus roseus</i> , (madagascar periwinkle)	ST	Lamb <i>et al.</i> 1998 ³⁰⁵
CYP71D12 (tabersonine 16-hydroxylase)	<i>Catharanthus roseus</i>	<i>Catharanthus roseus</i>	ST	Schröder <i>et al.</i> 1999 ³⁰¹
CYP72A1 (secologanin synthase)	<i>Catharanthus roseus</i>	<i>Catharanthus roseus</i>	ST	Irmeler <i>et al.</i> 2000 ³⁰²
CYP73A4 (cinnamate 4-hydroxylase)	<i>Catharanthus roseus</i>	<i>Catharanthus roseus</i>	ST	Hotze <i>et al.</i> 1995 ²⁹⁹
CYP75 (flavonoid 3',5'-hydroxylase)	<i>Catharanthus roseus</i>	<i>Catharanthus roseus</i>	ST	Kaltenbach <i>et al.</i> 1999 ³⁰⁰
CYP75 (flavonoid 3',5'-hydroxylase)	<i>Petunia hybrid</i> (petunia)	<i>Catharanthus roseus</i>	ST	Kaltenbach <i>et al.</i> 1999 ³⁰⁰
IFS (isoflavone synthase I)	<i>Glycine max</i> (soy bean)	<i>Catharanthus roseus</i>	GST	Leonard & Koffas 2007 ³⁰⁶
isoflavone synthase	<i>Trifolium pratense</i> (red clover)	<i>Oryza sativa</i> (rice)	GST	Kim <i>et al.</i> 2009 ³⁰⁷

More recent publications have specially focused on fusions containing the isoflavone synthase I (IFS) from *Glycine max* (soy bean) and isoflavone synthase from red clover.^{306,307} The artificial plant fusion system IFS-CPR (reductase CPR from *C. roseus*) was created by Koffas's research group by imitating the powerful natural fusion P450 BM3 from *B. megaterium*.³⁰⁶ The IFS converts naringenin and liquiritigenin to genistein and daidzein, respectively (Figure 1.21).

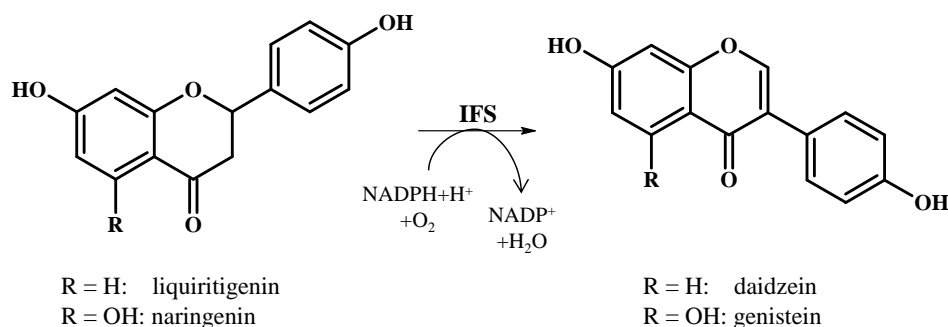


Figure 1.21: Conversion of the flavanones liquiritigenin and naringenin to the isoflavones daidzein and genistein, respectively, by the P450 isoflavone synthase I

The reaction mechanism catalysed by IFS starts with an oxidation in the presence of NADPH+H⁺ and molecular oxygen to a radical (**1**, Figure 1.22), followed by an aryl ring migration (**2**) and forming a 2,7,4'-trihydroxyisoflavanone (**3**). The last step is a dehydration (**4**), which yields genistein and is not performed by the P450. It is possible that a specific dehydratase is involved or that the water molecule is eliminated spontaneously.³⁰⁸⁻³¹⁰

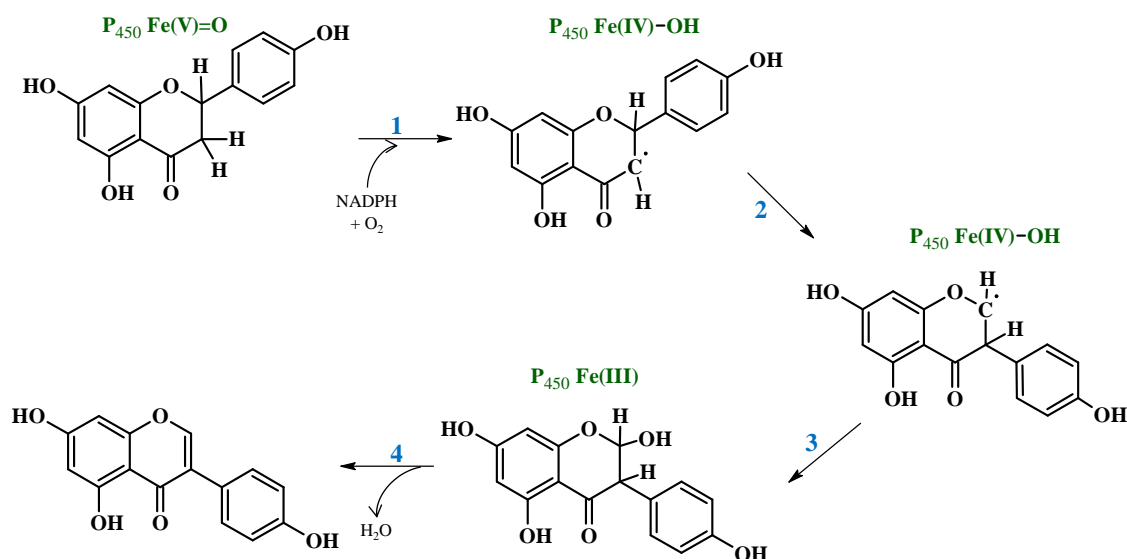


Figure 1.22: Reaction mechanism of the conversion of naringenin to genistein by the P450 isoflavone synthase I

Another artificial plant IFS-fusion for expression in *E. coli* BL21 (DE3) was developed by Kim *et al.* 2009³⁰⁷. Therefore, the IFS from red clover was fused to the rice reductase (rcIFS-riceCPR), deleting the membrane anchors of *rcIFS* (63 nucleotides) and *riceCPR* (49 nucleotides), and activity has been demonstrated in a growing cell assay.³⁰⁷

Isoflavones belong to the group of isoflavonoids and are predominantly produced as secondary metabolites in legumes.³¹¹ Isoflavones have a broad bioactivity spectrum: inhibition of tyrosine kinases and enzymes in steroid biosynthesis, antioxidant activity, prevention of carcinogenesis and inhibition of metastasis. In Asia, where soy bean (rich of isoflavones) is eaten much more than in western countries, a reduced frequency of heart diseases, osteoporosis, menopausal symptoms, breast and prostate cancer was recorded.³¹²⁻³¹⁷

1.5 Recombinant Expression Systems

There are a number of different expression systems available. The two least expensive and most commonly used systems are the bacterium *E. coli* (which has no endogenous P450 or P450 reductase genes) and the yeast *Saccharomyces cerevisiae* (containing three P450 and one associated NAD(P)H P450 reductase gene).^{28,318} Furthermore, insect cells, another heterologous eukaryotic expression

system, are often used for the expression of plant P450s together with the insect NADPH P450 reductase.³¹⁹ Duan and Schuler (2006)³¹⁹ give a useful summary of the expression of Arabidopsis P450s in different hosts.

1.5.1 Expression of P450s in *Escherichia coli*

The great advantage of bacterial expression over yeast or insect cells is the relatively fast growth rates, inexpensive cost and ease of cultivation. However, expression of unmodified plant P450s in *E. coli* can be complicated due to differences in codon preference and because eukaryotic P450s are mostly membrane bound and bacteria do not have such a developed membrane system. Expression of plant P450s in *E. coli* is therefore challenging and it is often difficult to obtain soluble protein.^{320,321} If the P450 is only anchored in the membrane, with the majority of the enzyme, including the catalytic centre in the cytosol, then removal of the hydrophobic membrane bound part may result in soluble enzyme. Studies on mammalian P450s have shown activity towards their specific substrates after the deletion of around 2-20 of the hydrophobic residues from the N-terminus.^{57,59,322} Additionally, the microsomal human P450 2C3 could be expressed solubly after the modification of the N-terminal hydrophobic membrane bound segment.⁵⁸

Many plant P450s have been expressed in *E. coli*, none of them soluble, for biochemistry studies. The two Arabidopsis CYP79F1 and CYP79F2, both involved in the biosynthesis of aliphatic glucosinolates have been characterised after recombinant expression in *E. coli*.^{210,212}

Artificial P450 fusion proteins have been expressed also in *E. coli* (more information in Chapter 1.4.2, page 43).

1.5.2 Expression in Yeast

The yeast *Saccharomyces cerevisiae* contains an endogenous reductase capable of efficient electron transfer to P450s³²³ and was the first host where mammalian^{324,325} and plant³²⁶ P450s were successfully expressed. *S. cerevisiae* contains three P450s and has therefore also its own reductases. Additionally, yeast supports posttranslational machinery (e. g. glycosylation, membrane association, correct protein folding) for the expression of active eukaryotic P450s.

More than twenty years ago it was found that the P450 activity is limited by the quantity and availability of the P450 reductase. For example CYP71A1 from avocado, CYP73A1 from artichoke and CYP73A3 from alfalfa have been expressed successfully in *S. cerevisiae*, however activity was reduced.³²⁶⁻³²⁸ Possible reasons for this could be that the yeast reductase is inadequate for the amount of expressed P450, and that the electron transfer is not optimal between yeast reductase and plant P450.³²⁹ Thus the activity was increased when the partnering plant reductase was expressed simultaneously.^{325,330,331}

The group of Ohkawa reported the successful expression of different mammalian membrane bound P450 together with the corresponding reductase in yeast.³³²⁻³³⁶ For example, the 17 α -hydroxylase (P450c17) was ten times more active than the wild-type when the native P450c17 was fused to the 23 amino acid truncated yeast reductase.³³³

Plant P450 co-expression systems with its corresponding NADPH P450 reductase in yeast have been generated. Examples of co-expression include the CYP98A14 from *Coleus blumei*, which catalyses the 3-hydroxylation of 4-coumaroyl-3',4'-dihydroxyphenyllactate and the 3'-hydroxylation of caffeoyl-4'-hydroxyl-phenyl lactate by forming rosmarinic acid.³³⁷

One of the first vectors used for expression of plant P450s in yeast was the shuttle vector pYeDP60 (Figure 2.3) which has a high copy number when expressed in *E. coli*. This vector, which contains the galactose-inducible GAL10-CYC1 promoter is coupled with the yeast P450 reductase and is still used due to its high stability in rich medium at high cell density.^{326,338}

To overcome coupling problems between the plant P450 and the yeast reductase, special yeast strains WAT11 and WAT21, which express the Arabidopsis NADPH P450 reductase ATR1 and ATR2, respectively, were constructed.³³⁸ Over twenty Arabidopsis P450s (CYP71B15, 71A1, 72B1, 73A5, 77A4, 77A6, 82C2, 82C4, 82F1, 82G1, 83A1, 83B1, 84A1, 85A1-2, 86A2, 86A8, 88A4, 94B1-3, 94C1, 86A1-4, 97B3, 98A3, 703A2, 704A2, 704B1, 707A1-4, 709C1, 711A1 and 734A1) have been successfully expressed using the pYeDP60 vector and the WAT11 strain.^{167,168,178,190,192,202,212,218,221,222,225,230,231,235,236,244,247,256,274,275,279,292,339-}

341

The alternate *Pichia pastoris* system can also be used to overcome the expression problems describe above for plant P450s in *E. coli*.³⁴² The Arabidopsis CYP85A2 – which converts teasterone and also typhasterol to 7-oxa-teasterone and 7-oxatyphasterol, respectively – and ATR1 have been expressed simultaneously in *Pichia pastoris* and activity was found.³⁴³

1.6 Aim of the project

The plant cytochrome P450 superfamily is a very attractive target for industrial applications, due to the high number of different reactions which they are able to catalyse. Cytochromes P450 work most efficiently when combined with their endogenous cytochrome P450 reductases as electron donor. The development of a fusion protein containing plant P450s and appropriate reductase to produce robust and efficient biocatalysts would be of relevance to industry.

The aim of this project is to develop a platform technology by cloning plant P450s for recombinant expression, for physiological characterisation studies and industrial application. Different expression systems were tested to get functional enzymes. The simplest expression system used was *E. coli*; however, as plant P450s are membrane bound, functional expression is more likely to occur in eukaryotic expression systems. Therefore, the yeast *S. cerevisiae* was also tested as host.

2 Materials and Methods

2.1 Reagents and consumables

The reagents and consumables used in this study were purchased from AccuStandard (New Haven, US), Bio-Rad Laboratories Ltd. (Hemel Hempstead, UK), Bruker Ltd. (Coventry, UK), Carl Zeiss Ltd. (Rugby, UK), Daicel Chemical Industries Ltd. (Tokyo, Japan), Difco (BD, Oxford, UK), Expedeon Ltd. (Harston, UK), Fisher Scientific UK Ltd. (Loughborough, UK), Finnzymes (Vantaa, Finland), Formedium (Norfolk, UK), Invitrogen Ltd. (Paisley, UK), Kartell spa (Noviglio, Italy), Levington F2 compost (Scotts, Bamford, Ipswich, UK), Matrix Science Ltd. (London, UK), Melford Laboratories Ltd. (Ipswich, Suffolk UK), Merck Chemicals Ltd. (Nottingham, UK), Millipore (Tullagreen, Ireland), New England Biolabs (Ipswich, UK), Oxoid Ltd. (Basingstoke, UK), Promega UK Ltd. (Southampton, UK), Qiagen Ltd. (West Sussex, UK), Sarstedt Ltd. (Leicester, UK), Sartorius AG (Göttingen, Germany), Scientific Laboratory Supplies Ltd. (Nottingham, UK), SelectScience Ltd. (Bath, UK), Sigma-Aldrich Company Ltd. (Dorset, UK), Starlab Ltd. (Milton Keynes, UK), Sterilin Ltd. (Newport, UK), Thermo Fisher Scientific p/a Perbio Science UK, Ltd. (Cramlington, UK), UVitec Ltd. (Cambridge, UK) and VWR International Ltd. (Lutterworth, UK).

TNT was donated by the Defence Science and Technology Laboratory (Dstl; Fort Halsted, UK), dinitrotoluenes (Sigma-Aldrich), aminodinitrotoluenes by Supelco (Sigma-Aldrich) and hydroxyaminodinitrotoluenes by AccuStandard.

DNA Polymerases and restriction enzymes were bought from New England Biolabs and Finnzymes.

PCR Primers were synthesised by Sigma-Aldrich and genes by GeneArt (Regensburg, Germany).

The construct of the artificial fusion construct IFS-CPR (IFS = isoflavone synthase 1 from *Glycine max* fused to the P450 reductase from *Catharanthus roseus*) was kindly provided by Prof. Mattheos Koffas (State University of New York, Buffalo, USA) and the nicotine-*N*-demethylase (CYP82E4) from *Nicotiana tabacum* from Prof. Ralph Dewey (Department of Crop Science, North Carolina State University, Raleigh, USA).

The water used to produce buffers and solutions was molecular biology grade water purified using an Elga Purelab Ultra water polisher (Elga Labwater, High Wycombe, UK).

2.2 Media, strains and plasmids

2.2.1 Bacterial media

Escherichia coli was grown in Lysogeny broth (LB), Terrific broth (TB), auto-induction and M9 minimal media. Super Optimal broth with Catabolite repression (SOC) was used for recovering *E. coli* cells after plasmid DNA transformation.

LB contained 10 g/l tryptone (Formedium), 10 g/l sodium chloride (NaCl) (Fisher Scientific) and 5 g/l yeast extract (Formedium). For the preparation of the solid agar plates, 15 g/l agar (Formedium) was added to LB prior autoclaving and then poured into petri dishes (Sterilin).

TB contained 12 g tryptone (Oxoid), 24 g yeast extract (Oxoid), 4 ml Glycerol (Fisher Scientific) and water to a final volume of 900 ml and sterilised. Before use, 100 ml of sterile 10x TB salt (170 mM KH_2PO_4 and 720 mM K_2HPO_4 , Fisher Scientific) were added.

Auto-induction medium³⁴⁴ (1 l) was made of 950 ml ZY solution (10 g tryptone, 5 g yeast extract and water until a final volume of 950 ml), 25 ml 50x M-solution (0.25 M sodium sulphate (Fisher Scientific), 2.5 M ammonium chloride (Fisher Scientific), 1.25 M monopotassium phosphate (Fisher Scientific), 1.25 M disodium phosphate (Fisher Scientific)), 10 ml 50x 5052 solution (25% glycerol (Fisher Scientific), 0.14 M glucose (Sigma-Aldrich), 0.3 M α -Lactose (Sigma-Aldrich)), 1 ml 1 M MgSO_4 and 1 ml 1000x trace metal solution.

100 ml 1000x trace metal solution contained 0.25 M iron(III)chloride hexahydrate (Fisons) (in 0.1 M HCl), 20 mM calcium chloride (Fisher Scientific), 10 mM manganese(II)chloride tetrahydrate (Sigma-Aldrich), 10 mM zinc(II)sulphate (Fisher Scientific), 2 mM cobalt(II)chloride hexahydrate (Sigma-Aldrich), 2 mM copper(II)chloride dehydrate (Sigma-Aldrich), 2 mM nickel(II)chloride hexahydrate (Sigma-Aldrich), 2 mM sodium molybdate pentahydrate (Sigma-

Aldrich), 2 mM sodium selenite pentahydrate (Fluka, Sigma-Aldrich) and 2 mM boric acid (Fisher Scientific).

Five times **M9** was made of 33.9 g/l Na₂HPO₄ (Fisher Scientific), 15 g/l KH₂PO₄, 2.5 g/l NaCl (Fisher Scientific), 5 g/l NH₄Cl (Fisher Scientific) and sterilised by autoclaving before use. For 1x M9 media was used 200 ml/l 5x M9, 800 ml/l water, 10 ml/l 1 M glucose (sterile filtrated, Fisher Scientific), 2 ml/l 1 M MgSO₄ (Fisher Scientific, sterile filtrated in Millex-MP filter unit, 0.22 µm from Millipore) and 100 µl 1 M CaCl₂ (sterile filtrated, Fisher Scientific).

SOC, used for transformation reactions, contained 5 g yeast extract (Formedium), 0.5 g NaCl (Fisher Scientific), 20 g tryptone (Formedium) and 950 ml water. After autoclaving, sterile filtrated glucose was added to a final concentration of 20 mM.

2.2.2 Bacterial strains

Different *E. coli* strains (Table 2.1) stored in 20% glycerol (Fisher Scientific) at -80 °C or after fresh transformation were streaked onto LB agar plates containing the appropriate antibiotics as necessary. Plates were incubated over night at 37 °C. One colony was used to inoculate a 10 ml starter culture, which was grown shaking at 250 rpm over night at 37 °C (Incubators used were from Gallenkamp, Jencons and Heraeus). Starter cultures were either used for plasmid preparation (Chapter 2.5, page 60) or to inoculate growth media for protein expression as described in Chapter 2.10.1 (page 67). TOP10, DH5α and NovaBlue were used for cloning and Rosetta 2 (DE3) and Rosetta gami 2 (DE3) for protein expression (Table 2.1).

Table 2.1: List of *E. coli* strains used for cloning and recombinant expression in this project

Strain name	Genotype	Manufacturer
TOP10	F ⁻ <i>mcrA</i> Δ(<i>mrr-hsdRMS mcrBC</i>) Φ80 <i>lacZ</i> ΔM15 Δ <i>lacX74 recA1 araD139</i> Δ(<i>ara leu</i>) 7697 <i>galU galK rpsL</i> (Str ^R) <i>endA1 nupG</i>	Invitrogen
DH5α	F ⁻ Φ80 <i>lacZ</i> ΔM15 Δ(<i>lacZYA-argF</i>) U169 <i>recA1 endA1 hsdR17</i> (rK ⁻ , mK ⁺) <i>phoA supE44 λ- thi-1 gyrA96 relA1</i>	Invitrogen
JM109	F' [<i>traD36 proA⁺B⁺ lacI^q Δ(lacZ)M15</i>] <i>supE44 endA1 hsdR17 gyrA96 relA1 thi</i> Δ(<i>lac-proAB</i>)	Stratagene
BL21 (DE3)	F ⁻ <i>ompT hsdSB</i> (rB ⁻ , mB ⁻) <i>gal dcm</i> (DE3)	Invitrogen
NovaBlue (DE3)	<i>endA1 hsdR17</i> (r _{K12} ⁻ m _{K12} ⁺) <i>supE44 thi-1 recA1 gyrA96 relA1 lac</i> F' [<i>proA⁺B⁺ lacI^qZΔM15::Tn10</i>] (Tet ^R)	Novagen-Merck
Rosetta 2 (DE3)	F ⁻ <i>ompT hsdS_B</i> (r _B ⁻ m _B ⁻) <i>gal dcm</i> (DE3) pRARE2 (Cam ^R) The pRARE2 plasmid contains tRNA genes for the rare codons AUA (Ile), AGG (Arg), AGA (Arg), CUA (Leu), CCC (Pro), CGG (Arg) and GGA (Gly).	Novagen-Merck
Rosetta gami 2 (DE3)	Δ(<i>ara-leu</i>)7697 Δ <i>lacX74 ΔphoA PvuII phoR araD139 ahpC galE galK rpsL</i> (DE3) F' [<i>lac⁺ lacI^q pro</i>] <i>gor522::Tn10 trxB</i> pRARE2 (Cam ^R , Str ^R , Tet ^R) The pRARE2 plasmid contains tRNA genes for the rare codons AUA (Ile), AGG (Arg), AGA (Arg), CUA (Leu), CCC (Pro), CGG (Arg) and GGA (Gly).	Novagen-Merck

2.2.3 Plasmids for gene cloning and enzyme expression

Plasmids for gene cloning and enzyme expression are shown in Table 2.2.

Table 2.2: Plasmids for gene cloning and enzyme expression

vector	antibiotica resistance	features	source
pCR2.1-TOPO	Kanamycin	T-overhang vector for cloning PCR products, topoisomerase	Invitrogen
pTrcHis2/ <i>lacZ</i>	Ampicillin	contained <i>isoflavone synthase 1</i> gene from <i>Glycine max</i> , vector pTrcHis2/ <i>lacZ</i> originall from Invitrogen	Prof. Koffas ³⁰⁶
LIC	Kanamycin	pETYSBLIC3C vector, cleavable his tagged N-terminus	Dr. Gideon Grogan ³⁴⁵
LicRed	Kanamycin	pETYSBLIC3C vector, cleavable his tagged N-terminus, contains RhF reductases from <i>Rhodococcus</i> sp.	Dr. Federico Sabbadin ¹⁴⁶
lamATR2tr	Kanamycin	pETYSBLIC3C vector, cleavable his tagged N-terminus, contains lamda linker and truncated ATR2 reductases from Arabidopsis	this work, chapter 5
licATR2tr	Kanamycin	pETYSBLIC3C vector, cleavable his tagged N-terminus, contains lic linker and truncated ATR2 reductases from Arabidopsis	this work, chapter 5
pYeDP60	Ampicillin	GAL10-CYC1 promoter	Prof. Daniele Werck-Reichert ³³⁸

The pTrcHis2/*lacZ*-vector (Figure 2.1, Invitrogen) containing the fusion IFS-CPR was derived from Prof. Mattheos Koffas (State University of New York, Buffalo, USA).³⁰⁶

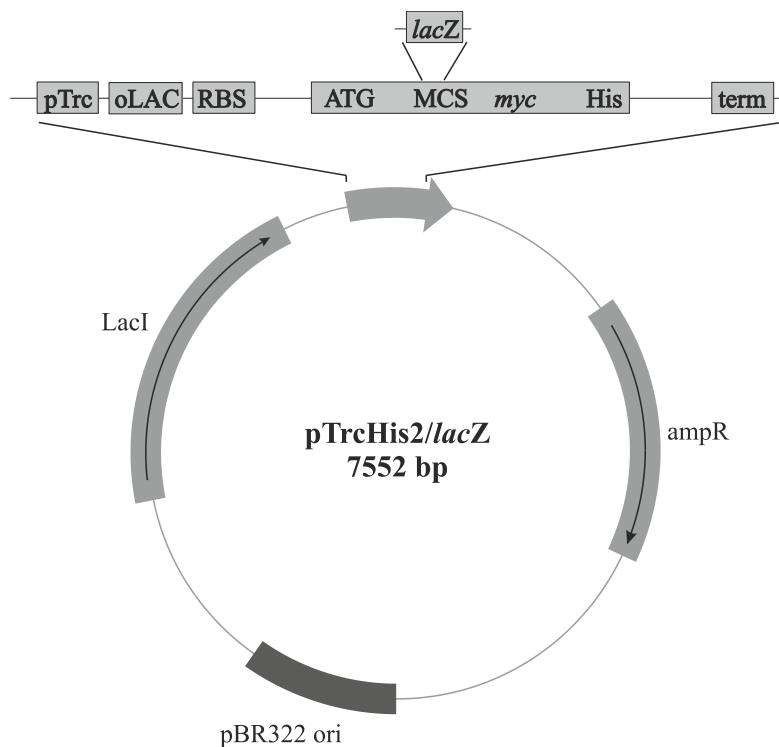


Figure 2.1: Vector map for pTrcHis2/*lacZ*

(pTrc = *trc* promoter, oLAC = Lac operator, RBS = ribosome binding site, ATG = expression start codon, MCS = multiple cloning site, *myc* = *myc* epitope, His = 6x histidines residues, *lacZ* = β -galactosidase gene, term = terminator, ampR = ampicillin resistance gene, pBR322 ori = origin of replication of the plasmid pBR322, LacI = repressor gene for IPTG induction)

The LIC-vector (Figure 2.2), LicRed¹⁴⁶ and the in this work developed lamATR2tr and licATR2tr vector are based on pETYSBLIC3C vector³⁴⁵, which contains an additional cleavable his tagged N-terminus.

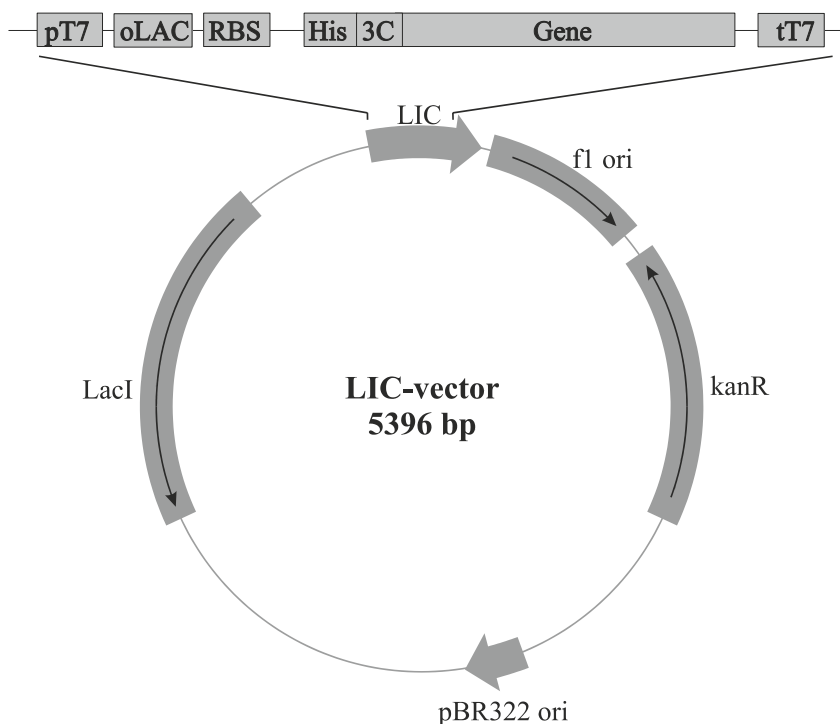


Figure 2.2: Vector map of LIC-vector

(pT7 = T7 promoter, oLAC = Lac operator, RBS = ribosome binding site, His = 6x histidines residues, which can be cleaved HRV 2C protease site = 3C, tT7 = T7 terminator, fl ori = fl phage origin of replication, pBR322 ori = origin of replication of the plasmid pBR322, kanR = kanamycin resistance gene, LacI = repressor gene for IPTG induction)

The vector pYeDP60 (vector map Figure 2.3) is a shuttle vector for cloning in *E. coli* and an expression in yeast.³³⁸

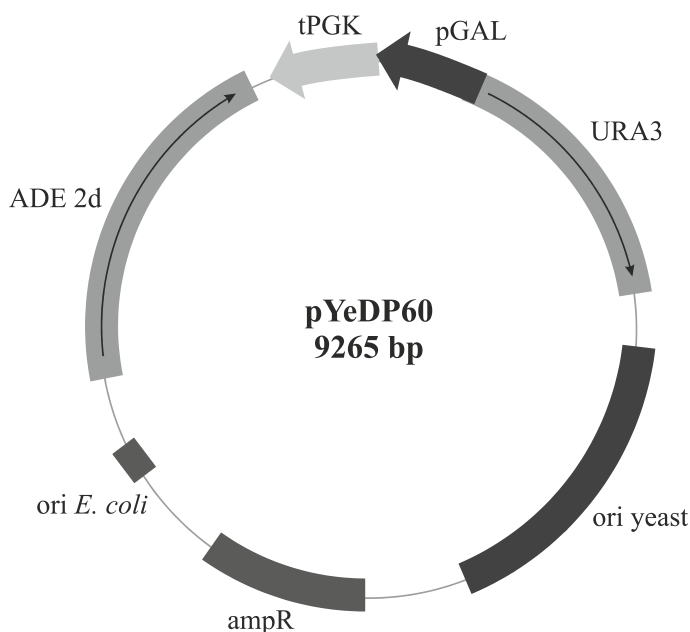


Figure 2.3: pYeDP60 shuttle vector map with an origin of replication for *E. coli* and yeast
(tPGK = phosphoglycerate kinase terminator, pGAL = galactose promoter, ADE 2d and URA3 = selection marker for adenine and uracil auxotrophy, ampR = ampicillin resistance gene)

2.3 Preparation of chemically competent *Escherichia coli* cells

All steps were performed with the appropriate antibiotics for the different *E. coli* strains (Table 2.1) in the growth media. For the preparation of chemically competent cells, *E. coli* strains were streaked on agar plates and incubated overnight at 37 °C. A starter culture (10 ml LB inoculated by a single colony from plate) was used to inoculate 100 ml LB to an OD₆₀₀ of 0.1. This culture was grown to an OD₆₀₀ of 0.4-0.5 and then centrifuged in 25 ml batches in 50 ml falcon tubes (Sarstedt) at 4000 rpm for 5 min and 4 °C in a CR312 Swinging Bucket Rotor Centrifuge (Jouan). The pellets were resuspended in 10 ml of an ice cold, sterile 50 mM MgCl₂/20 mM CaCl₂ solution per tube and incubated on ice for 30 min. Cells were then centrifuged at 4000 rpm for 5 min (CR312 Swinging Bucket Rotor Centrifuge, Jouan) and the pellet resuspended in 1 ml ice cold,

sterile 100 mM CaCl₂ (Fisher Scientific). Sterile glycerol (10% v/v Fisher Scientific) was added and the cells were incubated on ice for further 30 min. Aliquots of 50 µl were snap frozen in liquid nitrogen and stored at -80 °C until use.

2.4 Plant media, growth conditions and strains

Wild type *Arabidopsis thaliana* (Columbia 0, NASC Stock acc. No. N50193) was used for the isolation of CYP81D8, CYP81D11 and the two Arabidopsis reductases ATR1 and ATR2. All steps were carried out under sterile conditions by preparing media and handling plant material in the laminar flow cabinet.

Arabidopsis was grown in half MS (0.215% Murashige and Skoog Basal Salt mixture, Sigma-Aldrich) liquid culture containing sucrose (0.68%, Fisher Scientific), adjusted to pH 5.7 with KOH (Fisher Scientific) and if required 60 µM TNT. To solidify the medium, 0.8% (w/v) agar (Formedium) was added.

Seeds were sterilised in a fume cupboard as follows: Seeds were transferred to 1.5 ml micro tubes (Sarstedt) which were placed with open lids into a plastic box. The lid of the plastic box was closed immediately after the addition of 3 ml concentrated hydrochloric acid to 100 ml Bleach haychlor (Scientific Laboratories Supplies) in a glass beaker. After 3 h the lid of the plastic box was opened, the micro tubes were closed and then placed into the sterile flow hood with opened lids for 10 min to allow evaporation of remaining hydrogen chloride. Seeds were then transferred to half MS agar plates and imbibed at 4 °C for at least three nights.

Eight one-day-old seedlings were transferred from agar plates into 100 ml sterile glass flasks containing 10 ml half MS. Seeds were grown for a further 13 days under light condition of 80 µmol·m⁻²·s⁻¹, 16 h photoperiod at 25 °C and 130 rpm.

2.5 Plasmid DNA preparation

For a plasmid preparation, 5 ml cultures of *E. coli* were grown overnight at 37 °C, 200 rpm, in LB containing the appropriate antibiotics. The cultures were harvested by centrifugation at 4000 rpm for 10 min (Jouan Model CR 312 Centrifuge, Swinging Bucket Rotor, SelectScience). The plasmids were purified using the QIAprep Spin Miniprep kit (Qiagen) according to the manufacturer's instructions.

2.6 Purification of DNA fragments

The DNA fragments resulting from PCR amplification and restriction digest were purified using the Wizard SV Gel and PCR Clean-Up System (Promega), according to the manufacturer's protocol. Where required, DNA fragments were separated using agarose gel electrophoresis and excised from the gel before purification.

2.7 Detection of the mRNA transcript

2.7.1 RNA extraction from *Escherichia coli*

The RNA was extracted by using the RNeasy Mini Kit from Qiagen for RNA isolation following by a reverse transcription PCR reaction.

For the RNA isolation, *E. coli* Rosetta 2 (DE3) cells containing the plasmid with the gene of interest were grown in 100 ml M9 media (37 °C, 200 rpm) until the OD₆₀₀ reached 0.6-0.8 and then induced by adding 1 mM IPTG, 1 mM δ -aminolevulinic acid (ALA), 0.5 mM FeCl₃ (Fisons), 5 μ g/l riboflavin and incubated at 20 °C shaking (200 rpm) overnight.

The RNA was protected by using 2 ml RNAprotect Bacteria Reagent (Qiagen) to 1 ml culture, vortexed for 5 sec, incubated for 5 min at room temperature and centrifuged at 5000x g for 10 min (bench top microlitre centrifuge Sigma 1-15P). The supernatant was discarded and 200 μ l TE buffer (30 mM Tris-HCl, 1 mM EDTA, pH 8.0) containing 0.4 mg proteinase K and 4 mg lysozyme were added to the cell pellet, resuspended by pipetting and incubated for 10 min at room temperature (vortex at least every two min). Then, 700 μ l RTL buffer containing

β -mercaptoethanol (10 μ l β -mercaptoethanol/1 ml RTL) were added, vortexed, centrifuged for 5 min at full speed (bench top microlitre centrifuge Sigma 1-15P) and the supernatant transferred into a new tube. After adding 500 μ l 100% ethanol and mixing by inverting, the solution was transferred to a column, spun at 8000x g for 15 sec (bench top microlitre centrifuge Sigma 1-15P) and the flow-through discarded. The column was washed using 350 μ l RW1 buffer and spun 15 sec at 8000x g. DNA was removed by adding 70 μ l RDD buffer containing 10 μ l DNase stock (RNase free DNase Set, Qiagen) and incubated for 15 min at room temperature. The column was washed twice as described above with 350 μ l RW1 buffer followed by adding 500 μ l RW1 buffer to the column. The column was transferred to a 1.5 ml collection tube, 45 μ l RNase free water was added, spun 1 min at 8000x g and the RNA concentration measured with the Nanodrop ND-1000 spectrophotometer.

2.7.2 RNA extraction from plant tissue

Fourteen-day-old liquid culture grown Arabidopsis plants were harvested after six hours incubation with 60 μ M TNT (in 10 μ l DMSO). 10 μ l of DMSO alone were added to the cultures for negative control. Arabidopsis RNA was isolated by grinding eight whole plants in a pestle and mortar cooled in liquid nitrogen. The RNA was isolated using a plant RNeasy Mini Kit from Qiagen according to the manufacturer's instructions. An on-column, DNA digestion using RNAase-free DNAase (Qiagen) was included. The RNA content was quantified using a Nanodrop ND-1000 Spectrophotometer.

Ten μ g RNA were added to a total of 24 μ l RNase free water. 1 μ l of oligo dT primer (Invitrogen) was added and the mixture was incubated in the thermocycler for 2 min at 95 $^{\circ}$ C and then chilled on ice. Then the following substances were added: 8 μ l 5 x 1st strand buffer (Invitrogen), 2 μ l 2.5 mM dNTPs (Bioline), 2 μ l 0.1M DTT (Invitrogen), 1 μ l RNAsin (RNase inhibitor), 2 μ l Superscript II (Invitrogen). The total volume was brought to 40 μ l using RNase free water. The mixture was incubated at 42 $^{\circ}$ C for 2 h. Samples were frozen at -80 $^{\circ}$ C.

2.7.3 Reverse transcription from plant mRNA to cDNA

To 10 µg plant mRNA was added 1 µl oligo dT primer (0.5 µg/µl, Invitrogen) and RNase free water to a final volume of 25 µl, incubated at 95 °C for 2 min and then chilled on ice. After adding 8 µl 5x 1st strand buffer (Invitrogen), 125 µM dNTPs (Invitrogen), 5 µM DTT (Invitrogen), 40 U RNAsin ribonuclease inhibitor (Promega), 400 U Superscript II (Invitrogen), the total volume was brought to 40 µl using RNase free water and the solution was incubated at 42 °C for 2 h. Samples were frozen at -80 °C until use for PCR.

2.8 Traditional cloning method

2.8.1 Designing primers for truncated P450 and reductase genes

Plant P450s and P450 reductases are membrane associated through an N-terminal hydrophobic membrane anchor of around 25 to 70 amino acids. The association to the membrane is causing mainly the insolubility of these proteins. The catalytic centre is situated in the cytoplasm and a removal of the N-terminus potentially increasing the solubility will not reduce the enzyme activity.^{330,333,346}

To design forward primers, the amino acid sequence was analysed with TMHMM (<http://www.cbs.dtu.dk/services/TMHMM/>) and SignalP3.0 software (<http://www.cbs.dtu.dk/services/SignalP/>). The TMHMM program predicts membrane regions and SignalP 3.0 can identify the location of a signal peptide and cleavage sites.

2.8.2 Polymerase chain reaction (PCR)

Primers were designed using primer3 software (<http://frodo.wi.mit.edu>) and synthesised by Sigma-Aldrich.

PCRs for amplifying the genes of interest were performed using the Phusion DNA Polymerase (Finnzymes), which is a highly accurate proof reading polymerase in a Peltier Thermal Cycler PTC-200. PCR amplifications were performed in volumes ranging from 25 µl to 50 µl using 5x buffer HF. Primers were employed at an ultimate concentration of 400 nM, dNTPs (Invitrogen) at a final concentration of 200 µM each and template DNA at 200 ng.

The programme used was, if not otherwise indicated, 5 min at 98 °C for denaturation, 30 cycles of 10 sec denaturing at 98 °C, 30 sec annealing at 60-65 °C, 1.00-1.20 min extension at 72 °C and 10 min at 72 °C. PCR products were stored at -20 °C and a part of each PCR product was visualised on agarose gels. By appearance of unspecific PCR products, 400 mM NDSB 201 (3-(1-Pyridinio)-1-propanesulfonate) was added to improve the specificity of the PCR reaction.

The Taq polymerase (New England Biolabs) was used for colony PCR after a transformation reactions to identify the presence of the gene. Therefore, 2 µl cell template from a single colony (preparation according to Chapter 2.8.5, page 64) were mixed with 2.5 µl 10x Thermo pol buffer, 200 µM dNTP mix (Invitrogen), 44 mM DMSO, 400 nM primer (forward and reverse) in a total volume of 25 µl. The PCR used a 5 min denaturation at 94 °C, followed by 35 cycles of 94 °C denaturation for 15 sec, 55 °C annealing for 30 s and 72 °C extension for 1.00-1.20 min and a final extension step of 72 °C for 10 min.

2.8.3 Preparation of PCR products for cloning

Immediately after purifying the PCR product (see Chapter 2.6, page 60), A-tail overhangs were added to create blunt-ended PCR products. 3 µl cleaned PCR product (negative control with water) was added to 0.5 µl 10 x thermo pol buffer, 0.2 mM dATPs, 0.25 U Taq-polymerase and water to a final volume of 5 µl. After incubation at 72 °C for 10 min, 1 µl TOPO vector and 1 µl salt solution (both from TOPO TA Cloning Kit from Invitrogen) was added and the whole mix placed at room temperature for 30 min.

2.8.4 Transformation of plasmid DNA into chemically competent

***Escherichia coli* cells**

An aliquot 50 µl of frozen competent *E. coli* DH5α was defrosted on ice for 10-15 min and then 2 µl of plasmid DNA was added, mixed by stirring with pipette and left on ice for 5 min. *E. coli* cells were then heat-shocked, in a water bath at 42 °C for 40 sec and again chilled on ice. After 5 min, 200 µl SOC-medium was added and the freshly transformed cells were allowed to recover at 37 °C under shaking. After 1 h, aliquots were spread onto LB agar plates, containing antibiotics if necessary and grown at 37 °C overnight. For TOPO blue / white

screening cells were spread onto plates containing 64 µg/ml 5-Bromo-4-chloro-3-indolyl-β-D-galactopyranoside (X-gal).

2.8.5 Screening transformants for recombinant genes by PCR

Single colonies were picked with a pipette tip and resuspended in 20 µl sterile water. Bacteria cell walls were destroyed by incubation at 95 °C for 5 min and then cycled 5 times through 15 °C for 30 sec followed by 95 °C for 30 sec and then frozen at -80 °C for 10 min. 2 µl of this solution was used as template for the PCR reaction using Taq polymerase (Chapter 2.8.2, page 62).

2.8.6 Restriction endonuclease digest of DNA

Restriction enzymes were obtained from New England Biolabs and used with the buffer system supplied by the manufacturer. Digests were used to create diagnostic restriction maps for construct analysis or in preparation for subsequent cloning steps.

For restriction mapping 200 ng DNA was digested with 10-20 U of enzyme in a 10 µl reaction and if necessary 1 µg BSA was added. For preparation of DNA fragments 1-5 µg DNA was digested with 5-10 U of enzyme and 5 µg BSA. All reactions were incubated for 1.5 h at 37 °C. For restriction mapping, 5 µl of the reaction were analysed using agarose gel electrophoresis (0.8% agarose gel, see Chapter 2.11, page 72). For preparative digests, products of the reaction were purified, if necessary using gel purification (Chapter 2.6, page 60). When buffering systems for digests using multiple enzymes, which were not compatible, sequential digests with both enzymes on the same plasmid were conducted.

2.8.7 Dephosphorylation of DNA 5' end of the vector

The dephosphorylation of the DNA 5' ends was performed using 45 µl digested vector (cleaned from gel after digestion), 5 µl 10x arctic phosphatase buffer and 1 µl arctic phosphatase (5000 U/ml, New England Biolabs). The samples were incubated at 37 °C for 45 min and then the phosphatase was heat inactivated at 65 °C for 5 min before the solution was used for the ligation reaction (Chapter 2.8.8).

2.8.8 DNA ligation reaction

Ligation reactions were performed with dephosphorylated plasmid DNA (Chapter 2.8.7) and phosphorylated insert DNA. Ligation was performed on 100 ng of DNA, in 3:1, 1:1 or 1:3 ratios of vector to insert. Controls included phosphorylated and dephosphorylated vector only. Ligation reactions were performed using T4 DNA ligase (New England Biolabs). The reactions were buffered in 50 mM Tris-HCl, 10 mM MgCl₂, 1 mM ATP (Invitrogen), 10 mM dithiothreitol (DTT, Invitrogen), pH 7.5 at 25 °C and 400 U of ligase used in a total volume of 20 µl.

2.8.9 DNA sequencing and analysis

Sequencing reactions were performed by the Genomics Laboratory, Technology Facility, University of York (York, UK). A list of primers used for sequencing is shown in Table 2.3. PCR primer of the insert were used for the sequencing of the yeast shuttle vector pYeDP60. Sequence chromatograms were analysed using Applied Biosystems Sequence Scanner 1.0 and sequences were aligned using the BLAST packages available at the National Centre for Biotechnology information (www.ncbi.nlm.nih.gov/blast/).

Table 2.3: List of primers used for sequencing

name	sequence (5'-->3')
M13 forward	GTAAAACGACGGCCAGTG
M13 reverse	GGAAACAGCTATGACCATG
T7	TTATACGACTCACTATAGGG
T7term	TATGCTAGTTATTGCTCAGCGGT
ATR2seq R	CATAACGTGCTTTTGCCTCTTCACCCA
RhF rev	TGCCGCCGGCGACGAACACGTAGTGCTC

2.9 Ligation independent cloning method

The Ligation Independent Cloning (LIC) enables a rapid high-throughput cloning without any ligation steps due to the complementary long overhangs on insert and vector (Figure 2.4).³⁴⁵

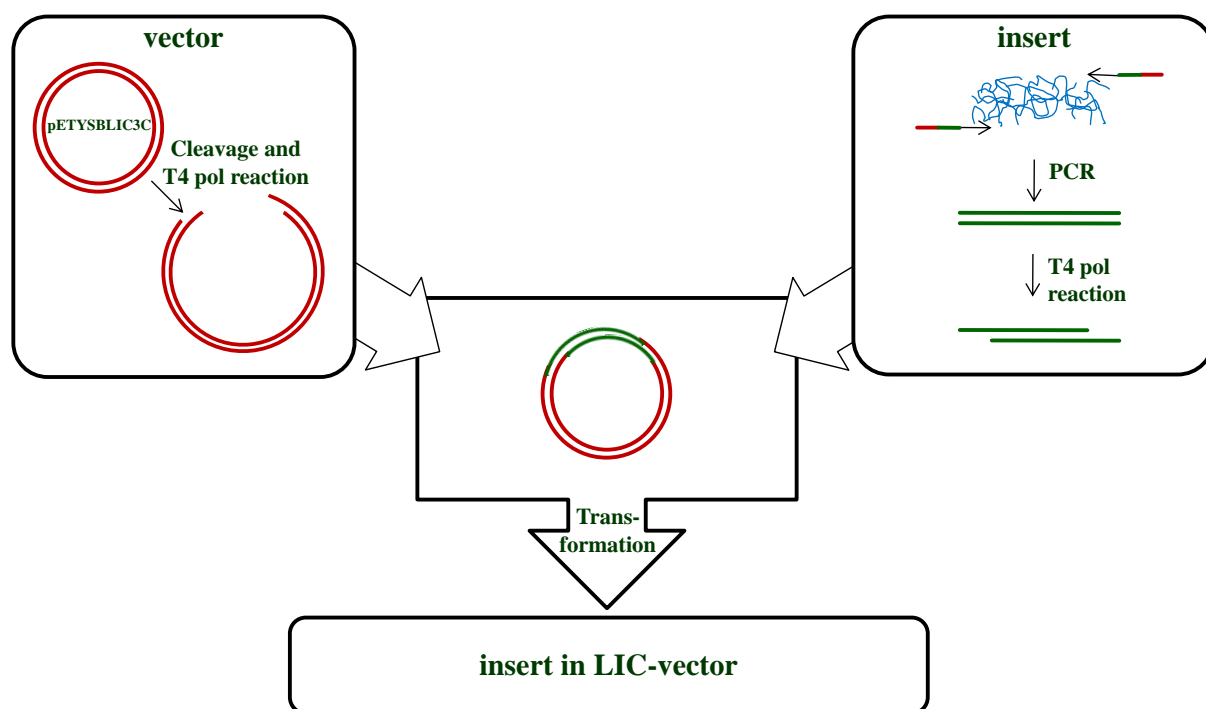


Figure 2.4: Schematic procedure for ligation independent cloning

Therefore, the LIC-vector, based on pETYSBLIC3C vector³⁴⁵ containing six cleavable N-terminal histidines, was digested using *BseR1*. Briefly, 100 ng LIC-vector, 10 μ l NEB4 buffer, 20 U *BseR1* and water to a final volume of 100 μ l were incubated for 1 h 50 min, then separated on a 0.6% agarose gel and purified (Chapter 2.6, page 60). The insert was amplified by PCR using Phusion polymerase (Chapter 2.8.2, page 62) and primers designed using HiTel software (TF Protein Production Laboratory, University of York, <http://bioltfws1.york.ac.uk/cgi-bin/primers.cgi?>). The purified insert and vector were treated with T4 polymerase (LIC qualified, Novagen-Merck) and the complementary bases A and T (Table 2.4) to create the long sticky ends (Figure 2.5). The reaction was performed at 22 $^{\circ}$ C for 30 min and stopped with further incubation of 75 $^{\circ}$ C for 20 min.

kanamycin after confirmation of the presence of the insert by PCR and incubated overnight at 37 °C and 200 rpm. M9 minimal medium was used to grow bacteria cells expressing P450s and fusion enzymes and LB medium for ATR1tr or ATR2tr. The main culture was inoculated with the preculture at an OD₆₀₀ of 0.1 and incubated shaking at 37 °C until an OD₆₀₀= 0.6-0.8. Protein expression was then induced by adding 1 mM IPTG. Additionally, 5 µg/l riboflavin was added for reductases as precursor of FMN and FAD and 0.5 mM FeCl₃ (Fisons), 1 mM ALA (δ-aminolevulinic acid, a heme ring precursor) for P450 expression. The proteins were expressed shaking (200 rpm) at 15 °C or 20 °C overnight.

2.10.2 Solubilisation buffers

To increase the solubility of the truncated Arabidopsis reductases, different solubilisation buffers were tested following the protocol from Lindwall *et al.* 2000³⁴⁷.

The ATR1tr was transformed into *E. coli* Rosetta 2 (DE3) and expressed in LB medium under the conditions described in Chapter 2.8.4.

Cells were harvested and resuspended in 35 ml 10 mM Tris, pH 8.5 containing 100 mM NaCl and 1 mM EDTA and then divided in 30 1 ml aliquots. Cells were spun (2300x g, 1 min), the supernatant discarded and the cell pellets resuspended in 1 ml of the different solubilisation buffers listed in Table 2.5. Buffer 0 was the buffer used for the batch purification of the Arabidopsis reductases in Chapter 2.10.4, which resulted in precipitated protein after purification.

Table 2.5: List of solubilisations buffer adapted from Lindwall *et al.* 2000³⁴⁷

buffer	Reagents to solubilise overexpressed protein
buffer 0	HIS-binding buffer: 50 mM sodium phosphate pH 8.0, 300 mM NaCl
buffer 1	100 mM Tris, 10 % glycerol, pH 7.6
buffer 2	100 mM Tris, 50 mM LiCl, pH 7.6
buffer 3	100 mM HEPES, 50 mM (NH ₄) ₂ SO ₄ , 10 % glycerol, pH 7.0
buffer 4	100 mM HEPES, 100 mM KCl, pH 7.0
buffer 5	100 mM Tris, 50 mM NaCl, 10 % isopropanol, pH 8.2
buffer 6	100 mM K ₂ HPO ₄ /KH ₂ PO ₄ , 50 mM (NH ₄) ₂ SO ₄ , 1% Triton X-100, pH 6.0
buffer 7	100 mM triethanolamine, 100 mM KCl, 10 mM DTT, pH 8.5
buffer 8	100 mM Tris, 100 mM sodium glutamate, 10 mM DTT, pH 8.2
buffer 9	250 mM K ₂ HPO ₄ /KH ₂ PO ₄ , 0.1 % CHAPS, pH 6.0
buffer 10	100 mM triethanolamine, 50 mM LiCl, 5 mM EDTA, pH 8.5
buffer 11	100 mM sodium acetate, 100 mM glutamine, 10 mM DTT, pH 5.5
buffer 12	100 mM sodium acetate, 100 mM KCl, 0.1% <i>n</i> -octyl-β-D-glucoside, pH 5.5
buffer 13	100 mM HEPES, 1 M MgSO ₄ , pH 7.0
buffer 14	100 mM HEPES, 50 mM LiCl, 0.1% CHAPS, pH 7.0
buffer 15	100 mM K ₂ HPO ₄ /KH ₂ PO ₄ , 2.5 mM ZnCl ₂ , pH 4.3
buffer 16	100 mM Tris, 50 mM NaCl, 5 mM calcium acetate, pH 7.6
buffer 17	100 mM triethanolamine, 50 mM (NH ₄) ₂ SO ₄ , 10 mM MgSO ₄ , pH 8.5
buffer 18	100 mM Tris, 100 mM KCl, 2 mM EDTA, 1% Triton X-100, pH 8.2
buffer 19	100 mM sodium acetate, 1 M MgSO ₄ , pH 5.5
buffer 20	100 mM Tris, 2 M NaCl, 0.1% <i>n</i> -octyl-β-D-glucoside, pH 7.6
buffer 21	100 mM Tris, 1 M (NH ₄) ₂ SO ₄ , 10 mM DTT, pH 8.2
buffer 22	100 mM sodium acetate, 50 mM LiCl, 5 mM calcium acetate, pH 5.5
buffer 23	100 mM HEPES, 100 mM sodium glutamate, 5 mM DTT, pH 7.0
buffer 24	100 mM triethanolamine, 100 mM sodium glutamate, 0.02% <i>n</i> -octyl-β-D-glucoside, 10% glycerol, pH 8.5
buffer 25	100 mM Tris, 50 mM NaCl, 100 mM urea, pH 8.2
buffer 26	100 mM triethanolamine, 100 mM KCl, 0.05% dextran sulfate, pH 8.5
buffer 27	100 mM K ₂ HPO ₄ /KH ₂ PO ₄ , 50 mM (NH ₄) ₂ SO ₄ , 0.05% dextran sulfate, pH 6.0
buffer 28	100 mM HEPES, 50 mM LiCl, 0.1% deoxycholate, pH 7.0
buffer 29	100 mM Tris, 100 mM KCl, 0.1% deoxycholate, 25% glycerol, pH 7.6
buffer 30	100 mM potassium acetate, 50 mM NaCl, 0.05% dextran sulfate, 0.1% CHAPS, pH 5.5

Lysozyme (from chicken egg white, Sigma) was added and the suspension incubated for 5 min on ice. Cells of each aliquot were lysed (Misonix S-4000 sonicator at 70% maximum amplitude, 1 sec sonication bursts, 4 sec cooling intervals at 0 °C for a total processing time of 1 min) and then incubated gently shaking for 10 min at 4 °C. After centrifugation at 16000x g for 10 min, the soluble proteins in the supernatant were analysed by Bradford assay (Chapter 2.12), SDS PAGE (Chapter 2.13) and western blot (Chapter 2.14).

2.10.3 Cell lysis by sonication

1 l cell culture was harvest by centrifugation (7 min at 2500 xg, High Speed Sorvall RC5B+rotor, SLC-1500) after 20 h of expression and resuspended in 30 ml HIS-binding buffer (HIS-Binding buffer: 50 mM sodium phosphate pH 8, 300 mM NaCl) or buffer 18A (100 mM Tris, 100 mM KCl and 1% Triton X-100, pH 8.2) containing 37.5 µl 0.1 M PMSF (protease inhibitor solved in isopropanol). Lysozyme (from chicken egg white, Sigma) was added to a final concentration of 2 µg/ml to the cells and incubated on ice for 5 min. Cells were lysed usually in 35 ml batches with a Misonix S-4000 sonicator at 70% maximum amplitude alternating 3 sec sonication bursts with 7 sec cooling intervals at 0 °C for a total processing time of 4 min. The effect of the sonication was visualised by light microscopy (Carl Zeiss, Axiovert 200, AxioCam HRm) (Figure 2.6).

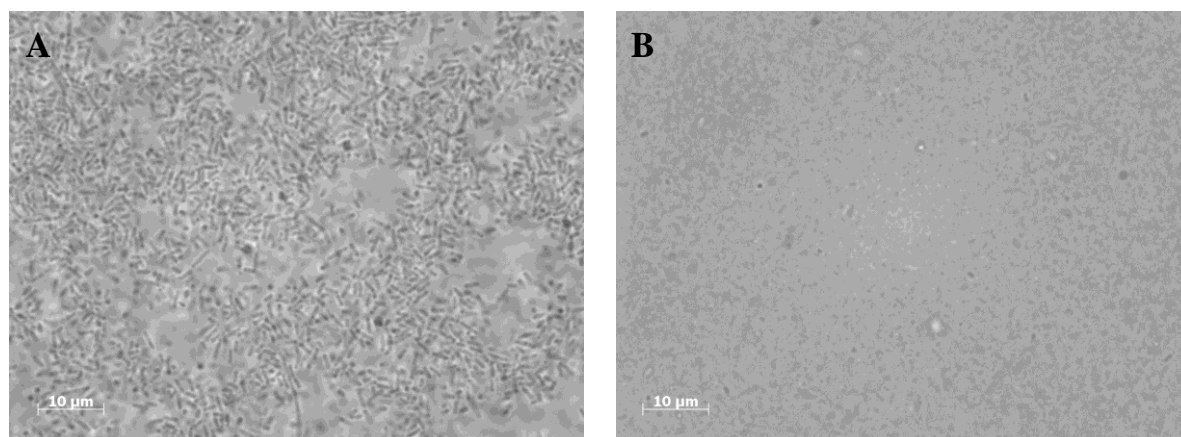


Figure 2.6: *E. coli* Rosetta 2 (DE3) cells A before and B after sonication

The soluble protein, present in the supernatant after centrifugation (15 min at 15000 rpm, High Speed Sorvall RC5B+rotor, SS-34) was used for protein purification (Chapter 2.10.4 and 2.10.5).

2.10.4 Protein purification in a batch process

All steps to purify the His-tagged protein were performed at room temperature and individual samples were taken for analysis by SDS PAGE (Chapter 2.13) and western blot analysis (Chapter 2.14). Protein purification was performed in a batch process by using His-Select Nickel Affinity Gel (Sigma) in a 50 ml falcon tube (500 μ l slurry per 10 ml supernatant containing the protein). The resin was equilibrated with 10 resin volumes of buffer, mixed by inverting, spun at 1200 xg for 1 min (Jouan Model CR 312 Centrifuge, Swinging Bucket Rotor) and the supernatant was discarded. This step was repeated twice. The soluble protein fraction after sonication (Chapter 2.10.3, page 70) containing the protein of interest was applied to the resin material and gently shaken at room temperature for 1 h up to 4 h. After centrifugation at 1200 xg (Jouan Model CR 312 Centrifuge, Swinging Bucket Rotor), the supernatant was removed and the resin washed three times with fifteen resin volumes of buffer. To remove non specific bound protein, the resin was washed with one resin volume of buffer containing 5 mM imidazole (Fisher Scientific) shaking for 5 min. After centrifugation (1200 xg, 5 min, Jouan Model CR 312 Centrifuge), the supernatant was discarded and the His-tagged protein eluted by incubation of one resin volume of buffer containing 500 mM imidazole (Fisher Scientific) for 10 min to 1 h by gently shaking. After centrifugation (2400 xg, 5 min, Jouan Model CR 312 Centrifuge, Swinging Bucket Rotor), the supernatant was transferred to a spin column (Agilent Technologies, 0.22 μ m cellulose acetate) to remove all resin traces by spinning 2 min at 13000 rpm (table centrifuge). The protein solution was dialysed twice against 5 l potassium phosphate (50 mM, pH 7.0) at 4 °C, if not otherwise specified.

2.10.5 Protein purification in a continuous process

A column (Chromatography column from Novagen) containing 1.5 ml His-Select Nickel Affinity Gel (Sigma) was equilibrated with 10 ml buffer.

The soluble supernatant containing the protein of interest was applied to the resin material and then washed twice with 10 ml buffer. Unspecific bound protein was eluted with 5 ml of 5 mM imidazole (Fisher Scientific) in buffer and the His-tagged protein with 500 mM imidazole in buffer. The eluted protein was dialysed

against two batches 5 l potassium phosphate (50 mM, pH 7.0) at 4 °C, if not otherwise specified.

2.11 Agarose gel electrophoresis

Agarose gel electrophoresis was used to visualise and to separate digestion and PCR products. The concentration of agarose (Melford) was varied between 0.8-1.0% (w/v), according to the size of the fragments to be separated. Agarose was dissolved in 1x Tris-acetate-EDTA (TAE) buffer, made from a 50x TAE stock, which contained: 242 g/l Tris (Invitrogen), 57.1 ml/l glacial acetic acid (Fisher Scientific) and 100 ml/l 500 mM EDTA (Sigma-Aldrich), pH 7.0. To visualise DNA under UV light (UVItec system and the software UVIpro) ethidium bromide (Fluka, Sigma-Aldrich) was added to a final concentration of 0.2 µg/ml. DNA was diluted in 6x loading dye comprising 0.25% w/v bromophenol blue and 30% glycerol. To determine the product size 1 kb DNA ladder or 2-Log DNA Ladder (both from New England Biolabs) were used according to the manufacturer's instruction. The DNA was typically separated using a voltage of 90-130 V.

2.12 Protein detection

Protein concentrations were determined using the Coomassie (Bradford) Protein Assay Kit (Thermo Fisher Scientific). For quantification a standard curve was prepared using bovine serum albumin (BSA) solutions of known concentrations between 0-2 mg/ml measured at 595 nm in the spectrophotometer Varian Cary 50 Bio UV/Vis Spectrophotometer (Agilent Technologies). Measurements were taken in triplicates.

2.13 Sodium dodecyl sulphate-polyacrylamide gel electrophoresis (SDS-PAGE)

2.13.1 SDS PAGE with the Bio-Rad system

Standard procedures were followed according to Laemmli.³⁴⁸ Gels were poured and run with the Mini-Protean 3 system (Bio-Rad). Gels were polymerised with

12% w/v acrylamide (Fisher Scientific) in the resolving gel and 4% w/v acrylamide in the stacking gel. Four times SDS loading buffer contained 2 ml of 625 mM Tris (Invitrogen), pH 6.8, 4 ml of 10% (w/v) SDS (Melford), 2 ml of glycerol (Fisher Scientific), 1 ml of β -mercaptoethanol (Sigma-Aldrich), 30 mg of bromphenol blue (Sigma-Aldrich), 1 ml of H₂O. Two times loading buffer was added in equivalent volumes to the samples, denatured for 5 min at 100 °C, cooled to room temperature, centrifuged to bring down the condensation and pellet any insoluble substances and 15 to 20 μ l loaded on the gel. Running buffer contained 25 mM Tris, 180 mM glycine (Fisher Scientific), 0.1% (w/v) SDS (pH 8.3). Electrophoresis was performed for approximately 45 min at 200 V. Prestained protein marker was purchased from New England Biolabs or Fermentas and gels were stained with Instant Blue (Expedeon). An UVItect system and the software UVIpro was used for the documentation.

2.13.2 SDS PAGE with the RunBlue system from Expedeon

SDS gradient gels (4 to 20% (w/v) acrylamide) were purchased from Expedeon. As running buffer was used 1x RunBlue RAPID. Twenty times of RunBlue RAPID was made of 0.6 M MOPS (Sigma), 1.2 M Tris (Invitrogen), 2% (w/v) SDS (Melford) and 130 mM sodium bisulphate (Expedeon). The sample preparation was done following the manufacturer's instructions. The gels were run at 90 mA and then stained with Instant Blue (Expedeon) and documented using an UVItect system and the software UVIpro.

2.14 Western blot analysis

For the western blot transfer a Trans-Blot SD Semi-Dry Transfer Cell (Bio-Rad) and a Model 200/2.0 power supply (Bio-Rad) were used. All western Blot analysis steps were performed at room temperature under gently shaking on a gel rocker (Stuart, Bibby Scientific Limited). An UVItect system and the software UVIpro was used for the documentation of the western Blot results.

2.14.1 Protein detection with anti-poly Histidine peroxidase conjugate

Protein SDS gels and nitrocellulose membrane (0.45 μ M, BioRad) were incubated in pre-chilled Towbin transfer buffer (25 mM Tris, 192 mM Glycine, 0.1% (w/v)

SDS, 20% (v/v) methanol, pH 8.3) for 15 min, prior assembling the gel/membrane sandwich complex. The blotting paper (extra thick, BioRad) briefly soaked in Tobwin transfer buffer was placed on to the anode of the transfer unit, followed by the membrane, the gel and again by a pre-soaked blot paper avoiding air bubbles. For the transfer, the cathode was placed onto the complex and the transfer was done with a voltage of 10 V for 1 h. After protein transfer to the membrane, the membrane was briefly rinsed in PBS buffer (137 mM NaCl, 2.5 mM KCl, 10 mM Na₂HPO₄, 1.5 mM KH₂PO₄, pH 7.4) and then blocked with 1x PBS containing 3% (w/v) non-fat milk powder (Fluka, Sigma-Aldrich) for 1 h at room temperature. After washing the membrane three times with PBS containing 0.05% Tween 20 (Sigma-Aldrich), the membrane was incubated with PBS, 3% BSA (Fisher Scientific) and the Monoclonal Anti-polyHistidine Peroxidase Conjugate (Sigma), followed by three washes for 5 min with PBS containing 0.05% Tween 20. The membrane was developed in a solution of 2 ml of 4-Chloro-1-naphtol (Sigma-Aldrich, one tablet dissolved in 10 ml methanol), 10 ml triethanolamine buffer saline (137 mM NaCl, 27 mM KCl, 12 mM triethanolamine, pH 7.5) and 5 µl H₂O₂. The reaction was stopped by washing the membrane in water.

2.14.2 Protein detection with alkaline phosphatase conjugate

The SDS gel and the nitrocellulose membrane were prepared under the same conditions as described in Chapter 2.14.1. After the protein transfer onto the membrane, the membrane was washed in PBS buffer (137 mM NaCl, 2.5 mM KCl, 10 mM Na₂HPO₄, 1.5 mM KH₂PO₄, pH 7.4) and then incubated in PBS containing 3% BSA (Fisher Scientific) and 2% milk powder (Fluka, Sigma-Aldrich) for 60 min to block the membrane. The membrane was incubated with the primary antibody, specific for the target protein (ATR2tr and RhF reductases produced in rabbit, Covalab, 1:10000 dilution) in PBS containing 3% BSA for 60 min. The membrane was then washed twice in PBS with 0.1% Tween 20 (Sigma-Aldrich) for 5 min, followed by washes in PBS, 0.5% Tween 20 and 1 M NaCl for 5 min, rinsed briefly in PBS and again in PBS containing 3% BSA before incubating the membrane with the secondary antibody (goat Anti-rabbit IgG conjugated to alkaline phosphatase, Sigma, 1:20000 dilution) for 60 min. The membrane was then washed twice in PBS containing 0.1% Tween 20 for 5 min,

twice in PBS containing 0.5% Tween 20 and 1 M NaCl for 5 min, briefly rinsed in PBS and then incubated in 10 mM Tris pH 9.6 for 5 min. The membrane was developed with nitroblue tetrazolium and 5-bromo-4-chloro-3-indolyl phosphate dipotassium (from Sigma as a tablet containing both ingredients, dissolved in 10 ml water) and the reaction was stopped by washing the membrane several times in water.

2.15 Protein characterisation

2.15.1 Characterisation of the P450 reductases

The characterisation of ATR1tr and ATR2tr was done, if not otherwise specified, with purified enzyme dialysed in buffer B: 30 mM potassium phosphate buffer (pH 7.8), 20% glycerol (Fisher Scientific), 0.1 mM EDTA (Fisher Scientific) and 20 μ M FMN (Sigma-Aldrich).

2.15.1.1 Spectrophotometric characterisation

Spectrophotometric work was performed at 30 °C using a Varian Cary 50 Bio UV/Vis Spectrophotometer (Agilent Technologies). High Quality Polystyrene Disposable Cells, Semi Micro, (1.5 ml, Kartell) were used for Bradford protein quantification and UV-transparent disposable cuvette (ultra-micro, 15 mm window height, BrandTech Scientific) for activity assays and wavescan measurements.

The absorption of ATR2tr (5.1 mg/ml, dialysed in 50 mM potassium phosphate buffer pH 7.5) was measured between the wavelength 300 and 600 nm with one point for each nanometre. Expressed and purified empty LIC-vector (without dialysis, protein concentration of 0.4 mg/ml) was used for negative control.

FMN and FAD were dissolved in 50 mM potassium phosphate buffer pH 7.5 to a final concentration of 100 μ M. The spectra of 10 μ M of both substances were recorded between 300 and 600 nm.

2.15.1.2 Activity assay with cytochrome c

Activity of ATR2tr to transfer single electrons from the cofactor (NADH or NADPH) was detected by using cytochrome c as the electron donor. The protocol adapted from Guengerich *et al.* 2009³⁴⁹ was modified to a 500 μ l volume and the

reaction measured spectrophotometrically by following the increase in absorbance at 550 nm. Each reaction contained 50 μ M horse heart cytochrome c (Sigma-Aldrich) with a certain amount of sample to a final volume of 495 μ l with 300 mM potassium phosphate buffer, pH 7.7. A baseline was recorded at 550 nm for 1 min and the reaction started by adding 5 μ l 10 mg/ml NAD(P)H (Melford). NADH and NADPH were tested as cofactor and ferredoxin reductase (from spinach, Sigma-Aldrich) as well as cytochrome c reductase (from porcine heart, Sigma-Aldrich) as positive control. Expressed and purified empty LIC-vector sample was used for negative control.

2.15.1.3 Temperature and pH optima of ATR1tr and ATR2tr

The temperature optimum for the two *Arabidopsis* reductases was determined using the activity assay with cytochrome c (Chapter 2.15.1.2) between 10 °C to 70 °C. The buffer was preheated in a water bath (Grant JB1, Scientific Laboratory Supplies) and the cuvette holder tempered.

For elucidation of the pH optimum of ATR1tr and ATR2tr, the activity for cytochrome c reduction was tested in three different buffers (Table 2.6) covering the pH range from pH 2.0-11.0. The pH optimum for both reductases was also determined in Britton Robinson buffer, which covered a pH range between pH 3.4 to 11.0.

Table 2.6: Buffers used for analyzing the pH optima of ATR1tr and ATR2tr

buffer	pH region	content	concentration
potassium phosphate	4.0 - 10.0	H ₂ KPO ₄ [*] and HK ₂ PO ₄ [*]	300 mM
citrate	2.0 - 7.6	citric acid [*] and tri sodium citrate [*]	300 mM
Britton Robinson	3.4 - 11.0	1:1:1 mixture of boric acid [*] , phosphoric acid [#] and acetic acid [*] , pH regulated with NaOH [*]	300 mM

^{*} chemical from Fisher Scientific, [#] from Sigma-Aldrich

For the reaction, 40 μ l of a 0.5 mM solution of the cytochrome c (horse heart, Sigma, dissolved in water), 1 μ g/ml ATR2tr (or 100 μ g/ml ATR1tr), 5 μ l 10 mM NADPH (Melford) and buffer were mixed to a final volume of 500 μ l (Table 4.2). The absorbance was observed at 550 nm at 30 °C. The activity (mM/min) was

calculated by using the average of three measurements divided by the extinction coefficient of cytochrome c at 550 nm ($\epsilon = 19.6 \text{ mM}^{-1}\text{cm}^{-1}$). Each point was measured as triplicates to get a standard deviation.

2.15.1.4 Stability test of ATR2tr in different buffers

The purified ATR2tr in 500 mM imidazole was divided in two batches and one was dialysed against two 5 l volumes of buffer A (50 mM potassium phosphate buffer pH 7.5) and the other against buffer B (30 mM potassium phosphate pH 7.8, 20% glycerol, 0.1 mM EDTA, 2.0 μM FMN) at 4 °C. Buffer B containing FMN should stabilise the activity of ATR2tr due to the low affinity of ATR2 to FMN.³⁵⁰ Glycerol can stabilise enzymes and protect hydrophobic sites of proteins.

The ATR2tr samples in buffer A or B were aliquoted and stored at -80 °C, -20 °C, 4 °C and 21 °C. The samples were assayed for activity with cytochrome c (see Chapter 2.15.1.2) after 2, 6, 16 and 41 days.

A Michaelis-Menten-diagram was generated with samples of purified ATR2tr before dialysis (containing 500 mM imidazole) and after dialysis in the two different buffers A and B using the same substrate concentrations published by Hull and Celenza 2000.³⁵¹ Error bars were calculated using the standard derivation of three replicas.

2.15.1.5 Kinetic studies of the reductases

The reaction was performed at 25 °C and the absorbance change of cytochrome c was monitored at 550 nm.

The reductases ATR1tr and ATR2tr (dialysed in buffer B) were used in a final concentration of 1 mg/ml and 0.01 mg/ml, respectively. The protein solution was mixed with different cytochrome c substrate concentrations (5, 6, 10, 20, 50, 100 and 150 μM , from horse heart, Sigma) in a total volume of 495 μl 300 mM potassium phosphate buffer (pH 7.7) and the reaction was started by adding 5 μl NADPH (10 mg/ml, Melford). Measurements were taken in triplicates.

Kinetic data (K_M and V_{max}) were calculated using Michaelis Menten kinetics (Software: GraFit) for the substrate concentration of 6 μM up to 100 μM .

The specific activity is defined by the activity of enzyme per milligram of total protein (in $\mu\text{mol min}^{-1}\text{mg}^{-1}$) and was calculated using following formula:

$$\text{specific activity} = V_{\text{max}} \cdot [\text{E}] \quad [\text{E}] = \text{enzyme concentration}$$

The protein concentration of 0.01 mg and 1 mg/ml reaction for ATR1tr and ATR2tr, respectively was used for kinetic activity assays. The turnover number k_{cat} is the number of moles of substrate, which are converted into product per mol of enzyme (per active site) under saturated conditions.

$$k_{cat} = V_{max}/[E]$$

2.15.2 Protein identification by MALDI-MS analysis

Protein identification was performed by the Proteomics Laboratory, Technology Facility University of York using a Bruker autoflex III MALDI-TOF/TOF and data were analysed by Mascot (Matrix Science).

2.15.3 P450 enzyme activity assays

A Waters (Milford, USA) HPLC system consisting of a 510 pump, a Waters Alliance 2695 separations module and a Waters 2996 Photodiode Array was used, if not otherwise specified, to detect the chemical compounds used in the different assays. The substrates and products were identified by comparing the spectra generated from the Waters photodiode array detector with the retention times and spectra of commercial compounds. Data analysis was performed using Empower-Pro Analysis Software.

2.15.3.1 Activity assay for CYP71D15 with limonene

E. coli JM109 whole cells and the total protein fraction containing CYP71D15 PM2-2 were used for activity assay with the native substrate limonene. Resting cell assays were performed in a total volume of 1 ml containing 5 mM limonene, 0.5 mM NADPH, 20 µg/ml spinach ferredoxin and 10 U/ml spinach ferredoxin reductase (Sigma-Aldrich) and buffer (100 mM Tris-HCl (pH 7.4), 250 mM KCl, 50 mM MgCl₂). Samples were taken over a time course, cells spun down and then an equal volume of ethyl acetate added, vortexed, centrifuged and the organic layer analysed by GC-MS (7890A GC System, 5975C inert XL MSD with Triple-Axis Detector, 7693 autosampler, Supelco HP5 GC column, software: ChemStation) following the temperature program in Figure 2.7.

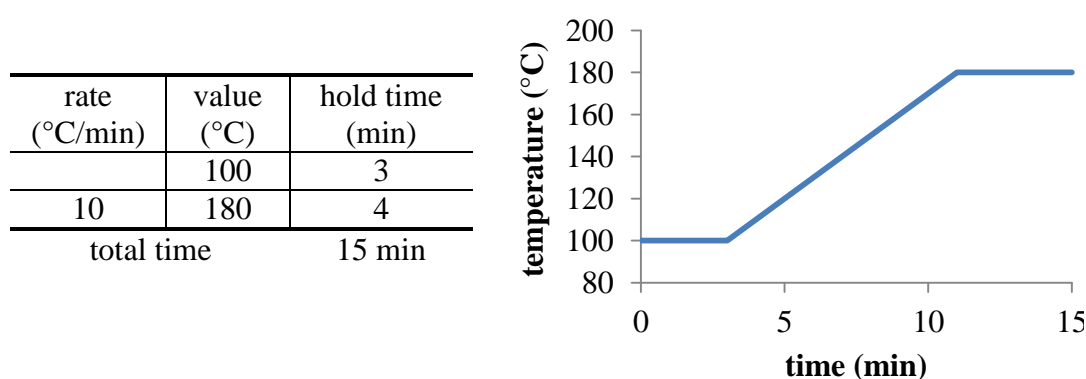


Figure 2.7: GC-MS program for analysing limonene and its hydroxylated products

2.15.3.2 Activity assay for CYP81D8 and CYP81D11 with methyl-tolyl-sulphide

The native substrate of Arabidopsis CYP81D8 and CYP81D11 are not known, however oxidising activity was tested towards the substrate methyl-tolyl-sulphide. The reaction contained 250 µg of protein (purified with Ni-chromatography), reductase (0.1 ng/ml spinach ferredoxin and 1 U/ml spinach ferredoxin reductase (Sigma-Aldrich) or Arabidopsis ATR1tr purified see Chapter 4), 100 mM sodium phosphate buffer pH 7.0, 1 mM methyl-tolyl-sulphide and was initiated by the addition of 300 µM NADPH. The reaction (100 µl) was stopped by adding acetonitrile (30 µl) at different time points and the products were analysed by HPLC. As a positive control the heme domain of XplA^{141,352} was used.

HPLC was performed with 50 µl sample injected to a Techsphere column (column temperature: 45 °C, sample temperature: 4 °C, water (Elga Labwater) and methanol (Fisher Scientific), flow: 1 ml/min) following the program in Table 2.7. The retention time of the substrate methyl-tolyl-sulphide was at 14 min and of methyl-tolyl-sulphoxide at 5 min.

Table 2.7: HPLC program for the separation of methyl-tolyl-sulphide and its oxidised derivatives

time (min)	water (%)	methanol (%)
0.00	50	50
5.00	50	50
10.00	40	60
10.01	5	95
15.00	5	95
15.01	50	50
25.00	50	50

2.15.3.3 Isoflavone synthase activity assay

For an *in vivo* assay in growing cell culture, the substrate naringenin (Sigma-Aldrich) was added to a final concentration of 50 μ M to the growing culture at the start of induction. Flavonoids are excreted by *E. coli* and can be analysed from the culture supernatant. Therefore, 5 ml samples were collected at different time points during the expression and analysed by HPLC after extraction.

For activity tests in resting cells, cultures were harvested and resuspended in potassium phosphate buffer (50 mM, pH 7.0) with 20 mg wet cells per 1 ml buffer. After adding the substrate naringenin (Sigma, final concentration: 100 μ M), the tubes were incubated at 28 °C and 160 rpm. Samples (2.5 ml) were collected at different time points for HPLC analysis after extraction.

Extraction method:

The samples were prepared according to the protocol of Leonard and Koffas³⁰⁶: To 5 ml sample the internal standard (5 μ l of 50 mM scopoletin) and 5 ml ethyl acetate for extraction was added. After mixing and centrifugation (Jouan Model CR 312 Centrifuge, Swinging Bucket Rotor, SelectScience), the organic phase was transferred into a glass vial for complete evaporation. To dissolve the flavonoids, 500 μ l methanol were added and the samples incubated at 60 °C for 15 min, followed by incubation at room temperature for 20 min. 50 μ l were injected to a TechSphere ODS 80A 5 μ column (250 x 4.6 mm, Fischer Thermo Scientific), with an isocratic flow of 1 ml/min of 50% (v/v) methanol containing 0.1% (v/v) acetic acid and 50% (v/v) water (column temperature: 25 °C, sample temperature: 21 °C). The standards of the substrate naringenin (Sigma-Aldrich) and the product genistein (Sigma-Aldrich) eluted at 17.5 min and 12 min,

respectively. The peak area was converted into concentration using a calibration with commercial available naringenin, genistein and scopoletin purchased from Sigma.

2.15.3.4 Cinnamate-4-hydroxylase (CYP73A5) activity assay

Cinnamate-4-hydroxylase activity was tested in resting cell assays. Therefore, the fusion proteins were expressed in LB and M9 medium following the protocol described in 2.10.1 (page 67) overnight at 15 °C and 200 rpm. The activity of the 73A5-fusions in the resting cell assays were optimised by variation of the expression temperature (15 °C and 20 °C) as well as the aeration (speed of 50 rpm and 200 rpm).

Cells were harvested by centrifugation (7 min at 4000 rpm, High Speed Sorvall RC5B+rotor, SLC-1500) and resuspended in 50 mM potassium phosphate buffer pH 7.0 to a final cell concentration of 100 mg/ml.

The resting cell assays were performed in glass vials in a total volume of 15 ml, the reaction started by adding the substrate cinnamic acid (Sigma-Aldrich) to a final concentration of 200 µM. Vials were shaken (300 rpm) at 28 °C. Samples (100 µl) were taken at different time point, and quenched with equal volume of methanol. After centrifugation (5 min at full speed, bench top microlitre centrifuge Sigma 1-15P), 20 µl of the supernatant were analysed by HPLC following a modified program (Table 2.8) according to Chen and Morgan³⁵³ using a Techsphere column (column temperature: 30 °C, sample temperature: 4 °C, buffer: water (Elga Labwater) and methanol (Fisher Scientific) containing 0.1% (v/v) acetic acid (Fisher Scientific) buffered to pH 7.25 with triethylamine (Sigma-Aldrich). Cinnamic acid (absorption maximum: 278 nm) eluted at 9.4 min and coumaric acid (absorption maximum: 310 nm) at 7.7 min under these conditions.

Table 2.8: HPLC program for the separation cinnamic acid and coumaric acid at 1 ml/min

time (min)	water (%)	methanol containing 0.1% acetic acid, pH 7.25 with triethylamine (%)
0.00	90	10
3.00	90	10
4.00	55	45
9.00	55	45
9.01	90	10
14.00	90	10

Ni-affinity chromatographic treated 73A5tr-ATR2tr (expressed in M9 at 15 °C and 200 rpm and purified in a continued process, see Chapter 2.10, page 67), protein bound to the resin material (0.5 ml resin material after two washing steps) as well as the insoluble protein (700 mg wet cells after sonication) were used for crude extract assays. The reactions were performed in glass vials in a total volume of 4 ml containing 4 U alcohol dehydrogenase (ADH, from *T. brockii*, Sigma-Aldrich), 2.5% (v/v) isopropanol (Fisher Scientific, substrate for ADH), 500 µM substrate cinnamic acid and 300 µM NADPH (Melford) shaking (300 rpm) at 30 °C. Samples were taken and prepared as described for the resting cell assay (see above).

A standard curve was measured for cinnamic acid and coumaric acid in the range of 10 µM to 500 µM with four replicas for each concentration.

2.15.3.5 Activity assay for CYP82E4

The *N*-demethylase (CYP82E4) from *Nicotiana tabacum* converts nicotine to nornicotine, both substances are possible to detect by HPLC analysis according to Saunders and Blume 1981.³⁵⁴ Samples (sample temperature: 4 °C) were separated on a SunFire C18 column (3.5 µm, 4.6 x 150 mm, Waters, column temperature: 20 °C), 1 ml/min flow of isocratic mobile phase of 70% water containing 0.2% phosphoric acid (pH 7.25 with triethylamine) and 30% methanol containing 0.2% phosphoric acid (pH 7.25 with triethylamine) with a run time of 28 min. The retention time of substrate (±) nicotine (Sigma) was at 18.9 min and of the product (±) nornicotine (Sigma) at 4.2 min (Figure 2.8). Both have an absorption maximum of 260 nm.

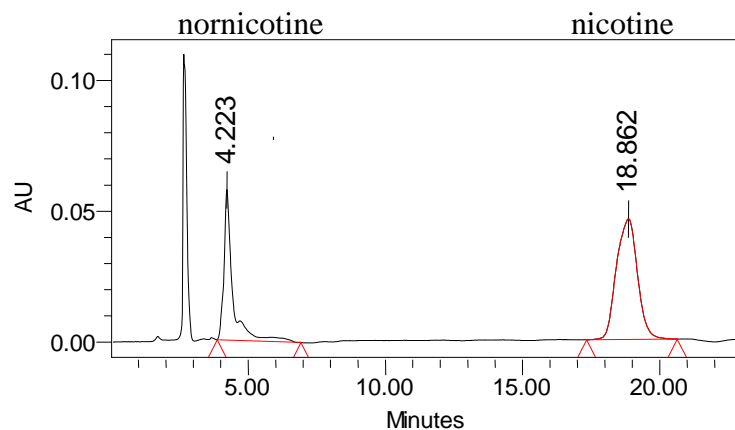


Figure 2.8: HPLC chromatogram for the separation of nicotine and nornicotine

HPLC-conditions: SunFire C18 column, 1 ml/min flow isocratic 70% water (0.2% phosphoric acid, pH 7.25 with triethylamine) and 30 % methanol (0.2% phosphoric acid pH 7.25 with triethylamine), column temperature: 20 °C, sample temperature: 4 °C

The activity for the fusions 82E4tr-lamATR2tr and 82E4tr-licATR2tr (sequences see appendix 2) was tested in a resting cell assay. The assay was performed in glass vials containing 25 mg cells per ml 50 mM potassium phosphate buffer (pH 7.0) and 100 μ M substrate nicotine in a final reaction volume of 20 ml, shaking at 28 °C and 300 rpm. Samples of 1.2 ml were taken at different time points, centrifuged (5 min at full speed, bench top microlitre centrifuge Sigma 1-15P) and 1 ml of the supernatant was evaporated completely (Savant SpeedVac DNA 110 Concentrator). The pellet was resuspended in 100 μ l water : methanol (70% : 30%) and 50 μ l were analysed by HPLC.

Additionally, HPLC separation of 1 mM nicotine and 1 mM nornicotine was tested with a ChiralPak IA column (Daicel Chemical Industries). Compounds were separated in a mobile phase of 35% (v/v) ethanol and 65% (v/v) (heptane : isopropanol : TFA =90:10:0.1%) with a isocratic flow of 0.5 ml/min and a column temperature of 20 °C. The substances were detected at 260 nm.

2.15.3.6 Activity assay for CYP81D8 with TNT and aminodinitrotoluenes

The resting cell assay against TNT was performed with CYP81D8tr, 81D8tr-lamATR2tr, 81D8tr-licATR2tr (all cloned into the LIC-vector) in 50 mM potassium phosphate buffer (pH 7.0) after an expression in *E. coli* Rosetta 2 (DE3) in M9 medium (2.10.1, page 67). For negative controls lamATR2tr,

licATR2tr (both in LIC-vector) and Rosetta 2 (DE3) cells without a plasmid were used.

The total reaction volume of 5 ml contained 50 mg wet cells per ml buffer (50 mM potassium phosphate buffer, pH 7.0). TNT (stock: 100 mM TNT in DMSO) was added to a final concentration of 100 μ M and samples incubated at 28 °C shaking at 200 rpm. Samples were taken over a time course, quenched by adding 10% of 1.5 M trichloroacetic acid (TCA), snap frozen in liquid nitrogen and stored at -80 °C, due to the instability of hydroxylaminodinitrotoluenes in presence of oxygen.^{355,356} Defrosted samples were centrifuged (10 min at full speed, bench top microlitre centrifuge Sigma 1-15P) and 50 μ l applied for HPLC analysis. For the separation of the TNT derivatives a TechSphere ODS 80A 5 μ column (250 x 4.6 mm, Fischer Thermo Scientific) was used. 50 μ l of each sample were run in the solvent conditions of 40% (v/v) water and 60% (v/v) methanol with a flow of 1 ml/min for 10 min (column temperature: 35 °C, sample temperature: 4 °C). TNT eluted after 5.6 min and the derivatives 4-hydroxylamino-2,6-dinitrotoluene (4-HADNT) at 4.7 min, 2-amino-4,6-dinitrotoluene (2-ADNT) at 6.1 min, 4-amino-2,6-dinitrotoluene (4-ADNT) at 5.6 min, 2,4-dinitrotoluene at 6.7 min and 2,6-dinitrotoluene at 7.2 min.

2.15.3.7 Activity assay for CYP81D8 with 7-ethoxycoumarin

Recombinant expressed CYP81D8 (in *E. coli* Rosetta 2 (DE3) and M9 medium, Chapter 2.10.1, page 67) 81D8tr-lamATR2tr and 81D8tr-licATR2tr (negative controls: control-lamATR2tr, control-licATR2tr and Rosetta 2 (DE3) cells without a plasmid) were tested in a resting cells assay with 7-ethoxycoumarin, which is a common P450 substrate³⁵⁷.

Therefore, 50 mg cells per ml buffer (50 mM potassium phosphate buffer, pH 7.0) and 200 μ M 7-ethoxycoumarin (Sigma-Aldrich) in a final volume of 5 ml were incubated in glass vials at 28 °C shaking at 200 rpm. Samples (300 μ l) were taken over a time course, centrifuged (10 min at full speed, bench top microlitre centrifuge Sigma 1-15P) to remove the cells. Fifty μ l of the supernatant were analysed by HPLC (Waters 717 Plus Autosampler, 2487 dual λ absorbance detector, Waters SunFire C18 column, 3.5 μ m, 4.6 x 150 mm) at a wavelength of 325 nm under isocratic 50% (v/v) water and 50% (v/v) methanol with 0.1% (v/v) acetic acid, flow: 0.7 ml/min (run time: 35 min, column temperature: 21 °C,

sample temperature: 4 °C).³⁵⁸ The retention times of 7-ethoxycoumarin and 3-hydroxycoumarin (Sigma-Aldrich), a possible product, were 18.2 and 10.2 min, respectively.

3 Chapter: Expression of Cytochromes P450

3.1 Introduction

Hosts such as yeast (eukaryotic host) or bacteria (prokaryotic host) have been traditionally used to express recombinant P450s for characterisation studies and for industrial applications. Both have advantages and disadvantages: The yeast expression is efficient and inexpensive and can be up-scaled for industrial applications; moreover, it allows expression of native membrane associated P450s in microsomes. The yeast *Saccharomyces cerevisiae* possesses three endogeneous P450s and one reductase representing a potential disadvantage of this system as endogeneous P450s could interfere with the P450 of interest.

The bacterium *E. coli* lacks P450s and can be more easily, faster and more economically cultivated in the lab. Expression problems can occur through different codon bias and protein misfolding due to the absence of complex membrane systems like the ER and post-translational machinery.

S. cerevisiae contains an endogenous P450 reductase which is able to efficiently transfer electrons to foreign P450s.³²³ *S. cerevisiae* was the first host used to successfully express mammalian^{324,325} and plant³²⁶ P450s with activity of membrane associated proteins being detected in the microsomes. A *S. cerevisiae* strain has been specially modified by introducing the Arabidopsis P450 reductase ATR1 and ATR2 genes and silencing the endogeneous yeast P450 reductase. These strains were named WAT11 and WAT21 (Table 3.1).^{166,338} More than 20 Arabidopsis P450s have been expressed using these engineered yeast strains (Chapter 1.5.2).

Table 3.1: *Saccharomyces cerevisiae* strains used in this work

<i>S. cerevisiae</i>	genotype	obtained from
WAT11	<i>MATa; ade2-1; his3-11,-15; leu2-3,-112; ura3-1; can^R; cyr⁺</i> (a derivative of the W303-B strain)	Prof. D. Werck Reichhart (CNRS-Institute de Biologie moléculaire des plantes, Strasbourg)
WAT12	<i>MATa; ade2-1; his3-11,-15; leu2-3,-112; ura3-1; can^R; cyr⁺</i> (a derivative of the W303-B strain)	

E. coli was also used as host for an expression of membrane-associated Arabidopsis P450s such as CYP74A1, 79A2, 79B2, 79B3, 79F1, 90B1, 98A3 and 701A3,^{37,203-205,210,212,243,251,273,359} however so far, Arabidopsis P450s have been not expressed solubly in *E. coli*.

Activity of recombinant P450s has mostly been detected using radiolabelled substrates.^{200,203-205,210,212,222,230,235,237,238,244,292,339,340,360,361} Other methods used for activity detection include HPLC^{37,278,362}, LC-MS²⁹⁴, GC-MS^{37,212,247,287} and Solid State Nuclear Magnetic Resonance (SSNMR)²⁴³.

The two Arabidopsis P450s CYP81D8 and CYP81D11 were selected for this project as these enzymes were upregulated in response to TNT (2,4,6-trinitrotoluene, Figure 3.1) and might play a role in general detoxification via a broad substrate specificity (Table 3.2).^{363,364}

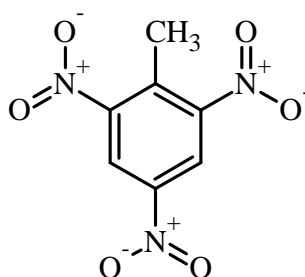


Figure 3.1: Chemical structure of 2,4,6-trinitrotoluene (TNT)

Table 3.2: P450s upregulated after TNT treatment from microarray data³⁶³

Fold increase	Accession number	Gene family name
30.7	At4g37370	CYP81D8
25.1	At3g28740	CYP81D11
14.5	At5g57220	CYP81F2
13.1	At2g30750	CYP71A12
8.7	At3g26830	CYP71B15
5.8	At5g67310	CYP81G1
3.4	At5g45340	CYP707A3
2.3	At3g26210	CYP71B23

The explosive TNT is highly toxic, recalcitrant to degradation in the environment and a major world-wide pollutant of our environment. This modern, synthetic compound is used for military purposes and also for the demolition industry. The TNT molecule is not a natural compound and has existed in the environment for a

relatively short time. These factors are likely to have contributed to the fact that there are not many organisms able to transform TNT to a less toxic compound. It is known, using microarray analyses, that expression of genes encoding enzymes from *Arabidopsis*, such as uridine diphosphate glycosyltransferases (UGTs), oxyphytodienoate reductases (OPRs), glutathione transferases (GSTs) and P450s, are upregulated in response to TNT stress. UGTs, OPRs and GSTs have been shown to have activity towards TNT and its metabolites.³⁶⁴⁻³⁶⁶

Microarray data available on the Internet (Geninvestigator, www.genevestigator.com) were used to find out details on the expression profiles of the two P450s chosen from the microarray experiment. CYP81D8 is expressed predominantly in the seedling and the young rosette and again in the mature siliques (Figure 3.2). CYP81D11 is expressed predominantly in the seedling and the young rosette and again in the mature siliques (Figure 3.2). CYP81D11 is mainly produced during and after germination and in the first stage of rosette growth. Transcripts of CYP81D11 are less abundant in the later stages of plant development.

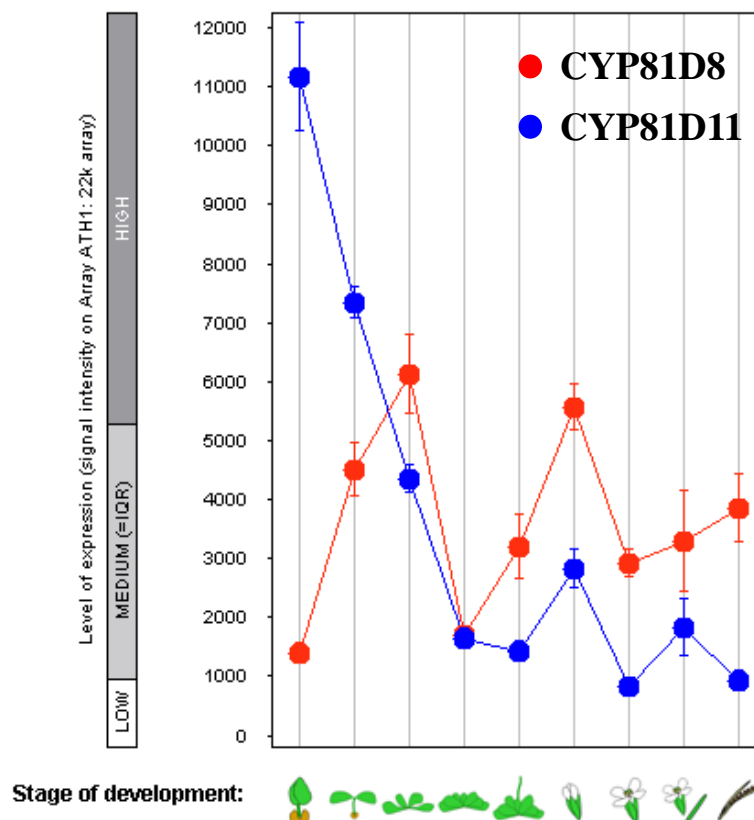


Figure 3.2: Occurrence of CYP81D8 and CYP81D11 in the development of *Arabidopsis*

(<https://www.genevestigator.com/gv/>, 15/12/2011)

Another P450, the (-)-4*S*-limonene-3-hydroxylase (CYP71D15) from peppermint (*Mentha x piperta*), a hybrid of spearmint (*Mentha spicata*) and watermint (*Mentha aquatica*), was studied in this chapter, because the limonene activity have been measured *in vitro* by GC-MS after solubilisation of the membrane associated protein CYP71D15.³⁶⁷

CYP71D15 hydroxylates (-)-4*S*-limonene in the C3 position regio- and stereospecifically to (-)-*trans*-isopiperitenol, which is a precursor of (-)-menthol (Figure 3.3).³⁶⁸ (-)-Menthol is a well studied monoterpene that occurs naturally as essential oil in peppermint. It is used in the food industry, for oral health care, cosmetics and tobacco due to its pleasant aroma and flavour and the cooling-anaesthetic effect.³⁶⁹

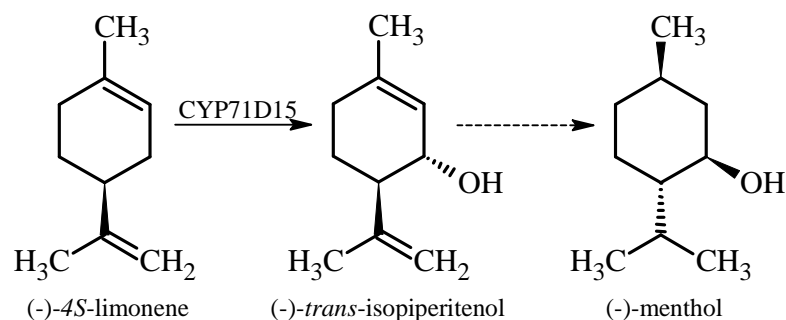


Figure 3.3: Regiospecific hydroxylation of (-)-4*S*-limonene to (-)-*trans*-isopiperitenol within the biosynthesis of (-)-menthol

Prof. Rodney Croteau's research group studied the limonene-3-hydroxylase after recombinant expression in *E. coli* JM109 and in the yeast strains WAT11 and WAT21. Hydroxylation rates of more than 2000 nmol·h⁻¹·mg⁻¹ by the membrane associated CYP71D15 were achieved after expression in *E. coli*, whereas only 35 nmol·h⁻¹·mg⁻¹ were obtained with yeast microsomes, independent of the strain (WAT11 or WAT21).^{367,370}

The hydrophobic membrane anchor of P450s and its reductase can be removed to increase the solubility with no activity loss as suggested in the literature. Kempf *et al.* reported that the human CYP2D6 was expressed solubly in the cytosol after removing the hydrophobic membrane anchor.³⁷¹

3.2 Objectives

Different strains of *E. coli* as well as *S. cerevisiae* were tested as hosts for the expression of the plant P450s: CYP81D8 and CYP81D11, both from Arabidopsis and the peppermint CYP71D15. Therefore, the native gene sequences were expressed in *S. cerevisiae* and then tested for activity. Truncated versions (without the hydrophobic membrane anchor to increase the solubility) of the P450s were used for expression in *E. coli*.

E. coli expression was carried out for the three P450s and the expression yield optimised by testing a range of strains and experimental conditions.

The yeast work was done in York and in Prof. Danièle Werck-Reichhart's laboratory (Institute de Biologie Moléculaire des plants du CNRS, Département Réponses au Stress, Strasbourg, France). Two modified yeast strains, WAT11 and WAT21³³⁸ for coexpression of the Arabidopsis reductases ATR1 and ATR2, respectively, were provided by Prof. Danièle Werck-Reichhart for the expression of full length plant P450s.

3.3 Materials and Methods

3.3.1 Analysis of CYP73D15 PM2-2 construct

Prof. Rodney Croteau (Institute of Biological Chemistry, Washington State University, Pullman, US) provided the CYP71D15 in the vector pCWori+ (construct PM2-2³⁶⁷). The amino acid sequence of the N-terminus in the construct PM2-2 was altered incorporating seven residues of a bovine 17 α -hydroxylase (Figure 3.4).^{321,367} A vector map is shown in Figure 3.5.

native CYP71D15	MELLQWSALILV
PM2-2	MALLAVFWSALILV
native CYP71D15	ATGGAGCTCCTCCAGCTTTGGTCGGCGCTTATAATCCTCGTAG
PM2-2	ATGGCTCTGTTATTAGCAGTTTTTTGGTCGGCGCTTATAATCCTCGTAG

Figure 3.4: N-terminal modification of CYP71D15 creating construct PM2-2³⁶⁷

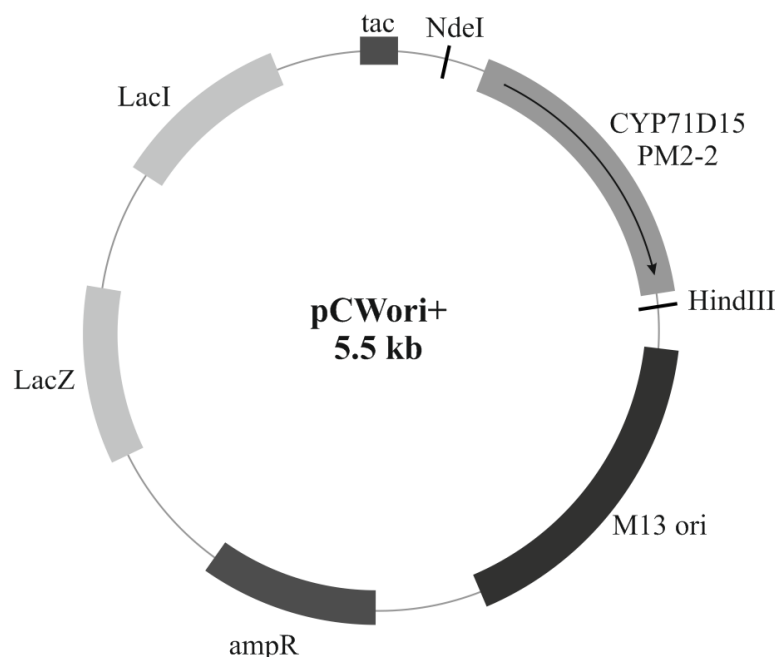


Figure 3.5: Vector map for pCWori+

LacZ = β -galactosidase gene, LacI = repressor gene for IPTG induction, tac = tac promoter, CYP71D15 PM2-2 = gene of interest, M13 ori = origin of replication of filamentous phage M13, ampR = ampicillin resistance gene, NdeI and HindIII = restriction sites

The CYP71D15 PM2-2 insert was analysed by a restriction digest using NdeI and HindIII and sequenced using primers listed in Table 3.3 (Chapter 2.8.9).

Table 3.3: Primer used for sequence analysis of CYP71D15 PM2-2

primer	sequence (5' → 3')
Tac promotor F	CCATGGTGACAATTAATCATCGGCTC
PM2-2int1263 F	GGGAAATGATTTTCGAGTTCGTCCCGTTCGG
Pm2-2int242 R	GGAGAACACCTCACCCAGCTGCACG
CYP71D15 PM2-2 R	GAGGAGAAGGCGGTCATGATGAAGGATCGTAGGGTGTGGGAAC

3.3.2 Materials and Methods for P450 expression in *Escherichia coli*

3.3.2.1 Isolation and cloning of the plant P450s

RNA was isolated from 14 days old Arabidopsis plants grown in liquid medium treated with TNT (Chapter 2.7.2) and transcribed into cDNA (Chapter 2.7.3).

Usually, P450s have a hydrophobic N-terminal region, allowing association with the membrane. The P450 amino acid sequences were analysed using the software TMHMM and SignalP3.0 (Chapter 2.8.1). The hydrophobic N-termini were removed by designing special LIC primers (Chapter 1.1) for the PCR amplification of Arabidopsis CYP81D8 and CYP81D11 (Primer see Table 3.4).

Table 3.4: Primer used for PCR amplification of the truncated versions of CYP81D8 and CYP81D11

primer	sequence
CYP81D8nat F	CCAGGGACCAGCAATGGAAACCAAAACCCTAATTTTCTCAATTCTCTCTCG
CYP81D8tr F	CCAGGGACCAGCAATGGGAAAACCTCAAGCGAAAGCCAAATCTACCTCC
CYP81D8 R	GAGGAGAAGGCGCGTCAAACGGACTCGTTGAAGATTTTAACAACAGAGG
CYP81D11nat F	CCAGGGACCAGCAATGTCATCAACAAAGACAATAATGGAAACTATATACC
CYP81D11tr F	CCAGGGACCAGCAATGCCACGGCCGCGTAAACTAAACCTACC
CYP81D11 R	GAGGAGAAGGCGCGTTATGGACAAGAAGCATCTAAAACCTTATGGAC
CYP71D15 PM2-2 F	CCAGGGACCAGCAATGGCTCTGTTATTAGCAGTTTTTTGGAGTGCG
CYP71D15 PM2-2 R	GAGGAGAAGGCGCGTCATGATGAAGGATCGTAGGGTGTGGGAAC

The peppermint CYP71D15 PM2-2 and the two truncated versions of Arabidopsis P450s (81D8tr and 81D11tr) were amplified using Phusion polymerase (Chapter 2.8.2) and primer listed in Table 3.4 before cloning into the LIC-vector (Chapter 1.1).

3.3.3 Expression of PM2-2 in *Escherichia coli*

For microsome preparation^{367,372} *E. coli* JM109 cells transformed with CYP71D15 PM2-2 were grown with shaking (200 rpm) at 37 °C in TB (Chapter 2.2.1) containing 100 µg/ml ampicillin. Expression was induced at OD_{600nm} = 0.85 by adding 1 mM IPTG, 1 mM thiamine and 75 µg/ml ALA (*E. coli* JM109 without the vector was used as negative control) and samples incubated with shaking (200 rpm) at 28 °C following the published protocol.³⁶⁷ After 40 h the cells (800 ml) were harvested by centrifugation (5000 rpm, rotor:

SLC1500, 10 min at 4 °C), resuspended in 35 ml 100 mM Tris buffer (pH 7.5) containing 20% glycerol, 0.5 M EDTA, 1 mM DTT and 0.2 mg/ml lysozyme. Cells were incubated with stirring for 10 min at 4 °C. Cell were centrifuged again (7000 rpm, rotor: SLC1500, 10 min at 4 °C) and resuspended in 30 ml 100 mM Tris buffer (pH 7.5) containing 20% glycerol, 0.5 M EDTA, 1 mM DTT and PMSF. Cells were sonicated (Chapter 2.10.3) and centrifuged at low speed (SS34-rotor, 3250 rpm). The supernatant was then spun in an ultracentrifuge (40 krpm for 1 h at 4 °C, rotor type 45Ti) to separate the soluble proteins from the membrane fraction. Membrane proteins were resuspended in 100 mM sodium phosphate buffer (pH 7.5) containing 30% glycerol using a glass homogeniser and proteins were detected by SDS-PAGE and western blot analysis.

For soluble, non membrane associated expression of the truncated Arabidopsis P450s 81D8tr and 81D11tr as well as the peppermint CYP71D15 PM2-2 several different strains (DH5 α , BL21(DE3), Rosetta 2, Rosetta gami 2) and media (LB, TB, M9 and auto-induction) was trialled. Incubations were all performed overnight with shaking (200 rpm) at 20 °C following the protocol Chapter 2.10.1. The purification was done in a batch process (Chapter 2.10.3-2.10.4).

3.3.4 Materials and Methods for P450 expression in yeast

3.3.4.1 Media

For yeast cultivation YPAG (yeast, bacto**p**eptone, **a**denine and **g**lucose) medium was used containing 10 g/l yeast extract (Formedium), 10 g/l bacto peptone (Difco), 20 g/l glucose (Fisher Scientific) and 200 mg/l sterile filtrated adenine was added after sterilisation. SGI medium (glucose based yeast minimal medium) was used for the selection of transformants on agar containing 1 g/l bacto casamino acids, 7 g/l yeast nitrogen base without amino acids (Difco), 20 g/l glucose, 20 g/l agar (Formedium) and 20 mg/l sterile tryptophane (Sigma-Aldrich) was added after sterilisation. The cultivation of the transformants in liquid culture was done in YPGE (yeast, bacto**p**eptone, **g**lucose and **e**thanol): 10 g/l yeast extract, 10 g/l bacto**p**eptone and 5 g/l glucose. Ethanol (50.6 ml/l) was added after autoclaving.

3.3.4.2 Transformation and expression in yeast

CYP71D15 from peppermint, CYP81D8 and CYP81D11 from *Arabidopsis* were cloned into the pYeDP60 vector. The vector pYeDP60 (vector map see Figure 2.3) is a shuttle vector for cloning in *E. coli* and expression in yeast.³³⁸

The transformation was carried out following the protocol adapted from Schiestl & Gietz, 1989³⁷³. Briefly, 50 ml YPGA liquid preculture was inoculated with an isolated yeast colony and incubated with shaking (140 rpm) at 28 °C over night. Then the main YPGA culture was inoculated to an OD_{700nm} 0.2 and incubated for five hours with shaking (140 rpm) at 28 °C. Cells were then centrifuged at low speed (500x g) for 10 min, the pellet resuspended in sterile water (1/10 of the original culture volume), transferred in 2 ml Eppendorf tubes (1 ml/tube) and centrifuged at low speed (500x g) for 10 min. The pellet was resuspended in 1.5 ml 0.1 M LiAc/TE (0.1 M LiAc, 10 mM Tris-HCl, 1 mM EDTA), centrifuged at low speed (500x g for 10 min) and the supernatant discarded leaving approximately 50 µl yeast cell suspension. To this yeast cell suspension, 1-5 µg plasmid-DNA, 10 µl carrier DNA solution (100 µl 10 mg/ml salmon sperm DNA in sterile water denatured for 20 min at 100 °C and then chilled on ice) and 40% PEG in 0.1 M LiAc/TE were added and cells were incubated gently shaking for one hour at 30 °C. After heat shock at 42 °C for 15 min, the suspension was centrifuged for 10 sec at low speed, the pellet washed with 1 ml sterile water, centrifuged again and resuspended in 200 µl SGI and plated on SGI agar. Agar plates were incubated at 30 °C for 3-4 days until colonies appeared.

For the expression, 10 ml SGI liquid preculture were inoculated with white transformants (colonies without a plasmid have a lack in adenine and turn red) and incubated at 28 °C with shaking (140 rpm) over night. The main culture was done in 6 x 200 ml YPGE, which was inoculated with 1.2-2 ml preculture and incubated with shaking (140 rpm) at 28 °C for 24 hours. After this time the glucose is used up by the yeast and it is using now the ethanol for its metabolism until 20 ml galactose (200g/l) were added for induction to each flask and incubated shaking (140 rpm) for 16 hours at 25 °C. Then the yeast was harvested and the microsoms isolated (see 3.3.4.3).

3.3.4.3 Yeast microsome preparation

After the expression, the yeast cells were centrifuged for 15 min at 7500 g at 4 °C and washed with TEK buffer (1 ml TEK/0.5 g yeast, TEK: 50 mM Tris-HCl pH 7.5, 1 mM EDTA, 100 mM KCl). The pellet was washed twice with 1 ml TES/0.5 g yeast (TES: 50 mM Tris-HCl pH 7.5, 1 mM EDTA, 600 mM sorbitol, fresh added 10 g/l BSA and 120 µl β-mercaptoethanol), glass beads (glass beads, 0.40-0.60 mm, Sartorius) were added to a fifth of the volume and shaken for 5 min at 4 °C (1 min shaking, 1 min chilled on ice). Glass beads were allowed to settle and the supernatant was transferred into fresh tubes. Glass beads were then washed twice with TES and the washings combined with the supernatant. The solution containing the shared cells was centrifuged (15 min at 7500x g at 4 °C) for removing cell membranes, leaving membrane fractions and soluble proteins in the supernatant. The supernatant was filtered with micra cloth (Calbiochem, Merck) to remove all glass beads and then ultracentrifuged at 100000x g at 4 °C (60 Ti-32000 rpm, 45 Ti-30000 rpm) for 45 min to pellet the microsomes. The pellet was transferred into a potter homogeniser, 500 µl TEG (50 mM Tris-HCl pH 7.5, 1 mM EDTA, 30% glycerol) added and homogenised on ice avoiding the build up of air bubbles.

To test the presence of active P450, sodium dithionite (Fluka, Sigma-Aldrich) and CO was added by bubbling the cuvette for 30 sec to create the CO bound form of the P450. Absorption was measured between 400 and 500 nm. Purified XplA heme³⁵² was used as positive control.

3.4 Results

3.4.1 P450 amino acid sequence analysis

Plant P450s have a membrane anchor of around 25 amino acids at the N-terminal sequence, which is hydrophobic and known to cause the insolubility of these proteins. The catalytic centre is situated in the cytoplasm, so that a deletion of the N-terminus should not reduce the enzyme activity.

The amino acid sequence was analysed with SignalP and TMHMM software (Chapter 2.8.1, result in Figure 3.6) and primers designed excluding the first 22 amino acids from the N-terminus in order to clone 81D8tr without the membrane

anchor. To ensure expression an ATG start codon was added to the 5' end of the forward primer.

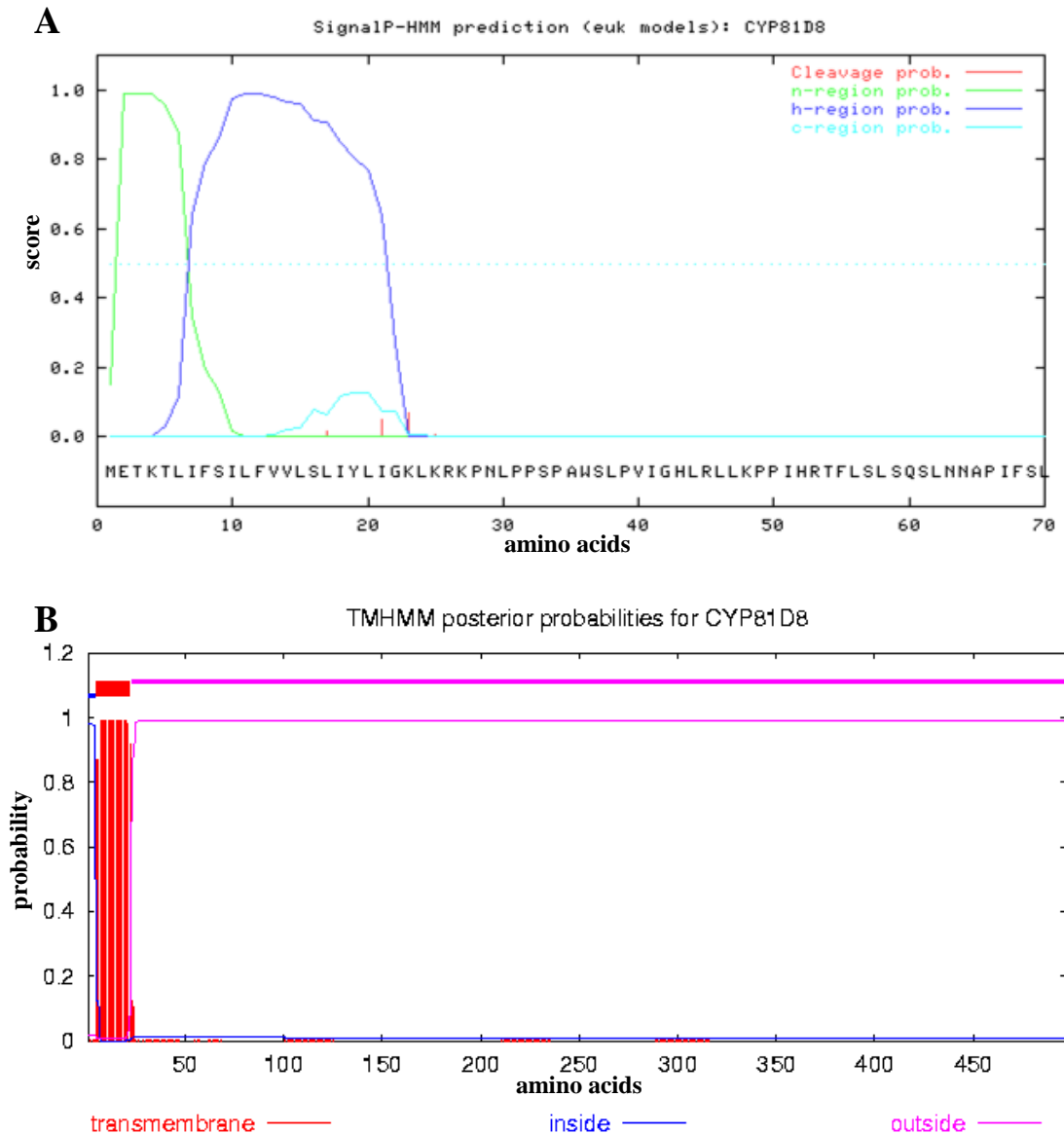


Figure 3.6: Analysis of the CYP81D8 amino acid sequence

A SignalP blot (cleavage prob = probability of cleavage site, n-region prob = probability of N-terminus of the signal peptide, h-region prob = probability of hydrophobic region of signal peptide, c-region prob= probability of C-terminus of signal peptide) and **B** TMHMM

A similar approach was taken to the cloning of CYP81D11. Here the first 32 amino acids (Figure 3.7) were removed to expressed 81D11tr without a membrane anchor. Again an ATG start codon was added to the 5'end of the forward primer.

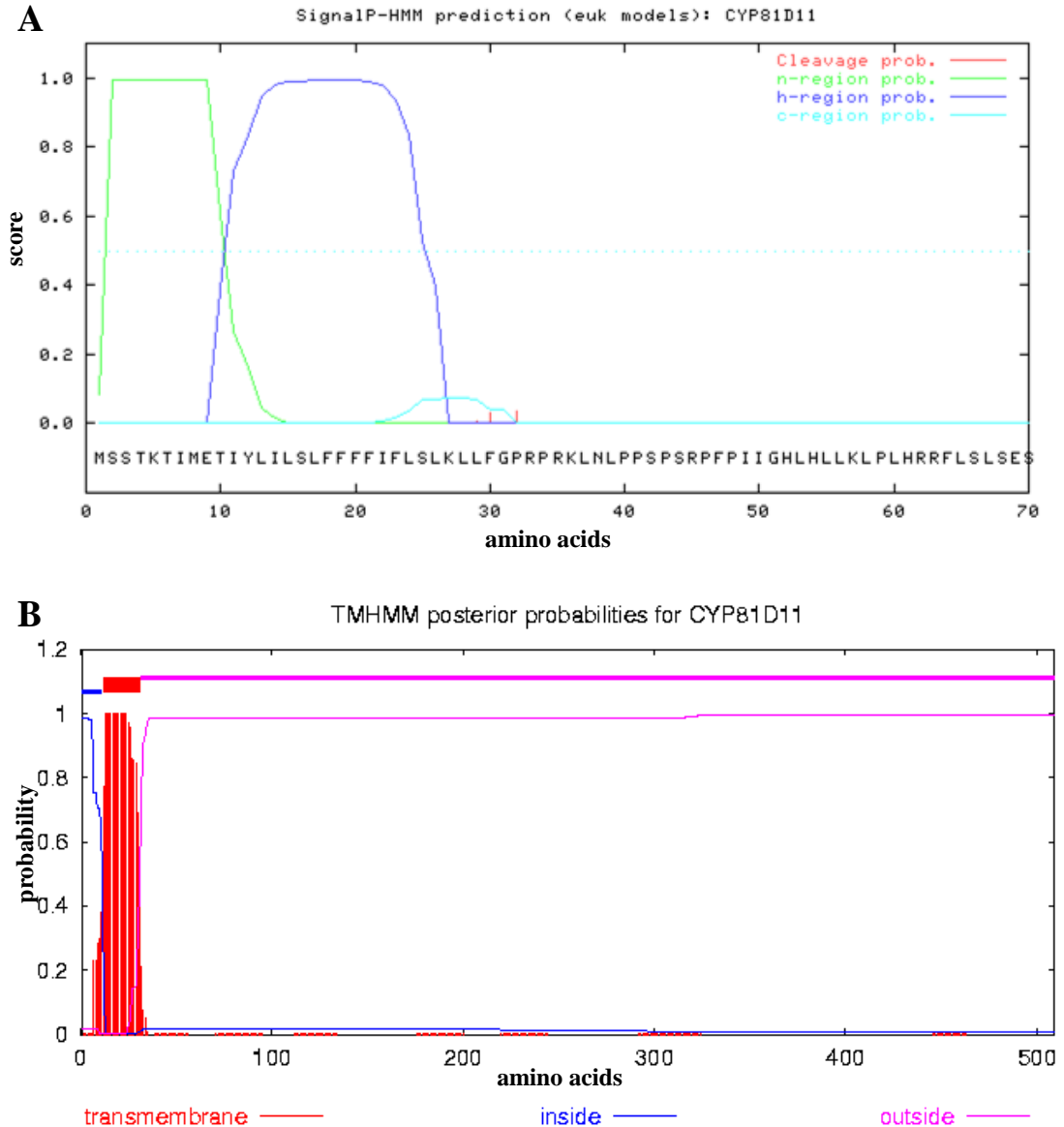


Figure 3.7: Analysis of the CYP81D11 amino acid sequence

A SignalP blot (cleavage prob = probability of cleavage site, n-region prob = probability of N-terminus of the signal peptide, h-region prob = probability of hydrophobic region of signal peptide, c-region prob = probability of C-terminus of signal peptide) and **B** TMHMM

The analysis result of the N-terminal amino acid sequence of CYP71D15 PM2-2 (Figure 3.8) was similar to the two Arabidopsis P450s described above. The full length of the CYP71D15 PM2-2 was used due to the fact that the N-terminus of the construct PM2-2 was already optimised for *E. coli* expression by Haudenschild *et al.* 2000³⁶⁷.

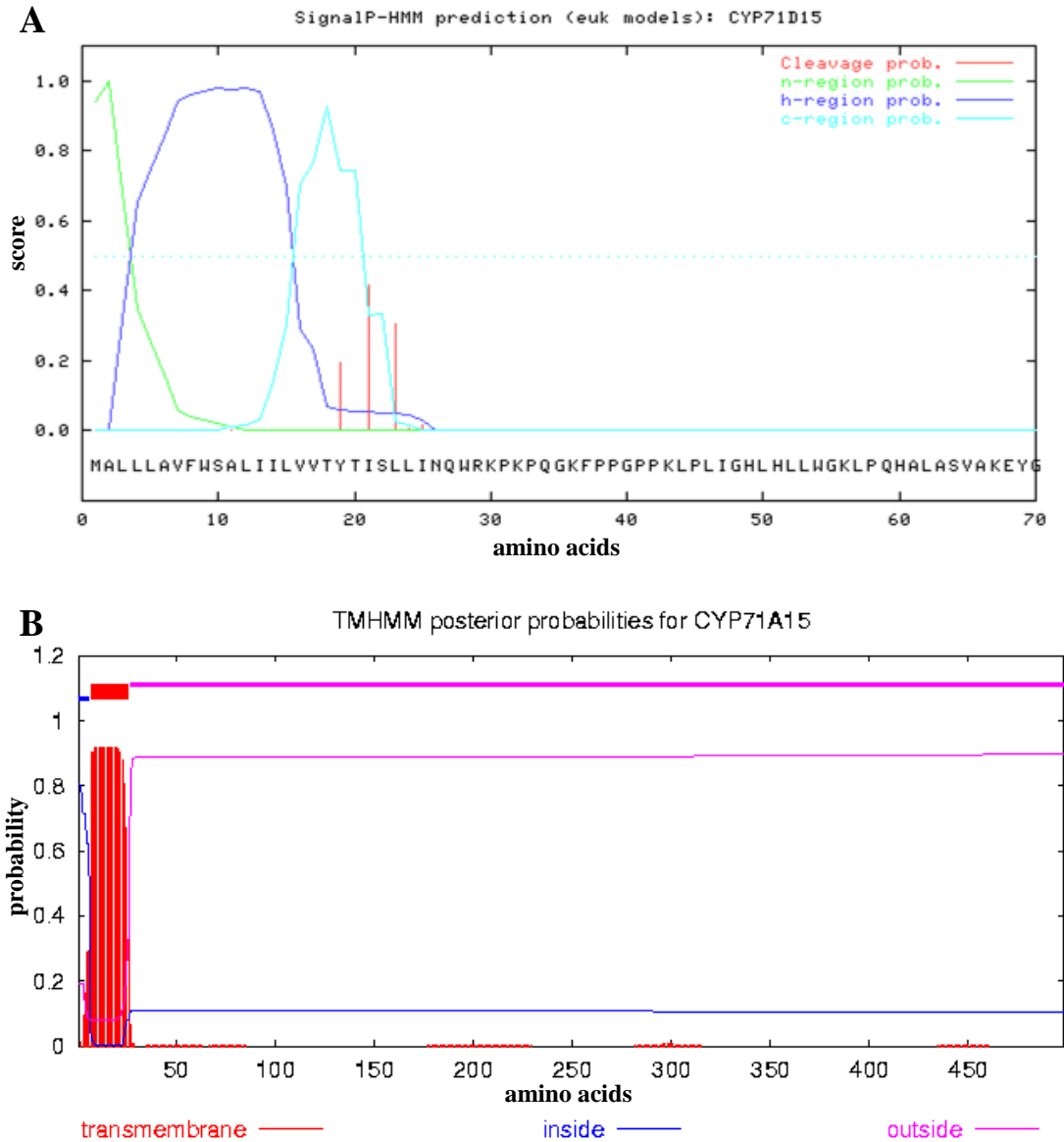


Figure 3.8: Analysis of the CYP71D15 amino acid sequence

A SignalP blot (cleavage prob = probability of cleavage site, n-region prob = probability of N-terminus of the signal peptide, h-region prob = probability of hydrophobic region of signal peptide, c-region prob= probability of C-terminus of signal peptide) and **B** TMHMM

3.4.2 Analysis of CYP71D15 PM2-2

The pCWori+ vector (5.5 kb) containing the insert CYP71D15 PM2-2 (1.5 kb) was digested and fragments separated using an agarose gel (Figure 3.9).

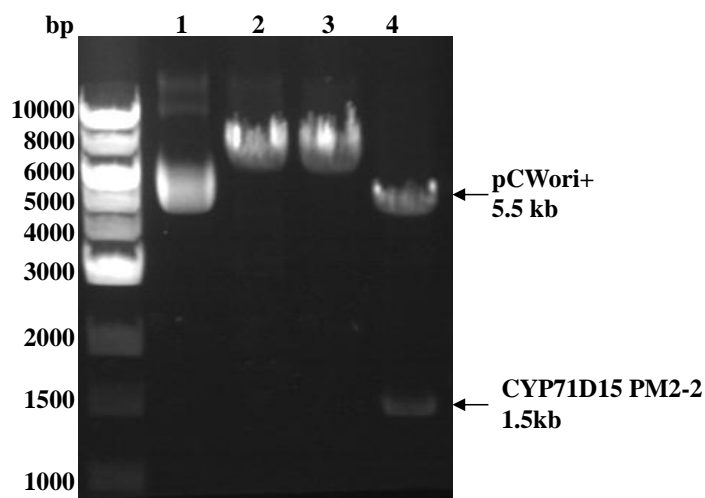


Figure 3.9: Analysis of CYP71D15 PM2-2 in pCWori+-vector after digestion
1 = no enzyme, 2 = HindIII, 3 = NdeI, 4 = HindIII and NdeI linearised the plasmid and isolated the insert CYP71D15 PM2-2 with a size of 1.5

Different internal and external primers were used for sequencing the PM2-2 gene and flanking regions. Sequencing confirmed the *CYP71D15 PM2-2* gene and C-terminal His-Tag comprising four histidine residues. The complete nucleotide sequence is found in Appendix B.

3.4.3 P450 cloning into the LIC-vector

All three P450s were amplified by PCR using Phusion polymerase (Figure 3.10) and then cloned into the LIC-vector.

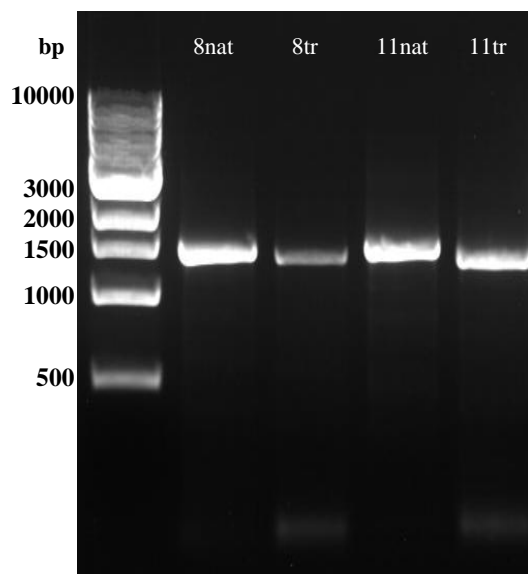


Figure 3.10: Analysis of PCR products for native CYP81D8 (8nat), N-truncated CYP81D8 (8tr), native CYP81D11 (11nat) and N-truncated CYP81D11 (11tr)

3.4.4 P450 expression in *Escherichia coli*

The peppermint CYP71D15 PM2-2 was expressed in *E. coli* JM109 following the published protocol from Prof. Rodney Croteau's research group (Chapter 3.3.3). SDS-PAGE analysis was performed to verify the expression of CYP71D15 PM2-2. The expected size of CYP71D15 PM2-2 was 57 kDa, however no signal for CYP71D15 PM2-2 was detected (Figure 3.11).

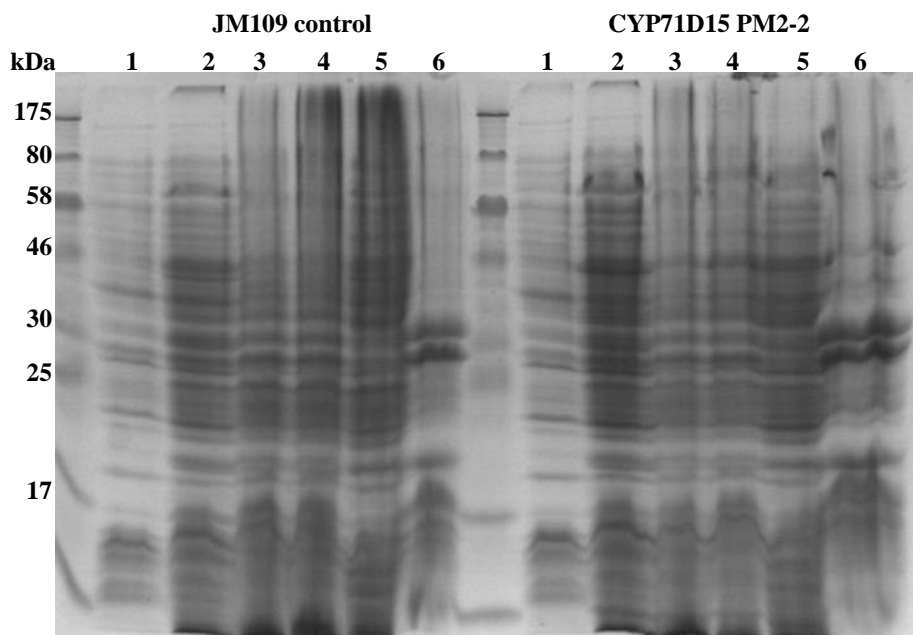


Figure 3.11: Analysis of crude extract of JM109 cells after expression of CYP71D15 PM2-2 (57 kDa)

JM109 cells without plasmid was used for negative control (**1** = cells before induction, **2** = cells after induction, **3** = disrupted cells after sonication, **4** = supernatant after sonication, **5** = soluble protein after ultracentrifugation, **6** = insoluble protein fraction containing membrane proteins after ultracentrifugation)

The different fractions were also analysed using a spectrophotometer, but the typical shift of the absorption maximum from 420 nm to 450 nm when bound carbon monoxide was absent.

All three P450s were expressed in different *E. coli* strains (DH5 α , BL21(DE3), Rosetta 2, Rosetta gami 2) and various media were tested. The results are summarised in Table 3.5.

Table 3.5: Scheme of the test expression of the Arabidopsis P450s in the Lic-vector using different *E. coli* strains and media

	LB-medium	TB-medium	M9-medium	
CYP71D15 PM2-2	no expression	no expression	not tested	BL21(DE3)
	no expression	no expression	not tested	Rosetta 2
	no expression	no expression	not tested	Rosetta gami 2
81D8tr	no expression	not tested	not tested	BL21(DE3)
	expression	not tested	no expression	Rosetta 2
	no expression	no expression	not tested	Rosetta gami 2
	no expression	not tested	not tested	DH5a
81D11tr	no expression	not tested	not tested	BL21(DE3)
	expression	not tested	no expression	Rosetta 2
	no expression	no expression	not tested	Rosetta gami 2
	no expression	not tested	not tested	DH5a

Expression was detected for 81D8tr (54 kDa) and 81D11tr (53 kDa) when expressed in *E. coli* Rosetta 2 and LB medium (Figure 3.12 and Figure 3.13). Uninduced culture and induced empty vector culture were used as negative control.

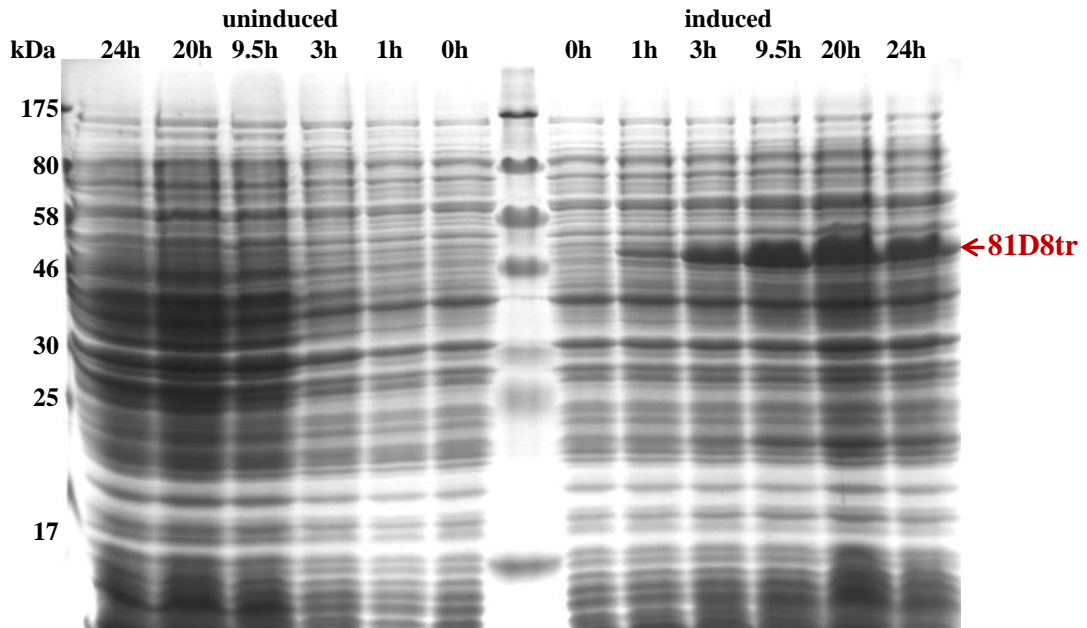


Figure 3.12: SDS PAGE analysis of crude extract from *E. coli* Rosetta 2 cells expressing 81D8tr (54 kDa) in LB medium with and without induction
An increase in signal could be seen from 3 h on.

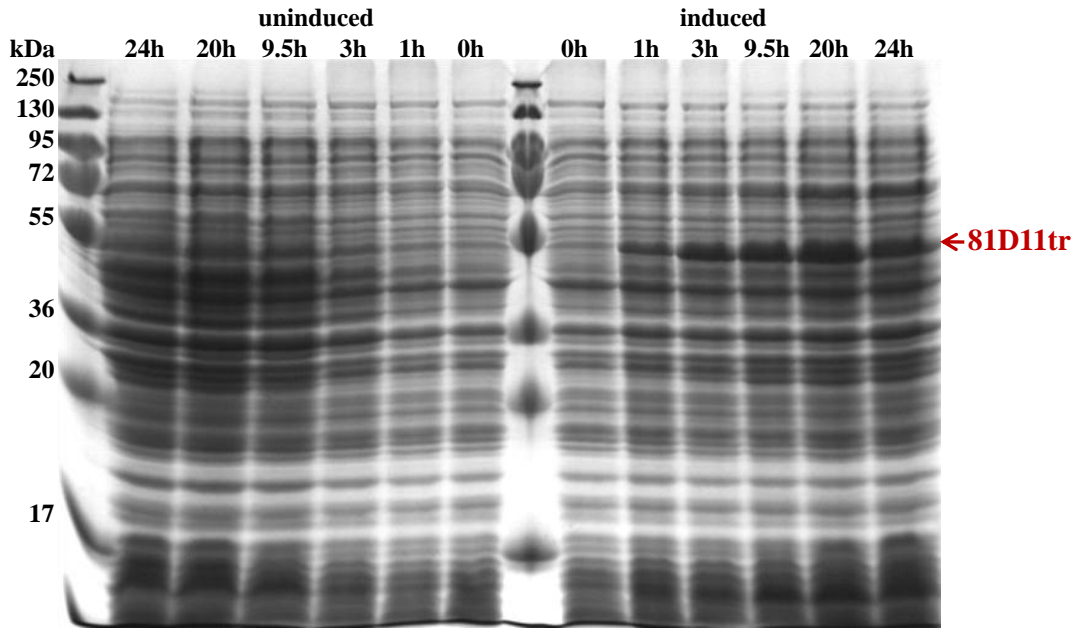


Figure 3.13: SDS PAGE analysis of crude extract from *E. coli* Rosetta 2 cells expressing 81D11tr (53 kDa) in LB medium with and without induction
An increase in signal could be seen from 3 h on.

Additionally auto-induction medium was tested and P450s were purified in a single step using Ni-affinity chromatography. Fractions were analysed using SDS PAGE gel electrophoresis. No signal was detected for 81D8tr and 81D11tr in whole cells, disrupted cells, soluble or insoluble protein fractions, possibly due to low expression levels. However, a strong signal was found in the eluted protein fractions for both P450s (Figure 3.14).

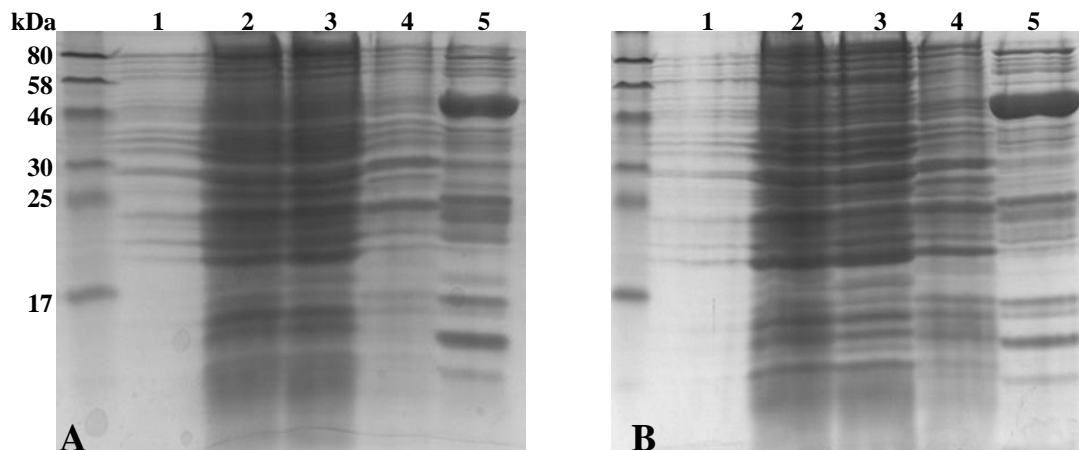


Figure 3.14: SDS PAGE analysis of protein fractions containing 81D8tr and 81D11tr after purification on Ni-resin material

A 81D8tr (54 kDa) and **B** 81D11tr (53 kDa) after expression in *E. coli* Rosetta gami 2 in auto-induction medium (1 = whole cells before sonication, 2 = disrupted cells, 3 = soluble protein fraction, 4 = insoluble protein fraction, 5 = eluted protein fraction)

A similar result was seen after purification of 81D8tr, 81D1tr (Figure 3.15). No signal was detected for 71D15 PM2-2 (57 kDa, Figure 3.16A) when expressed in *E. coli* Rosetta gami 2 and LB medium. Cells harbouring the empty were used as negative control and purified as the P450s (Figure 3.16B).

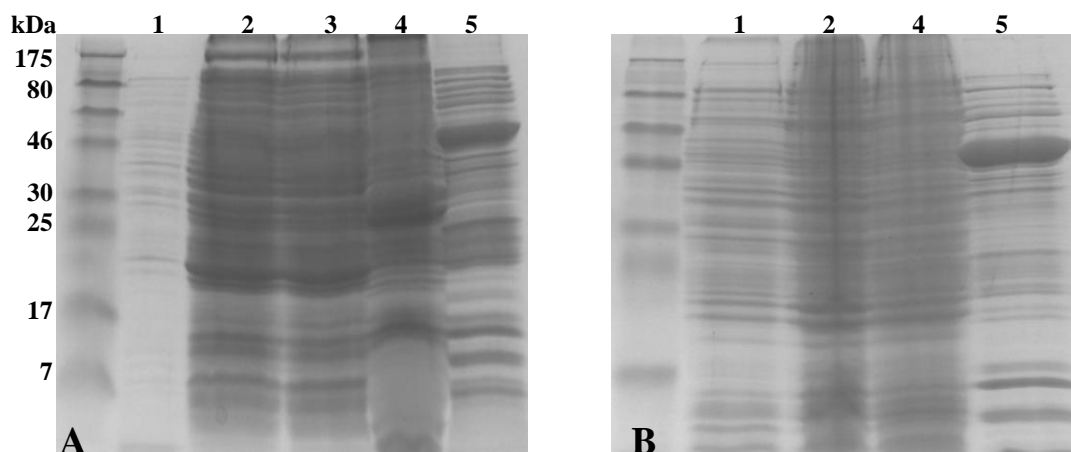


Figure 3.15: SDS PAGE analysis of protein fractions containing 81D8tr and 81D11tr after purification on Ni-resin material

A 81D8tr (54 kDa) and **B** 81D11tr (53 kDa) after expression in *E. coli* Rosetta gami 2 in LB medium (1 = whole cells before sonication, 2 = disrupted cells, 3 = soluble protein fraction, 4 = insoluble protein fraction, 5 = eluted protein fraction)

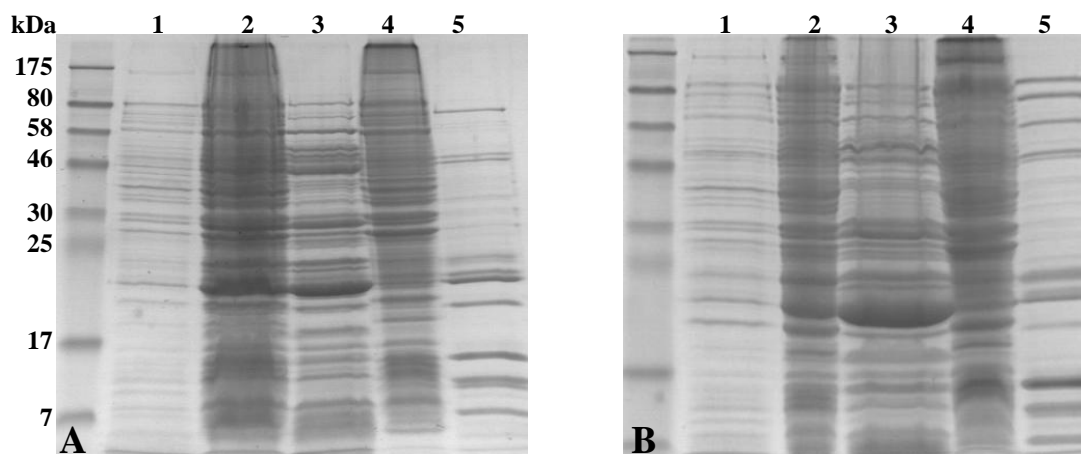


Figure 3.16: SDS PAGE analysis of protein fractions containing CYP71D15 PM2-2 and empty vector control after purification on Ni-resin material

A CYP71D15 PM2-2 (57 kDa) and **B** empty vector control after expression in *E. coli* Rosetta gami 2 in LB medium (1 = uninduced cells, 2 = disrupted cells, 3 = soluble protein fraction, 4 = insoluble protein fraction, 5 = dialysed protein fraction)

Additionally a western blot analysis was performed to check if there were proteins possessing a His-Tag, but no signal was detected for any of the three P450s (Figure 3.17).

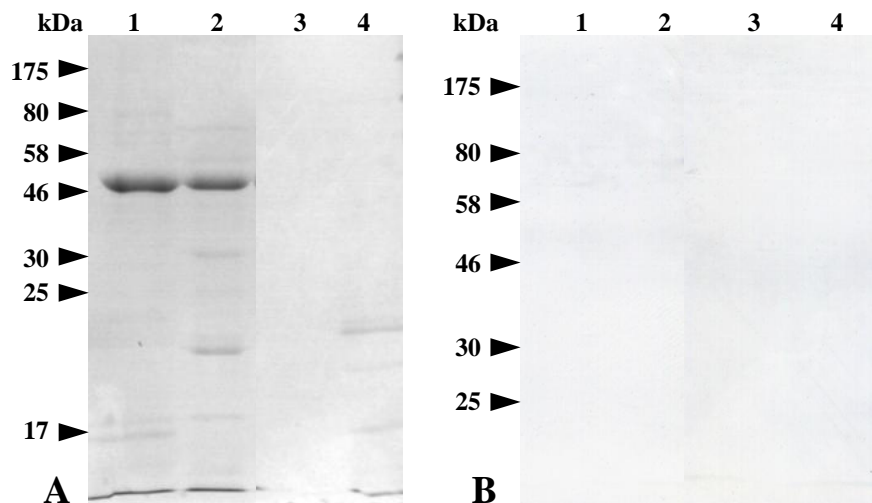


Figure 3.17: Analysis of plant P450s after purification on Ni-resin material
A SDS-PAGE and **B** western blot of purified P450s (1 = 81D8tr , 2 = 81D11tr, 3 = potassium phosphate buffer negative control, 4 = CYP71D15 PM2-2)

3.4.5 Activity assay for 81D8tr, 81D11tr and CYP71D15 PM2-2

P450 activity was tested in resting cell assays, disrupted (sonicated) cells and Ni-chromatography purified protein although P450 expression could be not detected by SDS PAGE and western blot analysis, possibly due to too low expression.

No native substrate is known for the two *Arabidopsis* CYP81D8 and CYP81D11. Thus to test the ability of these P450s to perform an oxidative reaction methyl-tolyl-sulphide was tested as substrate. The bacterial P450 XplA heme domain (with ferredoxin and ferredoxin reductase from spinach as reductase part) can oxidise methyl-tolyl-sulphide to methyl-tolyl-sulphoxide and was used as positive control.

For the bacterial P450 XplA the substrate peak decreased and a corresponding peak for methyl-tolyl-sulphoxide appeared (Figure 3.16). For all other tested samples, the concentration of the volatile methyl-tolyl-sulphide substrate decreased over time, but no product peak was detected. Therefore, it is possible that a reaction has occurred, however, not producing the predicted reaction product methyl-tolyl-sulphoxide. Additionally, whole cells and total protein

fraction were tested for activity against methyl-tolyl-sulphide, but no activity could be detected (results not shown).

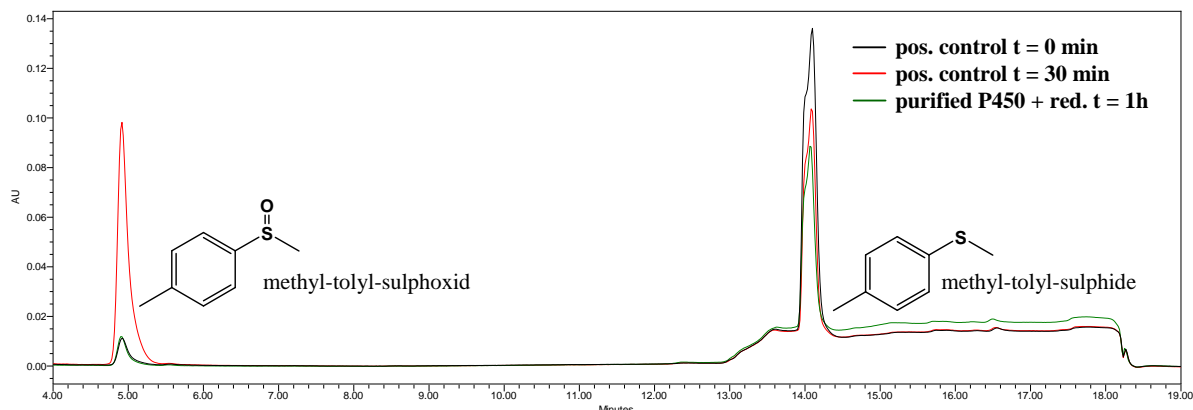


Figure 3.18: HPLC chromatogram of the methyl-tolyl-sulphide assay
(black line = positive control at time zero)

CYP71D15 PM2-2 was tested with its native substrate limonene using whole cells and total protein. The substrate limonene (10 $\mu\text{g/ml}$) had a retention time of 3.45 min. No additional peak of hydroxylated limonene was detected for any of the samples. Additionally 81D8tr and 81D11tr was tested against limonene, however no conversion was found.

3.4.6 P450 expression in yeast

P450s show a typical absorption maximum at 420 nm. Activity of P450s can be determined by measuring a shift in absorption to 450 nm when CO is bound.

P450 transformation into yeast, expression and microsome isolation for CYP71D15 from peppermint was done in Strasbourg and in York and CYP81D11 from Arabidopsis in York. The diluted, reduced microsomes (1:1 in TEG buffer) were analysed by UV/Vis and used for the baseline. The solution was bubbled with CO and analysed again. As a positive control, purified XplA heme was analysed and the typical shift to 450 nm of the CO bound form was observed (Figure 3.19A). There was a higher absorption around 420 nm for CYP71D15 (Figure 3.19B), implying that the P450 was not correctly folded and therefore inactive.

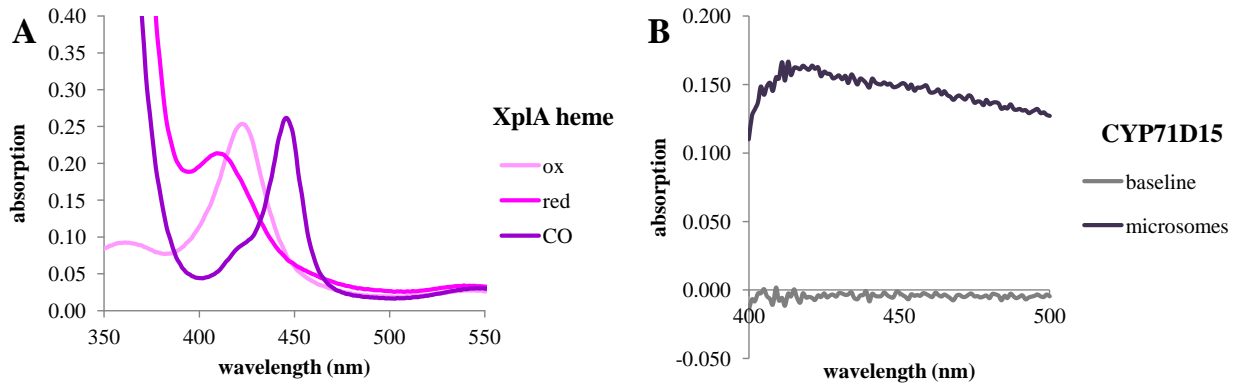


Figure 3.19: CO difference spectrum of the microsoms for XplA heme from *Rhodococcus* sp. and CYP71D15 from peppermint
A XplA heme (ox = oxidised form, red = reduced form, CO = CO bound form) and **B** CYP71D15

The expression of CYP71D15 from peppermint was repeated in York and additionally CYP81D11 was expressed. During the microsome preparation, surprisingly, the supernatant after the ultracentrifugation of CYP81D11 appeared reddish (the microsomes containing the P450 should be in the pellet) and due to that it was analysed with the UV/Vis spectrophotometer.

The supernatant of the ultracentrifugation and the diluted microsomes (1:1 in TEG buffer) with sodium dithionite were used for baseline correction. Then the solution was bubbled with CO and analysed again. However a P450 characteristic spectrum was not obtained (Figure 3.20).

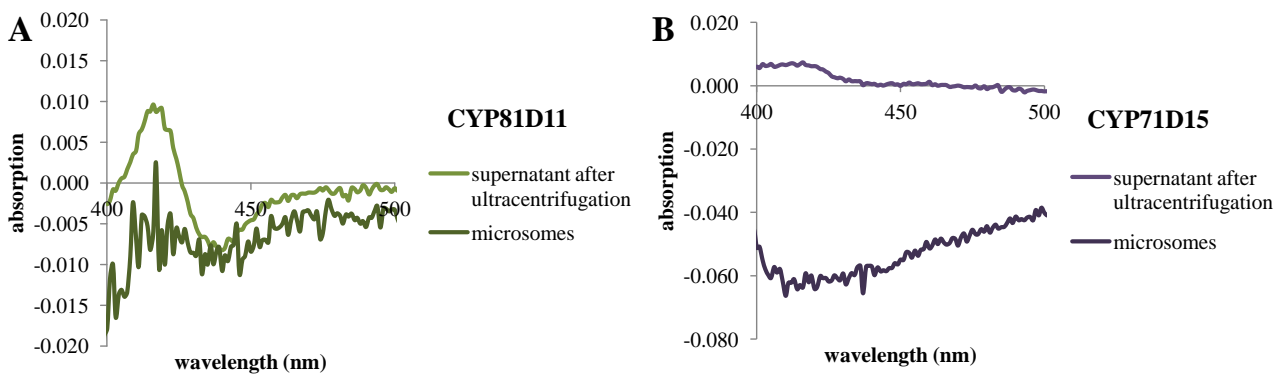


Figure 3.20: CO difference spectrum of the microsomes and the supernatant after the ultracentrifugation for CYP81A11 from Arabidopsis and CYP71D15 from peppermint
A CYP81A11 and **B** CYP71D15

There was no peak at 450 nm for both P450 microsomes, but again a higher absorption around 420 nm. The supernatant (after ultracentrifugation) of CYP81D11 showed also an absorption maximum at around 420 nm.

An SDS PAGE analysis was performed to detect the P450s (Chapter 2.13.2). Three different samples were tested: the supernatant after the sonication of the cells (**1** in Figure 3.21), the supernatant after ultracentrifugation (**2**) and the microsome solution (**3**).

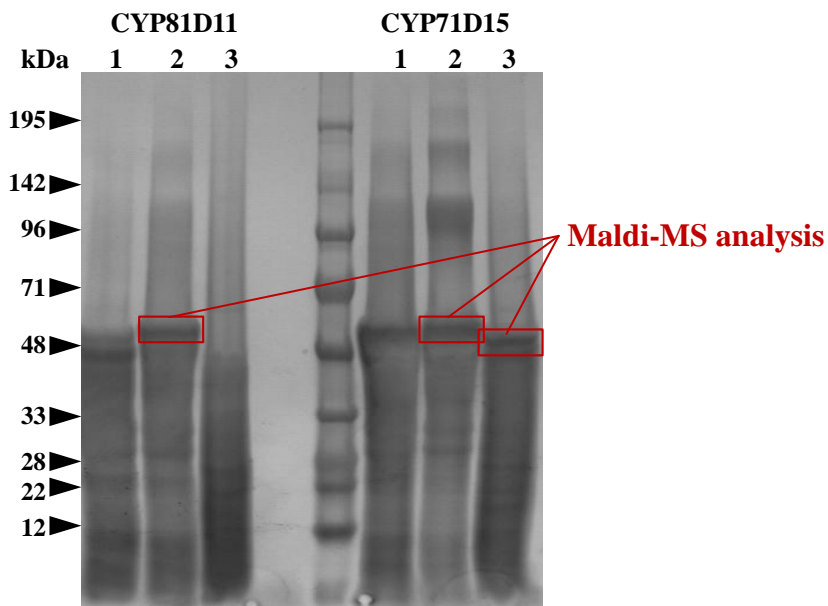


Figure 3.21: SDS PAGE analysis of yeast microsomes containing CYP81D11(57 kDa) and CYP71D15 PM2-2 (57 kDa).

1 = supernatant after the sonication of the cells, **2** = supernatant after ultracentrifugation, **3** = microsome solution. Bands in the red corners were sent for Maldi-MS analysis,

Signals of the expected sizes for CYP81D11 (57 kDa) and CYP71D15 (57 kDa) could be detected, but MALDI-MS analysis identified the samples as bovine serum albumin and no P450 sequence was detected (Chapter 2.15.2).

3.5 Discussion

3.5.1 P450s expressed in *Escherichia coli*

The function of CYP81D8 and CYP81D11 from *Arabidopsis* is not known (Appendix A). Both have been found to be induced in response to biotic and abiotic stress, such as osmotic stress, treatment with hydrogen peroxide, jasmonic acid, salicylic acid, abscisic acid, rose bengal and paraquat.^{374,375} Prof. Johnathan

Napier's research group studied CYP81D11 in more detail and postulated an important role of this P450 in the plant defence response and that it is induced by *cis*-jasmonate (an activator for genes involved in the pathway of secondary metabolic defence chemicals³⁷⁶).^{377,378}

The P450s CYP81D8, CYP81D11 and the peppermint CYP71D15 PM2-2 were expressed in *E. coli* and were found in the insoluble protein fraction. There was no improvement in the solubility when CYP81D8 and CYP81D11 were lacking the hydrophobic membrane anchor region. Different *E. coli* strains were tested to increase the yield of the expressed P450s. The *E. coli* Rosetta 2 strain, containing a supplementary plasmid for rare codons, resulted in the highest expression yield for 81D8tr and 81D11tr identified by SDS-PAGE when compared with uninduced Rosetta 2 cells.

Additionally, various media were tested for further optimisation of the P450 expression. No expression was achieved in TB, auto-induction and M9 media. The Arabidopsis 81D8tr and 81D11tr have been successfully expressed only in LB medium. However, no signal was seen in western blot analysis, possibly due to P450 protein folding so that the His-Tag cannot be recognised or through detection limitation.

Oxidative activity of 81D8tr and 81D11tr was tested in resting cell assays towards methyl-tolyl-sulphide, because the sulphoxide product is commercially available. It was not necessary to co-express a corresponding plant reductase, due to the native presence of the bacterial flavodoxin reductase (encoded by FPR³⁷⁹ and used as protection against oxidative stress³⁸⁰), which was shown to support plant P450s, for example the CYP97 carotene hydroxylase^{381,382}. However, no activity was found for Arabidopsis 81D8tr and 81D11tr to methyl-tolyl-sulphide in whole cells, which is possibly caused by limitation of the electron transfer through the *E. coli* reductase or through inactive P450s. Another reason may be that methyl-tolyl-sulphide is not a substrate of CYP81D8. Additionally, the P450s, present in the disrupted cell solution after sonication, were tested with two different reductases (commercially available spinach ferredoxin/ferredoxin reductase and recombinant expressed Arabidopsis ATR1tr, Chapter 4), nevertheless no product was detected. Although the expression of both P450s was shown by SDS PAGE analysis, activity could not be detected.

The peppermint CYP71D15 (limonene-3-hydroxylase) is part of the complex pathway leading to the monoterpene (-)-menthol³⁸³ and has been recombinantly expressed in insect cells, yeast and *E. coli* by Prof. Rodney Croteau's research group.^{367,368} The CYP71D15 construct PM2-2 (provided by Prof. Rodney Croteau) was expressed in *E. coli* following their publications and tested for the hydroxylation of (-)-(4*S*)-limonene to (-)-*trans*-isopiperitenol in resting cell assays as well as in different fractions containing protein. No hydroxylation activity was detected possibly caused by too low expression levels, which gave no signal in SDS PAGE and western blot analysis.

3.5.2 P450s expressed in *Saccharomyces cerevisiae*

For yeast expression the two *S. cerevisiae* strains WAT11 and WAT21, co-expressing the Arabidopsis reductase ATR1 and ATR2, respectively were used. Several research groups using these two strains have found that the amount of product is dependent on the P450, e.g. the CYP76B1 (from *Helianthus tuberosus*) worked better with WAT11 in the dealkylation of 7-ethoxycoumarin³⁸⁴ and CYP88A3 and CYP88A4 with WAT21 in the oxidation of *ent*-kaurenoic acid²⁴⁷. Additional to the activity assays, P450s can be characterised for their typical carbon monoxide difference spectra by shifting the absorption maximum sodium dithionite reduced P450 from 420 nm to the carbon monoxide bound form at 450 nm.

The three P450s CYP89A9 (from Arabidopsis with unknown function), CYP81D11 and CYP71D15 PM2-2 were expressed in *S. cerevisiae* WAT11 and WAT21 and microsomes containing the membrane associated P450s were isolated. P450s were detected by performing a CO difference spectrum. No maximum was seen for these P450s at 450 nm implying that incorrectly folded P450 had been produced. The reason for this is currently unknown. It was hypothesised that the expression of these P450s as fusion proteins would improve expression and facilitate the formation of active protein.

4 Expression, purification and characterisation of truncated, soluble Arabidopsis Cytochrome P450 reductases

4.1 Introduction

Cytochrome P450 reductases (CPR) are important partner enzymes for P450s because they supply electrons for all the different reactions.^{385,386} They are dependent on a flavin cofactor and NAD(P)H as a source of reducing equivalents. In yeast and animal species, only one single reductase is responsible for providing the necessary electrons for all the P450s.³⁸⁷ Plant genomes have usually more than one reductase (three in Arabidopsis and also in *Helianthus tuberosus*³⁸⁸), possibly due to the higher number of P450 genes in plant (246 P450 genes in Arabidopsis in comparison to 57 P450 genes in humans or three P450 genes in *S. cerevisiae*).³⁸⁹ Angiosperm reductases are usually classified into two distinct classes dependent on their N-terminal amino acid sequence. Class I is usually targeted to membrane of the ER whereas class II contains often more than 20% of the amino acids Serine and Threonine in the N-terminus and is then anchored in different membranes, such as chloroplasts.^{166,390-392}

In the late 1990s, two Arabidopsis cytochrome P450 reductases, named ATR1 (genetic locus: At4g24520) and ATR2 (At4g30210), were characterised after recombinant expression.^{166,391} A third reductases, ATR3 (At3g02280), was found in the Arabidopsis genome sequence³⁹³ and was shown to be an authentic reductase supporting cinnamate-4-hydroxylase activity *in vitro*.^{394,395}

Low sequence identity (33%) in the first 86 or 106 amino acids between ATR1 and ATR2, respectively, give rise to the suspicion that the reductases are anchored in different membranes such as endoplasmic reticulum (ER) or chloroplast membrane³⁵¹. The sequence of ATR2 contains two possible start codons, separated by a Serine and Threonine rich sequence, which is thought to act as membrane signal for chloroplast translocation.^{166,351,396} For this reason, ATR2 belongs to class II reductases whereas ATR1 to class I. Interestingly, ATR3 lacks this hydrophobic N-terminus and is located in the cytoplasm as well as in the nucleus, which was demonstrated by fluorescent spectroscopy of transiently

expressed ATR3 fused to GFP (together with the ER-located mRFP-HDEL ER marker) in tobacco leaves as well as in tobacco By-2 cells.³⁹⁵

Amino acid sequence analyses demonstrated that ATR1 and ATR2 share 64% sequence identity. The ATR2 amino acid sequence shares an identity of 73% with the P450 reductase from *Catharanthus roseus*³⁹¹, whereas the ATR1 shares 65% to this reductase. The reductase ATR3 shares only 26% and 24% sequence identity with ATR1 and ATR2, respectively, and belongs rather to the subfamily of diflavin reductases with a sequence identity of 42% to the human nitroreductase NR1 (Figure 4.1).³⁹⁵ ATR3 has been shown to interact with CIAPIN1, a mammalian cytokine-induced inhibitor of apoptosis, and therefore thought to take part in the cell division and programmed cell death.³⁹⁵

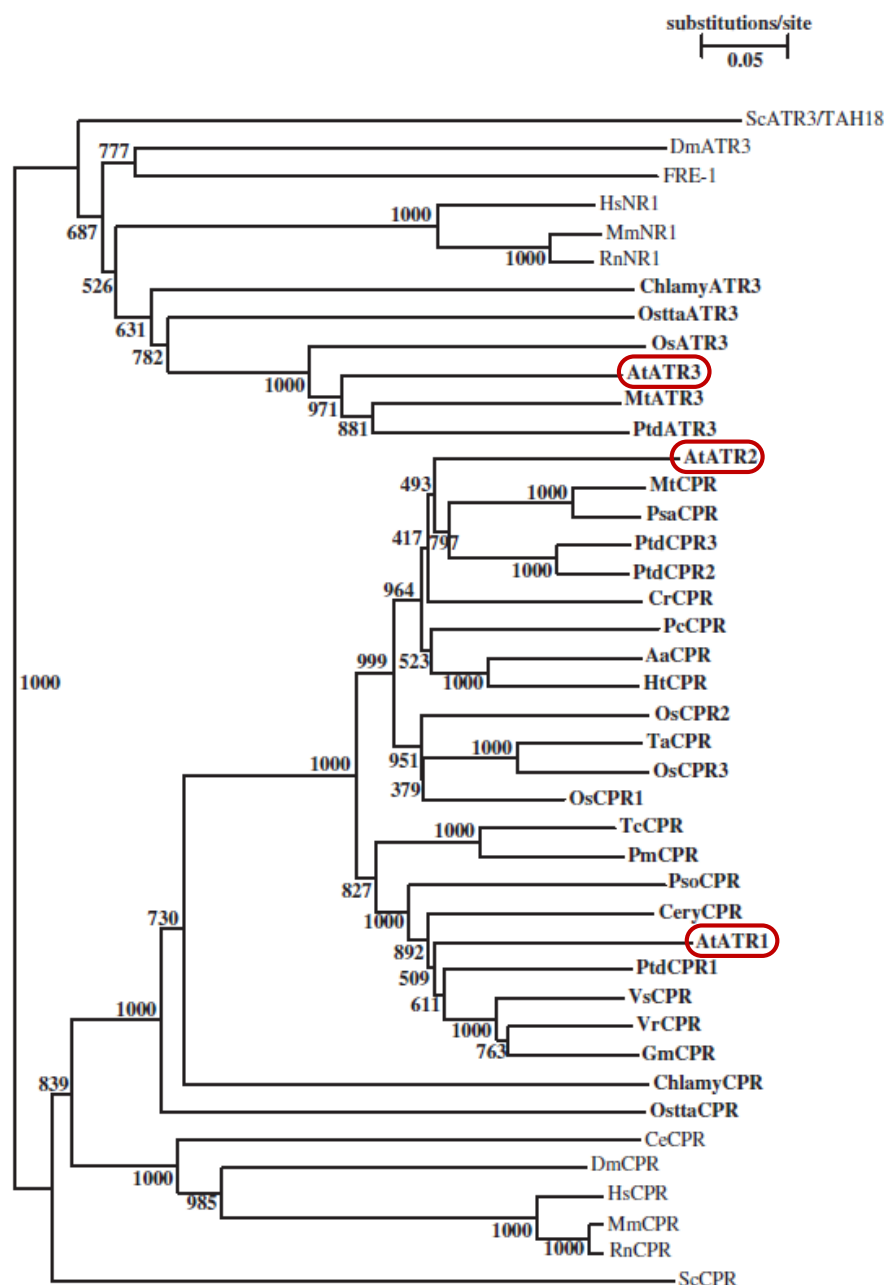


Figure 4.1: Phylogenetic tree of eukaryotic cytochrome P450 reductases with per cent bootstrap value (1000 bootstrap) of 30 CPR sequences and 12 ATR3-like sequences according to Varadarajan *et al.* 2010³⁹⁵ (Aa: *Artemisia annua*, At: *Arabidopsis thaliana*, Ce: *Caenorhabditis elegans*, Cery: *Centaurium erythraea*, Chlamy: *Chlamydomonas reinhardtii*, Cr: *Catharanthus roseus*, Dm: *Drosophila melanogaster*, Gm: *Glycine max*; Hs, *Homo sapiens*; Ht, *Helianthus tuberosus*; Mm, *Mus musculus*; Mt, *Medicago truncatula*, Os: *Oryza sativa*, Ostta: *Ostreococcus tauri*, Pc: *Petroselinum crispum*, Pm: *Pseudotsuga menziesii*, Ps: *Pisum sativum*, Pso: *Papaver somniferum*, Ptd: *Populus balsamifera subsp. Trichocarpa x Populus deltoids*, Rn: *Rattus norvegicus*, Sc: *Saccharomyces cerevisiae*, Ta: *Triticum aestivum*, Tc: *Taxus chinensis*, Vr: *Vigna radiate*, Vs: *Vicia sativa*)

ATR1 and ATR2 have conserved binding motifs for FMN, FAD and NADPH, which are shown in Figure 4.2.

CHAPTER 4 – ARABIDOPSIS REDUCTASES

ATR1				MTSALYASD	LFKQLKSIMG	TDSLSDDV--	-VLVIATTSL	36
ATR2	MSSSSSSSTS	MIDLMAAIK	GEPVIVSDPA	NASAYESVAA	ELSSMLIENR	QFAMIVTTSI		60
C. roseus	MDSSSEKLSF	F-ELMSAILK	GAKLDGNS-	-SDSGVAVSP	AVMAMLENK	ELVMILTTSV		57
							FMN-pyrophosphate	
ATR1	ALVAG-FVVL	LWKKTTADRS	GELKPLMIPK	SLMAKDEDDD	LDLGSBKTRV	SIFFGTQTGT		95
ATR2	AVLIGCIVML	VWRRSGSGNS	K--R-VEPLK	PLVIKPREE-	-EIDDGRKKV	TIFFGTQTGT		115
C. roseus	AVLIGCVVVL	IWRRSSGS-G	K--KVVEPPK	LIVPKSVVEP	EEIDEGKKKF	TIFFGTQTGT		114
							FMN-isoalloxazine-ring	
ATR1	AEGFAKALSE	EIKARYEKAA	VKVIDLDDYA	ADDDQYEEKL	KKETLAFFCV	ATYGDGPTD		155
ATR2	AEGFAKALGE	EAKARYEKTR	FKIVLDDYA	ADDDEYEEKL	KKEDVAFFFL	ATYGDGPTD		175
C. roseus	AEGFAKALAE	EAKARYEKAV	IKVIDIDDDYA	ADDEEYEEKF	RKETLAFFIL	ATYGDGPTD		174
							FMN-isoalloxazine-ring	
ATR1	NAARFYKWFT	EENERDIKIQ	QLAYGVFALG	NRQYEHFNKI	GIVLDEELCK	KGAKRLIEVG		215
ATR2	NAARFYKWFT	EGNDRGEWLK	NLKYGVFGLG	NRQYEHFNKV	AKVDDILVE	QGAQLRVQVG		235
C. roseus	NAARFYKWFV	EGNDRGDWLK	NLQYGVFGLG	NRQYEHFNKI	AKVDEKVAE	QGGKRIVPLV		234
							cytochrome c	
ATR1	LGDDDQSIED	DFNAWKESLW	SELDKLLKDE	DDKSVATPYT	AVIPEYRVVT	HDPRT----		271
ATR2	LGDDDQCIED	DFTAWREALW	PELDTILREE	GDTAVATPYT	AAVLEYRVSI	HDSEDAKFND		295
C. roseus	LGDDDQCIED	DFAAWRENVW	PELDNLLRDE	DDTVSTTYT	AAIPEYRVVF	PDKSDSLISE		294
							FAD-pyrophosphate	
ATR1	TQKSMESNVA	NGNTTIDIHH	PCRVDVAVQK	ELHTHESDRS	CIHLEFDISR	TGITYETGDH		331
ATR2	INMANGNGY-	---TVFDAQH	PYKANVAVKR	ELHTPESDRS	CIHLEFDIAG	SGLTYETGDH		351
C. roseus	AN-GHANGYA	NGNTVYDAQH	PCRSNVAVRK	ELHTPASDRS	CTHLDFDIAG	TGLSYGTGDH		353
							FAD-isoalloxazine-ring	
ATR1	VGUYAENHVE	IVVEAGKLLG	HSLDLVFSIH	ADKEDGSPLE	SA-VPPPPFP	PCTLTGTGLAR		390
ATR2	VGVLCDNLSE	TVDEALRLLD	MSPDITYFSLH	AEKEDGTPIS	-SSLPPPPF-	PCNLRTALTR		409
C. roseus	VGUYCDNLSE	TVEEAERLLN	LPPEYFSLH	ADKEDGTPLA	GSSLPPPPF-	PCTLRALTR		412
							FAD-isoalloxazine-ring	
ATR1	YADLLNPPRK	SALVALAAYA	TEPSEAEKLK	HLTSPDGKDE	YSQWIVASQR	SLLEVMAAFP		450
ATR2	YACLLSSPKK	SALVALAAHA	SDPTEAERLK	HLASPAGKDE	YSKWVVESQR	SLLEVMAEFP		469
C. roseus	YADLLNTPKK	SALLALAAYA	SDPNEADRKL	YLASPAGKDE	YAQSLVANQR	SLLEVMAEFP		472
							FAD-isoalloxazine-ring	
ATR1	SAKPPLGVFF	AAIAPRLQPR	YYSISSPRL	APSRVHVTS	LVYGPPTGR	IHKGVCSTWM		510
ATR2	SAKPPLGVFF	AGVAPRLQPR	FYSISSPKI	AETRIHVTCA	LVYEKMPTR	IHKGVCSTWM		529
C. roseus	SAKPPLGVFF	AAIAPRLQPR	FYSISSPRM	APSRHVVTCA	LVYEKTPGGR	IHKGVCSTWM		532
							NADPH-ribose, pyrophosphate	
ATR1	KNAVPAEKSH	ECSGAPIFIR	ASNFKLPSNP	STPIVMVGP	TGLAPFRGFL	QERMALKEDG		570
ATR2	KNAVPEYKSE	NCSSAPIFVR	QSNFKLPSDS	KVPIIMIGPG	TGLAPFRGFL	QERLALVESG		589
C. roseus	KNAIPLEESR	DCSWAPIFVR	QSNFKLPADP	KVPVIMIGPG	TGLAPFRGFL	QERLALKEEG		592
							NADPH-ribose, pyrophosphate	
ATR1	EELGSSLLFF	GCRNRQMDFI	YEDELNNFVD	QGVISELIMA	FSREGAQKEY	VQHKMMEKAA		630
ATR2	VELGPSVLFF	GCRNRMDFI	YEEELQRFVE	SGALAELSVA	FSREGPTKEY	VQHKMDKAS		649
C. roseus	AELGTAVFFF	GCRNRKMDYI	YEDELNHFLE	IGALSELLVA	FSREGPTKQY	VQHKMAEKAS		652
							NADPH-nicotineamide	
ATR1	QVWDLIKEEG	YLYVCGDAKG	MARDVHRTLH	TIVQEQEVS	SSEAEIVKK	LQTEGRYLRD		690
ATR2	DIWNMISQGA	YLYVCGDAKG	MARDVHRSLLH	TIAQEQQSMD	STKAEGFVKN	LQTSGRYLRD		709
C. roseus	DIWRMISDGA	YVYVCGDAKG	MARDVHRTLH	TIAQEQQSMD	STQAEQFVKN	LQMTGRYLRD		712
ATR1	VW							692
ATR2	VW							711
C. roseus	VW							714

Figure 4.2: Amino acid sequence alignment between the CPR from *C. roseus* and the two Arabidopsis reductases ATR1 and ATR2 modified from Mizutani and Otha 1998³⁹¹

The typical absorption maxima of flavoproteins³⁹⁷ at 455 and 380 nm, with the 455 nm peak disappearing when reduced with dithionite had been shown by Mizutani and Ohta³⁹¹ for ATR1 and ATR2.

The ATR1 and ATR2 proteins were recombinantly expressed in *Saccharomyces cerevisiae*¹⁶⁶ and *Spodoptera frugiperda*³⁹¹ insect cells and shown to have activity *in vivo* and *in vitro* with cytochrome c and with the Arabidopsis CYP73A5 (cinnamate-4-hydroxylase). Microarray analysis (<https://www.genevestigator.com/gv/>) showed that ATR1 is expressed constitutively at all developmental stage whereas ATR2 has more fluctuation in its expression pattern and showed the highest expression in young flowers (Figure 4.3). Expression of ATR3 is at least six times lower at all developmental stages than ATR1 or ATR2.

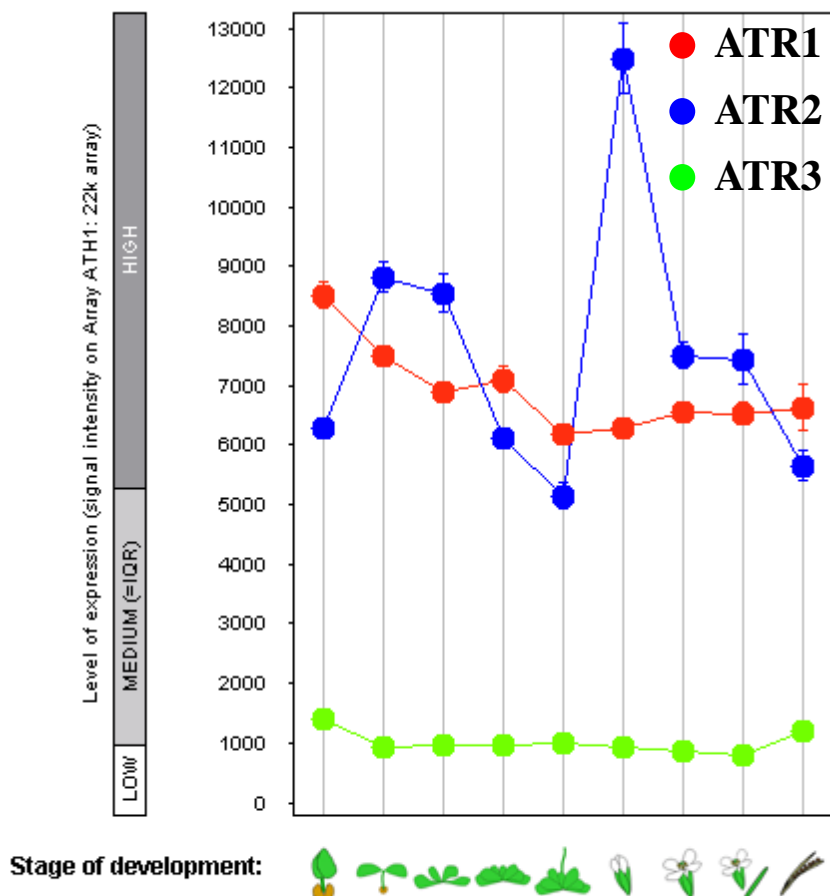


Figure 4.3: Expression levels of the three Arabidopsis cytochrome P450 reductases ATR1, ATR2 and ATR3 during the plant life cycle

(from genevestigator, <https://www.genevestigator.com/gv/>, 15/12/2011)

The full length ATR1 contains 692 amino acids with an estimated size of 77 kDa and ATR2 712 amino acids (79 kDa).¹⁶⁶ The molecular weight of both reductases is similar to that of other higher plant CPRs.^{388,398,399}

4.2 Objectives

The common host for recombinant expression of plant cytochromes P450 as well as for the partnering reductases are yeast cells (*S. cerevisiae*) or insect cells. Both are eukaryotic systems which provide all the post-translational machinery for the production of proteins associated with eukaryotic membranes. Expression in *E. coli*, however, has the advantages that it is an easy to use and an inexpensive expression system. Interestingly, Barnes *et al.* 1991³¹⁸ reported that P450 reactions are supported in *E. coli* without the additional expression of a specific reductase. The use of *E. coli* also has disadvantages. It is a prokaryotic expression system and expression can be hindered by different codon bias. Nevertheless, soluble enzyme has been produced in bacteria following deletion of the hydrophobic N-terminus encoding the membrane anchor region.⁵⁷

In this chapter, the two membrane-associated reductases ATR1 and ATR2 were cloned from Arabidopsis and modified at the N-terminus to increase solubility. The truncated versions (ATR1tr and ATR2tr) were overexpressed in *E. coli*, purified and activities compared to find the most effective reductases for expression in *E. coli*. Furthermore, the biochemistry of both reductases was studied.

4.3 Results

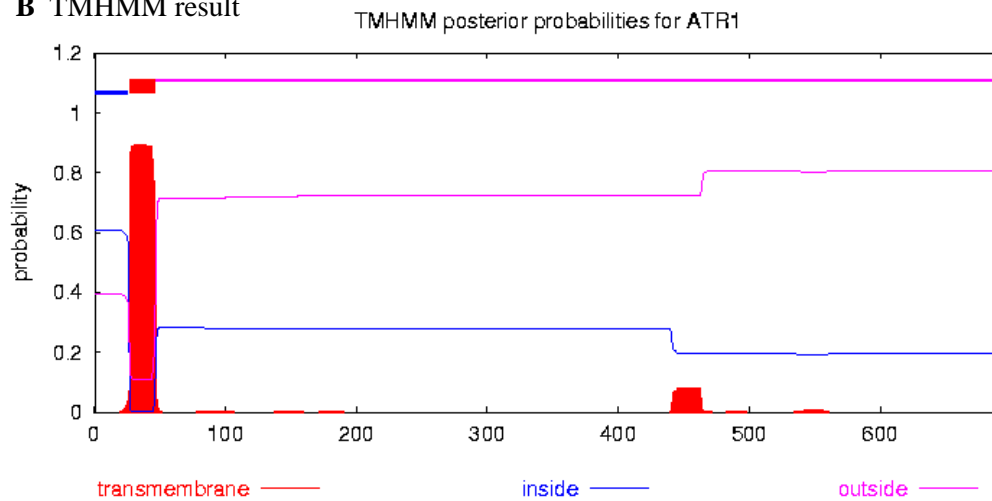
4.3.1 Primer design for the N-terminal membrane anchor truncated ATR1 and ATR2

The two Arabidopsis P450 reductases ATR1 (77 kDa) and ATR2 (79 kDa) have both a hydrophobic N-terminal region in the amino acid sequence, which allows association with a membrane. The amino acid sequence of both reductases was analysed using the software TMHMM and SignalP3.0 (Chapter 2.8.1) (Figure 4.4) and the hydrophobic N-termini removed (46 and 73 aa were deleted for ATR1 and ATR2, respectively).

A amino acid sequence of ATR1

MTSALYASDLFKQLKSIIMGTDSLSDVVLVIATTSALVAGFVLLWKKTTADRSGELK
 PLMIPKSLMAKDEDDDLGSGKTRVSIFFGTQTGTAEGFAKALSEEIKARYEKAARKV
 IDLDDYAADDDQYEEKLKKETLAFFCVATYGDGEPDNDNAARFYKWFTEENERDIKLLQQL
 AYGVFALGNRQYEHFNKIGIVLDEELCKKGAKRLIEVGLGDDDDQSIEDDFNAWKESLWS
 ELDKLLKDEDDKSVATPYTAVIPEYRVVTHDPRFTTQKSMESNVANGNTTIDIHPCRV
 DVAVQKELHTHESDRSCIHLEFDISRGTITYETGDHVGVAENHVEIVEEAGKLLGHSL
 DLVFSIHADKEDGSPLESAVPPPPGPGCTLGTGLARYADLLNPPRKSALVALAAYATEP
 SEAEKLLHLTSPDGKDEYSQWIVASQRSLEVMMAAFPSAKPPLGVFFAAIAPRLQPRYY
 SIISSPRLAPSRVHVTALVYGPTPTGRIHKGVCSTWMKNAVPAEKSHCESGAPIFIRA
 SNFKLPSNPSTPIVMVGPGLAPFRGFLQERMALKEDGEELGSSLLFFGCRNRQMDFI
 YEDELNNFVDQGVISELIMAFSREGAQKEYVQHKMMEKAAQVVDLIKEEGYLYVCGDAK
 GMARDVHRTLHTIVQEQEGVSSSEAEAIKKLQTEGRYL RDVW

B TMHMM result



C SignalP result

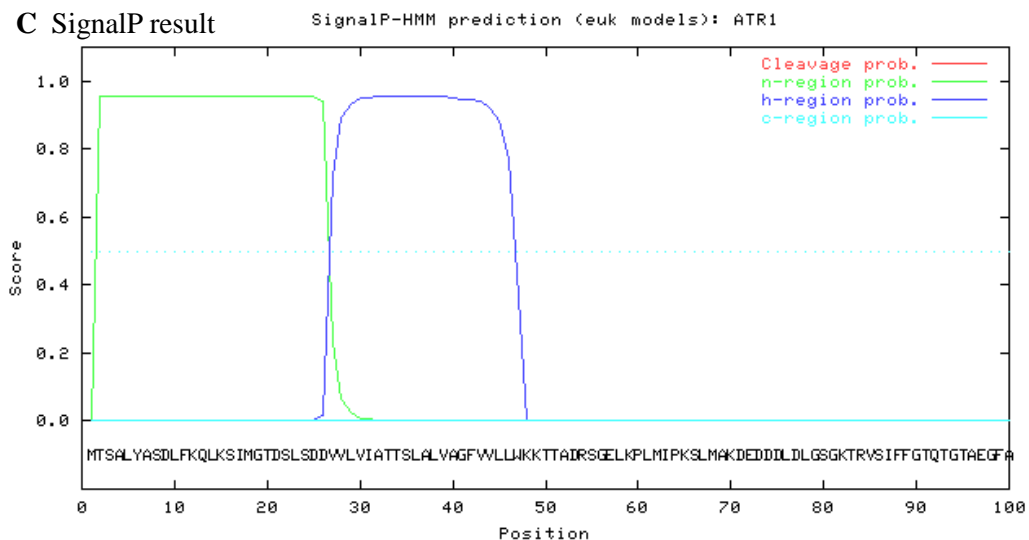


Figure 4.4: Amino acid sequence analysis of ATR1 N-terminus.

A full length amino acid sequence of ATR1, **B** TMHMM blot for analyzing the amino acid sequence of ATR1, which indicated a membrane region for around the first 50 amino acids, **C** result of SignalP 3.0 analysis (cleavage prob = probability of cleavage site, n-region prob = probability of N-terminus of the signal peptide, h-region prob = probability of hydrophobic region of signal peptide, c-region prob = probability of C-terminus of signal peptide)

4.3.2 Cloning of ATR1tr and ATR2tr

Genes encoding Arabidopsis reductases ATR1 and ATR2 were cloned following RNA extraction and reverse transcription into cDNA. The N-terminal truncated cDNAs of ATR1tr and ATR2tr were amplified using PCR (Chapter 2.8.2) and the truncated reductases were cloned into the LIC-vector using Ligation Independent Cloning (Chapter 1.1).

4.3.3 Expression of ATR1tr and ATR2tr in Escherichia coli

ATR1tr and ATR2tr were expressed at 20 °C in the two different *E. coli* expression strains Rosetta 2 (DE3) and Rosetta gami 2 (DE3) (conditions see Chapter 2.10.1).

The induced culture showed inhibited cell growth in comparison to the uninduced culture (Figure 4.5).

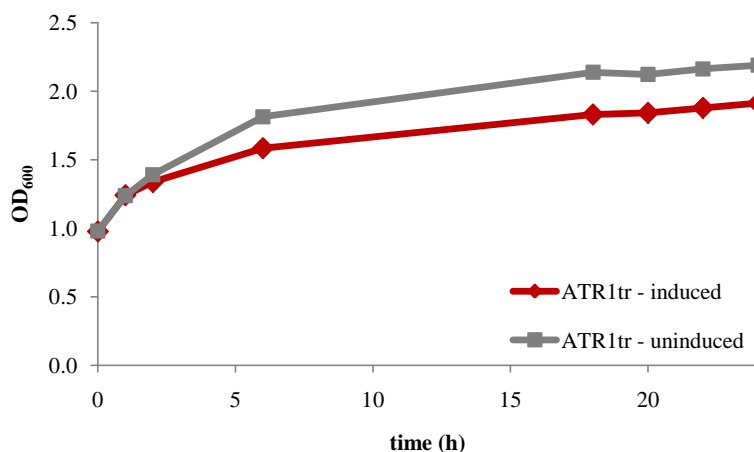


Figure 4.5: Cell growth (OD₆₀₀) after induction of ATR1tr in *E. coli* Rosetta 2 grown in LB medium

The expression of the 72 kDa ATR1tr in Rosetta 2 (DE3) cells was visible by SDS-PAGE (Figure 4.6A) and no expression could be detected in the uninduced control (Figure 4.6B). No overexpression of either reductases could be achieved when using strain Rosetta gami 2 (DE3), so Rosetta 2 (DE3) was used for the following experiments. Low amounts of ATR1tr could be expressed in Rosetta 2 (DE3) cells when M9 minimal media was used (Figure 4.6C and D).

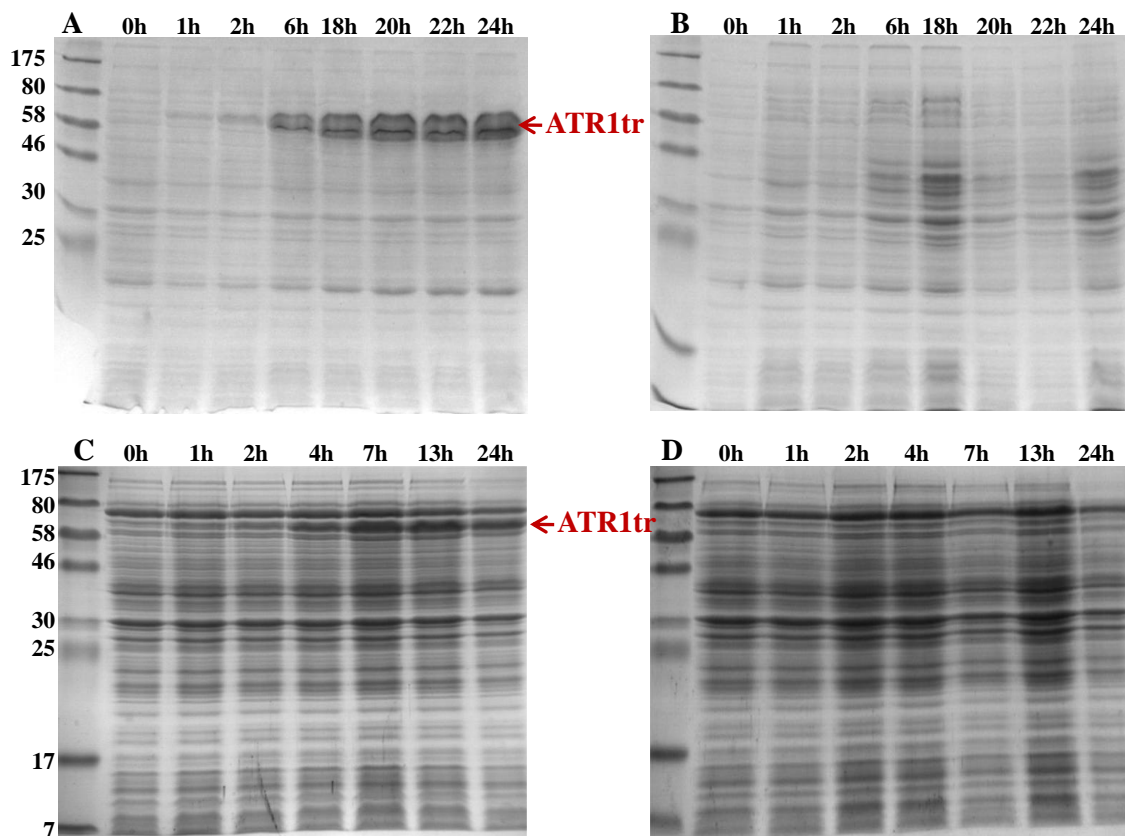


Figure 4.6: Analysis of crude extract by SDS PAGE

A induced and **B** uninduced *E. coli* Rosetta 2 (DE3) cells expressing ATR1tr (72 kDa) in LB medium and **C** induced and **D** uninduced *E. coli* Rosetta 2 (DE3) cells expressing ATR1tr in M9 minimal medium

ATR1tr was purified with Ni-resin material (Chapter 2.10.4). Purification was monitored using SDS PAGE (Figure 4.7) and showed that ATR1tr was partly soluble, which was purified using Ni-resin material. ATR1tr precipitated during dialysis and was again insoluble. To overcome these problems, different solubilisation buffers were tested (Chapter 2.10.2).

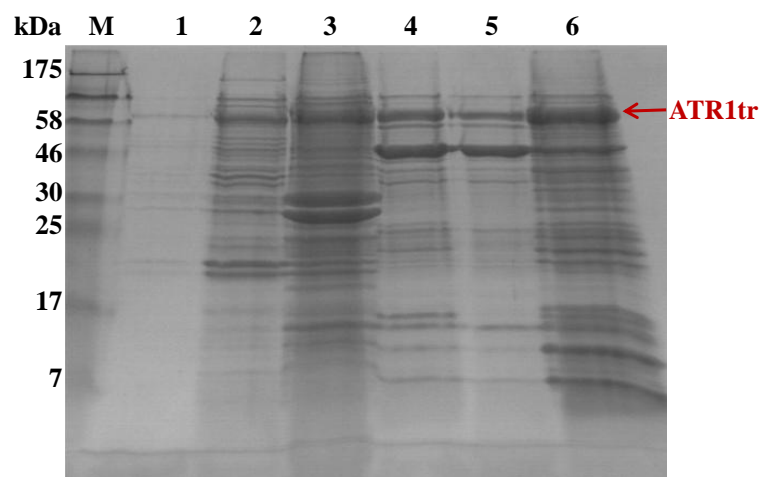


Figure 4.7: SDS PAGE analysis of ATR1tr (72kDa) during Ni-affinity purification
M marker, **1** whole cells prior sonication, **2** soluble protein fraction, **3** insoluble protein fraction, **4** eluted protein, **5** dialysed protein and **6** precipitated protein fraction after dialysis

4.3.4 Solubilisation of overexpressed ATR1tr

Thirty different buffers (Chapter 2.10.2) were tested to increase the solubility of the overexpressed ATR1tr and ten out of 30 buffers increased the concentration of soluble protein (Figure 4.8).

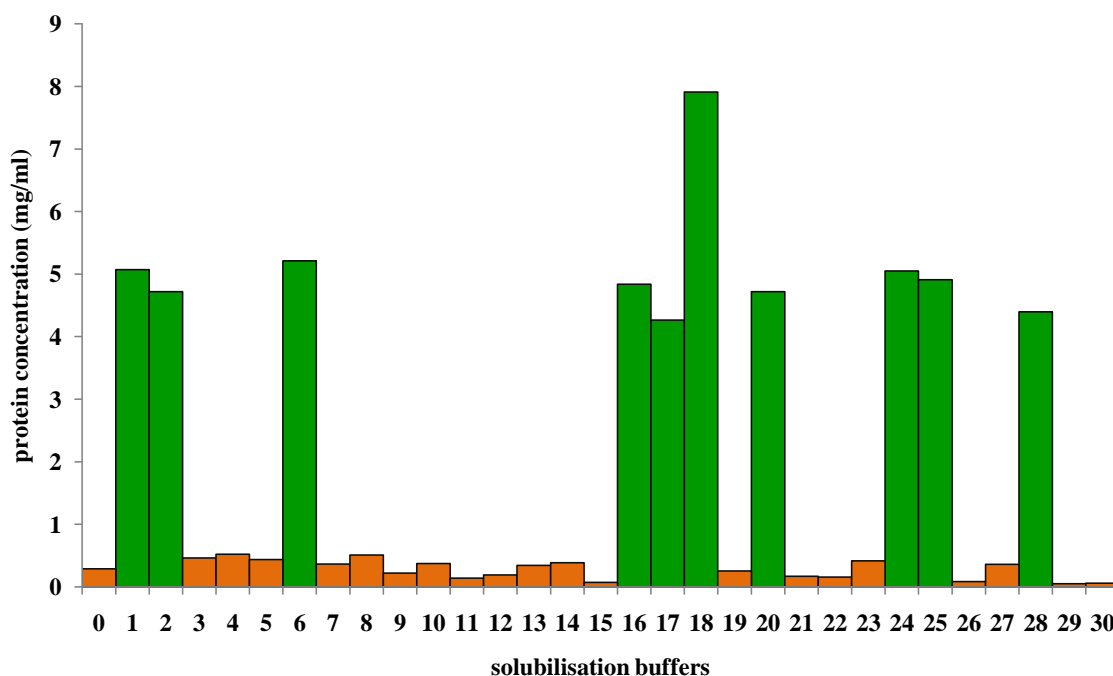


Figure 4.8: Protein concentration of the soluble total protein after overexpression in *E. coli* Rosetta 2 (DE3) using different solubilisation buffers 0-30

Protein fractions from all 30 buffers were analysed using SDS PAGE. The strongest signal for ATR1tr was obtained when using the buffers 1, 2, 6, 16, 17, 18, 20, 24, 25 and 28 (Figure 4.9). Western blot probing using anti-His antibodies confirmed these results (Figure 4.10). No signal was detected for the negative control containing the empty plasmid when resuspended in buffer 0 or solubilised in buffer 18 (lane 0c and 18c, respectively in Figure 4.10).

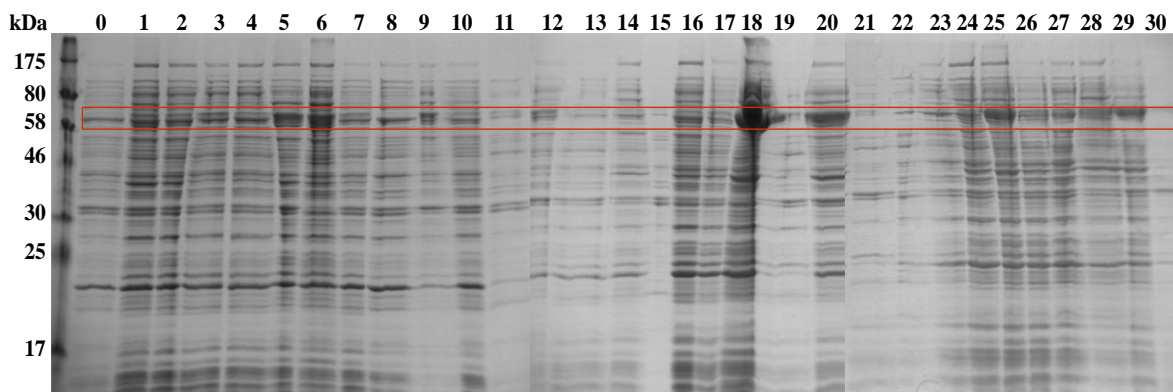


Figure 4.9: SDS PAGE analysis of the total soluble protein using solubilisation buffer 0-30. Red box show the overexpressed ATR1tr (72 kDa)

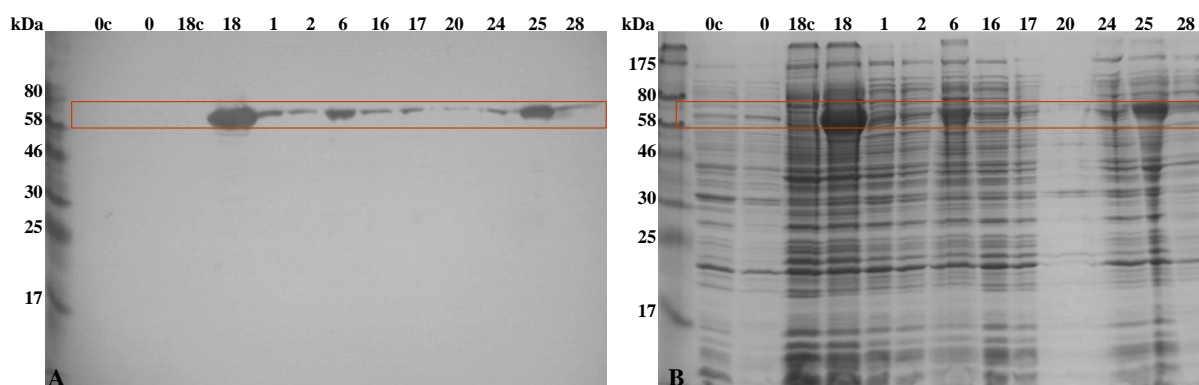


Figure 4.10: Analysis of ATR1tr after sonication in different solubilisation buffers
A Western blot analysis and **B** SDS PAGE of soluble protein fraction. Red boxes show the overexpressed ATR1tr. (Lane 0c = negative control in buffer 0, 18c = negative control in buffer 18, 0-28 = overexpressed ATR1tr in different solubilisation buffers)

4.3.5 Purification of ATR1tr and ATR2tr in solubilisation buffer 18A

ATR1tr and ATR2tr were overexpressed under the same conditions described in Chapter 2.10.1 and using buffer 18 to assist in the solubilisation of protein. However, buffer 18 contains EDTA, making it unsuitable for the purification with His-Select Nickel Affinity Gel column. EDTA can scavenge metal ions and

therefore complexes the nickel ions so that the His-tagged protein cannot bind. Therefore, buffer 18 without EDTA (buffer 18A) was used for the purification of ATR1tr and ATR2tr (Chapter 2.10.5).

A SDS PAGE analysis was performed after the purification of both reductases and ATR1tr and ATR2tr were detected (red box in gel A and B, Figure 4.11). The empty vector transformed into Rosetta 2 (DE3) was used as negative control (Figure 4.11C).

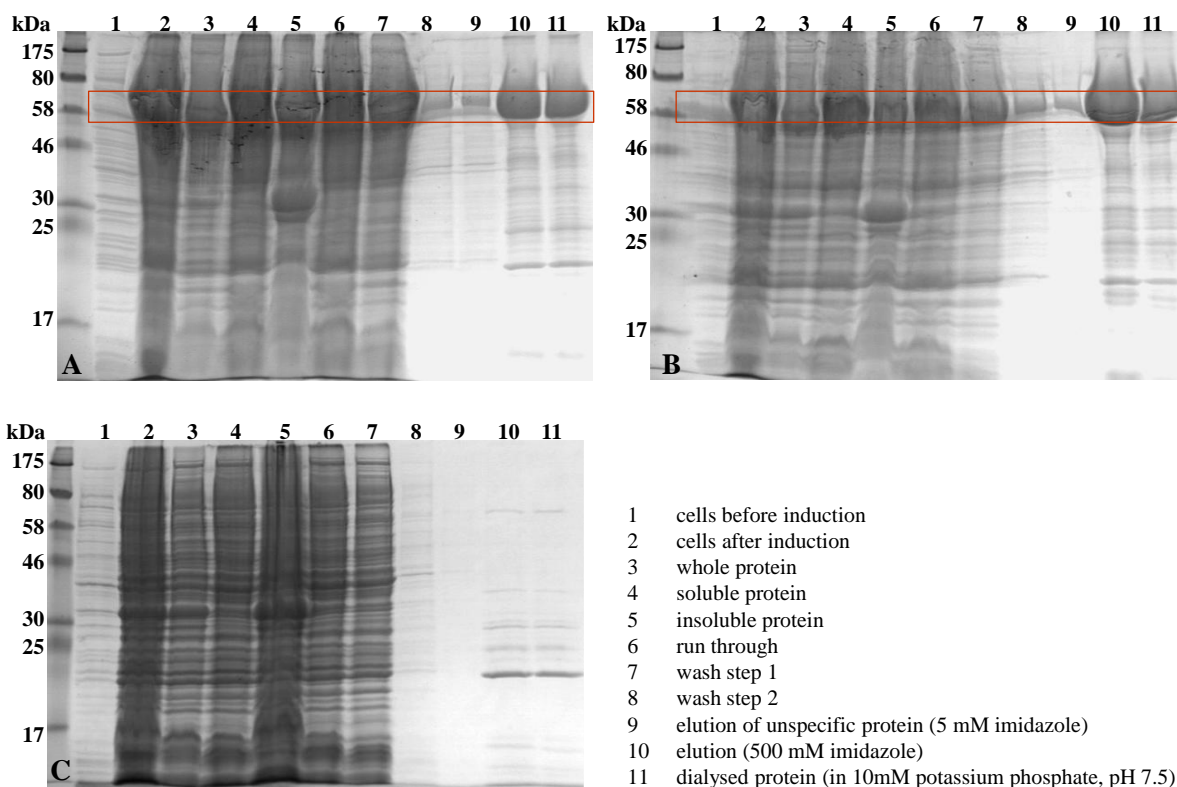


Figure 4.11: SDS PAGE Analysis of the purification of A) ATR1tr (72 kDa), B) ATR2tr (71 kDa) and C) negative control (empty vector expressed in *E. coli* Rosetta 2 (DE3))

4.3.6 Characterisation of Arabidopsis P450 reductase ATR2tr

4.3.6.1 Activity assay with cytochrome c

The activity of ATR1tr and ATR2tr with cytochrome c was tested for the two different co factors NADH and NADPH following the protocol described in (Chapter 2.15.1.2) to analyse the impact on the activity. Both Arabidopsis reductases displayed greater activity with NADPH over NADH as cofactor (Figure 4.12).

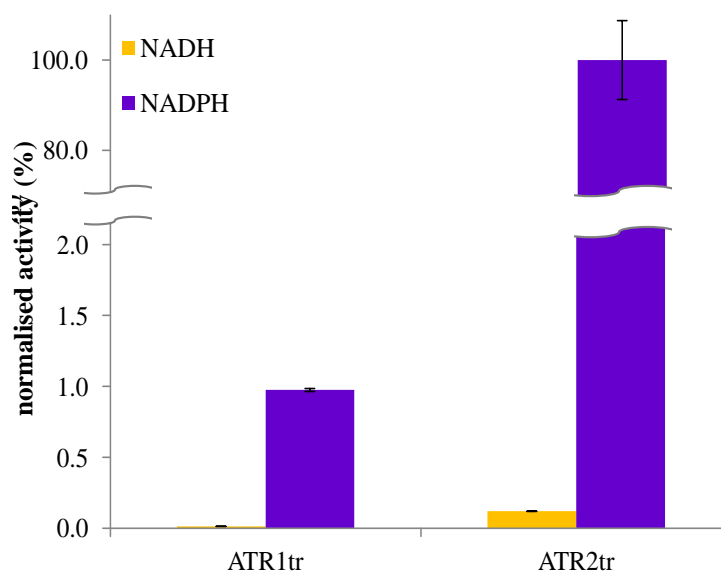


Figure 4.12: ATR1tr and ATR2tr activity dependence on the cofactor NADH and NADPH

Assay conditions: 1mg/ml reductase, 50 μ M cytochrome c, 110 μ M NAD(P)H in 300 mM potassium phosphate buffer (pH 7.7). The error bars represent the mean of three independent replicas \pm standard deviation.

ATR1tr and ATR2tr activity was compared with two commercial available reductases (ferredoxin reductase from spinach and cytochrome c reductase from porcine heart). Both, ATR1tr and ATR2tr, showed higher activity in comparison to the positive control reductase (Figure 4.13). ATR2tr was diluted from 1 mg/ml to 0.01 mg/ml to get a linear rate. The activity of cytochrome c reductase was not significant due to the fact that it showed a higher activity with the cofactor NADH than with NADPH.

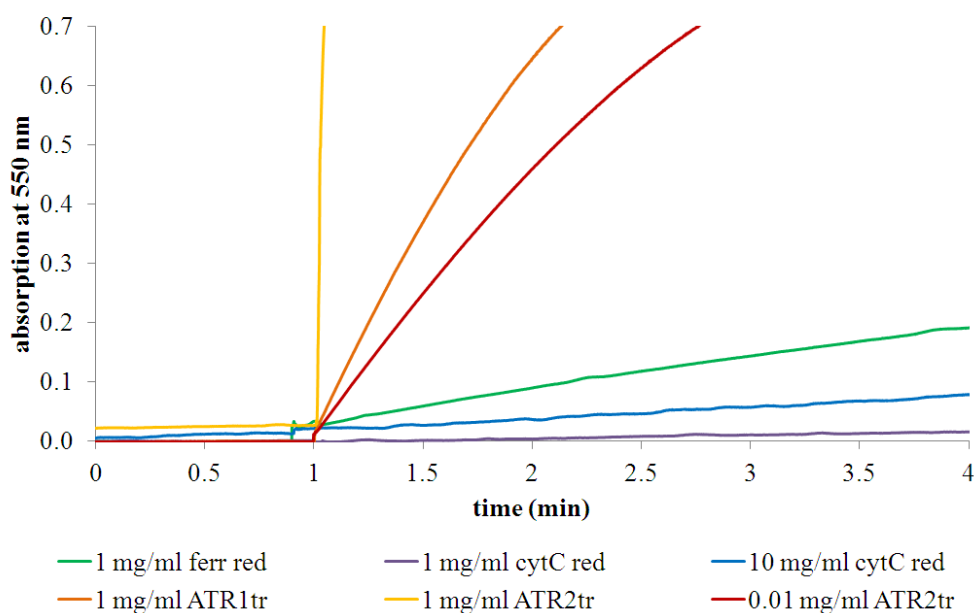


Figure 4.13: Cytochrome c conversion by different reductases in presence of the cofactor NADPH

Assay conditions: reductase (amount, see legend), 50 μ M cytochrome c in 300 mM potassium phosphate buffer (pH 7.7). The reaction was started after one minute by adding 110 μ M NADPH (ferr red = ferredoxin reductases from spinach, cytC red = cytochrome c reductase from porcine heart).

ATR2tr was with a conversion of 1500 μM cytochrome *c*/mg ATR2tr 20 times more active than ATR1tr (68 μM cytochrome *c*/min/mg ATR1tr, Figure 4.14). Porcine cytochrome *c* reductase and spinach ferredoxine reductase was used as positive control and showed a conversion of 0.5 μM and 7.5 μM cytochrome *c*/min/mg reductase, respectively. The low activity of cytochrome *c* reductase is caused by the cofactor NADPH. Higher values were detected by using the cofactor NADH.

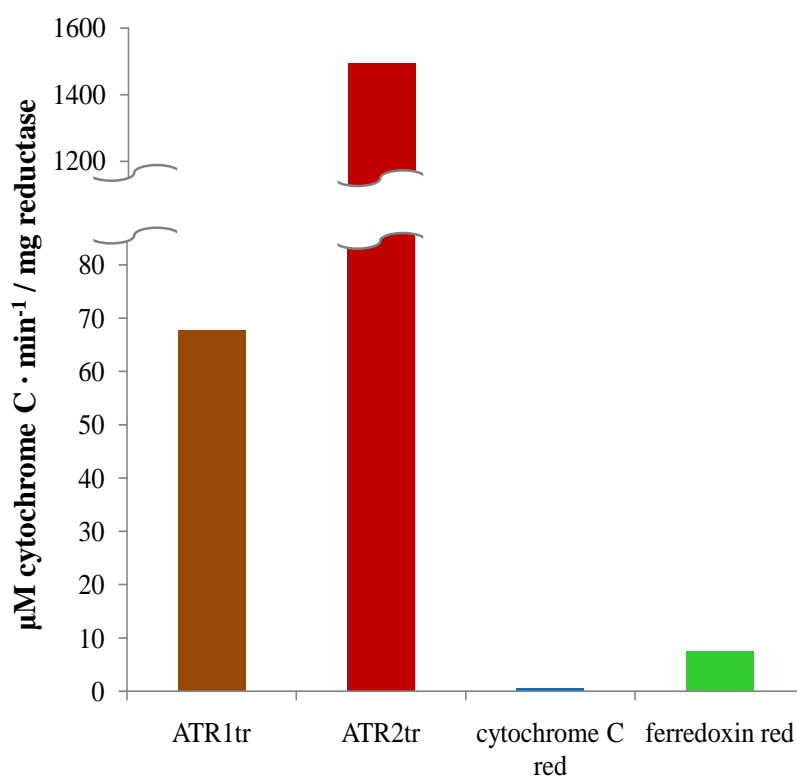


Figure 4.14: Cytochrome *c* conversion by different reductases in presence of the cofactor NADPH

ATR1tr = N-terminal truncated Arabidopsis reductase ATR1, ATR2tr = N-terminal truncated Arabidopsis reductase ATR2, cytochrome C red = cytochrome *c* reductase from porcine heart, ferredoxin red = ferredoxin reductase from spinach

4.3.6.2 Temperature and pH optima of ATR1tr and ATR2tr

Temperature and pH optima for ATR1tr and ATR2tr were performed as described in Chapter 2.15.1.3. The temperature optimum of ATR1tr and ATR2tr was determined to be 40 °C (Figure 4.15).

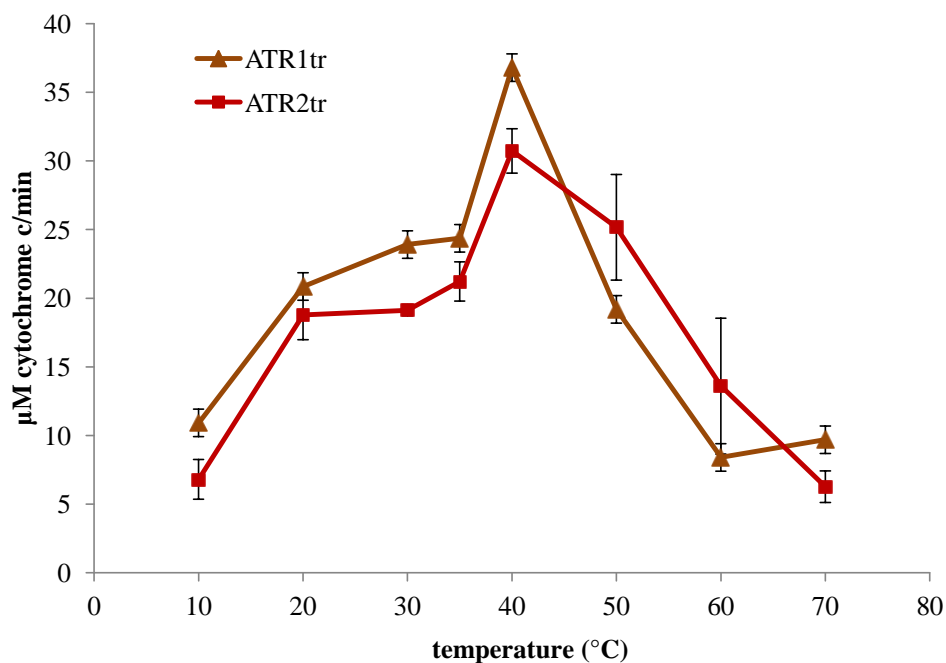


Figure 4.15: Temperature optimum for ATR1tr (1 mg/ml) and ATR2tr (0.01 mg/ml)
The error bars represent the mean of three independent replicas \pm standard deviation

The pH optima of both Arabidopsis reductases was analysed in Britton Robinson buffer (Chapter 2.15.1.3) covering a pH range of pH 3.4 to 11.0. The extinction coefficient of cytochrome c ($\epsilon(550\text{nm}) = 21 \text{ mM}^{-1}\text{cm}^{-1}$) was used to calculate the activity.

The pH optima of ATR1tr (100 $\mu\text{g/ml}$) and ATR2tr (1 $\mu\text{g/ml}$) were detected in 300 mM Britton Robinson buffer (Chapter 2.15.1.3). The optima of ATR1tr and ATR2tr were found to be pH 7.0 and pH 8.0, respectively (Figure 4.16).

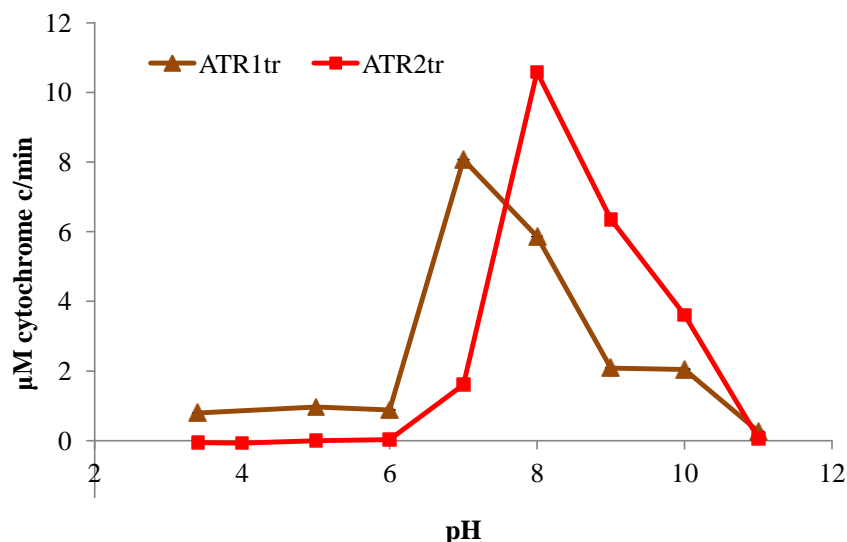


Figure 4.16: Activity of 100 µg/ml ATR1tr and 1 µg/ml ATR2tr in 300 mM Britton Robinson buffer (1:1:1 mixture of boric acid, phosphoric acid and acetic acid) at different pH values

The error bars represent the mean of three independent replicas \pm standard deviation.

The reductase activity of ATR2tr was also tested in citrate and phosphate buffer, covering a pH range of 4.0 to 7.6 (Chapter 2.15.1.3). ATR2tr showed approximately 10% more activity in the citrate and phosphate buffer when compared to Britton Robinson buffer (Figure 4.17).

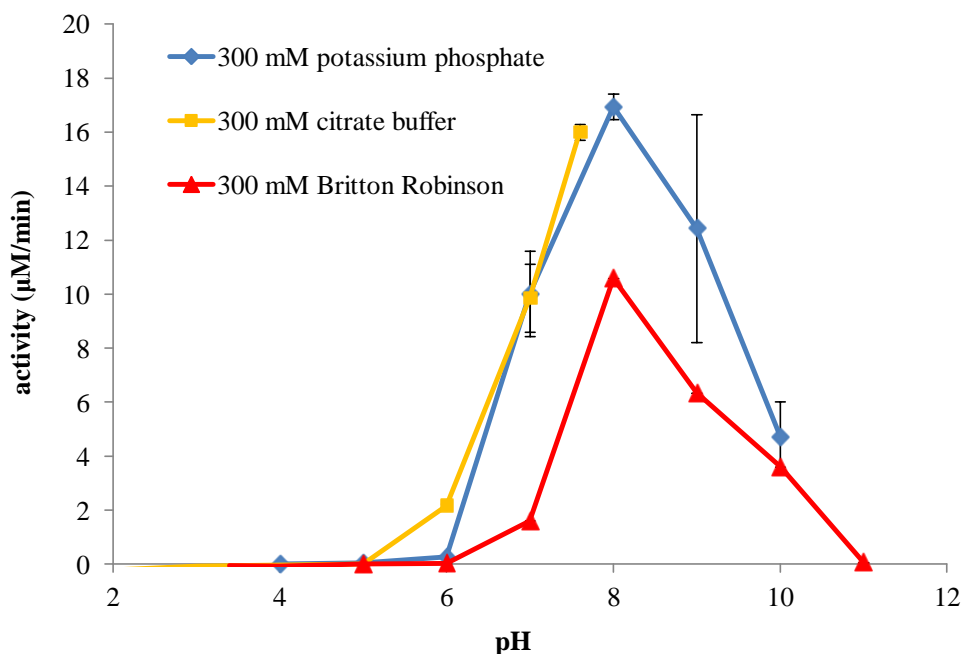


Figure 4.17: Activity of 1 µg/ml ATR2tr in diverse buffers covering different pH values

The error bars represent the mean of three independent replicas \pm standard deviation.

The activity of cytochrome c as well as the stability of the cofactor NADPH, both part of the reductase activity assay, are also pH dependent and can therefore change the pH optima of the two reductases.

Cytochrome c is changing the conformational state dependent on the pH and has an isoelectric point (number of positive and negative charges of the protein are equal) around pH 10.⁴⁰⁰⁻⁴⁰³ NADPH degrades at low pH values (Figure 4.18) and so fewer electrons are available for the reaction. Therefore, the reductases activity at a pH lower than pH 6.0 was reduced through the instability of NADPH.

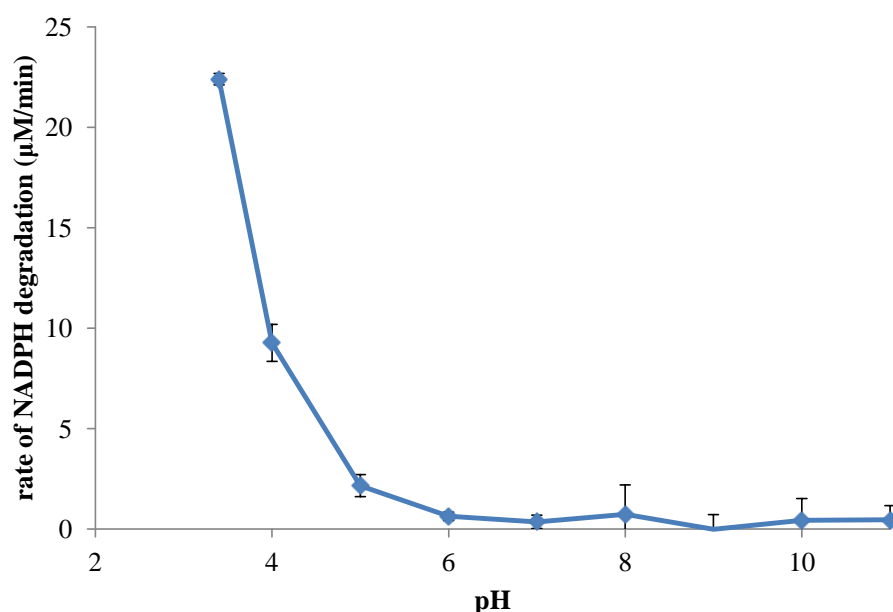


Figure 4.18: Stability of the cofactor NADPH at different pH values

Assay was performed using 50 µM cytochrome c and 110 µM NADPH in 300 mM potassium phosphate buffer (pH 7.7). The error bars represent the mean of three independent replicas \pm standard deviation.

4.3.6.3 Kinetic studies of the reductases ATR1tr and ATR2tr

The kinetic data for cytochrome c reduction were accomplished following the published protocol from Hull and Calenza³⁵¹ (Chapter 2.15.1.4). V_{\max} and K_M values were determined using Michaelis-Menten kinetics (software: GraFit) (Table 4.1). ATR2tr followed the common Michaelis-Menten kinetic, whereas ATR1tr was inhibited by the substrate cytochrome c for concentrations higher than 100 µM (Figure 4.19). The sample with the highest substrate concentration (150 µM cytochrome c) was ignored for the calculation of the kinetic data for ATR1tr by Michaelis-Menten (Figure 4.19A).

Table 4.1: Kinetic data for ATR1tr and ATR2tr (calculated by the program GraFit)

reductase	V_{\max} ($\mu\text{M}/\text{min}$)	K_M (μM)	inhibition constant	k_{cat} (s^{-1})
ATR1tr (Michaelis-Menten)	51 ± 5	23 ± 6		0.1 ± 0.02
ATR1tr (substrate inhibition)	261 ± 90	170 ± 68	21 ± 9	0.3 ± 0.1
ATR2tr (Michaelis-Menten)	38 ± 2	16 ± 3		5.0 ± 0.6

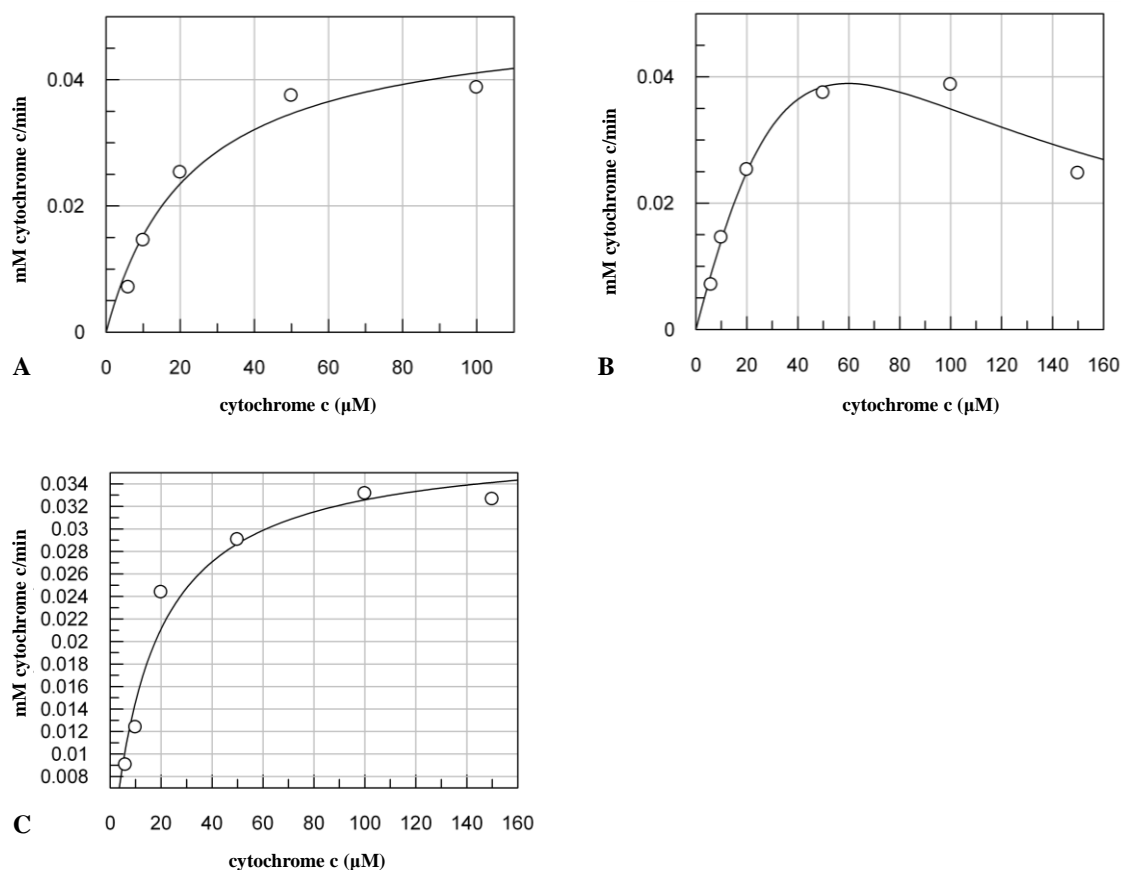


Figure 4.19: Michaelis-Menten blots by GraFit for A) ATR1tr by Michaelis-Menten equation and B) ATR1tr by equation for substrate inhibition and C) ATR2tr by Michaelis-Menten equation

To illustrate the accuracy of the kinetic data, the direct linear blot from Eisenthal and Cornish-Bowden was used.⁴⁰⁴ Here the median of all samples is used to estimate the K_M and V_{max} . As shown in Figure 4.20A the intersection for ATR1tr did not match as good as for ATR2tr (Figure 4.20).

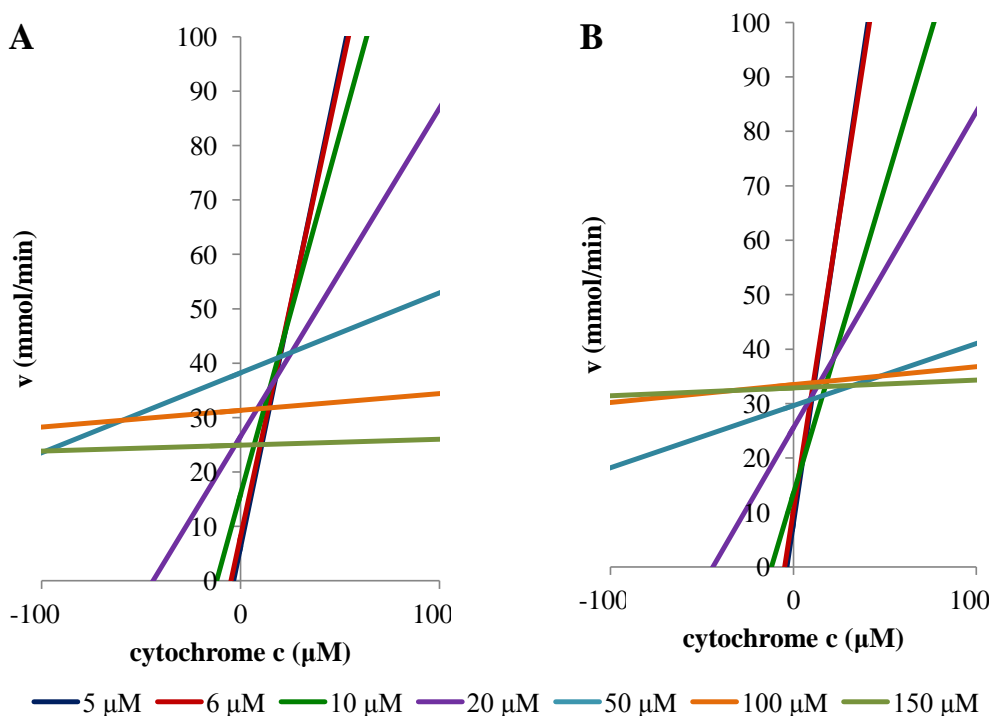


Figure 4.20: Cornish-Bowden blot for A) ATR1tr and B) ATR2tr
The different lines represent substrate concentrations between 4 μM and 150 μM cytochrome c.

The specific activity for ATR1tr considering substrate inhibition was $50.5 \mu\text{M}\cdot\text{min}^{-1}\cdot\text{mg}^{-1}$ and for ATR2tr $3770 \mu\text{M}\cdot\text{min}^{-1}\cdot\text{mg}^{-1}$.

4.3.6.4 Spectrophotometric characterisation of ATR2tr

P450 reductases have a typical absorption spectrum with a maximum at 375 and 450 nm. Dialysed ATR2tr (5.1 mg/ml in 10 mM potassium phosphate buffer, pH 7.5) was characterised for the presence of flavin by monitoring the absorption between 300 and 600 nm (Figure 4.21).

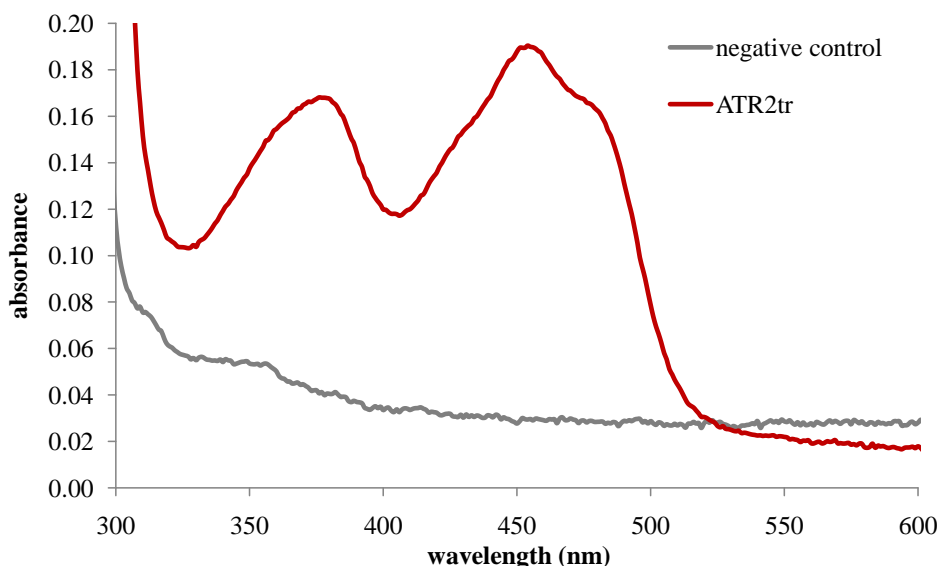


Figure 4.21: UV/Vis spectra of purified recombinant ATR2tr and negative control (expressed and purified empty vector)

The diagram illustrated a similar picture to published data with two absorption maxima, characteristic for flavins³⁹¹ at 383 and 458 nm. FMN and FAD alone have absorption maxima at around 370 and 452 nm (Figure 4.22).

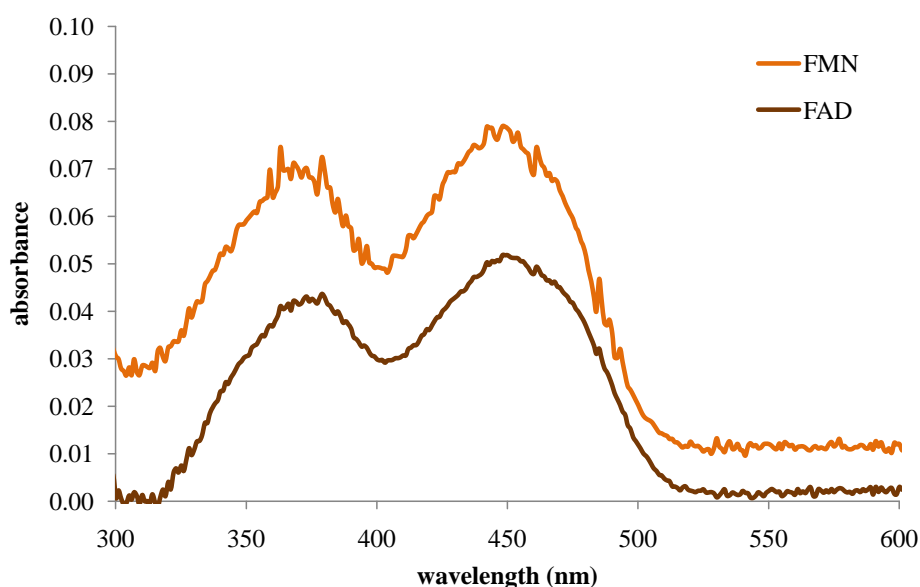


Figure 4.22: UV/Vis spectra of 10 μ M FMN and 10 μ M FAD in 50 mM potassium phosphate buffer pH 7.5

4.3.6.5 Activity test of purified ATR2tr in buffer A and B

As previously described, ATR2tr was purified using a column containing Ni-resin material, eluted with buffer 18A (100 mM Tris, 100 mM KCl and 1% Triton X-100, pH 8.2) containing 500 mM imidazole and dialysed in buffer A (50 mM potassium phosphate buffer pH 7.5). Hull and Calenza (2000) suggested another dialysis buffer of 30 mM potassium phosphate pH 7.8, 20% glycerol, 0.1 mM EDTA, 2.0 μ M FMN (called buffer B) stabilising the Arabidopsis reductase ATR2.³⁵¹

The reductase activity was tested using a cytochrome c assay following the protocol from Hull and Calenza 2000 (Chapter 2.15.1.2).³⁵¹ ATR2tr activity was inhibited in the presence of 500 mM imidazole in 100 mM Tris, 100 mM KCl and 1% Triton X-100, pH 8.2 (Figure 4.23). The highest activity for ATR2tr was obtained after the dialysis in buffer B.

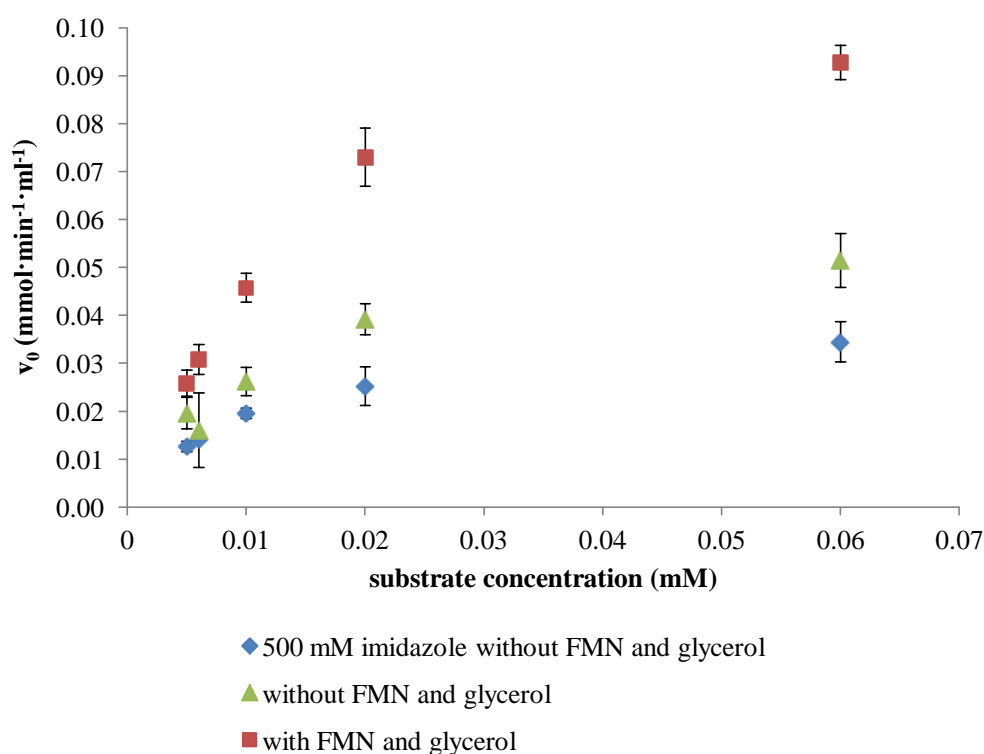


Figure 4.23: Michaelis-Menten-diagram of purified ATR2tr

In buffer 18A (100 mM Tris, 100 mM KCl and 1% Triton X-100, pH 8.2) containing 500 mM imidazole (blue rhombi), buffer A (50 mM potassium phosphate buffer pH 7.5, green triangles) and buffer B (30 mM potassium phosphate pH 7.8, 20% glycerol, 0.1 mM EDTA, 2.0 μ M FMN, red squares). The error bars represent the mean of three independent replicas \pm standard deviation.

4.3.6.6 Stability test of ATR2tr in different buffers

The reductase ATR2tr was analysed after dialysis in two different buffers: a general potassium phosphate buffer pH 7.5 (buffer A) and a potassium phosphate buffer pH 7.8 containing FMN and glycerol (buffer B). The samples were stored at four different temperatures (-80 °C, -20 °C, 4 °C and 21 °C) and the activity of ATR2tr was measured using a cytochrome c assay (Chapter 2.15.1.4).

ATR2tr was stable at 21 °C for at least two days and was inactive after less than six days independent from the storage buffer (Figure 4.24). A 75% and 50% decrease of the reductase activity was observed when stored at 4 °C in buffer A and B, respectively. ATR2tr was less stable in buffer A and lost activity steadily over time (Figure 4.24A). When ATR2tr was kept at -20 °C for 40 days, the activity was reduced to 30%, whereas storage at -80 °C meant that the activity was only reduced to 50% after the same period of time.

A 30% loss in activity of ATR2tr was observed upon freezing at -20 °C or -80 °C in buffer B; however, no further reduction in activity was found over time.

In summary, ATR2tr was more stable in buffer B due to the presence of FMN and glycerol.

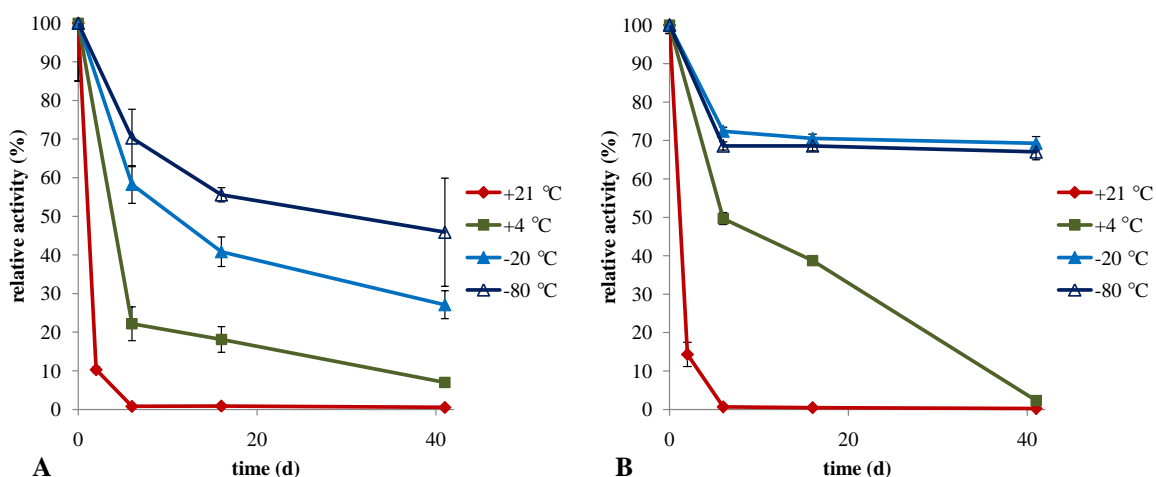


Figure 4.24: Stability of ATR2tr over time in A) buffer A (50 mM potassium phosphate buffer pH 7.5) and B) buffer B (30 mM potassium phosphate pH 7.8, 20 % glycerol, 0.1 mM EDTA, 2.0 μ M FMN)

The error bars represent the mean of three independent replicas \pm standard deviation. Sample at time 0 days was not frozen and activity measured at 21 °C.

4.4 Discussion

The two Arabidopsis reductases ATR1 and ATR2 are necessary partner enzymes for all the different P450 reactions in Arabidopsis and supply electrons in single steps from the co-factor NADPH to the heme iron in the catalytic centre of the P450 enzyme. Both reductases contain a membrane signal at the N-terminus and although active full length forms have been expressed previously in the eukaryotic hosts yeast¹⁶⁶ and insect cells³⁹¹, the proteins were predominantly insoluble. Activity assays established high stability for ATR1 while activity for ATR2 rapidly decreased when expressed in a eukaryotic host.³⁵⁰ Therefore, to increase the amount of soluble protein the hydrophobic N-termini of both enzymes were removed in this project and the two truncated reductases ATR1tr and ATR2tr (lacking 46 and 73 amino acids, respectively) expressed in *E. coli*.

Different *E. coli* expression strains were tested and the *E. coli* Rosetta 2 (DE3) strain was found to produce the highest yield for both truncated reductases. The recombinant, expressed enzymes were partly insoluble, although the N-terminus was deleted, and so 30 different solubilisation buffers were tested with ATR1tr to increase the solubility. The highest level of soluble ATR1tr, as confirmed by SDS PAGE and western blot analysis, was seen in buffer 18 containing 100 mM Tris, 100 mM KCl, 2 mM EDTA and 1% Triton X-100 (pH 8.2).

Both ATR1tr and ATR2tr were subsequently purified in buffer 18A (buffer 18 without the addition of EDTA). The absence of EDTA in buffer 18A did not affect the ability to solubilise ATR1tr and ATR2tr, as this characteristic was due to the high concentration (1%) of the detergent Triton X-100. Triton X-100, a non-ionic detergent used to solubilise membrane proteins.⁴⁰⁵

The temperature optima for both reductases was found to be at 40 °C and pH optima of ATR1tr and ATR2tr were pH 7.0 and pH 8.0, respectively. This pH optimum was also found to be similar for other plant reductases, such as the CPR from *Coleus blumei* with pH 7.5.³³⁷

Activity studies on the two N-terminal truncated Arabidopsis reductases showed that both were active with cytochrome c and NADH or NADPH, whereas the activity with NADPH as cofactor was 75 and 830 times higher for ATR1tr and ATR2tr, respectively. That NADPH is the more effective cofactor is not always the case, cytochrome c activity was better supported by NADH for example for

the CPR from cotton and the CPR from pea.^{406,407} Recombinant expressed ATR2tr was 20 fold more active than ATR1tr, or commercial available ferredoxin reductases.

Kinetic values for ATR1tr and ATR2tr were determined with V_{\max} 51 and 38 $\mu\text{M}/\text{min}$ and K_M 23 and 16 μM , respectively, using Michaelis-Menten kinetics. ATR1tr showed substrate inhibition, therefore, the interpretation of the data should be treated with caution. The kinetic data of ATR2tr were similar to published data of native ATR2 expressed in *S. cerevisiae* (K_M 15 μM)³⁵⁰ and of solubilised ATR2mod from the membrane fraction expressed in *E. coli* (K_M 15 μM and 9 U/mg)³⁵¹. The latter authors deleted only 45 amino acids of the predicted chloroplast signal, whereas in this project 73 amino acids (the whole hydrophobic membrane anchor) were removed. This shows that the N-terminus is not part of the catalytic centre, which was also demonstrated for the reductase of *S. cerevisiae*. The native reductase and a truncated soluble reductase (22 amino acids deleted at the N-terminus) of *S. cerevisiae* resulted in similar kinetic values for the activity with cytochrome c and CYP61 (forming ergosta-5,7-dienol to ergosterol).⁴⁰⁸

Soluble ATR2tr (K_M 16 μM) has a 1.4 to 14 lower affinity to cytochrome c compared to the K_M values of other soluble and truncated eukaryotic P450 reductases recombinantly expressed in *E. coli* (1.1 μM for *S. cerevisiae* CPR⁴⁰⁸ and 12 μM for *Phanerochaete chrysosporium* CPR⁴⁰⁹). Recombinantly expressed and then solubilised full length CPRs showed also a stronger affinity of cytochrome c, such as 5 μM for house fly CPR⁴¹⁰. Overexpressed and purified plant CPRs gave with 7 μM (*C. roseus*⁴¹¹) two times higher affinity than ATR2tr (16 μM , this work).

ATR2 has two possible start codons, so two possible proteins can be produced. ATR2-1 (712 aa) and ATR2-2 (702 aa) were expressed in *S. cerevisiae* reported by Urban *et al.* 1997¹⁶⁶. The specific microsomes activity with cytochrome c was 2.8 $\mu\text{mol}\cdot\text{l}^{-1}\cdot\text{min}^{-1}\cdot\text{mg}^{-1}$ and 0.3 $\mu\text{mol}\cdot\text{l}^{-1}\cdot\text{min}^{-1}\cdot\text{mg}^{-1}$ for ATR2-1 and ATR2-2, respectively. ATR2tr expressed in *E. coli* (this project) showed with 3770 $\mu\text{mol}\cdot\text{l}^{-1}\cdot\text{min}^{-1}\cdot\text{mg}^{-1}$ more than 1000 higher specific activity than native ATR2-1 (2.8 $\mu\text{mol}\cdot\text{l}^{-1}\cdot\text{min}^{-1}\cdot\text{mg}^{-1}$) or ATR2-2 (ten amino acids on the N-terminus deleted, 0.3 $\mu\text{mol}\cdot\text{l}^{-1}\cdot\text{min}^{-1}\cdot\text{mg}^{-1}$) expressed in yeast microsomes.¹⁶⁶ Albeit, characterisation studies of ATR1 and ATR2 resulted in similar specific activity for the conversion

of cinnamic acid to coumaric acid when tested with the Arabidopsis P450 cinnamate-4-hydroxylase (CYP73A5), possibly due to the limited velocity of the P450.^{166,391} ATR2tr showed also a higher specific activity when compared with other plant reductase, e. g. reductase of *Petunia hybrida* (30-60 $\mu\text{mol}\cdot\text{l}^{-1}\cdot\text{min}^{-1}\cdot\text{mg}^{-1}$)⁴¹² and *Mentha spicata* (43 $\mu\text{mol}\cdot\text{l}^{-1}\cdot\text{min}^{-1}\cdot\text{mg}^{-1}$)⁴¹³. Moreover, a lower specific activity was reported for P450 reductases from other organisms, for example 2.85 $\mu\text{mol}\cdot\text{l}^{-1}\cdot\text{min}^{-1}\cdot\text{mg}^{-1}$ for human reductases recombinant expressed in insect cells⁴¹⁴ or 10.7 $\mu\text{mol}\cdot\text{l}^{-1}\cdot\text{min}^{-1}\cdot\text{mg}^{-1}$ *Candida maltose* P450 reductase in microsomes after expression in *S. cerevisiae*⁴¹⁵.

The K_M value for ATR2tr found in this work was 16 μM and a similar value was found when expressed in yeast³⁵⁰. The turnover number k_{cat} (the maximum number of enzymatic reactions per second) was found to be around three times lower for ATR2tr (5 s^{-1}) than for native ATR2 expressed in yeast (14 sec^{-1})³⁵⁰.

ATR2tr, after dialysis in buffer B, exhibited more activity than when assayed in general potassium phosphate buffer A due to its low affinity for the coenzyme FMN³⁵⁰. ATR2tr expressed in *E. coli* and stored in buffer B at -21 °C or -80 °C kept 70% of the original reductases activity using cytochrome c over six weeks (Chapter 4.3.6.6).

In conclusion, the two recombinant expressed Arabidopsis reductases ATR1tr and ATR2tr were soluble and active after purification. ATR1tr showed substrate inhibition with cytochrome c and was 200 times less active than ATR2tr, which performed typical Michaelis-Menten kinetics. The kinetic data of ATR2tr were similar to published data, whereas the specific activity was higher and it was found to be more stable than reported in the literature. Therefore, ATR2tr was selected for the creation of the platform technology containing plant P450s and an Arabidopsis reductase (Chapter 5).

5 Development of the ATR2tr-LIC platform

5.1 Introduction

For industry, *E. coli* is generally the preferred heterologous host for recombinant protein expression and this robust bacterial expression system would be desirable for the characterization of Arabidopsis P450s. Plant P450s have been expressed as membrane associated proteins in *E. coli* (more information in Chapter 3). Unfortunately, there is no evidence in the literature that plant P450s can be soluble and actively expressed in *E. coli*. The difficulties in expression of plant P450s in bacteria are caused by the hydrophobic membrane anchor, the complex protein structure and different codon bias between plant and bacteria. Due to this challenge, plant P450s have been mainly expressed in mammalian³⁶, insect^{191,416} or yeast^{166,328} cells, but it also has been shown that it is possible to engineer plant P450 systems for expression in bacteria as membrane associated proteins²⁹⁹.

As a reductase is necessary for the P450 reaction it would be useful to fuse a P450 of choice to a reductase to create a self-sufficient system. In 1995, the first artificial plant P450 fusion enzyme was recombinantly expressed in *E. coli* and activity detected in membrane preparations.²⁹⁹

The following plant cytochromes P450 are described in this Chapter for the development of the platform technology where plant P450s are fused to Arabidopsis reductase ATR2tr: isoflavone synthase I (IFS), cinnamate-4-hydroxylase (CYP73A5), N-demethylase (CYP82E4) and CYP81D8 with unknown function.

The native isoflavone synthase I (IFS) from *Glycine max*, which was already used for the artificial fusion of the plant reductases CPR from *Catharanthus roseus* by Prof. Koffas' group³⁰⁶ was chosen. The enzyme IFS catalyses the two aryl migrations (from liquiritigenin to daidzein and from naringenin to genistein) in the phenylpropanoid pathway (Figure 5.1). The isoflavones daidzein and genistein belong to the class of phytoestrogens and have an antioxidant effect, which protects the DNA in the cells from oxidative damage.

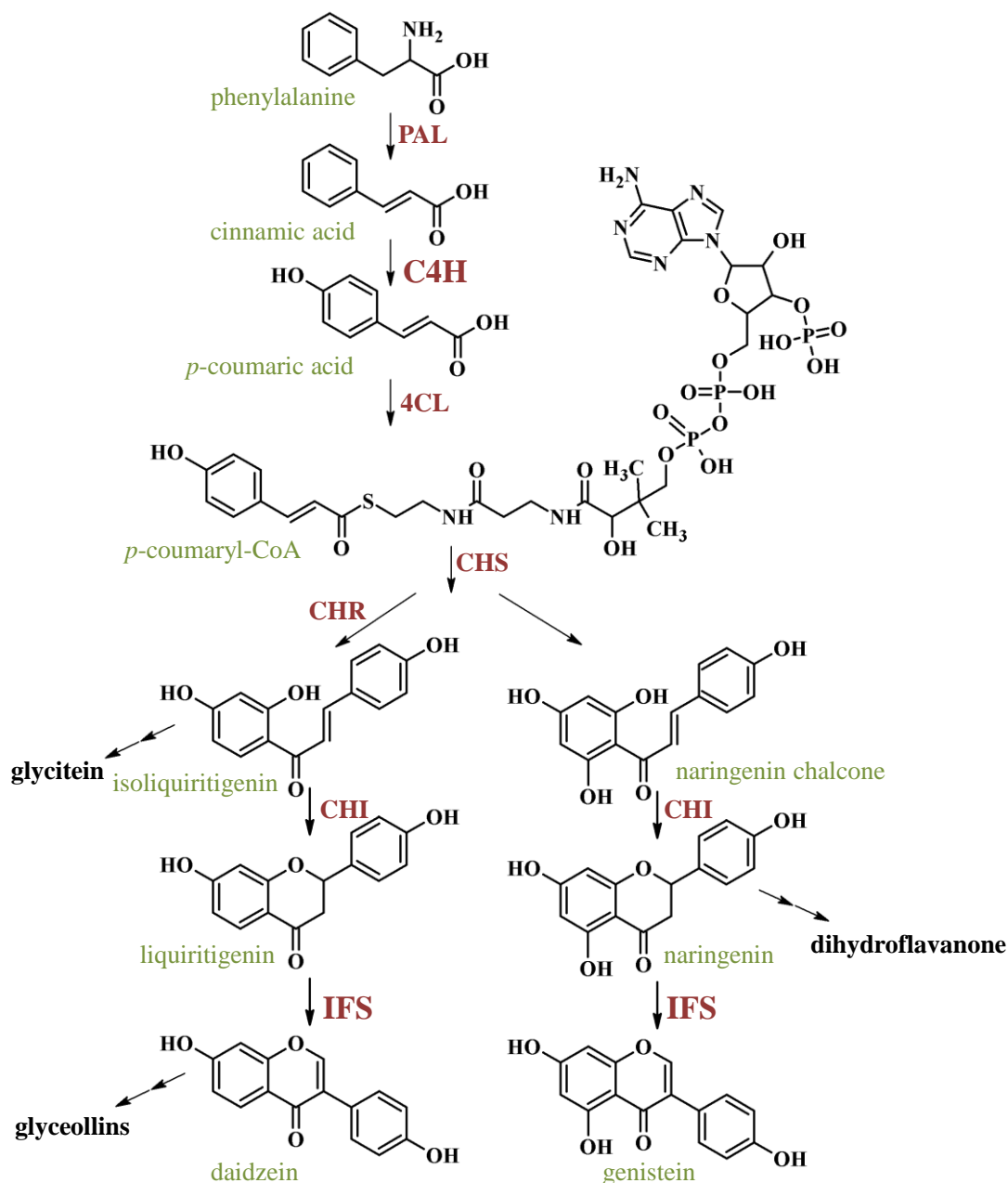


Figure 5.1: Phenylpropanoid pathway showing the key role of the two P450s IFS (CYP93C) and C4H (CYP73A5) used in this project

PAL = phenylalanine ammonia lyase, C4H = cinnamate-4-hydroxylase, 4CL = 4-coumarate-CoA-chalcone isomerase, CHS = chalcone synthase, CHR = chalcone reductase, CHI = chalcone isomerase, IFS: isoflavone synthase

The construct was kindly provided by Prof. Mattheos Koffas (State University of New York, Buffalo, USA) as the artificial fusion IFS-CPR E3³⁰⁶ (IFS = isoflavone synthase I from *G. max* fused to the P450 reductase from *C. roseus*). Modifications of the anchor region at the N-terminus of the P450 IFS gene, as well as the linker between the P450 and the reductase, were altered to increase the isoflavone synthase activity. The highest activity towards naringenin was seen

when an N-terminal modified IFS was used. Therefore, the first six N-terminal residues were replaced by the synthetic mammalian peptide (amino acid sequence: MALLLAVF; ϵ) and then fused to a truncated *C. roseus* reductase through the linker λ , encoding glycine-serine-threonine (Figure 5.2).³⁰⁶

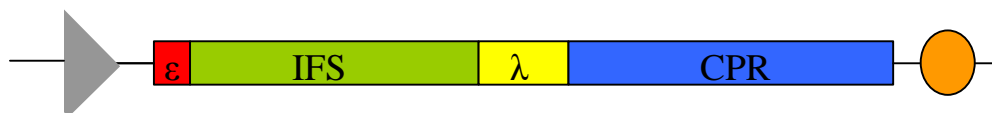


Figure 5.2: Arrangement of IFS-CPR fusion construct

IFS = isoflavone synthase I, ϵ = synthetic sequence encoding mammalian peptide, λ = linker, encoding glycine-serine-threonine, CPR = *Catharanthus roseus* reductases (Leonard and Koffas³⁰⁶)

IFS (GenBank accession number AF195798) belongs to the CYP93C subfamily and is closely related to CYP93C1 (97% amino acids sequence, AF022462)^{417, 418}. The native *IFSnat* as well as the codon optimised *IFSopt* (GeneArt) for expression in *E. coli* were both used in these studies.

The cinnamate-4-hydroxylase (CYP73A5) was selected, because it is a well studied P450 from Arabidopsis⁴¹⁹ and is involved in the phenylpropanoid pathway (Figure 5.1), hydroxylating *trans*-cinnamic acid to *p*-coumaric acid. It was characterised in 1997 after recombinant expression in insect cells.¹⁹¹

The CYP82E4 from *Nicotiana tabacum* was chosen due to its N-demethylase activity of nicotine (Figure 5.3), a desired reaction for the pharmaceutical industry. Tertiary N-methylamine products from alkaloids are attractive for the pharmaceutical industry, such as alkaloids from the opiate family, for example the analgesics morphine⁴²⁰ and codeine⁴²¹, or tropanes, for example cocaine⁴²² and the central nerve system stimulating atropine⁴²³. They are generally produced with different chemical methods that often require toxic reagents such as cyanogen bromide⁴²² or chloroformate esters⁴²⁴.

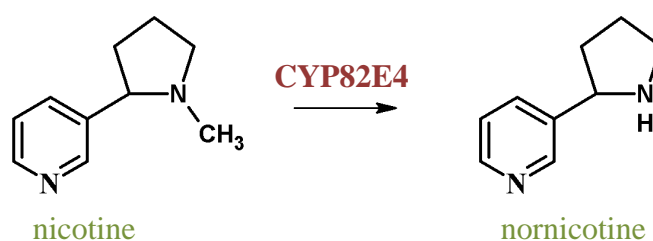


Figure 5.3: N-demethylation of nicotine to nornicotine by CYP82E4 from *Nicotiana tabacum*

The alkaloid nicotine is the main representative in tobacco products. Nornicotine can be reduced chemically or when incinerated to nitroso products, such as N'-nitrosornicotine, which are toxic and mostly carcinogenic.⁴²⁵

The function of CYP81D8 is not known yet. Nevertheless, this P450 gene was found to be more than 30 fold upregulated in Arabidopsis after treatment with the explosive 2,4,6-trinitrotoluene (TNT) in a microarray experiment (Chapter 3.1, Table 3.2).^{363,364} TNT is an artificial substance, which is highly toxic. It persists in the environment and so far no enzyme has been identified able to mineralise this compound.⁴²⁶ Due to the fact that CYP81D8 is responding to TNT, it may be that this P450 is also involved in the transformation of other organic xenobiotics.

5.2 Objectives

Plant cytochromes P450 are known to catalyse a diverse range of chemistries and are attractive targets for oxidative biocatalysis and detoxification of environmental pollutants. However, as plant P450s are membrane associated, recombinant expression of soluble protein is problematic and as a result very few of these enzymes have been characterised.¹⁴⁸ A strategy to obtain soluble protein when expressed in *E. coli* is the removal of the N-terminal hydrophobic membrane anchor region at a molecular level (Chapter 2.8.1). Fusing the N-terminal truncated heme domain of plant P450s with an appropriate N-terminal truncated reductase could provide the basis for developing robust, soluble redox-self-sufficient plant enzyme systems for characterisation studies.

This chapter describes the development of a new technology platform using a Ligation Independent Cloning (LIC) vector (Chapter 2.9), in which the truncated version of the Arabidopsis P450 reductase ATR2tr was integrated. This novel ATR2tr-vector was tested with a selection of plant P450s catalysing different P450 reaction types. The technology could be used in a high throughput screen of Arabidopsis P450s with the aim of determining plant P450 functions and engineering biocatalysts for industrial applications.

5.3 Methods

5.3.1.1 Developing the platform technology of plant P450-ATR2tr fusions

There are three cytochromes P450 reductases encoded in the Arabidopsis genome. A truncated version of the Arabidopsis reductase ATR2 was selected for developing the ATR2tr-LIC vector because studies (Chapter 4) had found that recombinant ATR2tr had approximately 20 times more activity than ATR1tr. ATR3 was not tested, but microarray analysis suggests that it has lower expression (Figure 4.3).

The Arabidopsis reductase ATR2tr was synthesised by GeneArt (Regensburg, Germany) to remove the four native *Bse*RI restriction sites and to codon optimise the sequence for expression in *E. coli*. ATR2tr was cloned into the LIC-vector using traditional cloning methods (described Chapter 2.8) with *Bse*RI (N-terminus) and *Nde*I (C-terminus) restriction sites.

The linker was inserted at the N-terminal sequence of ATR2tr by PCR. The forward primer (Lic_BseRI_F, Table 5.1) was designed to integrate the lic-linker and two primers for the lam-linker (lam_BseRI_F1 and lam_BseRI_F2, Table 5.1), due to its length. The reverse primer (Atr2_NdeI_Lic_R) was designed with a *Nde*I restriction site and lamATR2tr and licATR2tr was amplified by PCR using Phusion polymerase (Chapter 2.8.2).

Table 5.1: Primer sequences for cloning ATR2tr into the LIC-vector

Linker = underlined sequence, restriction site *Bse*RI in forward primer and *Nde*I in reverse primer = bold, start of ATR2tr synthesised sequence = italics

primer name	sequence
Lic_BseRI_F	AGAGAGGG <u>CGCGCCTTCTCCTC</u> <i>AGGTAGCGGTAATAGCAAACGTGTTG</i>
lam_BseRI_F1	<u>CTCCTCAGGATCGGGT</u> <i>GGTAGCGGTAATAGCAAACGTGTTG</i>
lam_BseRI_F2	AGAGAGGGGGCTCCTG CTCCTC <i>AGGATCGGGTGGTAGCGGT</i>
Atr2_NdeI_Lic_R	GAGAGAC CATATG <i>TTACCAAACATCACGCAGATAACG</i>

The ATR2tr inserts were purified (Chapter 2.6) and digested sequentially. Therefore, 13 µg insert DNA, 15 µl NEB4 buffer (New England Biolabs), 5 U NdeI (New England Biolabs) and water to a final volume of 150 µl were incubated overnight at 37 °C. Then a further 5 µl NEB4 buffer and 10 U BseRI (New England Biolabs) were added and incubated at 37 °C for 1h 50 min. The vector (15 µg) was digested under the same conditions as described above in a total volume of 300 µl and then separated by agarose gel electrophoresis (0.8% w/v agarose, Chapter 2.11) and purified (Chapter 2.6). To avoid re-ligation of the vector, the linearised vector (4 µg) was dephosphorylated in a reaction containing 8 µl 10x arctic phosphatase buffer (New England Biolabs) and 15 U arctic phosphatase (New England Biolabs) in a total volume of 80 µl for 1 h at 37 °C followed by heat inactivation at 65 °C for 5 min. The ligation of the lamATR2tr or licATR2tr insert and the LIC-vector was done in the ratios of 2:1 and 4:1. A total volume of 3 µl contained 0.5 µl 10x T4 DNA ligase reaction buffer and 120 U T4 DNA ligase (New England Biolabs) and the reaction was incubated overnight in a 2 l water bath with a temperature starting at 21 °C lowered to 4 °C. The ligation product was transformed into *E. coli* DH5α (Chapter 2.8.4), transformants screened on selective agar containing kanamycin and verified using the primer Lic_BseRI_F, lam_BseRI_F1 and Atr2_NdeI_Lic_R (Table 5.1). Positive clones were incubated overnight for plasmid preparation (Chapter 2.5) and a restriction digest performed with BseRI and NdeI (Chapter 2.8.6). For final confirmation that the right plasmid with the correct sequence was engineered, the gene was sequenced (Chapter 2.8.9) using T7 and T7term primers.

5.3.2 Cloning of P450s into lamATR2tr- and licATR2tr-vector

5.3.2.1 Primer design

In cloning experiments, P450 genes were cloned using either their native sequence or their codon-optimised sequence for expression in *E. coli*. Codon optimisation was performed by GeneArt (Table 5.2). The full length sequences are found in Appendix B.

Table 5.2: List of P450s used for the creation of artificial plant fusions with the reductase ATR2tr

P450	gene origin
<i>IFSnative</i>	construct containing the native gene derived from Prof. Mattheos Koffas ³⁰⁶
<i>IFSopt</i>	synthesized and codon optimized for <i>E. coli</i> expression by GeneArt
<i>CYP73A5</i>	synthesized and codon optimized for <i>E. coli</i> expression by GeneArt
<i>CYP82E4</i>	native gene derived from Prof. Ralph Dewey ⁴²⁷
<i>CYP81D8</i>	native gene isolated from <i>Arabidopsis thaliana</i>

To each forward primer the sequence CCAGGGACCAGCA was added upstream of the start codon of the P450 sequence to create the overhangs for the ligation independent cloning. The stop codons of the P450 inserts were removed in order to obtain a fusion to ATR2tr. The reverse primers were designed individually for each linker (Table 5.3). To prepare the sequence for T4 treatment, as described previously, the 3'-end of the sequence was engineered to end with an Adenine (A), resulting in a change of the last amino acid: in CYP73A5 the terminal Cysteine was changed to a Serine and in CYP82E4 the terminal Tyrosine to a Threonine. The last amino acids of IFSori, IFSsyn and CYP81D8 were silent mutations (see Appendix B).

Table 5.3: Primer sequences for cloning P450 inserts into ATR2tr-LIC-vector
Lic primer sequence addition in capital letters, insert sequence in small letters

primer name	sequence
e-IFS for ATR2 fusion F	CCAGGGACCAGCA atggctctgttattagcagttttcttggtttg
eIFSori-LicATR2tr R	GAGGAGAAGGCGCGtgaaaggagtttagatgcaacgccgatccttgc
eISFori-lamLicATR2tr R	GAGGAGCAGGAGCCtgaaaggagtttagatgcaacgccgatccttgc
eIFSsyn-native-Lic F	CCAGGGACCAGCA atggcactgctgctggcagttttctgggtctgtttg
IFSsyn-trunc-ATR2tr F	CCAGGGACCAGCA gcccgctccgaccccgagcgcaaaaagcaaacgactg
73A5syn-trunc-Lic F	CCAGGGACCAGCA ctgcgtggtaaaaaactgaaaatgcctccgggtccg
73A5syn-LicATR2tr R	GAGGAGAAGGCGCG tgagttacgcggtttcatcacaataatgctatg
73A5syn-lamLicATR2tr R	GAGGAGCAGGAGCC tgagttacgcggtttcatcacaataatgctatg
82E4-trunc-Lic F	CCAGGGACCAGCA acaaaaaaatctcaaaaacctcaaaaccttacc
82E4-LicATR2tr R	GAGGAGAAGGCGCG tgtaagctcaggtgccaggcgaggcgctattatc
82E4-lamLicATR2tr R	GAGGAGCAGGAGCC tgtaagctcaggtgccaggcgaggcgctattatc
81D8-trunc-Lic F	CCAGGGACCAGCA ggaaaac tcaagcgaac gccaaatcta cctccgag
81D8-LicATR2tr R	GAGGAGAAGGCGCG tacggactcgttgaagattttaacaacagaggac
81D8-lamLicATR2tr R	GAGGAGCAGGAGCC tacggactcgttgaagattttaacaacagaggac

5.3.2.2 Cloning strategy

The P450 inserts were amplified by PCR using the high fidelity Phusion polymerase. Primers are listed in Table 5.3 and 4 M NDSB 201 (Chapter 2.8.2). The purified P450 sequences (Chapter 2.6) as well as lamATR2tr- and licATR2tr-vector were prepared following the protocol for ligation independent cloning (Chapter 1.1). Primer T7 and ATR2seqR (Table 2.4) were used for sequence confirmation (Chapter 2.8.9).

5.3.3 Expression and activity assays of the novel plant fusions

The expression of the plant P450 fusion was performed overnight at 20 °C following the protocol described in Chapter 2.10.1 and activity assay in Chapter 2.15.3.

5.4 Results

5.4.1 Developing the platform technology for plant P450-ATR2tr fusions

5.4.1.1 Designing the linker region between P450 and reductase

Two different linkers between the P450s and the reductase ATR2tr were tested (Figure 5.4).

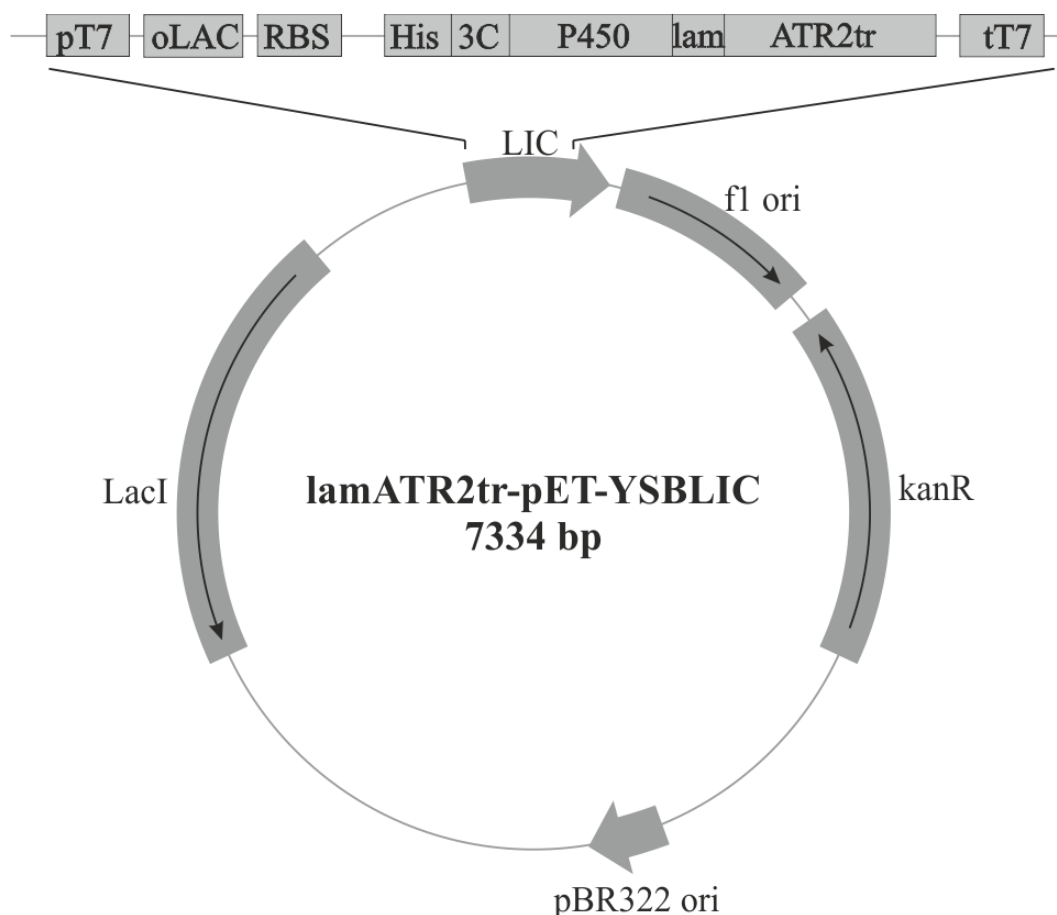


Figure 5.4: Schematic construction of the P450-ATR2tr fusion containing the lam-linker

(pT7 = T7 promotor, oLAC = Lac operator, RBS = ribosome binding site, His = 6x histidines residues, which can be cleaved HRV 2C protease site = 3C, P450 = cytochrome P450, lam = linker between P450 and reductase, ATR2tr = Arabidopsis reductase ATR2 without hydrophobic N-terminal membrane sequence, tT7 = T7 terminator, f1 ori = f1 phage origin of replication, pBR322 ori = origin of replication of the plasmid pBR322, kanR = kanamycin resistance gene, LacI = repressor gene for IPTG induction)

The first linker to be tested was the lic-linker (amino acid sequence: RAFSS), which is the necessary overhang in the LIC-vector for the LIC technology described in Chapter 1.1. The second linker was the λ -linker (amino acid sequence: GST) created by the Koffas group.³⁰⁶ The λ -linker and the first five

amino acids of the truncated CPR (from *C. roseus*) resulted in the sequence of GSTSSGSG (called lam-linker), which was modified by inserting a *Bse*RI restriction site. The codon for the first glycine and for threonine had to be changed to be compatible for the ligation independent cloning. Threonine is coded through four possible codons (ACN, where N is A, T, G or C), which could not be used, because the linker sequence is part of the overhangs created through the T4 polymerase reaction and therefore must not contain the base adenine. Threonine was changed to the similar, neutral, polar amino acid serine and the codon for glycine from GGA to GGC in a silent mutation to remove the adenine from the nucleotide sequence. However, these changes resulted in four subsequent serines and the formation of two *Bse*RI (CTCCTC) sites. Therefore, the threonine was changed to cysteine.

5.4.2 Cloning of ATR2tr into the LIC-vector

The ATR2tr with the lam-linker or the lic-linker at the N-terminus was cloned into the LIC-vector. The lamATR2tr- and licATR2tr-vectors were transformed into *E. coli* DH5 α and positive colonies screened using whole cell PCR (Chapter 2.8.2). Plasmids of positive clones were purified and digested to verify the correct insert (Figure 5.5).

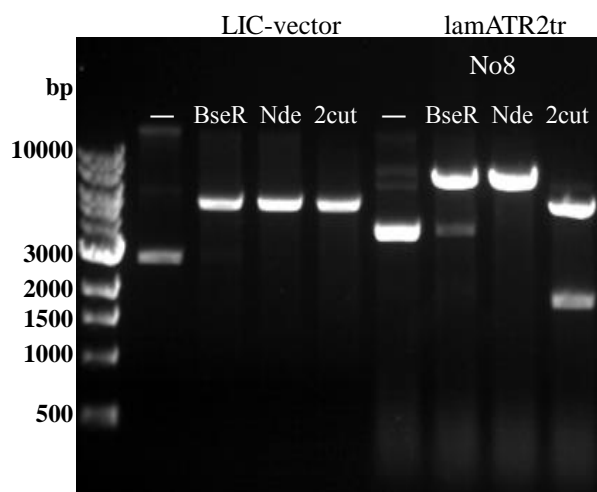


Figure 5.5: Analysis of positive transformants for the presence of the lam-ATR2tr in the LIC-vector

Restriction digest of the LIC-vector (negative control) and lamATR2tr by *Bse*RI (*Bse*R), *Nde*I (*Nde*) or with both enzymes (2cut)

5.4.3 Cloning of P450 inserts into lamATR2tr and licATR2tr

The P450 inserts were amplified by PCR using the high fidelity Phusion polymerase and cloned into the lamATR2tr- and the licATR2tr-vector. Again colonies containing the desired gene were detected by whole cell PCR and correct inserts were confirmed by restriction digest of the (Figure 5.6) and sequencing.

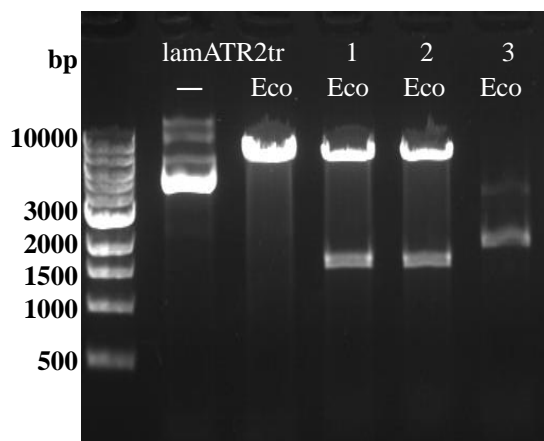


Figure 5.6: Analysis of positive transformants for the presence of the P450 73A5tr
Restriction digest with EcoR1 (Eco) of the empty lamATR2tr-vector and the transformants 73A5tr-lamATR2tr No1 and 2 containing the insert and No3 with no insert.

5.4.4 Expression and activity assays of the novel plant fusions

5.4.4.1 IFS-ATR2tr fusions

The isoflavone synthase activity was detected for the conversion of naringenin to genistein by HPLC after extraction of the culture supernatant in ethylacetate (Chapter 2.15.3.3). Great error bars were received due to the complex extraction method and an internal standard was required. Three compounds (syringic acid, biochanin A and scopoletin) were chosen to test for their use as internal standard for the detection of naringenin and genistein by HPLC (Chapter 2.15.3.3). Retention time and absorption maxima for each compound are listed in Table 5.4.

Table 5.4: List of chemical compounds considered to use as internal standard optimising the extraction method for the two flavonoids naringenin and genistein

chemical compound (IUPAC name)	molecular weight	absorption maximum	retention time
naringenin (5,7-dihydroxy-2-(4-hydroxyphenyl)chroman-4-one)	272 g/mol	291 nm	12.0 min
genistein (5,7-Dihydroxy-3-(4-hydroxyphenyl)chromen-4-one)	270 g/mol	261 nm	16.8 min
syringic acid (4-hydroxy-3,5-dimethoxybenzoic acid)	198 g/mol	276 nm	4.2 min
biochanin A (5,7-dihydroxy-3-(4-methoxyphenyl)chromen-4-one)	284 g/mol	260 nm	16.8 min
scopoletin (7-Hydroxy-6-methoxycoumarin)	192 g/mol	230 & 346 nm	4.8 min

Syringic acid could be not detected after extraction, however it was stable at room temperature in methanol over days. Syringic acid was lost during the extraction, due to the deprotonation of the carboxyl group and so it was not extracted into the organic phase of ethyl acetate. Therefore, syringic acid was not used as internal standard when using this method.

Biochanin A is a homologue of genistein and therefore, expected to have similar properties. Unfortunately, biochanin A is not very stable at room temperature and has the same retention time of 16.8 min as genistein (Figure 5.7) and therefore unsuitable as internal standard.

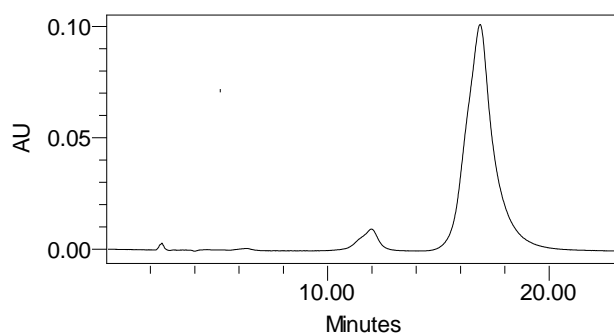


Figure 5.7: HPLC analysis of the flavonoids biochanine A, genistein and naringenin
HPLC chromatogram at 260 nm for a sample mix of biochanin A (50 μ M, retention time: 16.8 min), naringenin (50 μ M, retention time: 12.0 min) and genistein (50 μ M, retention time: 16.8 min); HPLC conditions: 50 μ l sample was applied to HPLC, TechSphere column, 1 ml/min isocratic flow 50% water, 50% methanol with 0.1% acetic acid, column temperature: 25 $^{\circ}$ C, sample temperature: 21 $^{\circ}$ C, run time 23 min

Scopoletin elutes earlier than naringenin and genistein with a retention time of 4.8 min (Figure 5.8). It is stable at room temperature over days and also during the extraction step and was therefore chosen as internal standard for the isoflavone synthase activity assay (Chapter 2.15.3.3).

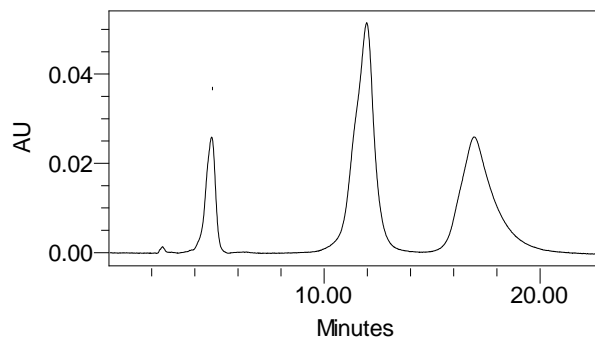


Figure 5.8: HPLC analysis of the flavonoids scopoletin, naringenin and genistein

HPLC chromatogram at 280 nm for scopoletin (50 μ M, retention time: 4.8 min), naringenin (50 μ M, retention time: 12.0 min) and genistein (50 μ M, retention time: 16.8 min); HPLC conditions: 50 μ l sample was applied to HPLC, TechSphere column, 1 ml/min isocratic flow 50% water, 50% methanol with 0.1% acetic acid, column temperature: 25 $^{\circ}$ C, sample temperature: 21 $^{\circ}$ C, run time 23 min

5.4.4.1.1 Activity in a growing cell assay

The isoflavone synthase I activity of the different artificial fusions was tested in a growing cell assay. The conversion of the substrate naringenin (50 μ M) to genistein was observed by analysing samples of the culture supernatant over time. No genistein was produced by the recombinant expressed fusions containing the native *IFS* gene (Figure 5.9). For the codon optimised IFSopt-lamATR2tr and IFSopt-licATR2tr 5 μ M (10% conversion) and 10 μ M (20% conversion) genistein were detected after 48 h, respectively. No activity was found for the negative controls IFS (in the LIC-vector, data not shown), empty lamATR2tr or empty licATR2tr.

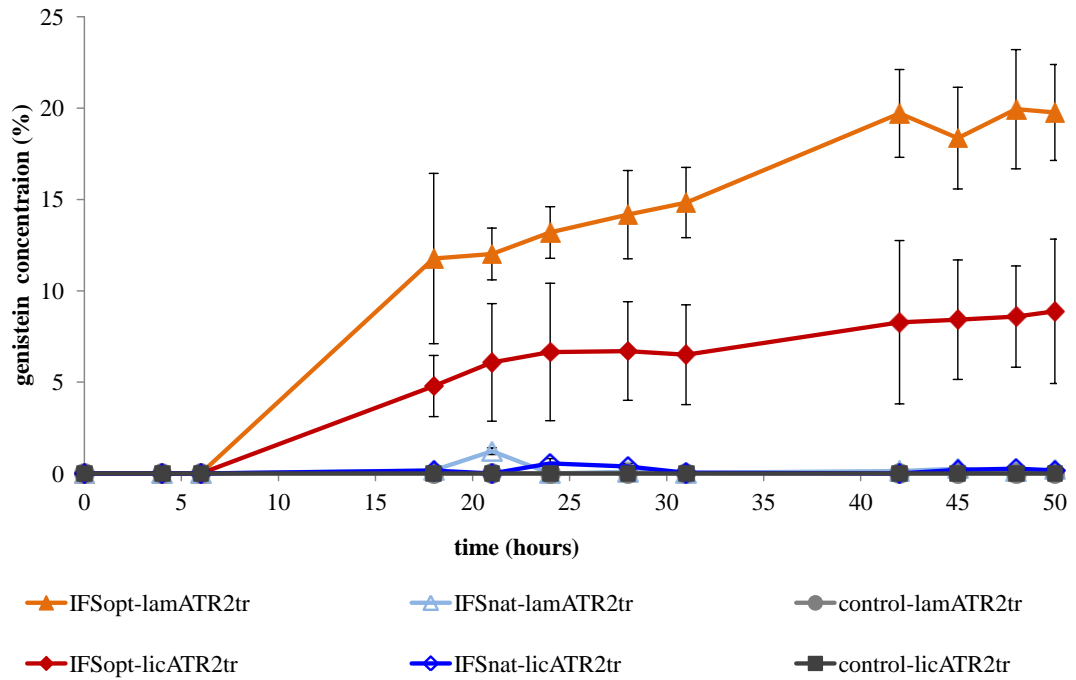


Figure 5.9: Activity of *Glycine max* IFS fused to *Arabidopsis* ATR2tr

Genistein production in a growing cell assay by artificial plant P450 fusions (IFSnat = native isoflavone synthase I from *G. max*, IFSopt = isoflavone synthase I codon optimized for *E. coli* expression, lamATR2tr = truncated ATR2 with lamda linker, licATR2tr = truncated ATR2 with lic-linker). The error bars represent the mean of five independent replicas \pm standard deviation.

The fusions containing the IFS and ATR2tr were analysed by SDS PAGE and western blot analysis using anti His-antibodies (Chapter 2.14.1) and anti ATR2-antibodies (Chapter 2.14.2). No signal was received for the fusions using anti His-antibodies, possibly a result of a not accessible His-tag.

The IFS fusions containing the native gene did not show a signal, possibly because expression levels were below detection limits.

The IFSopt-lamATR2tr and IFSopt-licATR2tr were detected only in the insoluble fraction (Figure 5.10) and were identified by MALDI-MS analysis (Chapter 2.15.2). In all sample (total protein, soluble and insoluble protein fraction) was found ATR2tr (72 kDa) implying a degradation of the fusions. For positive control was used lamATR2tr without IFS.

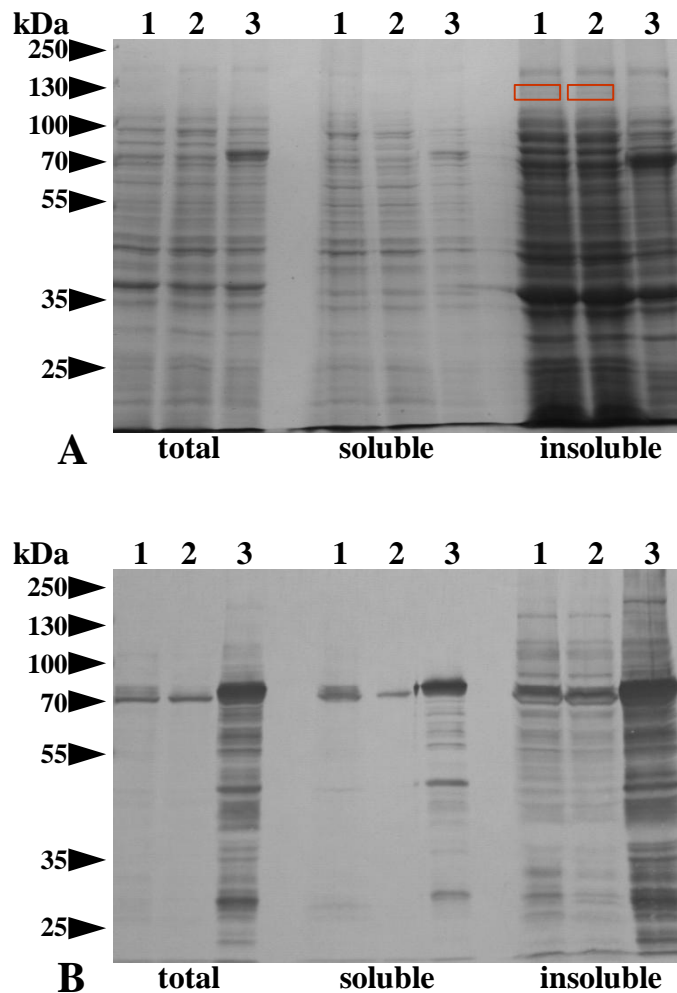


Figure 5.10: A) SDS-PAGE and B) western blot analysis (anti ATR2-antibodies) of *Glycine max* IFS fused to Arabidopsis ATR2tr

Analysis of total protein, soluble and insoluble protein (1 = IFSopt-lamATR2tr, 2 = IFSopt-licATR2tr, 3 = lamATR2tr control). The protein band with the expected size of IFSopt-lamATR2tr and IFSopt-licATR2tr (red boxes) from the insoluble protein fraction were sent for MalDI-MS analysis.

5.4.4.2 CYP73A5tr-ATR2tr fusions

5.4.4.2.1 Activity in a resting cell assay

The CYP73A5 codon optimised gene sequence without the hydrophobic N-terminus (73A5tr) was fused to ATR2tr using two different linkers. Both fusions, 73A5tr-lamATR2tr and 73A5tr-licATR2tr, converted cinnamic acid to coumaric acid in a resting cell assay, when grown in LB medium. The activity was three to five times greater when the fusions were grown in M9 minimal medium than in LB medium (Figure 5.11). No product was detected for the empty-ATR2tr controls, independent of the used linker.

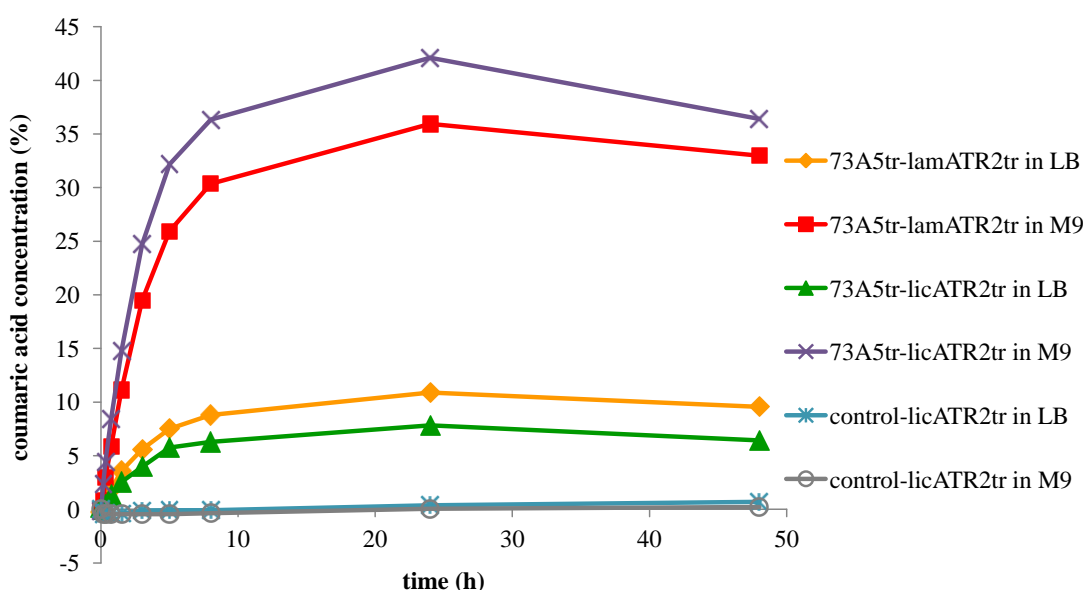


Figure 5.11: Activity of Arabidopsis P450 73A5tr fused to Arabidopsis ATR2tr in different media

Production of coumaric acid by 73A5tr-lamATR2tr and 73A5tr-licATR2tr in a resting cell assay after expression in M9 minimal or LB medium at 15 °C and 200 rpm.

Different expression conditions were tested in M9 medium to increase the activity of the CYP73A5-fusions. When fusions were expressed shaking (200 rpm) at 15 °C, resting cell assay showed more than 30% of the cinnamic acid was converted to coumaric acid in 24 h. Preliminary results indicated that the 73A5tr-licATR2tr produced approximately 5% more coumaric acid suggesting slightly higher activity than 73A5tr-lamATR2tr.

Activity was significantly reduced when cells were grown in M9 medium shaking (200 rpm) at 20 °C and 200 rpm (Figure 5.12) in comparison to the result above (Figure 5.11).

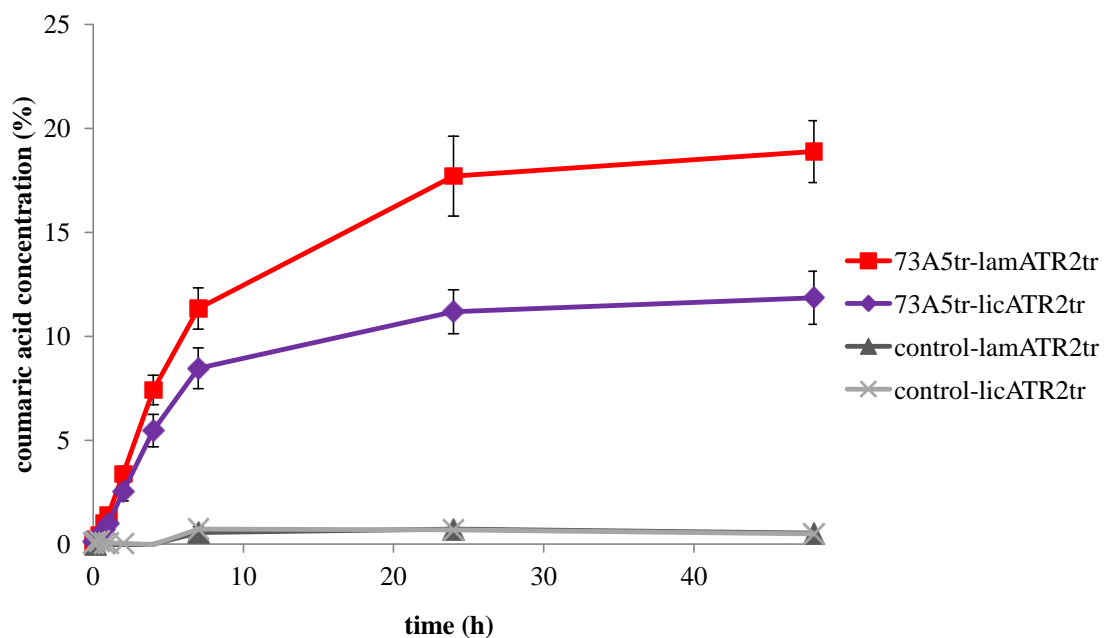


Figure 5.12: Activity of Arabidopsis P450 73A5tr fused to Arabidopsis ATR2tr in M9 medium

Production of coumaric acid by 73A5tr-lamATR2tr and 73A5tr-licATR2tr in a resting cell assay after expression in M9 minimal medium at 20 °C and 200 rpm. The error bars represent the mean of five independent replicas \pm standard deviation.

Similar amounts of coumaric acid product (30%) were detected for 73A5tr-lamATR2tr when expressed at 15 °C and 50 rpm (Figure 5.13) compared to 15 °C and 200 rpm. The fusion 73A5tr-licATR2tr only converted substrate to 20% coumaric acid at 15 °C and 50 rpm, which is 50% of the conversion received at 15 °C and 200 rpm (Figure 5.11).

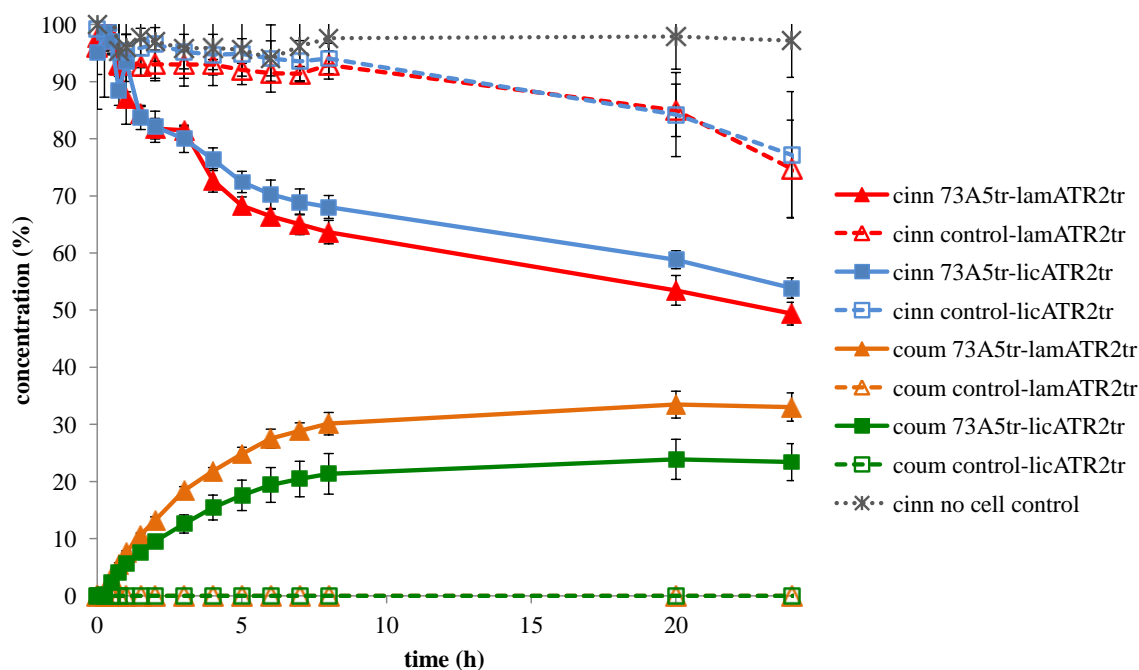


Figure 5.13: Conversion of cinnamic acid to coumaric acid by artificial plant fusions containing Arabidopsis P450 73A5tr and Arabidopsis ATR2tr in a resting cell assay Protein expression at 15 °C and 50 rpm (cinn = cinnamic acid, coum = coumaric acid, 73A5tr = truncated version of CYP73A5, synthesised and codon optimised for the expression in *E. coli*, lamATR2tr = truncated version of ATR2 with lam-linker, licATR2tr = truncated version of ATR2 with lic-linker, control-lamATR2tr and control-licATR2tr = empty vector control containing the ATR2tr with different linkers). The error bars represent the mean of four independent replicas \pm standard deviation.

5.4.4.2.2 Purification of 73A5tr-lamATR2tr

The fusion 73A5tr-lamATRtr (127 kDa) was subjected to nickel-affinity chromatography (Chapter 2.10.5) and then detected by SDS PAGE and western blot analysis (Figure 5.14). The 73A5tr-lamAR2tr was mainly present in the insoluble and in the eluted protein fraction. The protein band of the expected size for 73A5tr-lamATR2tr was sent for MALDI-MS analysis (Chapter 2.15.2) and the expected two proteins cinnamate-4-hydroxylase (from Arabidopsis) and NADPH-ferrihemoprotein reductase (Arabidopsis) were identified.

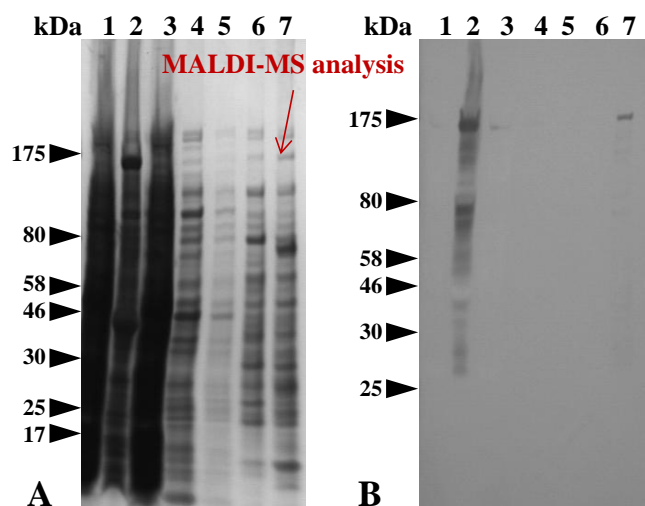


Figure 5.14: SDS-PAGE and western blot analysis (anti His-antibody) of Arabidopsis P450 73A5tr fused to Arabidopsis ATR2tr

A SDS PAGE and B western blot analysis of the different steps during the purification of 73A5tr-lamATR2tr (1 = soluble protein fraction, 2 = insoluble protein fraction, 3 = run through, 4 = wash step 1, 5 = wash step 2, 6 = elution of unspecific bound protein, 7 = elution of 73A5tr-lamATR2tr). The protein band with the expected size of 73A5tr-lamATR2tr was sent for Maldi-MS analysis

The different fractions were then tested for the ability to convert cinnamic acid. Results showed that activity was only found in the insoluble fraction (Figure 5.15).

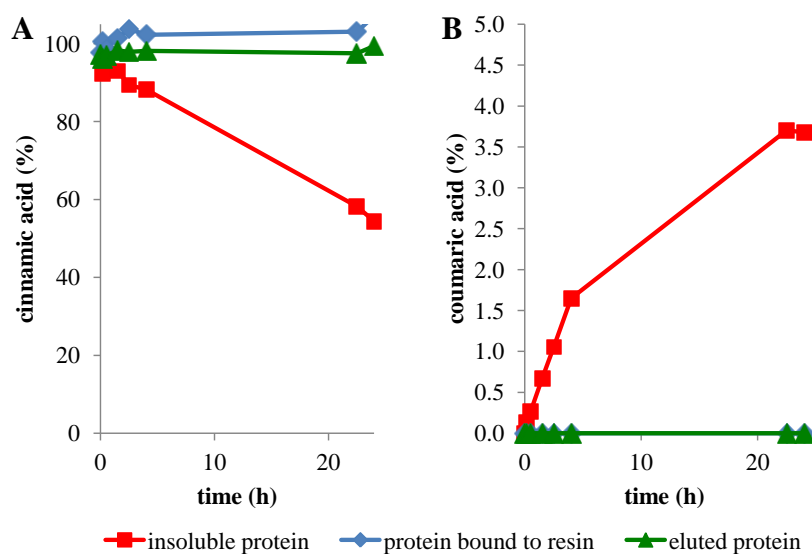


Figure 5.15: Cinnamate-4-hydroxylase activity in different fractions of the purification of 73A3tr-lamATR2tr

Observation of A the substrate cinnamic acid and B the product coumaric acid

To confirm this result, 73A5tr-lamATR2tr was expressed again in *E. coli* Rosetta 2 (DE3) and fractions of whole cells, sonicated cells (total protein), supernatant (soluble protein) and dissolved pellet (insoluble fraction) after sonication and centrifugation were tested for activity and analysed by SDS PAGE and western blot analysis. The activity found in whole cells (cell concentration:

50 mg/100ml, Figure 5.16A) with 170 μM coumaric acid was reduced to 10% in total and to 3% in the insoluble protein fraction (Figure 5.16B).

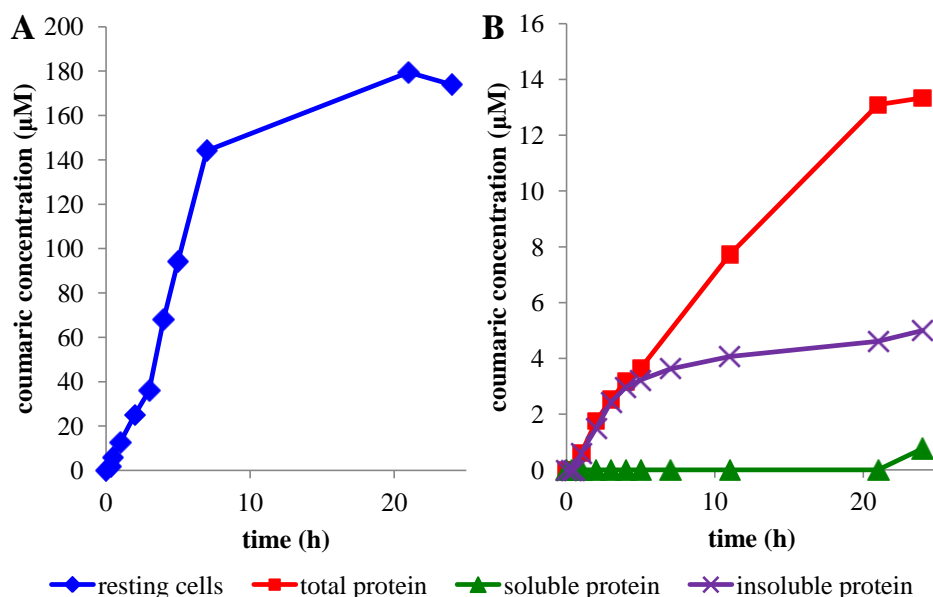


Figure 5.16: Cinnamate-4-hydroxylase activity of 73A3tr-lamATR2tr in different fractions after expression in *E. coli*

Production of coumaric acid by 73A5tr-lamATR2tr in **A** resting cells and **B** different fractions after the sonication

The 73A5tr-lamATR2tr fusion was detected by western blot analysis in the whole cells, total and insoluble protein fraction (Figure 5.17). No signal was seen in the soluble fraction.

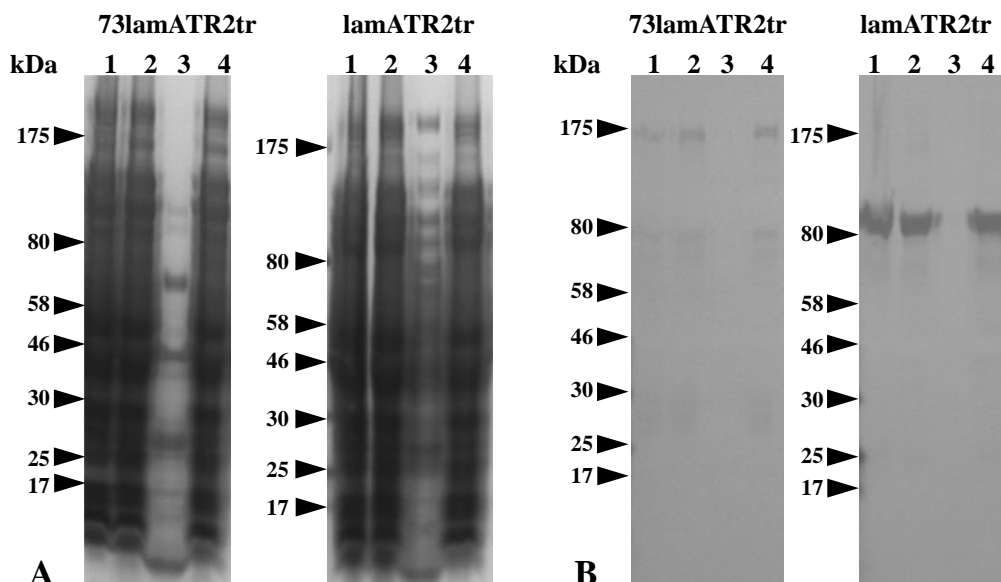


Figure 5.17: SDS-PAGE and western blot analysis of Arabidopsis P450 73A5tr fused to Arabidopsis ATR2tr as soluble and insoluble protein

73A5tr-lamATR2tr fusion (127 kDa) and lamATR2tr (negative control) detected by **A** SDS PAGE and **B** western blot analysis against anti His-antibodies (1 = whole cells, 2 = total protein fraction, 3 = fraction of soluble protein, 4 = fraction of insoluble protein)

5.4.4.3 CYP82E4tr-ATR2tr fusions

The N-demethylase (CYP82E4) was truncated to remove the membrane anchor (sequence, see Appendix B) and cloned into the lamATR2tr- and the licATR2tr-vector. The expression was performed in *E. coli* Rosetta2 (DE3) and M9 minimal medium (Chapter 2.10.1). The activity of the fusion was tested using resting cell assays following the conversion of nicotine to nornicotine (Chapter 2.15.3.5). Nicotine was removed from all samples, including negative controls (control-lamATR2tr, Rosetta 2 cells, and no cell control) within 45 min (Figure 5.18). The disappearance of nicotine was found to be due to the instability of nicotine in 70% water and 30% methanol (0.2% phosphoric acid, pH 7.25 with triethylamine).

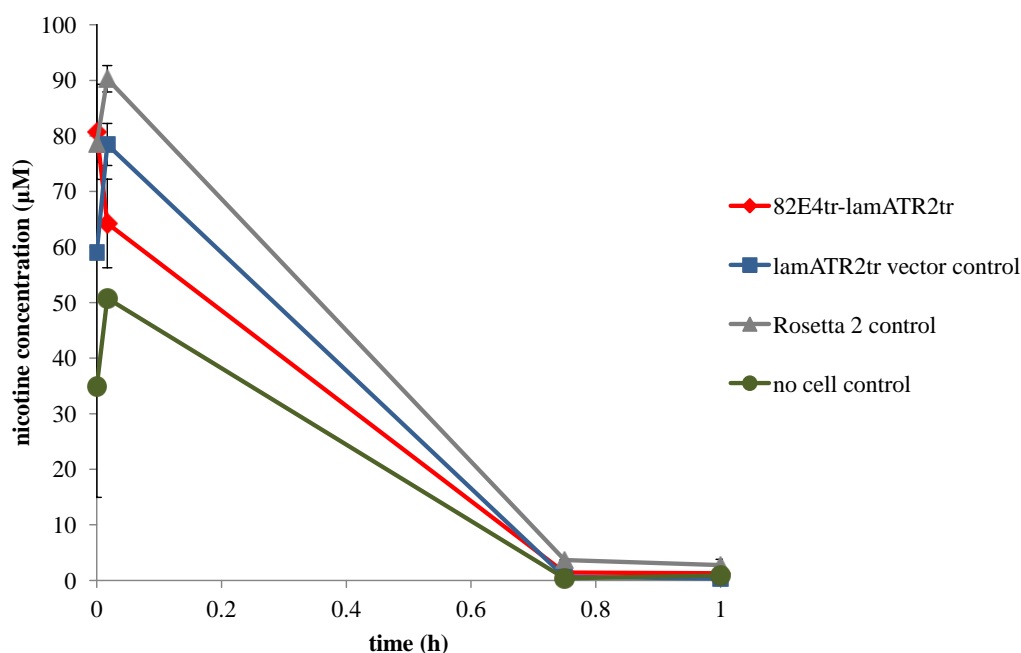


Figure 5.18: Nicotine removal in a resting cell assay

The error bars represent the mean of three independent replicas \pm standard deviation.

Nevertheless, the reaction mixture was analysed to see if nornicotine was produced. Nornicotine standard had a retention time of 4.2 min. Nornicotine could not be detected in any of the samples, due to other products of *E. coli* eluting between the retention time of 3.3 to 5.7 min and therefore was not detected (Figure 5.19).

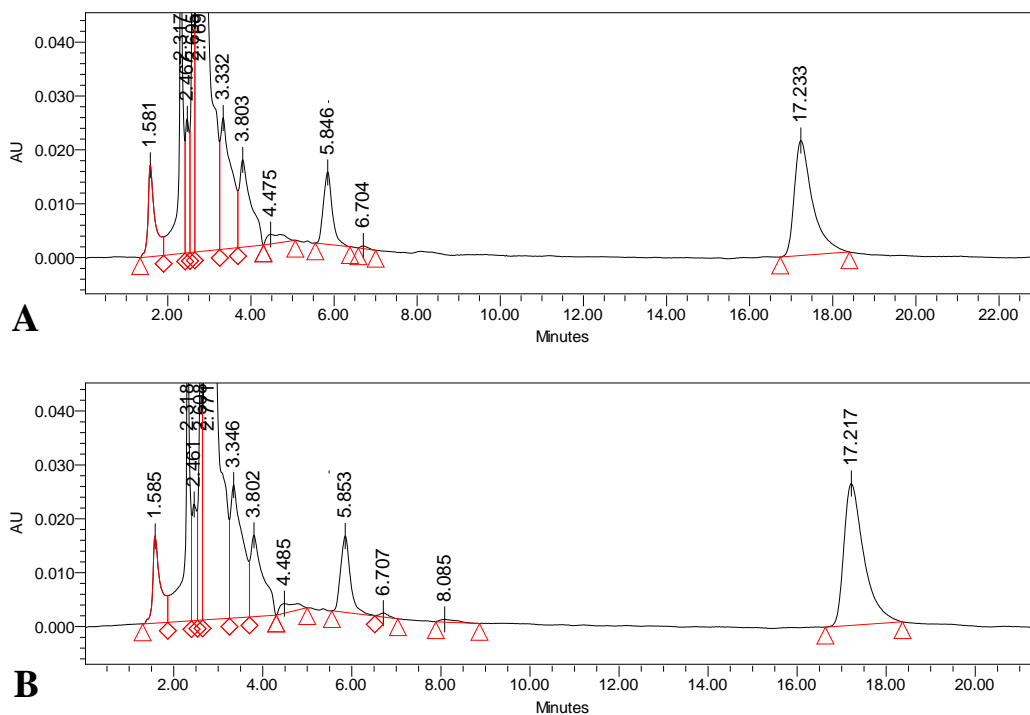


Figure 5.19: HPLC analysis (reversed-phase column) of the crude cell extract for nicotine and nornicotine.

HPLC chromatogram for **A** 82E4tr-lamATR2tr and **B** control-lamATR2tr after a reaction time of 10 min in a resting cell assay (17.2 min = nicotine), HPLC conditions: SunFire C18 column, 1 ml/min flow isocratic 70% water (0.2% phosphoric acid, pH 7.25 with triethylamine) and 30 % methanol (0.2% phosphoric acid pH 7.25 with triethylamine), column temperature: 20 °C, sample temperature: 4 °C.

To improve the identification of nornicotine, a chiral column (ChiralPak IA) was used. This column was able to separate a commercial racemic mixture of nornicotine (Figure 5.20). The enantiomers of nicotine eluted in one peak at 15.3 min. However, when extracts were tested, it was not possible to isolate nicotine or nornicotine using this method.

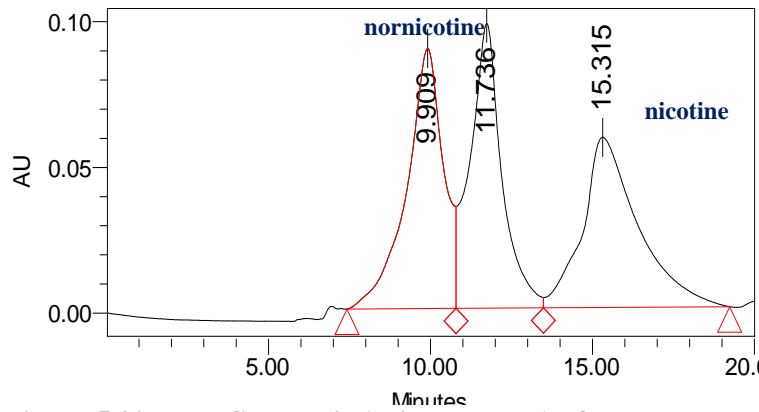


Figure 5.20: HPLC analysis (chiral column) of the crude cell extract for nicotine and nornicotine

HPLC separation of nicotine (retention time: 15.3 min), (R)-nornicotine (9.9 min) and (S)-nornicotine (11.7 min), HPLC conditions: ChiralPak IA column, isocratic 0.5 ml/min flow of 35% ethanol and 65% (heptanes ; isoporpanol : TFA = 90:10:0.1) , 1 mM (R/S)-nicotine, 1mM (R/S)- nornicotine

Both fusions, 82E4tr-lamATR2tr and 82E4tr-licATR2tr (128 kDa, red boxes in line 3 and 4, respectively, Figure 5.21), were detected by SDS PAGE and western blot analysis (with anti His-antibodies) in the insoluble fraction.

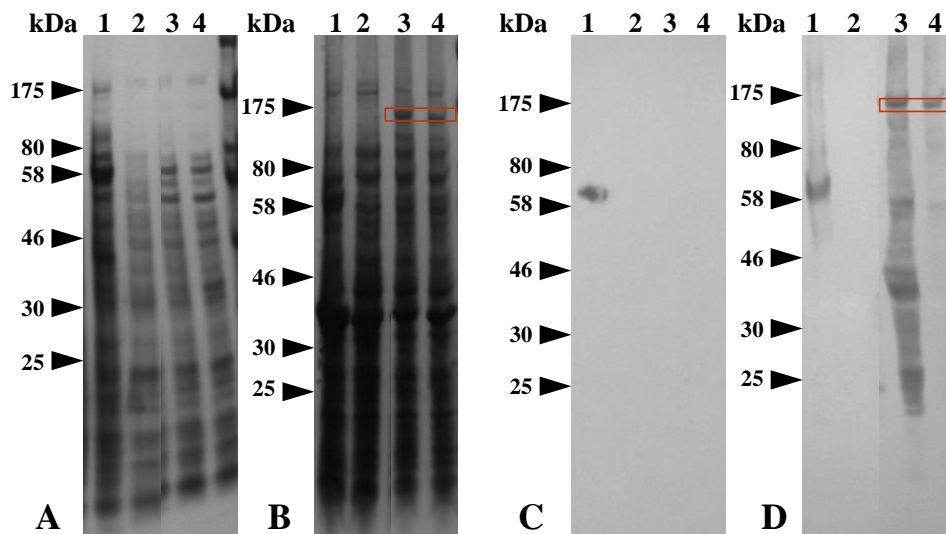


Figure 5.21: SDS-PAGE and western blot analysis of *Nicotiana tabacum* P450 82E4tr fused to *Arabidopsis* ATR2tr

Analysis of crude extract by SDS-PAGE **A** in soluble fraction and **B** in insoluble fraction as well as by western blot analysis against anti His-antibodies **C** in soluble fraction and **D** in insoluble fraction (1 = control-licATR2tr, 2 = Rosetta 2 cells, red boxes: 3 = 82E4tr-lamATR2tr, 4 = 82E4tr-licATR2tr)

5.4.4.4 CYP81D8tr-ATR2tr fusions

The 81D8tr-lamATR2tr and 81D8tr-licATR2tr were expressed in Rosetta 2 (DE3) and tested for activity against 100 μ M TNT. There were no differences in TNT transformation between the fusion proteins (81D8tr-lamATR2tr and 81D8tr-licATR2tr) and the negative control (Figure 5.22) and no additional peaks were seen.

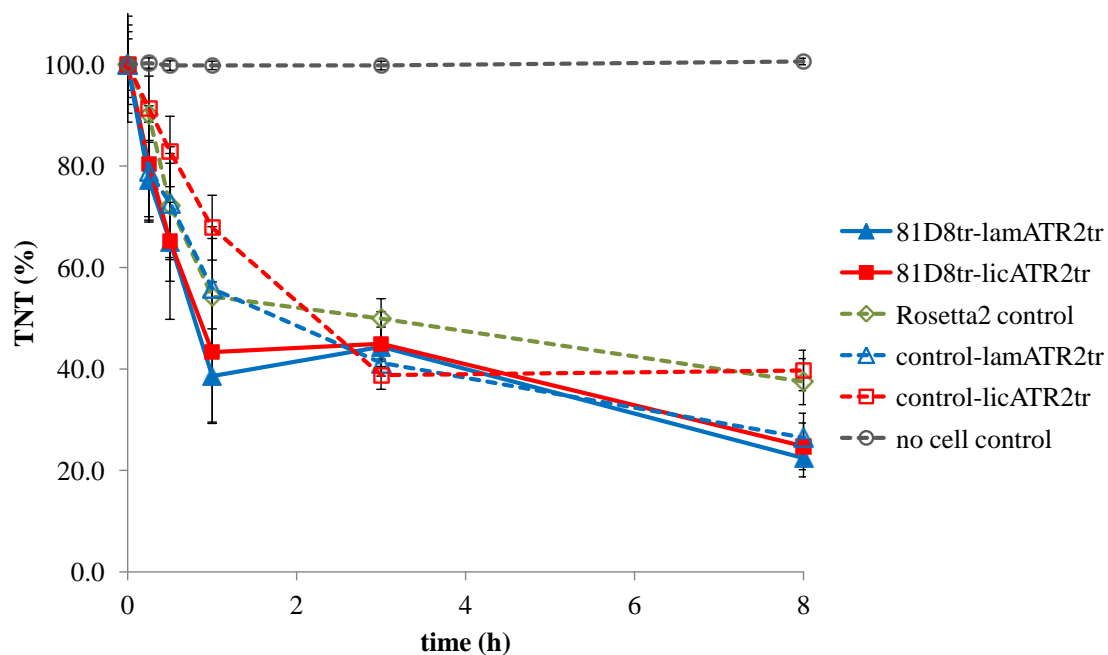


Figure 5.22: TNT removal in a resting cell assay over time

The error bars represent the mean of four independent replicas \pm standard deviation.

As the endogenous function of CYP81D8 is unknown, the 81D8tr-fusions were also tested with 7-ethoxycoumarin, a model P450 substrate, in resting cell assays. The concentration of 7-ethoxycoumarin remained constant (Figure 5.23) and no product peak appeared over time.

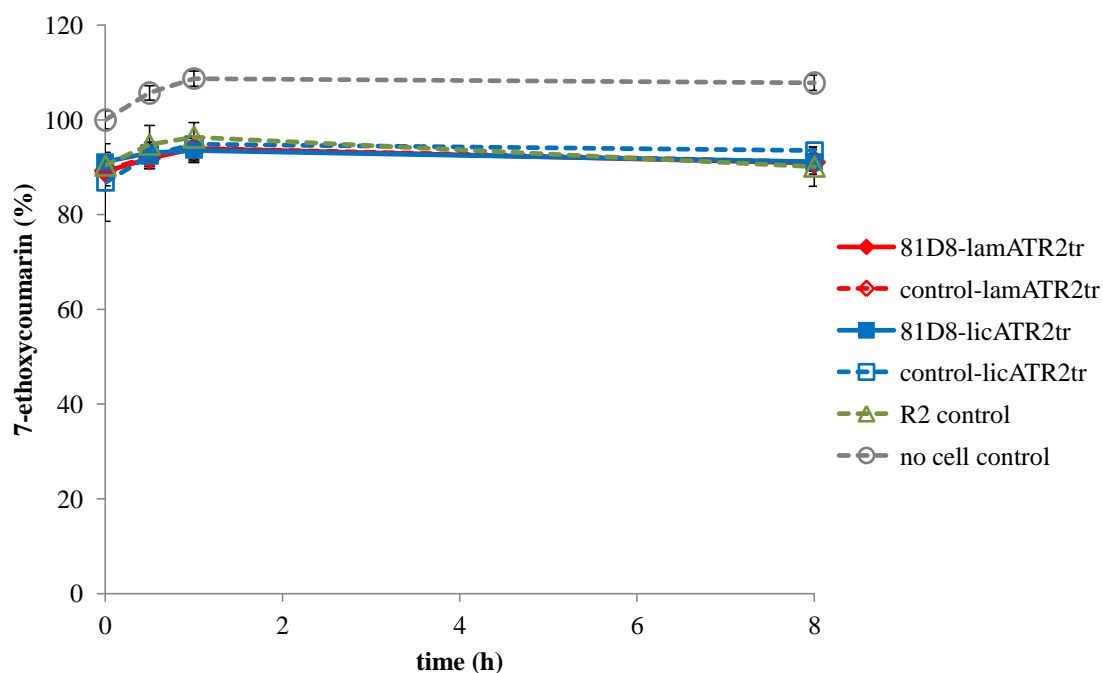


Figure 5.23: Resting cell assay using 7-ethoxycoumarin as substrate

The error bars represent the mean of four independent replicas \pm standard deviation.

The 81D8tr-lamATR2tr (125 kDa) and 81D8tr-licATR2tr (125 kDa) were detected in the insoluble fraction by SDS PAGE and western blot analysis (Figure 5.24). No signal was visible in the soluble fraction except for control-licATR2tr (72 kDa).

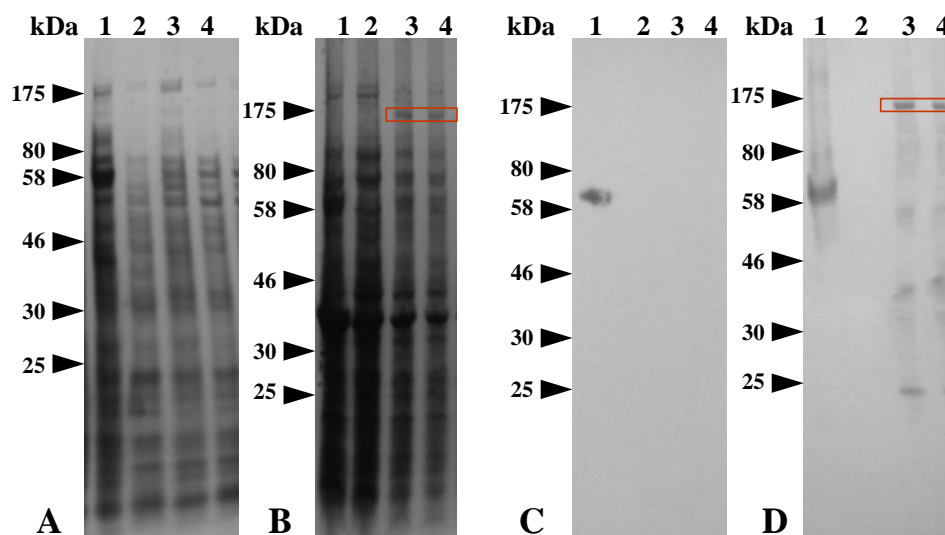


Figure 5.24: SDS-PAGE and western blot analysis of Arabidopsis P450 81D8tr fused to Arabidopsis ATR2tr

Detection of proteins by SDS A in soluble fraction and B in insoluble fraction as well as by western blot analysis against anti His-antibodies C in soluble fraction and D in insoluble fraction (1 = control-licATR2tr, 2 = Rosetta 2 cells, red boxes: 3 = 81D8tr-lamATR2tr, 4 = 81D8tr-licATR2tr)

5.5 Discussion

A platform for expression of plant P450s fused to plant P450 reductases was developed by cloning the Arabidopsis reductase ATR2tr. ATR2tr was expressed in a soluble form in *E. coli* and chosen for the development of the platform technology due to its higher activity than other plant reductases, such as Arabidopsis ATR1tr, ferredoxin reductase and cytochrome c reductase (Chapter 4).

ATR2tr was cloned into the LIC-vector using traditional cloning methods. The connection between the P450 and the reductases was realised by a linker. Two different linkers (lic-linker and lam-linker) were tested. To test this platform, four plant P450s catalysing different reaction types were selected as candidate P450s. The hydrophobic membrane anchor regions of the selected P450s, as identified using TMHMM and SignalP3.0 software (Chapter 2.8.1) were removed and P450s (except CYP93C1 was used with a modified N-terminus³⁰⁶) cloned into lamATR2tr- and licATR2tr-vector using ligation independent cloning, expressed and assayed.

Expression of the artificial plant fusions in the *E. coli* host did not affect the cell growth under the conditions tested here, although it was reported that the fusion of CYP73A4 (cinnamate-4-hydroxylase from *C. roseus*) to the reductases from *C. roseus* resulted in reduced *E. coli* growth.²⁹⁹

IFS-ATR2tr fusions

The isoflavin synthase (IFS) was first identified after functional expression in yeast and Arabidopsis.⁴²⁸

The activity of IFS from *Glycine max* fused to ATR2tr was tested in a growing cell assay for the conversion of naringenin to genistein. No genistein was produced using the native IFS gene (IFS_{nat}-lamATR2tr and IFS_{nat}-licATR2tr), however a conversion of 10% and 20% was seen after 48 h for the codon optimised IFS_{opt}-lamATR2tr and IFS_{opt}-licATR2tr, respectively. The fusion IFS_{syn}-lamATR2tr converted 5.9 μM cinnamic acid to coumaric acid in resting cell assays after 18 h. Other research groups produced similar amounts of genistein (3.7 μM) with yeast microsomes containing IFS after 10 h.⁴²⁸

An example of another artificial plant fusion of rcIFS-riceCPR (IFS from red clover fused to rice reductases) expressed in *E. coli* produced 63% genistein after

12 h in a growing cell assay (using LB medium),³⁰⁷ which was three times higher than when IFS fused to ATR2tr (this project).

73A5tr-ATR2tr fusions

The Arabidopsis CYP73A5 hydroxylates cinnamic acid to coumaric acid. Both fusions (73A5tr-lamATR2tr and 73A5tr-licATR2tr) were expressed in *E. coli* and activity was shown in resting cell assays. The conversion to coumaric acid was increased by altering the growth conditions prior to the resting cell assay. Expression overnight in M9 medium resulted in five fold higher activity (after 24 h cell assay). The opposite effect was demonstrated for rcIFS-riceCPR expressed in *E. coli*, where the production of genistein was reduced to 35% when M9 instead of LB medium was used.³⁰⁷ At a yield of 35% genistein after 48 h the substrate naringenin is not used up (still 50% remained), which could be a result of low enzyme activity when the substrate concentration is too low. This can be tested by adding again naringenin. Another reason of this phenomenon could be the consumption of the cofactor NADPH, which is only replaced when a carbon source in *E. coli* is available. Resting cell assays were usually performed in 50 mM potassium phosphate buffer (Chapter 2.15.3.4) without any additional carbon source. If the NADPH amount is the limiting factor can be tested by adding sugar, which will be transferred into the cell and transformed in the pentose phosphate pathway to create NADPH.

Furthermore, in this project it was found that an expression at 15 °C and 200 rpm increased the conversion of more than 30%, whereas the activity of 73A5tr-licATR2tr was 5% higher than for 73A5tr-lamATR2tr.

The fusion 73A5tr-lamATR2tr was subjected as soluble protein to nickel-affinity chromatography to prove the presence of the fusion protein as confirmed in western blot and MALDI-MS analysis, however no activity was detected. Activity studies and western blot analysis of the different fractions (whole cells, total, soluble and insoluble fraction) indicated that 73A5tr-lamATR2tr was present as membrane associated protein and therefore found in the insoluble fraction. CYP73A4 from *C. roseus* (a homolog of CYP73A5) and CYP71D12 (tabersonine 16-hydroxylase from *C. roseus*), both fused to the reductases from *C. roseus* were also found as active proteins in the membrane fraction.^{299,301} These observations

indicate that the association of the P450 with the endoplasmic reticulum is necessary for activity.

82E4tr-ATR2tr fusions

CYP82E4 from *Nicotiana tabacum* catalyses the *N*-demethylation of nicotine to nornicotine and both could be separated by HPLC. The novel fusions (82E4tr-lamATR2tr and 82E4tr-licATR2tr) were expressed in *E. coli* and activity tested in resting cell assays. The substrate nicotine was removed for all tested samples (also the negative controls) in less than 1 h, which indicated that nicotine is not very stable under the reaction conditions. Moreover, a product peak for nornicotine could not be definitively allocated due to the presence of interfering peaks from *E. coli* extract, which appeared around the same retention time as nornicotine. Other research groups have avoided this problem by using ¹⁴C-labelled nicotine as substrate for thin layer chromatographic analysis, which is a more sensitive method.^{427,429-431}

Nicotine and its derivatives were shown to be separated from urine using HPLC (reversed-phase C18 column).^{432,433} However, when a chiral column was used to identify nornicotine by adapting the method of Demetriou *et al.* 1993⁴³⁴ no improved separation could be seen when resting cell assay samples were separated. Further attempts to optimise this method were not made due to time constraints. These preliminary were unable to confirm whether fusions containing the CYP82E4 is active. In the future, GC-MS analysis could be used to detect both nicotine and nornicotine.

81D8tr-ATR2tr fusions

The Arabidopsis CYP81D8 was 30 times upregulated in a microarray experiment in Arabidopsis plants after TNT treatment.³⁶³ While activity towards TNT by the fusions (81D8tr-lamATR2tr and 81D8tr-licATR2tr) was not detected, when 7-ethoxycoumarin was tested as potential substrate also no product appeared. So whether the fusions were active has not yet been confirmed. *E. coli* can use TNT as nitrogen source.⁴³⁵⁻⁴³⁷ and TNT was reduced to hydroxylaminodinitrotoluenes in all samples by the nitroreductases naturally present in *E. coli*.

Two linkers (lic-linker with the amino acid sequence: RAFSS and lam-linker: GSTSSGSG) have been tested to create fusions of the P450s and the reductase ATR2tr. Generally, the lam-linker resulted in 5-10% higher activity than the lic-linker when tested with IFS or 73A5 fusions. However, preliminary results suggested that the 73A5tr-licATR2tr when grown in M9 medium at 15 °C and 200 rpm may have similar activity to 73A5tr-lamATR2tr.

The artificial lam-linker was originally engineered by Prof. Koffas' research group to create a junction of GSTSSGSG with the start of the truncated CPR, which should avoid the formation of secondary structure.³⁰⁶ In their work, they compared the activity of IFS-CPR connected with the lam-linker and the construct C, a fusion without a linker, where the IFS C-terminus was directly fused to the truncated CPR from *C. roseus*. Construct C did not produce any product when expressed in *E. coli* JM109, TOP10F' or BL21Star. However, construct C showed activity when expressed in DH5 α , which was 50% compared to IFS-CPR.³⁰⁶ Their findings showed the necessity of a linker to keep a distance between P450 and reductase. The same GST-linker was used successfully for the artificial plant fusion rcIFS-riceCPR (IFS from red clover fused to rice reductases) as rcIFS-CPR (IFS to *C. roseus* reductases) to allow the two enzymes a separate protein folding.³⁰⁷

Previously, Prof. Schröder's research group also used a ST-linker for engineering different plant fusions with the CPR from *C. roseus*.²⁹⁹⁻³⁰² The dipeptide ST was chosen to avoid forming of extensive secondary structures, which can affect the electron transfer between the reductase and the P450.

The detection of artificial plant fusion enzymes by western blot analysis seemed to be not straightforward, due to lack of data in the literature.^{302,305-307} An active fusion of CYP73A4-CPR was only detected when containing the membrane anchor of the P450, but then it was not active. Activity was found when the first 69 amino acids of the P450 have been removed, however no protein signal was visible in the immunoblot.²⁹⁹ The flavonoid hydroxylase (CYP75 from *C. roseus*) was detected as fusion with the reductase from *C. roseus* and the reductase from *Petunia hybrida* by western blot analysis.³⁰⁰

All fusions engineered with the Arabidopsis ATR2tr reductase were detected in the western blot analysis using anti His-antibodies. They were found mainly in the

insoluble protein fraction, which implied that these fusions are still membrane associated, despite lacking the hydrophobic N-terminus. The only exceptions with no signal in the SDS PAGE and the western blot were the IFS fusions containing the native IFS gene (IFS_{nat}-lamATR2tr and IFS_{nat}-licATR2tr), for which also no activity was detected, possibly caused by a too low protein expression. The presence of plant fusion proteins containing IFS from *G. max* or IFS from red clover was not confirmed so far.^{306,307}

This development of a vector, which contained the soluble Arabidopsis reductase ATR2tr, is usable for high-throughput cloning due to the Ligation Independent Cloning system. ATR2tr, one of the Arabidopsis reductase, would be expected to be an appropriate partner enzyme for creating fusion with the 178 Arabidopsis P450s with unknown function to discover their native role in the plant.

This system provides a platform technology, where also other plant P450s can be cloned fast and easily as fusion enzymes, which then can be studied further for their potential function.

6 Comparison of plant Cytochromes P450 fused to different reductases

6.1 Introduction

The electron transfer from P450 reductases to P450s is species unspecific, in all cases examined; for example *Nicotiana tabacum* was transformed with the rabbit liver P450 and showed to be supported endogeneous *N. tabacum* reductases⁴³⁸. However, the specific activity of the membrane associated CYP75 (flavonoid hydroxylase) from *Petunia hybridia* fused to its own reductase showed twice much activity after recombinant expression in *E. coli* than when fused to the reductase of *C. roseus*.³⁰⁰ Thus, it could be predicted that the reductases in each organism should be the most efficient for the support of their corresponding P450s considering that they have evolved together.

The CPR from *C. roseus*, firstly characterised from Madyastha and Coscia in 1979 after purification from five day old, etiolated seedlings,⁴¹¹ was used as the partnering reductase for the creation of artificial plant P450 fusion systems (see Table 1.2, page 45). For all the plant-plant fusions, the hydrophobic N-terminus of the CPR was deleted to avoid an association with the bacterial membrane and to increase the solubility.^{299-302,306,307}

The truncated form of ATR2 (ATR2tr) from Arabidopsis was expressed as a soluble and active reductase in *E. coli* (Chapter 4, page 111) and then used as partner enzyme to develop a platform technology of a plant P450 fused to a Arabidopsis reductase (Chapter 5, page 137).

The RhF reductase is originally part of the native fusion P450 RhF from *Rhodococcus* sp. which catalyses the *O*-dealkylation of 7-ethoxycoumarin to 7-hydroxycoumarin (Figure 1.12).^{136,137} Recently, it was used for the functional expression of bacterial P450 fusions.^{145,146,439-441}

6.2 Objectives

A technology platform comprising plant P450s fused to the truncated Arabidopsis reductase ATR2tr was engineered as described in Chapter 5 and in this chapter, the system was developed further by testing additional reductases and *E. coli* strains. The reductases were fused to: cinnamate-4-hydroxylase (CYP73A5) from

Arabidopsis and isoflavone synthase I (IFS) from *Glycine max* and the activities *in vivo* compared.

The IFS (CYP93C) gene was fused to three reductases:

- 1) the CPR from *C. roseus* (fusion construct obtained from Prof. Mattheos Koffas, Chapter 5.1),
- 2) the ATR2tr from Arabidopsis (developed in Chapter 5) and
- 3) the RhF reductase from *Rhodococcus* sp.

The IFS activity was tested by measuring the conversion of naringenin to genistein in growing and resting cell assays.

The cinnamate-4-hydroxylase (CYP73A5) gene was fused to two reductases:

- 1) the ATR2tr from Arabidopsis (developed in Chapter 5) and
- 2) the RhF reductase from *Rhodococcus* sp.

CYP73A5tr from Arabidopsis was chosen as its function in the phenylpropanoid pathway is known. The activity of CYP73A5tr was tested for the hydroxylation of cinnamic acid to coumaric acid in *in vitro* as well as in resting cell assays.

6.3 Methods

6.3.1 Expression of IFS-fusions

6.3.1.1 Expression conditions of IFS-CPR

The construct IFS-CPR (C-terminus of isoflavone synthase I from *G. max* fused to the N-terminus of the reductases from *C. roseus*) was kindly provided by Professor Koffas (University at Buffalo, The State University of New York)³⁰⁶ and was used as positive control for the IFS-P450-reductase fusion systems. Two different *E. coli* strains were tested: JM109, used for expression of IFS-CPR by Leonard and Koffas 2007³⁰⁶, and Rosetta 2 (DE3), which contains an additional plasmid for eukaryotic rare codons (chloramphenicol resistance, Novagen) (*E. coli* strains, see Table 2.1). Both *E. coli* strains were transformed with the IFS-CPR fusion construct in the pTrcHis2/LacZ vector (ampicillin resistant, Invitrogen) (Chapter 2.8.4).

For the expression of IFS-CPR, the published protocol from Leonard and Koffas, 2007³⁰⁶ was used. Briefly, a preculture of 10 ml LB medium containing 1% glucose and 100 µg/ml ampicillin (additionally 34 µg/ml chloramphenicol for Rosetta 2 cells) was inoculated with a single colony and incubated overnight shaking (200 rpm) at 37 °C. A volume of 100 ml LB containing 100 µg/ml ampicillin (and 34 µg/ml chloramphenicol for Rosetta 2) was inoculated with the preculture to an OD_{600} = 0.1 and incubated shaking (200 rpm) at 37 °C. When OD_{600} had reached 0.8, 1 mM IPTG was added and the culture incubated at 30 °C under shaking for 3 h. Cells were then harvested and resuspended to an OD_{600} = 0.6 in M9 minimal medium (final volume: 100 ml) containing 6 nM thiamine and 1 mM IPTG (Figure 6.1).

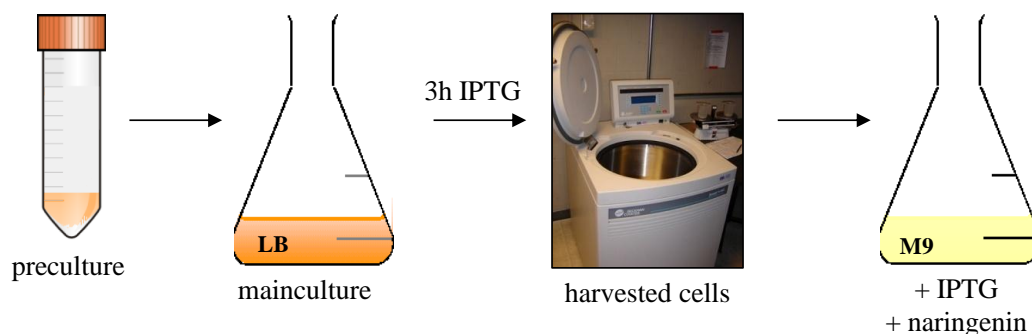


Figure 6.1: Flow scheme of the protocol for the expression of IFS-CPR fusion construct according to Leonard and Koffas³⁰⁶

6.3.1.2 Optimised conditions for the expression of the IFS-RhF fusion

The fusion protein IFS-RhF (isoflavone synthase 1 from *G. max* fused to the reductases RhF from *Rhodococcus* sp.) was expressed under the conditions described in Materials and Methods (Chapter 2.10.1), with the following alteration: After inoculation, the main culture was incubated shaking at 28 °C for approximately 16 h. Cultures were then further incubated shaking at 37 °C until the OD_{600} reached 0.6 to 0.8.

6.4 Results

6.4.1 IFS fusions

6.4.1.1 Expression of IFS-CPR

The fusion IFS-CPR (isoflavone synthase I from *G. max* fused to the reductases from *C. roseus*) was expressed in *E. coli* JM109 and Rosetta 2 (DE3) cells. The presence of the plasmid in the strains was confirmed by PCR.

Following the addition of IPTG, the cell density increased for all samples during the following 3 h incubation (Figure 6.2). However, following the addition of naringenin, during the subsequent growing cell assay, IFS-CPR expression in JM109 cells grew two-fold more slowly than the other cultures (Figure 6.2).

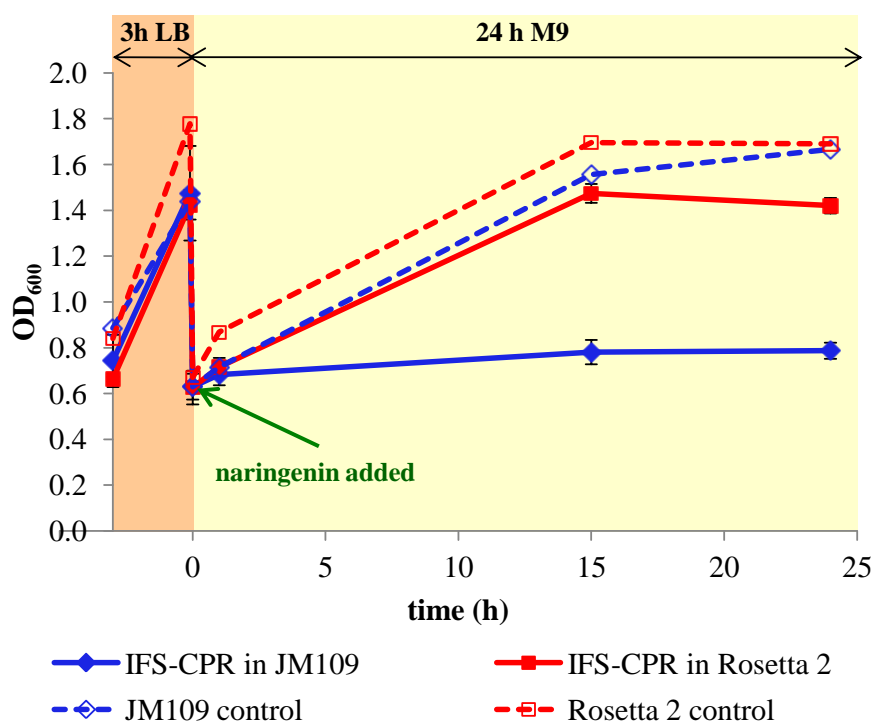


Figure 6.2: Observation of the cell growth of *E. coli* JM109 and Rosettas 2 during the expression of IFS-CPR

Data for IFS-CPR in JM109 and Rosetta 2 (DE3) cells represent the mean of three independent replicas \pm standard deviation.

In the cultures of Rosetta 2 (DE3) cells expressing IFS-CPR, 75% of the substrate naringenin was removed from the medium, whereas in the cultures of JM109 cells expressing IFS-CPR was no significant uptake of naringenin (Figure 6.3A), also small amount of 5 μ M genistein was produced. The naringenin concentration

increased in the cultures of the untransformed JM109 and Rosetta 2 (DE3) cells, possibly due to water evaporation over time. The product genistein was produced with IFS-CPR in both *E. coli* strains, with the conversion five times higher in Rosetta 2 (DE3) than in JM109 (Figure 6.3B). Rosetta 2 (DE3) was therefore chosen for further experiments.

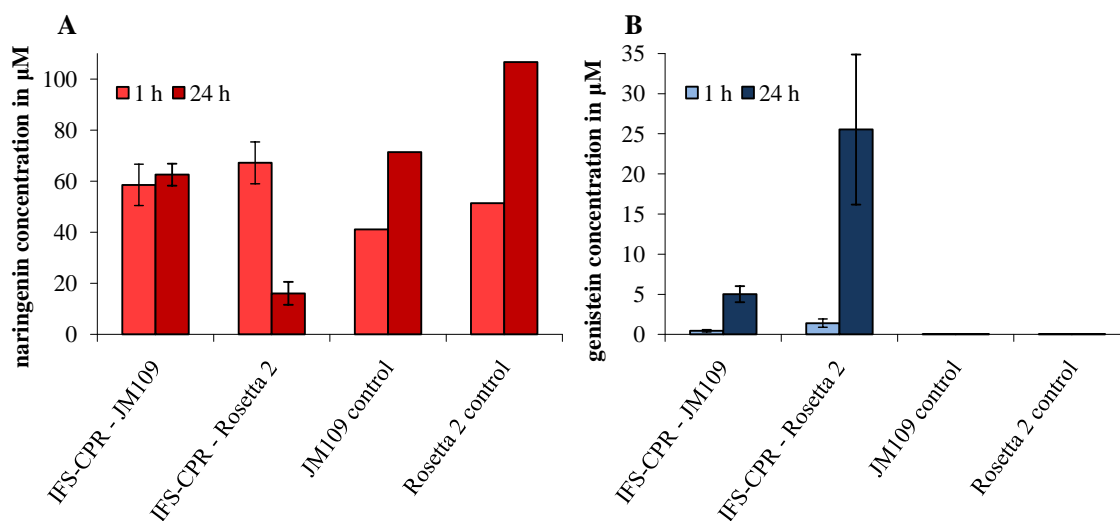


Figure 6.3: Activity of *Glycine max* IFS fused to *Catharanthus roseus* CPR when expressed with *E. coli* JM109 and Rosetta 2 cells.

A naringenin and **B** genistein concentration in the culture supernatant after an expression time of 1 and 24 h (IFS = isoflavone synthase 1 from *G. max*, CPR = P450 reductase from *C. roseus*). The error bars represent the mean of two to three independent replicas ± standard deviation.

6.4.1.2 Expression of IFS-RhF

The expression of IFS-RhF (plant-bacterial fusion) was performed under the same conditions as stated for IFS-CPR (Chapter 6.3.1.1). However, activity of the isoflavone synthase was lower than IFS-CPR: just 2 μM genistein was produced after 24 h (Figure 6.4), which is 12.5 times less than for IFS-CPR.

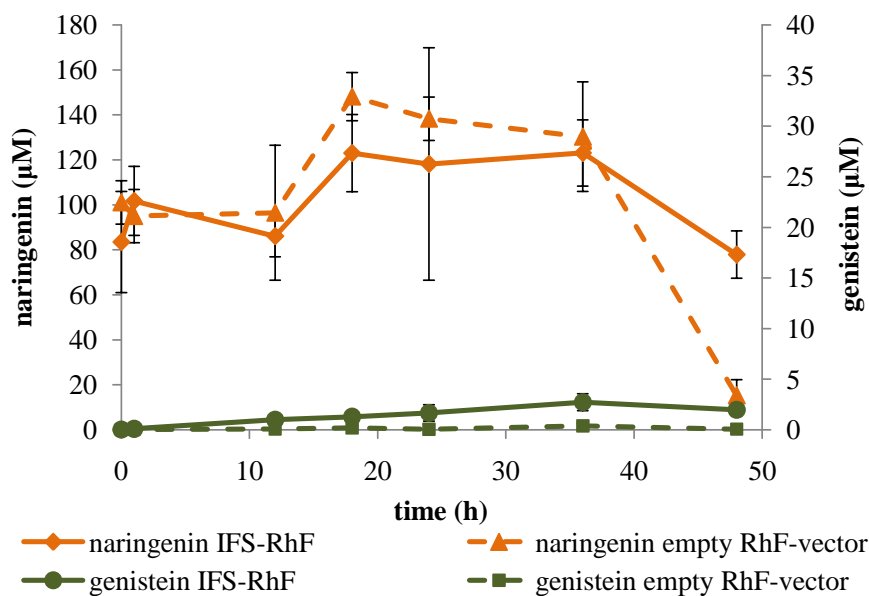


Figure 6.4: Activity of *Glycine max* IFS fused to *Rhodococcus sp.* RhF reductase
In vivo conversion of naringenin to genistein by IFS-RhF. The error bars represent the mean of four independent replicas \pm standard deviation.

By using the optimised protocol (Chapter 6.3.1.2), the *in vivo* genistein production in growing cells containing IFS-RhF over 24 h was improved 10-fold. Thus, the plant-bacterial fusion IFS-RhF (red in Figure 6.5) produced more genistein (23 μM after 48 h) than the plant-plant fusion IFS-CPR (green in Figure 6.5, 18 μM after 48 h) in the growing cell assay at 20 °C. No activity was detected for the expression of IFS without reductases, the RhF reductases alone, IFS-RhF boiled control or *E. coli* Rosetta 2 (DE3) cells without any plasmid.

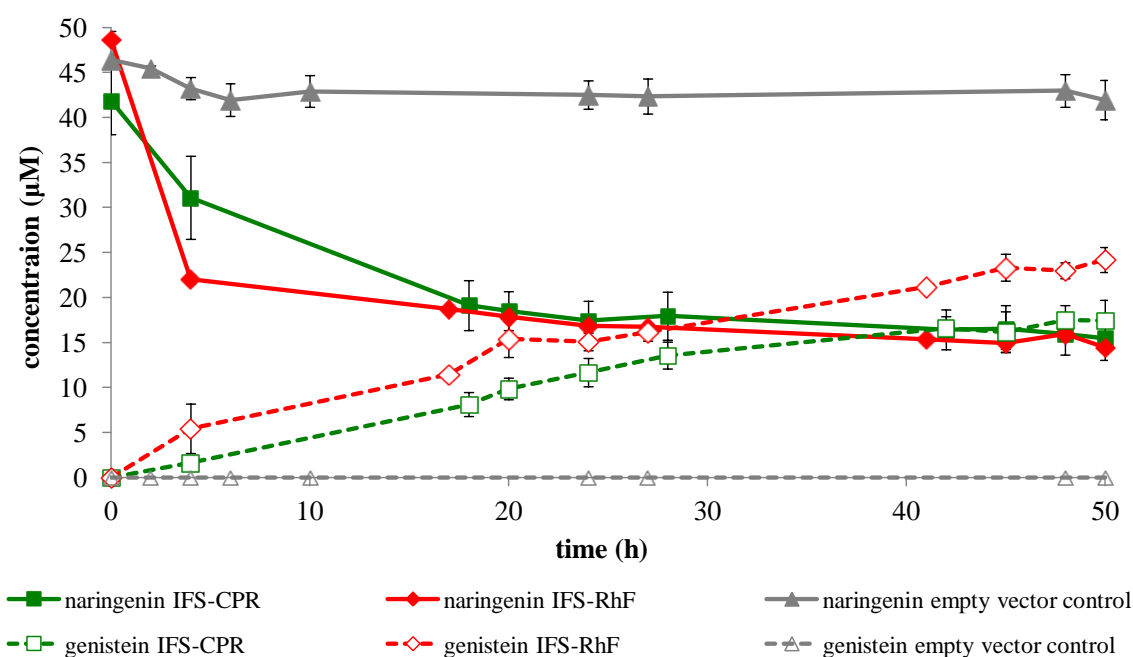


Figure 6.5: Conversion of naringenin to genistein by IFS-RhF and IFS-CPR in a growing cell assay at 20 °C

IFS = isoflavone synthase 1 from *G. max*, CPR = P450 reductase from *C. roseus*, RhF = P450 reductase domain from *Rhodococcus* sp. The error bars represent the mean of five independent replicas \pm standard deviation.

When cells were grown at 15 °C, activity of IFS-RhF and IFS-CPR was reduced to around 15 μM genistein for both after 48 h (Figure 6.6). This was 3.2-fold and 2.5-fold lower for IFS-RhF and IFS-CPR, respectively, than when cells were grown at 20 °C.

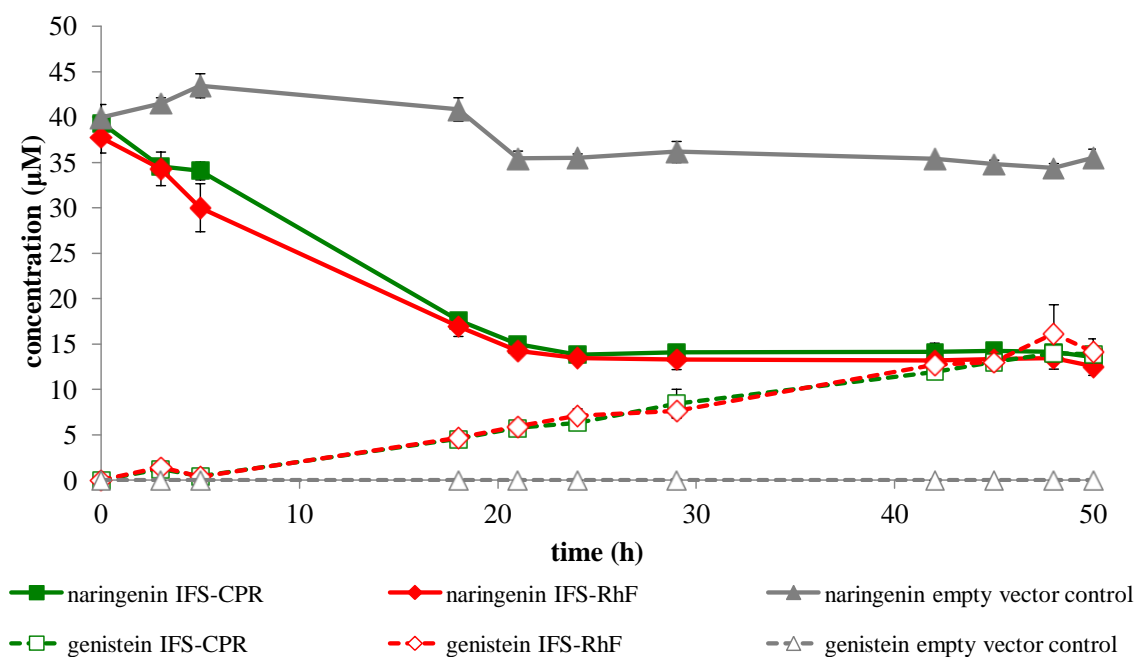


Figure 6.6: Conversion of naringenin to genistein by IFS-RhF and IFS-CPR in a growing cell assay at 15 °C

IFS = isoflavone synthase 1 from *G. max*, CPR = P450 reductase from *C. roseus*, RhF = P450 reductase domain from *Rhodococcus* sp. The error bars represent the mean of three independent replicas \pm standard deviation.

The activity seen for IFS-RhF was 10-fold higher than IFS-CPR in growing cell assays. Faster growth and an increase in cell mass may explain the rise in genistein production for IFS-RhF. Therefore, the OD_{600} of *E. coli* Rosetta 2 (DE3) was measured over a time course (Figure 6.7), however no significant difference was observed. The differences in genistein production might be due to the extraction method and the sensitivity in HPLC detection.

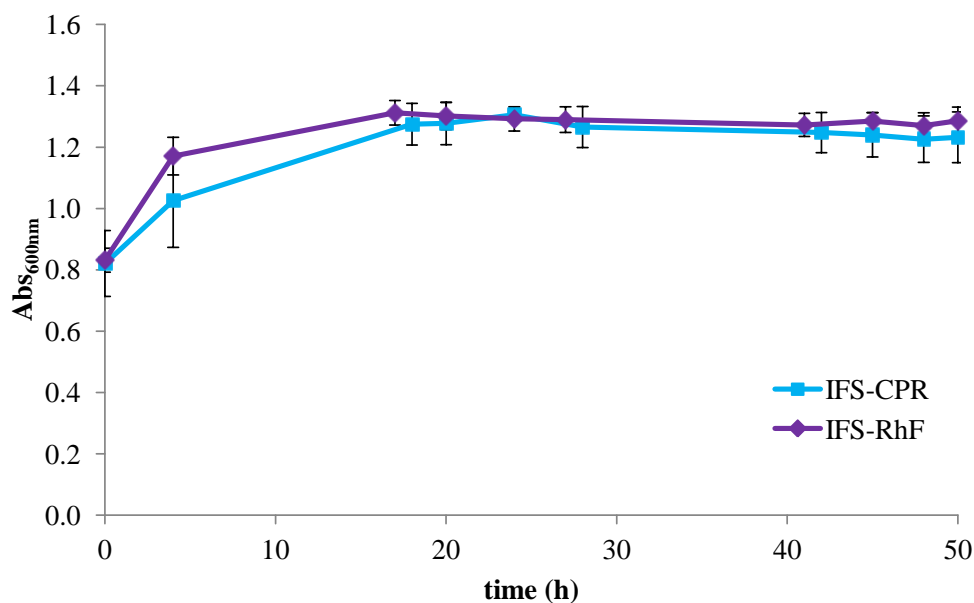


Figure 6.7: Observation of the optical density during the expression of IFS-CPR and IFS-RhF at 20 °C in M9 medium

The error bars represent the mean of five independent replicas \pm standard deviation.

The level of the conversion of naringenin to genistein was similar for IFS-CPR and IFS-RhF when tested in a resting cell assay (Figure 6.8).

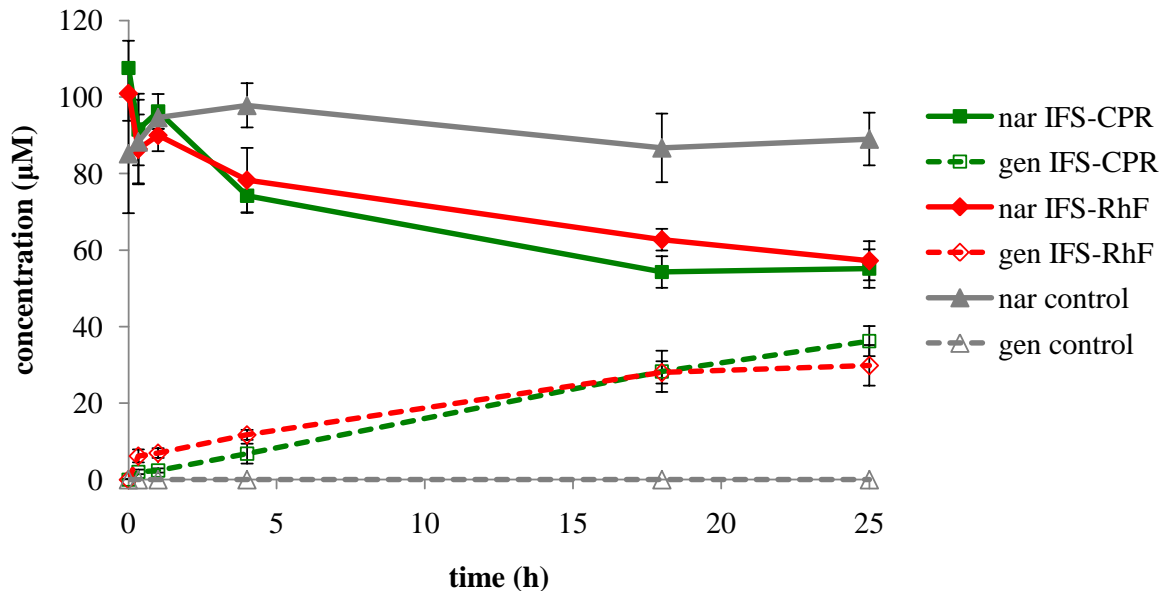


Figure 6.8: Conversion of naringenin to genistein in a resting cell assay

(nar = naringenin, gen = genistein, IFS = isoflavone synthase 1 from *G. max*, CPR = P450 reductase from *C. roseus*, RhF = P450 reductase domain from *Rhodococcus* sp., control = plasmid containing RhF reductase expressed in *E. coli*.) The error bars represent the mean of five independent replicas \pm standard deviation.

6.4.1.3 Comparison of the IFS fusions in their growing cell cultures

The production of genistein by IFS fused to different reductase was compared in growing cell assays (Rosetta 2 (DE3), 20 °C and 200 rpm). The IFS-RhF produced almost 50% genistein after 48 h and was found to have the highest activity in comparison to the other fusions under these conditions (Figure 6.9). IFS-CPR showed the second highest activity with 35% genistein production. Interestingly, activity for the IFS fusions containing the Arabidopsis ATR2tr as reductase partner was only achieved after codon optimisation of the IFS gene. No such modification was required for the other two fusions (IFS-RhF and IFS-CPR). Rosetta 2 (DE3) harbouring the empty vector did not produce coumaric acid and the substrate concentration of cinnamic acid remained unchanged, verifying the activity of the created fusion enzymes.

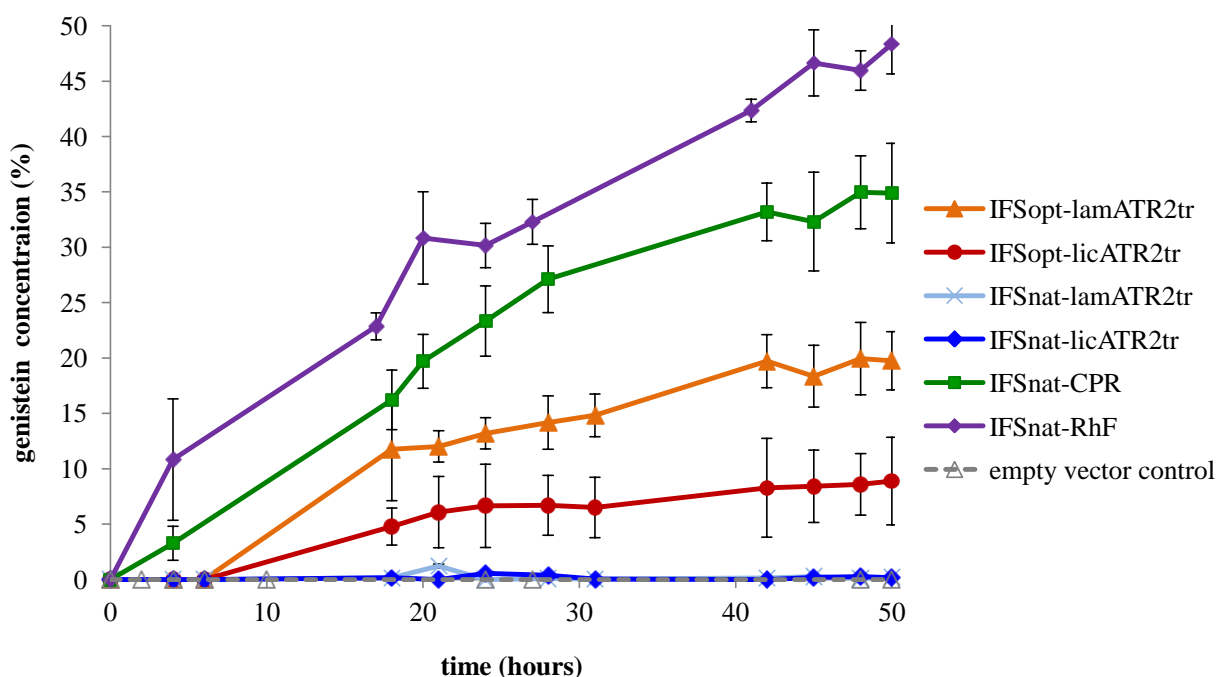


Figure 6.9: Production of genistein by IFS fusions in a growing cell assay

(IFS = isoflavone synthase 1 from *G. max*, opt = codon optimised gene for *E. coli* expression, nat = native gene of IFS, ATR2tr = truncated version of P450 reductase from Arabidopsis ATR2, CPR = P450 reductase from *C. roseus*, RhF = P450 reductase domain from *Rhodococcus* sp.) The error bars represent the mean of at least four independent replicas \pm standard deviation.

6.4.1.4 Detection of IFS fusion enzymes

To show the presence of IFS-CPR and IFS-RhF fusions, SDS PAGE and western blot analysis (anti-His antibody) were conducted. Faint signals on western blot were detected for IFS-RhF in the soluble and insoluble fraction (Figure 6.10). No signal was detected for IFS-CPR by western blot analysis, a result of possibly through a very low expression of IFS-CPR by the host cells.

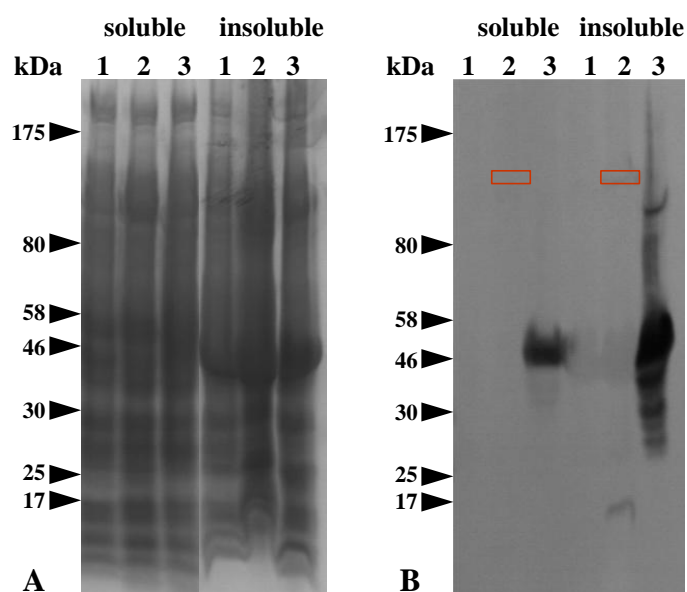


Figure 6.10: SDS-PAGE and western blot analysis of *Glycine max* IFS fused to *Catharanthus roseus* CPR and to *Rhodococcus* sp. RhF reductase in the soluble and insoluble fraction

Soluble and the insoluble fraction after the sonication: **A** SDS-PAGE and **B** western blot (anti-His antibody); (1 = IFS-CPR, 80 kDa; 2 = IFS-RhF, red boxes, 95 kDa, 3 = RhF-vector control, 36 kDa)

The western blot was repeated with specific antibodies raised against the reductase RhF in order to confirm the results obtained using His-antibodies.

The IFS-RhF fusion was detected in the soluble protein fraction as well as in the insoluble protein fraction (Figure 6.11). However, no signal difference was detected in the total protein fraction. No degradation product for the fusion (RhF alone, 35 kDa) was seen. The control RhF alone was detected in the total, the soluble and insoluble protein fraction.

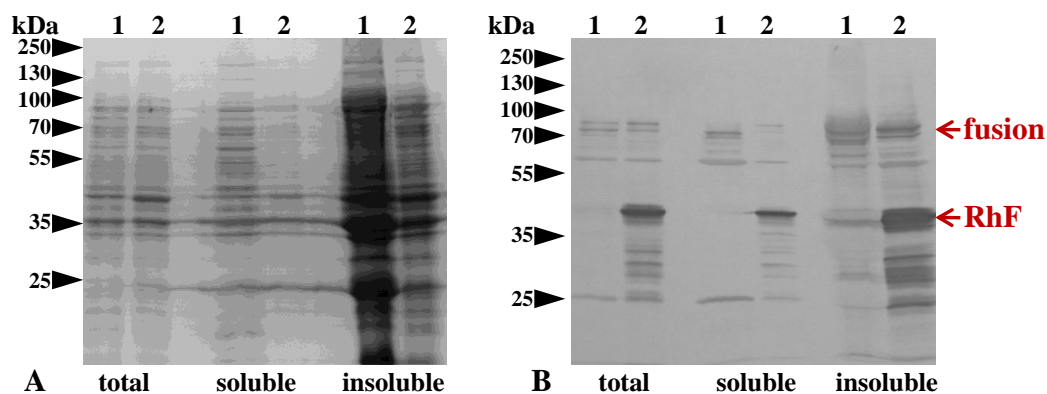


Figure 6.11: SDS-PAGE and western blot analysis of *Glycine max* IFS fused to the RhF reductase from *Rhodococcus* sp. in total, soluble and insoluble protein fraction
Total, soluble and the insoluble protein fraction after the sonication: **A** SDS-PAGE and **B** western blot (specific RhF antibody); (1 = IFS-RhF, 95 kDa; 2 = RhF control, 35 kDa)

The fusions IFS-lamATR2tr and IFS-licATR2tr could be not detected by western blot analysis using anti His-antibodies. However, both were detected as fusion proteins by western blot analysis against specific ATR2 antibodies in the insoluble protein fraction (Figure 6.12). No signal was found in the soluble protein fraction and also not in the total protein fraction, possibly due to too low concentration. The control ATR2tr was visible in the total, soluble and insoluble protein fraction (line 3 in Figure 6.12B). ATR2tr alone was also detected in samples containing the IFS-fusions suggesting the degradation of the fusion into IFS and ATR2tr.

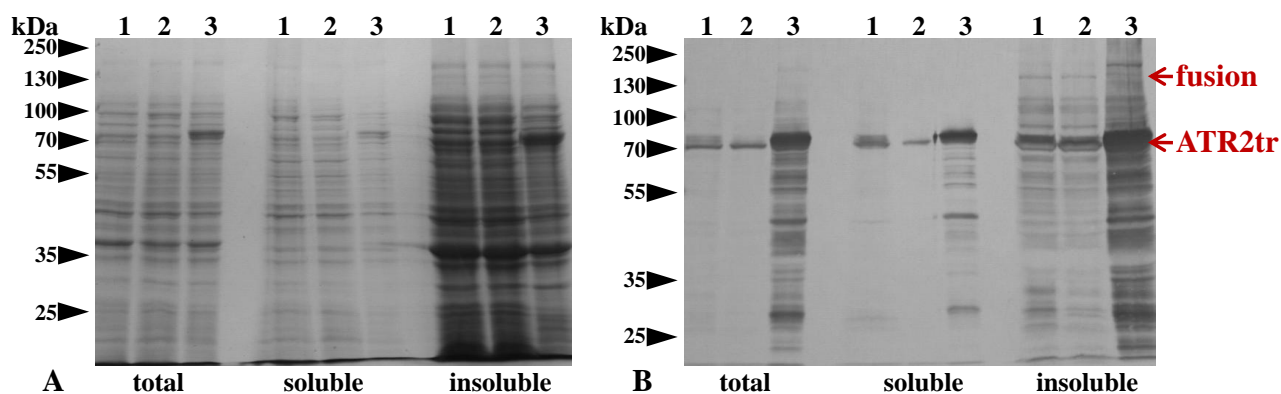


Figure 6.12: SDS-PAGE and western blot analysis of *Glycine max* IFS fused to Arabidopsis reductase ATR2tr in total, soluble and insoluble protein fraction
Total, soluble and the insoluble protein fraction after the sonication: **A** SDS-PAGE and **B** western blot (specific ATR2tr antibody); (1 = IFS-lamATR2tr, 131 kDa; 2 = IFS-licATR2tr, 131 kDa, 3 = lamATR2tr control, 72 kDa)

Reverse transcription PCR (Chapter 2.7) using primers to the IFS gene was used to test if the genes encoding IFS-RhF were transcribed (Figure 6.13). A band at the predicted size for IFS of 1500 bp was seen using cDNA from IFS-RhF expressing cells as *E. coli* Rosetta 2 (DE3) template. No signal was detected for the boiled IFS-RhF control (line b, Figure 6.13).

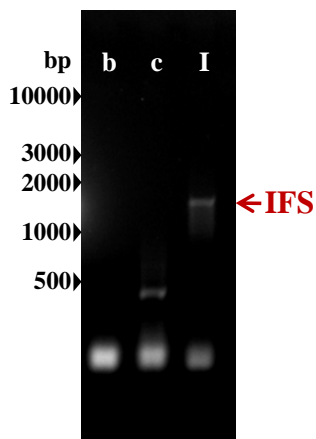


Figure 6.13: Reverse transcription PCR for IFS-RhF
b = boiled IFS-RhF control, c = RhF control, I = IFS-RhF

6.4.1.5 Purification of IFS-RhF

Fractions of Ni-chromatography purified Rosetta 2 (DE3) expressed IFS-RhF were analysed by SDS-PAGE and western blot. IFS-RhF fusion was detected in the insoluble (line 2, Figure 6.14) and in the eluted (line 5) fractions.

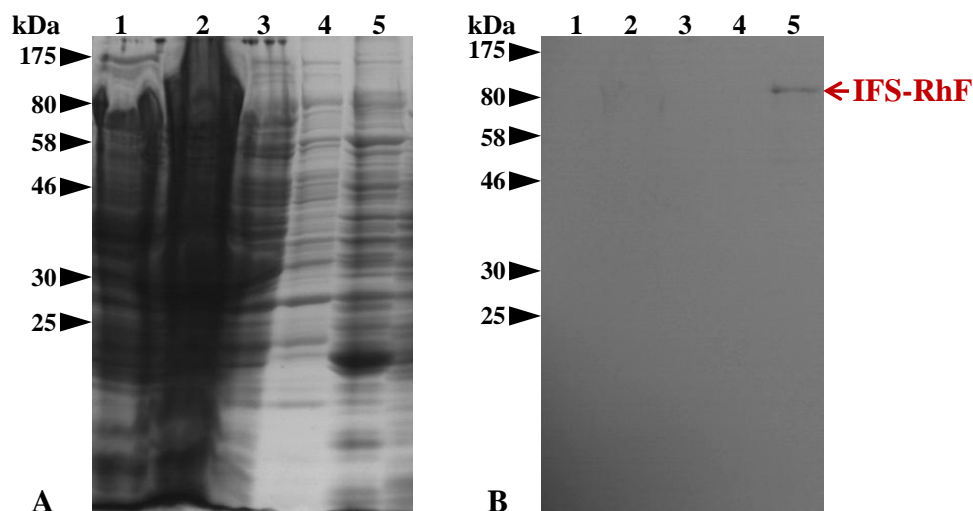


Figure 6.14: SDS-PAGE and western blot analysis of *Glycine max* IFS fused to *Rhodococcus sp.* RhF reductase after purification with Ni-affinity chromatography
A SDS PAGE and **B** western blot of the purification of IFS-RhF (1 = soluble fraction after sonication, 2 = insoluble fraction after sonication, 3 = wash step, 4 = elution of unspecific protein, 5 = eluted IFS-RhF)

6.4.2 CYP73A5tr fusions

Resting cell assays were conducted on 73A5tr-lamATR2tr, 73A5tr-licATR2tr and 73A5tr-RhF expressed in *E. coli* Rosetta 2 (DE3). All fusions converted cinnamic acid to coumaric acid, with 73A5tr-lamATR2tr and 73A5tr-licATR2tr producing 33% and 23% after 24 h, respectively (Figure 6.15). The plant bacterial fusion 73A5tr-RhF shown with 3.5% genistein production a much lower conversion after 24 h. There were no decrease in cinnamic acid, nor increase in coumaric acid in the cells harbouring the empty vector only (data not shown).

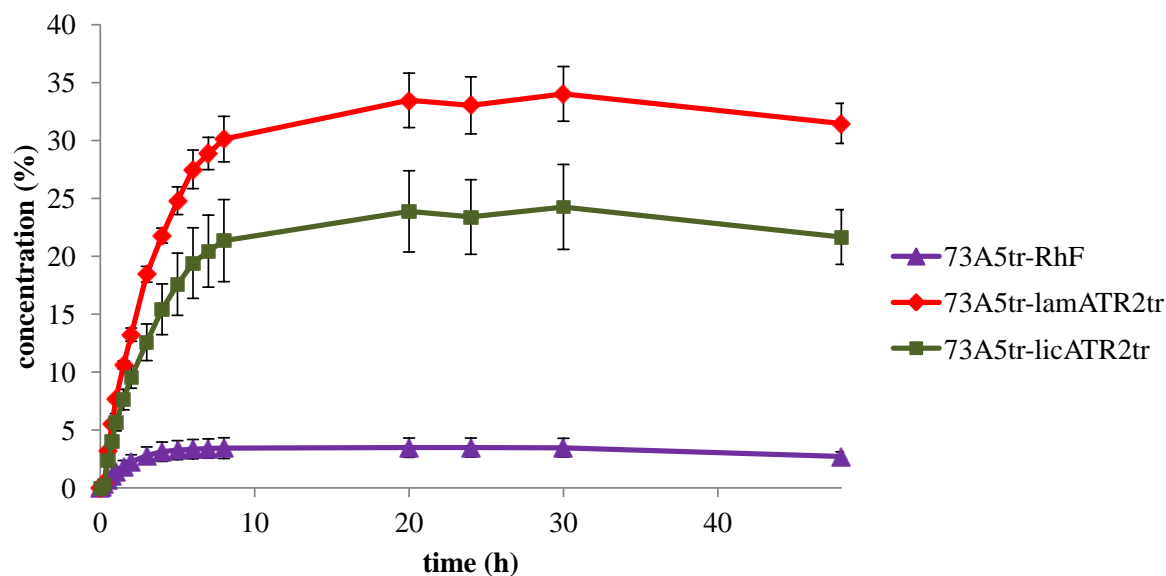


Figure 6.15: Cinnamate-4-hydroxylase activity of Arabidopsis P450 73A5tr fused to Arabidopsis ATR2tr in a resting cell assay

73A5tr = truncated version of cinnamate-4-hydroxylase, RhF = P450 reductase domain from *Rhodococcus* sp., ATR2tr = truncated version of P450 reductase from Arabidopsis ATR2. The error bars represent the mean of four independent replicas \pm standard deviation.

Subsequent, SDS PAGE as well as a western blot analyses were performed for the soluble and the insoluble fraction of the expressed 73A5tr fusions (Figure 6.16 and Figure 6.17). No bands at the predicted size of the fusion enzymes were found in the soluble protein fraction. However bands at the predicted size for all fusions (73A5tr-RhF = 91 kDa, 73A5tr-lamATR2tr = 127kDa, 73A5tr-licATR2tr = 127 kDa) and the RhF alone (36 kDa) were detected in the insoluble fraction. No band was visible for the negative Rosetta 2 cell control.

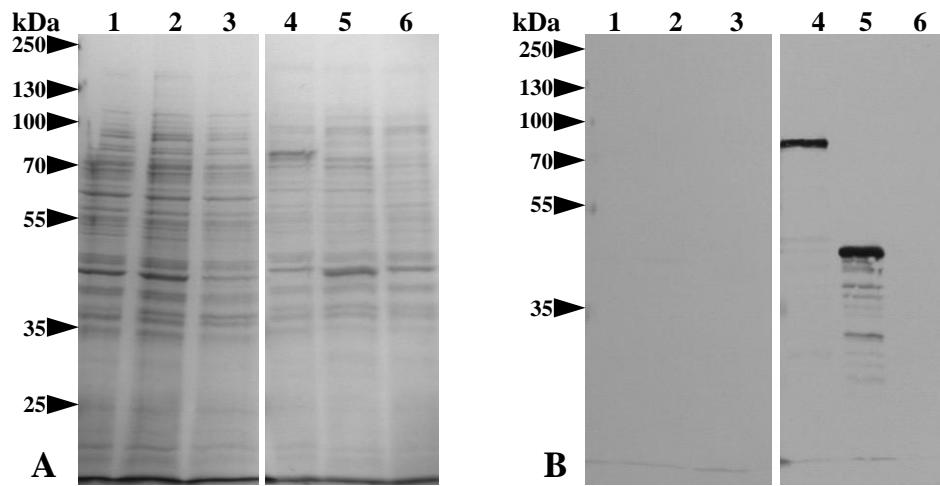


Figure 6.16: SDS-PAGE and western blot analysis of Arabidopsis P450 73A5tr fused Arabidopsis ATR2tr or to *Rhodococcus* sp. RhF reductase in the insoluble protein fraction

A SDS PAGE and B western blot analysis against anti His-antibodies (1 = 73A5tr-lamATR2tr, 2 = 73A5tr-licATR2tr 3 = 73A5tr-RhF, 4 = lamATR2tr control, 5 = RhF control, 6 = Rosetta 2 cells)

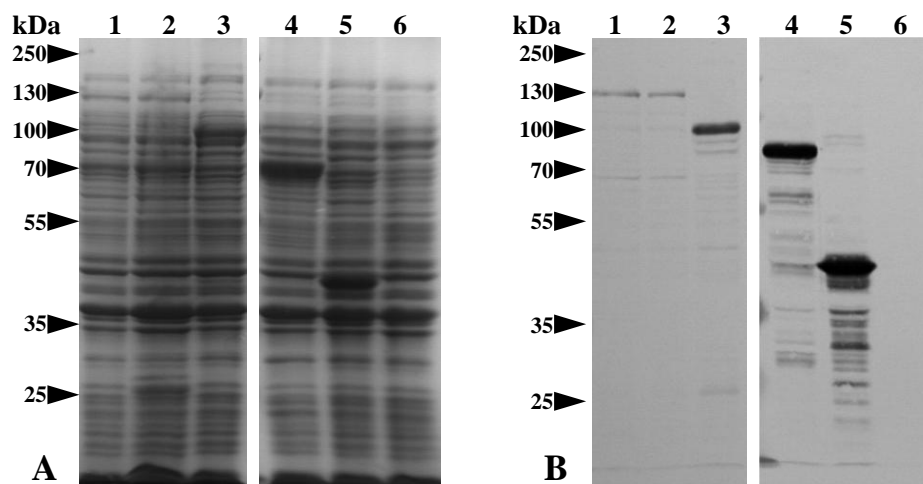


Figure 6.17: SDS-PAGE and western blot analysis of Arabidopsis P450 73A5tr fused Arabidopsis ATR2tr or to *Rhodococcus* sp. RhF reductase in the insoluble protein fraction

A SDS PAGE and **B** western blot analysis against anti His-antibodies (1 = 73A5tr-lamATR2tr, 2 = 73A5tr-licATR2tr 3 = 73A5tr-RhF, 4 = lamATR2tr control, 5 = RhF control, 6 = Rosetta 2 cells)

6.5 Discussion

The IFS-CPR fusion, an artificial fusion of IFS from *G. max* coupled to the 71 amino acid truncated reductase CPR from *C. roseus*, was developed by Prof. Koffas's research group.³⁰⁶ The genes were fused using an artificial linker λ (GST) to reduce the formation of secondary structure and different modifications of the IFS N-terminus were tested to try to increase activity as measured by the production of genistein from naringenin. In their studies, using JM109 cells, the highest yield with around 15 μ M (30%) genistein was seen when the construct contained the IFS with a synthetic mammalian peptide at the N-terminus fused to the 71 amino acid truncated CPR (*C. roseus*) through the linker λ .³⁰⁶ The published work was repeated here using the same cell strain and experimental methods, and the fusion protein tested: just 5 μ M (10%) genistein was produced after 24 h. Additionally, the Rosetta 2 (DE3) strain, which contained an additional plasmid for rare codons, was tested. Five times more genistein (25 μ M = 50%) *in vivo* was produced by this strain after 24 h and thus it was chosen for further analysis.

The plant P450 IFS was fused to the bacterial reductases RhF from *Rhodococcus* sp. creating the first plant-bacterial self-sufficient system. The RhF

reductase is part of a native P450-RhF fusion and was already used for engineering artificial fusions with various prokaryotic P450 such as P450cam and P450-XplA heme.¹⁴⁶

A conversion of 3% genistein was initially detected for IFS-RhF. This was optimized to almost 50% genistein production by simplifying the protocol to an expression in M9 minimal medium instead of changing the medium after 3 h pre expression in LB to M9. Under these optimised conditions, IFS-CPR made 12 μ M genistein, which is 15% less than IFS-CPR in Rosetta 2 (DE3) under the conditions reported by Leonard and Koffas 2007³⁰⁶.

Other groups tested the artificial plant fusion of the isoflavone synthase from red clover (*Trifolium pratense*) (rcIFS) fused to rice (*Oryza sativa*) reductase (rcIFS-riceCPR) or the reductases from *C. roseus* (rcIFS-CPR). While the experimental conditions were not identical to those used here, making comparisons difficult, the rcIFS-riceCPR fusion showed 75% conversion to genistein when expressed in LB after 12 h in resting cell assays, whereas only 26% conversion was detected by using M9 medium.³⁰⁷

In this project, two different expression temperatures (20 °C and 15 °C) were tested for IFS-CPR and IFS-RhF. The conversion of naringenin to genistein was reduced about 22% and 30% for IFS-CPR and IFS-RhF, respectively by dropping the temperature from 20 °C to 15 °C.

Kim *et al.* reported the conversion of naringenin to genistein by rcIFS-riceCPR, performed at 28 °C in a growing cell assay with 63% after 12 h,³⁰⁷ which was higher than by IFS-RhF (5% conversion to genistein after 12 h at 20 °C, this project), possibly caused by the lower temperature used in the growing cell assay.

The red clover IFS expressed in yeast produced 18% genistein, which was increased to 88% genistein when co expressed with the riceCPR in *S. cerevisiae*.⁴⁴² The endogeneous reductase of *S. cerevisiae* did not transfer the electrons from the cofactor to the P450 rcIFS as effectively as the plant reductase riceCPR.

While the isoflavone synthase activity was relatively easy to measure, detecting expressed IFS protein by SDS-PAGE or western blot analysis was difficult as these methods are less sensitive.

Unfortunately, no signal was detected for IFS-CPR by western blot analysis (anti-His-antibody), possibly through the protein fold not exposing the His-tag or

because this method is less sensitive than the enzyme assay and the level of IFS was below the limits of detection using this technique. Leonard and Koffas reported in their publication the *in vivo* activity of IFS-CPR without recognising any *in vitro* activity of purified enzyme or the detection of the fusion by SDS PAGE or western blot.³⁰⁶ The fusion IFS-RhF was detected after N-affinity chromatography by western blot analysis using His-antibodies. A stronger signal for the fusion IFS-RhF was received when blotted against specific RhF reductase antibodies. IFS fused to the Arabidopsis reductase ATR2tr (IFS-lamATR2tr and IFS-licATR2tr) was only detected in the insoluble protein fraction by western blot analysis with specific antibodies raised against the reductase ATR2tr, suggesting membrane associated fusion protein. Additional degradation of the fusion to IFS and ATR2tr was found.

The Arabidopsis CYP73A5 (cinnamate-4-hydroxylase), lacking 26 amino acids at its N-terminus of the hydrophobic membrane anchor, was fused to the truncated version of the Arabidopsis ATR2tr and to the RhF reductase from *Rhodococcus* sp. to compare their activities. Both fusions showed the ability to hydroxylate cinnamic acid to coumaric acid in resting cell assays. The 73A5tr fused to ATR2tr resulted showed 20% higher activity than 73A5tr-RhF (3.5% coumaric acid after 24 h) demonstrating in this case, that the coupling of a P450 and reductase originating from the same plant are more efficient than when the two enzymes are derived from different organisms. This is in agreement with the observation also made for the flavonoid-3',5'-hydroxylase (CYP75) from *C. roseus* fused to the CPR of *C. roseus*, which had a two-fold higher specific activity than the hydroxylase CYP75 from *C. roseus* fused to *Petunia hybrid* reductase.³⁰⁰ However, in conflict with this, studies by Mizutani found that the turnover number (amount of substrate molecules that the P450 can convert to product per catalytic site and per unit of time) of recombinant CYP73A5 expressed in insect cells was similar for the conversion of cinnamic acid to coumaric acid in combination with ATR2, or the reductase from *Vigna radiate* (mung bean) *in vitro*.^{191,391} Urban *et al.* detected a 4-fold higher turnover rate for cinnamate-4-hydroxylase from barley (*Helianthus tuberosus*) co-expressed with yeast (*S. cerevisiae*) reductase in yeast microsomes.³²⁶ This research group compared also the Arabidopsis CYP73A4 co-expressed in yeast with a yeast reductase,

Arabidopsis ATR1 and ATR2 (yeast strains WAT11 and WAT21, respectively) and found that the turnover rate of CYP73A5 with yeast reductase was two-fold higher than with either of the two Arabidopsis reductases.¹⁶⁶

Additionally, two different linkers (lam- and lic-linker) connecting the P450 73A5tr and the reductase ATR2tr were tested and the activity of the fusion containing the lam-linker was 10% higher than with the lic-linker. Similar was seen for the IFS fusions, where IFSsyn-lamATR2tr produced two-fold more genestein than IFSsyn-licATR2tr. Both linkers were dependent on the growth medium (Chapter 5, page 137). Modifications at the N-terminus, functioning as membrane anchor, and the linker region joining P450 and reductase may increase expression and activity.

The reductases ATR2tr and RhF were expressed independently and in a soluble and active form in *E. coli* Rosetta 2 (DE3). The P450s, lacking their hydrophobic membrane anchor, fused to the reductases (ATR2tr or RhF) were expressed as active enzymes; however, they still appear to be associated to the membrane and are found in the insoluble protein and membrane fraction. This finding implies even so the membrane anchor has been removed that the P450 may still be associated to the membrane. 73A5tr-fusions lacking the membrane anchor were still present in the insoluble fraction. The solubility may be increased by modification of the P450 N-terminus, for example replacing the N-terminal region with a signal sequence, such as the endogeneous *E. coli* OmpA signal sequence⁴⁴³ or the sequence of the bovine steroid 17 α -hydroxylase (CYP17A), which would also be useful for *in vitro* assays^{318,444}.

Previous studies reported that plant P450s fused to a plant reductase have been actively expressed in *E. coli*. Here, optimisation studies have shown that the expression strain is important and expression in the Rosetta 2 strain resulted in the highest activity in resting cell assays. Additional codon optimisation for *E. coli* expression of IFS increased the activity more than 10% as well as the linker region connecting P450 and reductase. Future further optimisation areas to test would include the linker region and also the N-terminus of the P450.

Soluble expression of plant P450s has been notoriously difficult and proven a bottleneck in characterisation of these enzymes. This platform technology shows promise for the study of plant P450s using artificial fusions with plant or bacterial reductases, because of the advantages of expressing a single fusion enzyme instead of two separate ones. Additionally, the platform could be used for *in vivo* activity tests screening a range of substrates, or conversely, to screen a large number of P450s for activity to a specific product of interest with the aim of identifying and characterising new P450 functions.

7 Final Discussion

Biotransformation is a fast growing sector in industry and is more and more displacing synthetic chemistry. The benefits of using biocatalysts for transformation include the ability to make enantio- and regiospecific products as well as frequently having more environmentally friendly production conditions when compared to traditional chemistries.^{445,446}

Cytochromes P450 are fascinating due to their occurrence in all kingdoms of life as well as their broad substrate range, regio- and stereospecificity. P450s require a corresponding reductase and the cofactor NAD(P)H for their reaction. Human P450s occur predominantly bound to the endoplasmic reticulum of liver cells, where they are involved in the metabolism of drugs and medicine, hence the activities of P450s are intensively studied. Bacterial P450 systems are cytosolic and have also been the subject of much research due to their solubility, as well as their roles in secondary metabolism. Plants possess significantly more P450s than found in mammals or bacteria, with often more than 200 P450s in a single plant species. Plant P450s are mainly involved in the reactions of secondary metabolism, and are stimulated under stress conditions. They are insoluble due to a strong association with an endoplasmic reticulum or organelle membrane, for example the membrane of the chloroplast by a serine-threonine rich sequence³⁵¹, and are therefore not easy to express actively as recombinant proteins. As a result the plant P450s have been examined in much less detail than their counterparts in other kingdoms and so for most plant P450s a function is still not known. For example, a search of publications on Arabidopsis P450s (reviewed in Chapter 1) showed that for 75% of Arabidopsis P450s the native substrate has not yet been identified. Given these limitations, the development of a specific system to express and assay active plant P450s is necessary.

A platform technology containing plant P450s fused to appropriate reductases was engineered in this project. This technology will provide a system for the study of artificial plant P450-reductase fusions and investigation of P450s with unknown function with the facility to readily clone P450s in frame, upstream of a reductase. Two great advantages of using fusion proteins are that just one protein needs to be prepared instead of two separate enzymes, and there is the potential to improve activity by more efficient electron transfer from the reductase to the P450. In this

project, attention was concentrated on P450s from *Arabidopsis* due to the availability of annotated gene sequences and that this species is of interest many members of the plant science community. Native *Arabidopsis* reductases were tested to optimise activity of the P450 fusions. Encoded in the *Arabidopsis* genome are three *Arabidopsis* P450 reductases: ATR1, ATR2 and ATR3. While ATR3 is involved primarily in embryo development³⁹⁵, ATR1 and ATR2 are expressed predominantly throughout the spatial and temporal development of the plant. Both proteins, along with their native membrane anchor regions, have been expressed and characterised as membrane proteins in yeast and insect cells.^{166,391} Although, the main focus of this project is the rapid screening recombinant P450s for activity *in vivo*, expression of soluble fusions would be advantageous for more detailed biochemical characterisation. Hence, truncated forms of the reductases (ATR1tr and ATR2tr) were expressed without N-terminal hydrophobic membrane anchors and cloned into pET-YSBLIC³⁴⁵. Expression in *E. coli* and purification by nickel-affinity chromatography were optimised to attain soluble, active ATR1tr and ATR2tr. Activity assays, using cytochrome *c*³⁴⁹, showed that ATR2tr was 20 times more active than ATR1tr. *ATR2tr* was therefore selected for creating the fusion platform technology and cloned into pET-YSBLIC using traditional, non-LIC, cloning methods. A linker sequence was also inserted at the 5' end of *ATR2tr* to connect the encoded P450 to the reductase. The lam-linker was developed based on the tripeptide linker GST which is often used for artificial plant P450 fusion systems^{306,307}. A second linker, called lic-linker, which has been successfully used for fusions of prokaryotic P450s with the RhF reductase from *Rhodococcus*^{146,441}, was used. In addition to the ATR2tr, the RhF reductase was cloned and tested for activity in *E. coli* with plant P450s to create plant-bacterial P450 fusions. Four different P450s (CYP93C, CYP73A5, CYP81D8 and CYP82E4) were selected to show proof-of-principle of the novel plant fusion system (Table 7.1).

Table 7.1: List of P450-reductase fusion constructs created in this project and their tested substrates

P450	activity		Conversion after 24 h in resting cell assays			
	substrate	product	CPR	RhF	lamATR2tr	licATR2tr
IFS (CYP93C)	naringenin	genistein	23%* 28%	30%* 28%	0%*	0%*
IFSopt (CYP93C)	naringenin	genistein	not tested	not tested	7%*	3%*
73A5tr (opt.)	cinnamic acid	coumaric acid	not tested	4%	33%	23%
CYP82E4	nicotine	normicotine	not tested	not tested	0%	0%
81D8tr	TNT, DNT, MTS, EC	not tested	not tested	0%	0%	0%

opt = gene codon optimized for *E. coli* expression, TNT = 2,4,6-trinitrotoluen, DNT = 2,4-dinitrolouene or 2,6-dinitrotoluene, MTS = methyl-tolyl-sulphide, EC = 7-ethoxycoumarin, * experiment performed as growing cell assay

Comparison of reductases, codon usage and linker regions for fusion expression

A comparison of isoflavone synthase (IFS) (CYP93C1 from *Glycine max*) fused to different reductases was performed to test that the P450 activity was dependent on the electron transfer by the reductase. As shown in Table 7.1, IFS-CPR and IFS-RhF resulted in the highest activities. While the activity of the nativeIFS-ATR2tr fusion was improved following codon optimisation for expression in *E. coli*, activity was still less than for the IFS-CPR and IFS-RhF fusions.

A similar comparison using the codon optimised Arabidopsis P450 cinnamate-4-hydroxylase without the hydrophobic membrane anchor (73A5tr) revealed that, as shown in Table 7.1, 73A5tr-ATR2tr had higher activity than the CYP73A5-bacterial fusion (73A5tr-RhF).

Expression of native CYP82E4, *N*-demethylase from *Nicotiana tabacum* and native Arabidopsis CYP81D8 (of unknown function) fused to ATR2tr did not result in activity using the tested substrates.

To assess linker sequences joining the P450 to the ATR2tr the lam- and lic-linkers were compared. Although results varied according to experimental conditions, overall the lam-linker gave higher activity.

The results show that plant P450s work best when fused to a reductase from the same species. In the absence of a species-specific reductase, the bacterial RhF reductase from *Rhodococcus* could be used as a universal reductase. RhF is part of

a native bacterial fusion which has evolved to live in an environment alongside the P450. Although in the native fusion the P450 is fused to the C-terminus of RhF reductase (Figure 1.11B), in the studies here the plant P450 was fused to the N-terminus of the RhF reductase (Figure 7.1). The results also show that codon optimisation for expression in *E. coli* improves activity. As the costs in gene synthesis have dropped significantly in recent years, along with improvements in software tools to optimise for *E. coli* codon bias and additional modifications, discussed below, at a large (100-1000 sequences) scale, this could now be a viable step in enhancing performance of the screen.

The plant P450-plant reductase fusions, or if the plant-specific reductase is unavailable, plantP450-RhF fusions, could be used as artificial fusion systems for preliminary, high-throughput substrate screens. A secondary screen for P450s not expressed during the preliminary screen, could be performed whereby activity is achieved by using codon optimisation for *E. coli* expression and alternative reductases. These procedures could also be applied to increase the expression and activity of promising P450s for more detailed characterisation.

Improving performance in cell assays

It was observed that the maximum conversion of substrate into product was 40 % (seen with cinnamic acid to coumaric acid after 48 hours). Given that substrate levels indicated no other products were being formed, this means that the assay is less sensitive than it could be, and potentially expensive, substrate is wasted. Analysis of the data (Figure 5.13) showed that the conversion was non-linear, with activity slowing down over time. Possible reasons for this are that the NADPH in the cells has been depleted to a limiting concentration. NADPH is produced via the pentose phosphate pathway. Adding glucose, as a supplemental carbon source, to the sample during the assay could address this possible limitation in substrate conversion in future experiments. Following Michaelis-Menten kinetics, at limiting substrate concentrations, enzyme rates decrease with substrate concentration decrease. The amount of conversion, and therefore sensitivity, could be increased by the addition of more substrate. Ensuring that a non-limiting substrate concentration is used, activity with increasing substrate concentration could be monitored.

Enhancing solubility of the fusions

All the reductases tested in this project were expressed as active, soluble forms in *E. coli*. However, while fusion proteins were found in both soluble and insoluble protein fractions, activity was only found in the insoluble fractions. These results indicate that active fusions are associated with a membrane even though the membrane targeting signal was removed during the cloning, and that this membrane association is P450-specific. Literature reported hydrophobic regions on the surface of the P450 like the F-G loop, which is also part of the substrate access channel, show interaction with membranes.^{97,447} Studying existing P450 structures, as well as analysing each target P450 amino acid sequence (used for the fusion), would show hydrophobic parts of the enzyme. These could be modified if the gene is re-synthesised for codon optimisation, as discussed above, to improve solubility of the whole fusion protein. Optimising the N-terminal truncation of the P450s further could also lead to improvements in solubility and expression yield.³²¹ Studying the hydrophobic regions of the P450s responsible for the insolubility by interacting with the membrane could identify regions to be modified. Beyond this, the mechanism of the electron transfer between reductase and P450 could be studied, with particular attention to the linker region, with the aim of improving efficiency.^{306,441}

Future directions for P450-reductase fusion systems

In this project two fusion systems containing plant P450s fused to the N-terminus of the Arabidopsis reductase ATR2tr (Figure 7.1A) or the *Rhodococcus* RhF (Figure 7.1B) reductase have been characterised. Overall, it was shown that both fusion systems resulted in active protein and the activity was dependent on the P450. This is the first reported artificial plant P450-bacterial reductase fusion. Even though the bacterial and plant reductases are structurally divergent, it is remarkable that they both support the P450 reaction.

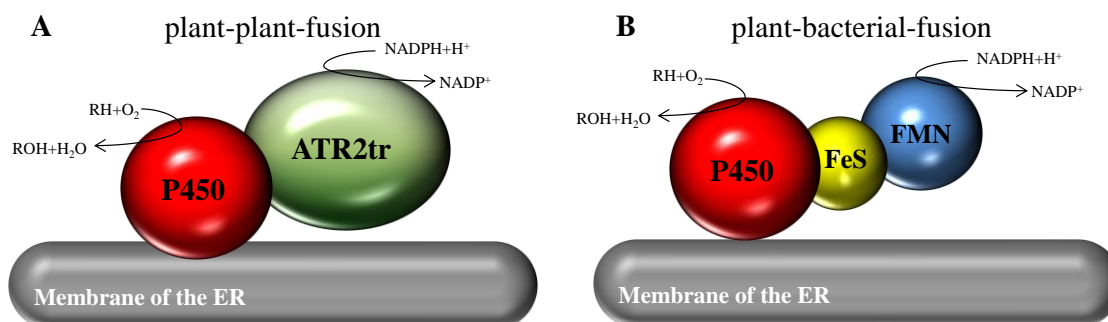


Figure 7.1: Schematic organisation of artificial A) plant-plant fusions (P450-ATR2tr) and B) plant bacterial (P450-RhF) fusions

Both fusions are lacking the hydrophobic membrane anchor at the N-terminus of the P450s and are fused C-terminally to the reductase. Due to hydrophobic regions on the surface of the P450 the fusion might be still membrane associated.

The main outcome of this project is a platform technology that is a useful tool for the investigation of novel plant P450 activities. It can be employed for high-throughput cloning via a ligation independent cloning system enabling a large number of P450s to be easily cloned, expressed as fusions in *E. coli* and screened using resting cell assays. However, there are still deficiencies to this system which can be addressed. In this way, this technology presents a new opportunity to search libraries of plant P450 fusions against a wide range of substrates to discover new activities and new biocatalysts for the industrial future.

Appendix A

Table A1: Cytochromes P450 in Arabidopsis

P450 (gene locus)	reaction	pathway	references
51G1 (At1g11680)	obtusifoliol 14 α -demethylase	sterols/steroids	183,184
51G2 (At2g17330)	obtusifoliol 14 α -demethylase (pseudogene)		184
71A12 (At2g30750)	hydroxylation and N-demethylation of pyrazoxyfen	metabolism of herbicide pyrazoxyfen, camalexin biosynthesis in roots	185,186
71A13 (At2g307700)	dehydration of indole acetaldoxime to indole-3-acetonitrile	camalexin biosynthesis	187
71A14 (At5g24960)	putative P450		
71A15 (At5g24950)	putative P450		
71A16 (At5g42590)	putative P450		
71A17P	pseudogene fragment		
71A18 (At1g11610)	putative P450		
71A19 (At4g13290)	putative P450		
71A20 (At4g13310)	putative P450		
71A21 (At3g48320)	putative P450		
71A22 (At3g48310)	putative P450		
71A23 (At3g48300)	putative P450		
71A24 (At3g48290)	putative P450		
71A25 (At3g48280)	putative P450		
71A26 (At3g48270)	putative P450		
71A27P (At4g20240)	pseudogene		
71A28 (At4g20235)	putative P450		
71B2 (At1g13080)	putative P450		
71B3 (At3g26220)	putative P450		
71B4 (At3g26280)	putative P450		
71B5 (At3g53280)	putative P450		
71B6 (At2g24180)	putative P450		
71B7 (At1g13110)	deethylation of 7-ethoxycoumarin (with cumene hydroperoxide as electron donor)		188
71B8 (At5g35715)	putative P450		
71B9 (At2g02580)	putative P450		
71B10 (At5g57260)	putative P450		
71B11 (At5g25120)	putative P450		
71B12 (At5g25130)	putative P450		
71B13 (At5g25140)	putative P450		
71B14 (At5g25180)	putative P450		
71B15 (At3g26830)	conversion of s-dihydrocamalexin acid to camalexin	camalexin	189,190
71A16 (At3g26150)	putative P450		
71B17 (At3g26160)	putative P450		
71B18P	pseudogene		

APPENDIX A

P450 (gene locus)	reaction	pathway	references
71B19 (At3g26170)	putative P450		
71B20 (At3g26180)	putative P450		
71B21 (At3g26190)	putative P450		
71B22 (At3g26200)	putative P450		
71B23 (At3g26210)	putative P450		
71B24 (At3g26230)	putative P450		
71B25 (At3g26270)	putative P450		
71B26 (At3g26290)	putative P450		
71B27 (At1g13070)	putative P450		
71B28 (At1g13090)	putative P450		
71B29 (At1g13100)	putative P450		
71B30P (At3g53290)	pseudogene		
71B31 (At3g53300)	putative P450		
71B32 (At3g53305)	putative P450		
71B33	pseudogene		
71B34 (At3g26300)	putative P450		
71B35 (At3g26310)	putative P450		
71B36 (At3g26320)	putative P450		
71B37 (At3g26330)	putative P450		
71B38 (At3g44250)	putative P450		
72A7 (At3g14610)	putative P450		
72A8 (At3g14620)	No native function known, hydroxylation of quinidine	quinidine metabolism	341
72A9 (At3g14630)	putative P450		
72A10 (At3g14640)	putative P450		
72A11 (At3g14650)	putative P450		
72A12P	pseudogene		
72A13 (At3g14660)	putative P450	upregulated in response to cis-jasmone	377
72A14 (At3g14680)	putative P450		
72A15 (At3g14690)	putative P450		
72C1 (At1g17060)	exact substrate not identified (binds typhasterol)	degradation of brassinosteroids	293,448-450
73A5 (At2g30490)	4-hydroxylation of <i>t</i> - cinnamic acid to <i>p</i> -coumaric acid; hydroxylation of cinnamic acid analogs	phenylpropanoid pathway, lignin biosynthesis	166,191,192
74A1 (At5g42650)	allene oxide synthase for linoleic acid hydroperoxide and linolenic acid hydroperoxide	jasmonate acid biosynthesis	37,45,193-196
74B2 (At4g15440)	hydroperoxide lyase for linoleic acid hydroperoxide and linolenic acid hydroperoxide	oxylipin pathway, jasmonate biosynthesis	197-199
75B1 (At5g07990)	3'-hydroxylation of naringenin and dihydrokaempferol	phenylpropanoid pathway, flavonoid biosynthesis	200
76C1 (At2g45560)	10-hydroxylation of geraniol	terpenoid indole alkaloid biosynthesis	201
76C2 (At2g45570)	putative P450	possibly involved in cell death	451

APPENDIX A

P450 (gene locus)	reaction	pathway	references
76C3 (At2g45580)	putative P450		
76C4 (At2g45550)	putative P450		
76C5 (At1g33730)	putative P450		
76C6 (At1g33720)	putative P450		
76C7 (At3g61040)	putative P450		
76C8P (At3g61035)	pseudogene fragment		
76G1 (At3g52970)	putative P450		
77A4 (At5g04660)	epoxidation of unsaturated C ₁₈ fatty acids (oleic, linoleic, α -linolenic acid)	fatty acid metabolism	178
77A5P	pseudogene		
77A6 (At3g10570)	in-chain 10-hydroxylation of 16-hydroxypalmitate	cutin biosynthesis	202
77A7 (At3g10560)	putative P450		
77A8P	pseudogene		
77A9 (At5g04630)	putative P450		
77B1 (At1g11600)	putative P450		
78A5 (At1g13710)	putative P450		
78A6 (At2g46660)	putative P450		
78A7 (At5g09970)	putative P450		
78A8 (At1g01190)	putative P450		
78A9 (At3g61880)	putative P450	possibly involved in fruit development	452
78A10 (At1g74110)	putative P450		
79A2 (At5g05260)	conversion of phenylalanine to oxime	benzylglucosinolate biosynthesis	203
79A3P (At5g35917)	pseudogene		
79A4P (At5g35920)	pseudogene		
79B2 (At4g39950)	conversion of tryptophan and tryptophan analogs to oxime	indole glucosinolate biosynthesis, camalexin biosynthesis, auxin biosynthesis	204-209
79B3 (At2g22330)	conversion of tryptophan and tryptophan analogs to oxime	indole glucosinolate biosynthesis, camalexin biosynthesis, auxin biosynthesis	204-209
79B4P	pseudogene		
79C1 (At1g79370)	putative P450		
79C2 (At1g58260)	putative P450		
79C3P	pseudogene		
79C4P	pseudogene		
79C5P (At1g58265)	pseudogene		
79F1 (At1g16410)	N-hydroxylation of homo- to tetrahydro-methionine ($n = 3$ to 6) (short-chain methionine derivatives to their aldoximes)	biosynthesis of aliphatic glucosinolates	210-213

APPENDIX A

P450 (gene locus)	reaction	pathway	references
79F2 (At1g16400)	N-hydroxylation of long chain penta and hexahomomethionine to their aldoxime	biosynthesis of aliphatic glucosinolates	211-213
81D1 (At5g36220)	putative P450		
81D2 (At4g37360)	putative P450		
81D3 (At4g37340)	putative P450		
81D4 (At4g37330)	putative P450		
81D5 (At4g37320)	putative P450		
81D6 (At2g23220)	putative P450		
81D7 (At2g23190)	putative P450		
81D8 (At4g37370)	putative P450		
81D10 (At1g66540)	putative P450		
81D11 (At3g28740)	putative P450	induced by cis-jasmone	377,378
81F1 (At4g37430)	putative P450		
81F2 (At5g57220)	4-hydroxylation of indole-3-ylmethyl to 4-hydroxy-indole-3-ylmethyl glucosinolate	indole glucosinolate biosynthesis	214-216
81F3 (At4g37400)	putative P450		
81F4 (At4g37410)	putative P450	possibly involved in the indole glucosinolate biosynthesis	217
81G1 (At5g67310)	putative P450		
81H1 (At4g37310)	putative P450		
81K1 (At5g10610)	putative P450		
81K2 (At5g10600)	putative P450		
82C2 (At4g31970)	5-hydroxylation of 8-methoxypsoralen to 5-hydroxy-8-methoxypsoralen	metabolism of tryptophan-derived secondary metabolites, possibly involved in jasmonic acid induced indole glucosinolates	218,219
82C3 (At4g31950)	putative P450		
82C4 (At4g31940)	5-hydroxylation of 8-methoxypsoralen to 5-hydroxy-8-methoxypsoralen	Fe deficiency response, possibly through an IDE1-like mediated pathway	218,220
82F1 (At2g25160)	putative P450		
82G1 (At3g25180)	(<i>E,E</i>)-geranylinalool and the sesquiterpenoid (<i>E</i>)-nerolidol into the acyclic volatile C ₁₆ -homoterpene 4,8, 12-trimethylthdeca-1,3,7, 11-tetraene (TMTT) and the C ₁₁ -homoterpene 4,8-dimethyl-1,3,7-nonathene (DMNT), respectively		221

APPENDIX A

P450 (gene locus)	reaction	pathway	references
83A1 (At4g13770)	oxidation of methionine-derived oximes oxidation of p-hydroxyphenyl-acetaldoxime, indole-3-acetaldoxime, conversion of aldoximes to thiohydroximates	biosynthesis of aliphatic glucosinolate	222-224
83B1 (At4g31500)	oxidation of indole-3-acetaldoxime	biosynthesis of indole glucosinolate	222,223,225
84A1 (At4g36220)	5-hydroxylation of coniferaldehyde, coniferyl alcohol and ferulic acid	phenylpropanoid pathway, biosynthesis of lignin	167,226,227
84A4 (At5g04330)	putative ferulate-5-hydroxylase		228,229
85A1 (At5g38970)	C6-oxidase for 6-deoxycastasterone to castasterone, other steroids conversion of castasterone to brassinolide	biosynthesis of brassinolide	230-234
85A2 (At3g30180)	C6-oxidase for 6-deoxycastasterone to castasterone, other steroids conversion of castasterone to brassinolide	biosynthesis of brassinolide	230-233,235,236
86A1 (At5g58860)	ω -hydroxylation of saturated and unsaturated C12 to C20 fatty acids	fatty acid metabolism, biosynthesis of cutin, biosynthesis of suberin	237-240
86A2 (At4g00360)	ω -hydroxylation of saturated and unsaturated C12 to C18 fatty acids	fatty acid metabolism, biosynthesis of cutin	238,241,242
86A4 (At1g01600)	ω -hydroxylation of saturated and unsaturated C12 to C18 fatty acids	fatty acid metabolism, biosynthesis of cutin	202,238,242,243
86A7 (At1g63710)	ω -hydroxylation of lauric acid	fatty acid metabolism, biosynthesis of cutin	238,242
86A8 (At2g45970)	ω -hydroxylation of saturated and unsaturated C12 to C18 fatty acids	fatty acid metabolism, biosynthesis of cutin	238,242,244
86B1 (At5g23190)	ω -hydroxylation for long chain fatty acid (C22 and C24)	biosynthesis of suberin, fatty acid metabolism, polyester monomer biosynthesis	38,245
86B2 (At5g08250)	putative P450		
86C1 (At1g24540)	putative P450		
86C2 (At3g26125)	putative P450		
86C3 (At1g13140)	hydroxylation of fatty acids (C12, C14, C14:1, C16)	fatty acid metabolism	246
86C4 (At1g13150)	putative P450		
87A2 (At1g12740)	putative P450	possibly involved in auxin signaling	453
87A3P	pseudogene		

APPENDIX A

P450 (gene locus)	reaction	pathway	references
88A3 (At1g05160)	oxidation of <i>ent</i> -kaurenoic acid to gibberillin A12 in three steps	biosynthesis of gibberellins	39,247
88A4 (At2g32440)	oxidation of <i>ent</i> -kaurenoic acid to gibberillin A12 in three steps	biosynthesis of gibberellins	39,247
89A2 (At1g64900)	putative P450		
89A3 (At5g61320)	putative P450		
89A4 (At2g12190)	putative P450		
89A5 (At1g64950)	putative P450		
89A6 (At1g64940)	putative P450		
89A7 (At1g64930)	putative P450		
89A9 (At3g03470)	putative P450		
90A1 (At5g05690)	23 α -hydroxylation of steroids	biosynthesis of brassinolide	171,172,248,249
90B1 (At3g50660)	22 α -hydroxylation of C27, C28, C29 sterols	biosynthesis of brassinolide	169,249-251
90C1 (At4g36380)	C23-hydroxylation of sterols (typhasterol to castasterone)	biosynthesis of brassinolide	252-255
90D1 (At3g13730)	C23-hydroxylation of sterols	biosynthesis of brassinolide	253-255
93D1 (At5g06900)	putative P450		
94B1 (At5g63450)	putative P450		
94B2 (At3g01900)	putative P450		
94B3 (At3g48520)	12-hydroxylation of jasmonoyl-L-isoleucine	oxidative catabolism of jasmonate, jasmonate mediated signaling pathway	256,257
94C1 (At2g27690)	ω -hydroxylation of saturated and unsaturated C12 to C18 fatty acids and hydroxylation of ω -hydroxy fatty acid into dicarboxylic fatty acid	fatty acid metabolism	240,258
94D1 (At1g34540)	putative P450		
94D2 (At3g56630)	putative P450		
94D3P	pseudogene		
96A1 (At2g23180)	putative P450		
96A2 (At4g32170)	putative P450		
96A3 (At1g65340)	putative P450		
96A4 (At5g52320)	putative P450		
96A5 (At2g21910)	putative P450		
96A6P (At5g51900)	pseudogene		
96A7 (At1g47630)	putative P450		
96A8 (At1g47620)	putative P450		
96A9 (At4g39480)	putative P450		
96A10 (At4g39490)	putative P450		
96A11 (At4g39500)	putative P450		
96A12 (At4g39510)	putative P450		

APPENDIX A

P450 (gene locus)	reaction	pathway	references
96A13 (At5g02900)	putative P450		
96A14P (At1g66030)	pseudogene		
96A15 (At1g57750)	hydroxylation of midchain alkane to alcohols and second hydroxylation to ketone	biosynthesis of wax	259
97A3 (At1g31800)	β -hydroxylation of carotene	carotenoid metabolism	260,261
97B3 (At4g15110)	β -hydroxylation of β -carotene to zeaxanthin via β -cryptoxanthin	carotenoid metabolism	262
97C1 (At3g53130)	ε -hydroxylation of β,ε -carotene	carotenoid metabolism	260,263
98A3 (At2g40890)	3-hydroxylation of <i>p</i> -coumarate to caffeic acid and 3-hydroxylation of coumaroyl-esters (shikimate and quinate esters)	phenylpropanoid pathway, biosynthesis of lignin monomers and soluble phenolics	168,264-267
98A8 (At1g74540)	<i>meta</i> -hydroxylation of the three triferuloylspermidine phenolic rings, oxygenation of resveratrol	alternative phenolic pathway, pollen development	268,269
98A9 (At1g74550)	<i>meta</i> -hydroxylation of the three triferuloylspermidine phenolic rings, oxygenation of resveratrol	alternative phenolic pathway, pollen development	268,269
701A3 (At5g25900)	oxidation of <i>ent</i> -kaurene to <i>ent</i> -kaurenoic acid in three steps	biosynthesis of gibberellin	39,270-273
702A1 (At1g65670)	putative P450		
702A2 (At4g15300)	putative P450		
702A3 (At4g15310)	putative P450		
702A4P	pseudogene		
702A5 (At4g15393)	putative P450		
702A6 (At4g15396)	putative P450		
702A7P	pseudogene		
702A8 (At3g30290)	putative P450		
703A2 (At1g01280)	in-chain monohydroxylation of saturated fatty acids (C10-C16)	biosynthesis of sporopollenin, pollen development	274
704A1 (At2g44890)	putative P450		
704A2 (At2g45510)	putative P450		
704B1 (At1g69500)	ω -hydroxylation of saturated, unsaturated and epoxy C16 and C18 fatty acids	biosynthesis of sporopollenin, pollen development	275,276
705A1 (At4g15330)	putative P450		
705A2 (At4g15350)	putative P450		
705A3 (At4g15360)	putative P450		
705A4 (At4g15380)	putative P450		
705A5 (At5g47990)	conversion of thaliandiol to desaturated thaliandiol	thalianol metabolic pathway	277
705A6 (At2g05180)	putative P450		
705A8 (At2g27000)	putative P450		

APPENDIX A

P450 (gene locus)	reaction	pathway	references
705A9 (At2g27010)	putative P450		
705A10P	pseudogene		
705A11P	pseudogene		
705A12 (At5g42580)	putative P450		
705A13 (At2g14100)	putative P450		
705A14P	pseudogene		
705A15 (At3g20080)	putative P450		
705A16 (At3g20083)	putative P450		
705A17P	pseudogene		
705A18 (At3g20090)	putative P450		
705A19 (At3g20100)	putative P450		
705A20 (At3g20110)	putative P450		
705A21 (At3g20120)	putative P450		
705A22 (At3g20130)	putative P450		
705A23 (At3g20140)	putative P450		
705A24 (At1g28430)	putative P450		
705A25 (At1g50560)	putative P450		
705A26P	pseudogene		
705A27 (At1g50520)	putative P450		
705A28	putative P450		
705A29P	pseudogene		
705A30 (At3g20940)	putative P450		
705A31P	pseudogene		
705A32 (At3g20950)	putative P450		
705A33 (At3g20960)	putative P450		
705A34P	pseudogene		
706A1 (At4g22690)	putative P450		
706A2 (At4g22710)	putative P450		
706A3 (At5g44620)	putative P450		
706A4 (At4g12300)	putative P450		
706A5 (At4g12310)	putative P450		
706A6 (At4g12320)	putative P450		
706A7 (At4g12330)	putative P450		
707A1 (At4g19230)	8-hydroxylation of abscisic acid	abscisic acid catabolism	278-280
707A2 (At2g29090)	8-hydroxylation of abscisic acid	abscisic acid catabolism	278-281
707A3 (At5g45340)	8-hydroxylation of abscisic acid	abscisic acid catabolism	278,279,281-286

APPENDIX A

P450 (gene locus)	reaction	pathway	references
707A4 (At3g19270)	8-hydroxylation of abscisic acid	abscisic acid catabolism	278,279
708A1 (At1g55940)	putative P450		
708A2 (At5g48000)	hydroxylation of thalianol to thaliandiol	thalianol metabolic pathway	277
708A3 (At1g78490)	putative P450		
708A4 (At3g44970)	putative P450		
709B1 (At2g46960)	putative P450		
709B2 (At2g46950)	putative P450		
709B3 (At4g27710)	putative P450		
710A1 (At2g34500)	C22-desaturation of β -sitosterol to stigmasterol	biosynthesis of sterols	287-289
710A2 (At2g34490)	C22-desaturation of β -sitosterol and 24- <i>epi</i> -campesterol to stigmasterol and brassicasterol	biosynthesis of sterols	287
710A3 (At2g28850)			
710A4 (At2g28860)	C22-desaturation of β -sitosterol to stigmasterol	biosynthesis of sterols	288
711A1 (At2g26170)	putative P450		
712A1 (At2g42250)	putative P450		
712A2 (At5g06905)	putative P450		
714A1 (At5g24910)	C13-hydroxylation of <i>ent</i> -kaurenoic acid to steviol	gibberillin catabolism	277,290
714A2 (At5g24900)	putative P450	gibberillin catabolism	290
715A1 (At5g52400)	putative P450		
716A1 (At5g36110)	putative P450		
716A2 (At5g36140)	putative P450		
718 (At2g42850)	putative P450		
720A1 (At1g73340)	putative P450		
721A1 (At1g75130)	putative P450		
722A1 (At1g19630)	putative P450		
724A1 (At5g14400)	22 α -hydroxylation of brassinosteroid	biosynthesis of brassinolide	291
734A1 (At2g26710) initially classified as CYP72B	C26-hydroxylation of brassinolide and castasterone	brassinolide catabolism	173,292,293
735A1 (At5g38450)	<i>trans</i> -hydroxylation of isopentenyladenine, tri/di/monophosphates	biosynthesis of zeatin, cytokinin metabolism	294
735A2 (At1g67110)	<i>trans</i> -hydroxylation of isopentenyladenine, tri/di/monophosphates	biosynthesis of zeatin, cytokinin metabolism	294

Appendix B

B1 Gene sequences used in Chapter 3

CYP81D8 (from *Arabidopsis*) was isolated from plant cultivated in liquid culture. The truncated version of CYP81D8 (*CYP81D8tr* in italics) was created by deleting the hydrophobic N-terminal region.

```
ATGGAACCAAACCCCTAATTTTCTCAATTCTCTTCGTTGTTCTCTCTCTCATTT
ACTTAATTGGAAAACCTCAAGCGAAAGCCAAATCTACCTCCGAGTCCGGCATGGTC
ATTACCGGTGATTGGTCATCTCCGCCCTTCTCAAACCACCGATTTCATCGCACATTC
CTCTCCCTCTCTCAATCCCTAAACAATGCTCCGATCTTCTCCCTCCGACTCGGTA
ACCGACTCGTTTTCGTGAACCTCGTCACACTCGATCGCCGAGGAATGTTTCACCAA
AAACGACGTCGTAAGTGGCGAACAGACCAAACCTTCATCCTCGCTAAACACGTTGCG
TACGATTACACAACCATGATCGCAGCTTCCCTACGGTGACCACTGGCGTAACCTCC
GCCGCATCGGCTCCGTGAGATATTCTCCAATCACCGTCTCAATAGCTTTTTGTGTC
TATTCGTAAAGACGAGATCCGACGACTTGTGTTTTCGTCTTCTCGGAACTTTTCA
CAAGAGTTTGTGAAAGTGGATATGAAATCAATGTTATCTGACTTAACATTCAACA
ACATTTTAAGAATGGTGGCCGAAAACGTTACTACGGAGACGGTGTGAGGATGA
TCCGGAGGCTAAACGTGTCCGGCAGCTTATAGCGGATGTGGTGGCTTGTGCTGGT
GCTGGAAACGCTGTTGATTACTTACCGTTTTGCGGTTGGTTTCAGATTACGAGA
CACGGGTTAAGAAGTTGGCGGGTAGGCTCGACGAGTTCTTGCAAGGATTGGTTGA
TGAGAAACGAGAAGCTAAGGAGAAAGGAAACACTATGATCGATCACTTGCTTACT
CTGCAAGAATCCCAACCGGATTACTTCACGGATCGTATCATTAAAGGAAACATGC
TCGCTTTGATACTAGCAGGGACCGACACATCAGCGGTTACGTTAGAATGGGCATT
GTCGAACGTGTTGAACCATCCGGATGTATTGAACAAGGCGAGAGATGAAATCGAT
AGAAAGATAGGTTTAGACAGGCTTATGGATGAATCAGATATCTCAAACCTGCCTT
ATCTCCAAAACATTGTGTCTGAAACGTTGCGCCTTTATCCTGCGGCTCCCATGCT
TCTTCTCACGTTGCCTCGGAAGATTGTAAAGTTGCAGGATACGATATGCCGCGT
GGCACGATACTATTGACCAATGTGTGGGCTATACACAGAGATCCTCAGCTATGGG
ATGATCCAATGAGCTTCAAGCCAGAGAGGTTTGAGAAAGAAGGAGAAGCTCAGAA
GCTAATGCCGTTTGGGTTAGGAAGAAGGGCGTGTCTGGTTCTGGACTGGCTCAT
CGGCTTATAAACCTGACTCTTGGATCATTGATTGAGTGTGTTGGAATGGGAGAAGA
TTGGAGAAGAAGTGGATATGAGTGAAGGCAAAGGTGTTACAATGCCTAAAGCCAA
GCCTTTGGAAGCCATGTGCAGAGCACGTCCCTCTGTTGTTAAATCTTCAACGAG
TCCGTTTGA
```

CYP81D11 (from *Arabidopsis*) was isolated from plant cultivated in liquid culture. The truncated version of CYP81D11 (*CYP81D11tr* in italics) was created by deleting the hydrophobic N-terminal region.

ATGTCATCAACAAAGACAATAATGGAAACTATATACCTAATTCTCTCTCTCTTCT
TCTTCTTCATCTTCCTATCTCTCAAACCTCTTGTTTCGGACCACGGCCGCGTAAACT
AAACCTACCGCCGAGTCCGAGTCGACCATTTCCGATCATCGGACACCTCCACCTT
CTAAAGCTACCACTCCACCGTAGATTTCTCTCTCTCTCAGAATCTTTAAACAACG
CCAAGATTTTCTCTCTCAGCCTCGGCTCTCGTCTAGTTTTTGTGTTTCTTCTCA
CGCCGTCGCGGAAGAATGTTTCACTAAGAACGACGTCGTGTTAGCTAACC GGCCG
GAGTTTCTCGTCGGGAAACATATAGGGTACAACCTCTACGACCATGGTTGGTGCGG
CTTATGGAGATAGTTGGAGGAATCTTCGACGTATTGGCACCATTGAGATCTTCTC
GTCTCTTAGGCTTAATAGCTTCGTATCTATCCGTCAAGATGAGATCCGACGGCTC
ATAATTTGTCTAGCGAAAACTCTCAACATGGGTTTGTGAAAGTGGAGATGAAAC
CATTGTTTATGTGTTTAACTATCAACAACATCATTAGAATGGTGGCCGGAAAAAG
ATTCTACGGTGATGGAACAGAGAACGACAACGAGGCTAAACACGTGAGACAGCTA
ATTGCCGAGGTAGTTGTTAGCGGCGGCGCAGGGAACGCAGCAGACTACTTCCCTA
TCCTTCGTTACGTAACGAACTATGAGAAACATGTTAAGAAGTTAGCAGGTCGTGT
TGATGAGTTTTTGC AAAGTCTAGTTAACGAGAAACGTGTGGAGAAAGTAAAAGGT
AACACAATGATCGATCATTACTTTCTCTACAAGAACTCAGCCTGATTACTACA
CGGATGTGATCATCAAAGGAATCATACTTGTTATGATACTTGCCGGGACTGATAC
ATCAGCTGGAACGTTAGAATGGGCGATGTGCAATTTGTTGAACCATCCAGAAGTA
TTACGAAAGGCAAAGACCGAAATCGACGACCAAATCGGTGTAGACCGGTTAGTAG
AGGAACAAGACATTGTGAAACTTCCCTTACCTTCAGCACATTGTGTCAGAGACTTT
ACGGCTTTATCCGGTGGCTCCAATGCTTTTACCCACTTAGCATCAGAAGATTGT
ATAGTTGATGGCTATGACGTTCCACGCGGCACAATCATCTTGGTGAATGCATGGG
CCATCCATAGAGATCCAAAGTTATGGGAAGAGCCAGAAAAATTTAAGCCGGAGAG
GTTTGAGAAAAAAGGAGAGGATAAAAAAGTTGATGCCATTTGGGATTGGACGACGA
TCTTGCCCTGGTTCAGGGCTAGCTCAACGGCTAGTGACTTTGGCTCTTGGATCAT
TGGTCCAATGTTTTGAGTGGGAGAGGGTTGAAGAAAAGTATCTAGACATGAGAGA
AAGTGAAAAAGGAACCACAATGCGAAAAGCTACATCGTTGCAAGCTATGTGTA
AAAGCTCGTCCCATTGTCCATAA

CYP71D15 construct PM2-2 (limonene-3-hydroxylase from peppermint) was provided by Prof. Rodney Croteau (Institute of Biological Chemistry, Washington State University, Pullman, US).³⁶⁷

```
ATGGCTCTGTTATTAGCAGTTTTTTGGTCGGCGCTTATAATCCTCGTAGTAACCT
ACACCATATCCCTCCTAATCAACCAATGGCGAAAACCGAAACCCCAAGGGAAGTT
CCCCCGGGCCCGCCGAAGCTGCCGCTGATCGGGCACCTCCACCTCCTGTGGGGG
AAGCTGCCGCAGCACGCGCTGGCCAGCGTGGCGAAGGAGTACGGCCCCGTGGCCC
ACGTGCAGCTGGGTGAGGTGTTCTCCGTCGTCCTTTCGTCGCGGGAGGCGACGAA
GGAGGCGATGAAGCTGGTAGACCCGGCGTGCGCGAACC GGTTTCGAGAGCATCGGG
ACGAGGATCATGTGGTACGACAACGAGGACATCATCTTCAGCCCCCTACAGCGAGC
ACTGGCGCCAGATGCGCAAGATCTGCGTCTCCGAGCTCCTCTCCTCCCGCAACGT
CCGCTCCTTCGGCTTCATCCGGCAGGACGAGGTGTCGCGCCTCCTCCGCCACCTC
CGTCCCTCGGCAGGGGCGGCCGTGGACATGACGGAGAGGATAGAGACGCTGACGT
GCTCCATCATCTGCAGGGCGGGCTTCGGGAGCGTGATCAGGGACAACGCGGAGCT
GGTGGGGCTGGTCAAGGACGCGCTCAGCATGGCCTCGGGGTTTCGAGCTCGCCGAC
ATGTTCCCCTCCTCCAAGCTCCTCAACCTCCTCTGCTGGAACAAGAGCAAGCTCT
GGAGGATGCGCCGCCGCGTCGACACCATCCTCGAGGCCATCGTCGACGAGCACAA
GTTCAAGAAAAGCGGCGAGTTCGGCGGCGAGGACATCATCGACGTCCTCTTCAGG
ATGCAGAAGGACACCCAGATCAAAGTCCCCATCACCACCAACTCCATCAAAGCCT
TCATCTTCGATACGTTCTCAGCAGGGACTGAGACATCCTCAACCACCACCCTATG
GGTGCTGGCGGAGCTGATGAGGAACCCGGCAGTGATGGCGAAAGCGCAGGCGGAG
GTGAGAGCGGCACTGAAGGAGAAGACGAACTGGGACGTGGACGACGTGCAAGAGC
TTAAGTACATGAAATCGGTGGTGAAGGAGACGATGAGGATGCACCCTCCGATCCC
GTTGATCCCGAGATCATGCAGAGAAGAATGCGTGGTTAACGGGTATACGATTCCG
AACAAAGGCCAGAATCATGATCAACGTCTGGTCCATGGGCAGGAATCCTCTCTACT
GGGAAAAACCCGATACCTTTTTGGCCCCGAAAGGTTTGACCAAGTTTCAAAGGATTT
CATGGGAAATGATTTTCGAGTTCGTCCCGTTTCGGAGCGGGAAGAAGAATCTGCCCC
GGCTTGAACCTTCGGGTTGGCAAACGTTGAGGTTCCATTGGCGCAGCTTCTTTACC
ACTTCGACTGGAAGTTGGCGGAAGGAATGAAACCTTCTGATATGGACATGTCTGA
GGCGGAAGGCCTTACCGGAATACTAAAGAACAATCTTCTTCTTGTGCCACACCC
TACGATCCTTCATCATGA
```

B2 Gene sequence used in Chapter 4

ATR1tr (P450 reductase from *Arabidopsis*) was isolated from plant cultivated in liquid culture. The truncated version of ATR1 was created by deleting the hydrophobic 46 amino acids of the N-terminal region.

```
TGGAAGAAAACGACGGCGGATCGGAGCGGGGAGCTGAAGCCTTTGATGATCCCTA
AGTCTCTTATGGCTAAGGACGAGGATGATGATTTGGATTTGGGATCCGGGAAGAC
TAGAGTCTCTATCTTCTTCGGTACGCAGACTGGAACAGCTGAGGGATTTGCTAAG
GCATTATCCGAAGAAATCAAAGCGAGATATGAAAAAGCAGCAGTCAAAGTCATTG
ACTTGGATGACTATGCTGCCGATGATGACCAGTATGAAGAGAAATTGAAGAAGGA
AACTTTGGCATTCTTCTGTGTTGCTACTTATGGAGATGGAGAGCCTACTGACAAT
GCTGCCAGATTTTACAAATGGTTTACGGAGGAAAATGAACGGGATATAAAGCTTC
AACAACTAGCATATGGTGTGTTTGCTCTTGGTAATCGCCAATATGAACATTTTAA
TAAGATCGGGATAGTTCTTGATGAAGAGTTATGTAAGAAAGGTGCAAAGCGTCTT
ATTGAAGTCGGTCTAGGAGATGATGATCAGAGCATTGAGGATGATTTTAATGCCT
GGAAAGAATCACTATGGTCTGAGCTAGACAAGCTCCTCAAAGACGAGGATGATAA
AAGTGTGGCAACTCCTTATACAGCTGTTATTCTGAATACCGGGTGGTGACTCAT
GATCCTCGGTTTACAACCTCAAAAATCAATGGAATCAAATGTGGCCAATGGAAATA
CTACTATTGACATTCATCATCCCTGCAGAGTTGATGTTGCTGTGCAGAAGGAGCT
TCACACACATGAATCTGATCGGTCTTGCAATTCATCTCGAGTTCGACATATCCAGG
ACGGGTATTACATATGAAACAGGTGACCATGTAGGTGTATATGCTGAAAATCATG
TTGAAATAGTTGAAGAAGCTGGAAAATTGCTTGGCCACTCTTTAGATTTAGTATT
TTCCATACATGCTGACAAGGAAGATGGCTCCCCATTGGAAAGCGCAGTGCCGCCT
CCTTTCCCTGGTCCATGCACACTTGGGACTGGTTTGGCAAGATACGCAGACCTTT
TGAACCCTCCTCGAAAGTCTGCGTTAGTTGCCTTGGCGGCCTATGCCACTGAACC
AAGTGAAGCCGAGAACTTAAGCACCTGACATCACCTGATGGAAAGGATGAGTAC
TCACAAATGGATTGTTGCAAGTCAGAGAAGTCTTTTAGAGGTGATGGCTGCTTTTC
CATCTGCAAAACCCCACTAGGTGTATTTTTTGGCTGCAATAGCTCCTCGTCTACA
ACCTCGTTACTACTCCATCTCATCCTCGCCAAGATTGGCGCCAAGTAGAGTTCAT
GTTACATCCGCACTAGTATATGGTCCAACCTCCTACTGGTAGAATCCACAAGGGTG
TGTGTTCTACGTGGATGAAGAATGCAGTTCCTGCGGAGAAAAGTCATGAATGTAG
TGAGGCCCAATCTTTATTCGAGCATCTAATTTCAAGTTACCATCCAACCCTTCA
ACTCCAATCGTTATGGTGGGACCTGGGACTGGGCTGGCACCTTTTAGAGGTTTTTC
TGCAGGAAAGGATGGCACTAAAAGAAGATGGAGAAGAACTAGGTTTCATCTTTGCT
CTTCTTTGGGTGTAGAAATCGACAGATGGACTTTATATACGAGGATGAGCTCAAT
AATTTTGTGATCAAGGCGTAATATCTGAGCTCATCATGGCATTCTCCCGTGAAG
GAGCTCAGAAGGAGTATGTTCAACATAAGATGATGGAGAAGGCAGCACAAAGTTTG
GGATCTAATAAAGGAAGAAGGATATCTCTATGTATGCGGTGATGCTAAGGGCATG
GCGAGGGACGTCCACCGAACTCTACACACCATTGTTTCAGGAGCAGGAAGGTGTGA
GTTTCGTCAGAGGCAGAGGCTATAGTTAAGAACTTCAAACCGAAGGAAGATACCT
CAGAGATGTCTGG
```

ATR2tr (P450 reductase from *Arabidopsis*) was isolated from plant cultivated in liquid culture. The truncated version of ATR2 was created by deleting the hydrophobic 75 amino acids of the N-terminal region.

```
GGTTCCTGGGAATTCAAAACGTGTCGAGCCTCTTAAGCCTTTGGTTATTAAGCCTC
GTGAGGAAGAGATTGATGATGGGCGTAAGAAAGTTACCATCTTTTTTCGGTACACA
AACTGGTACTGCTGAAGGTTTTGCAAAGGCTTTAGGAGAAGAAGCTAAAGCAAGA
TATGAAAAGACCAGATTCAAATCGTTGATTTGGATGATTACGCGGCTGATGATG
ATGAGTATGAGGAGAAATTGAAGAAAGAGGATGTGGCTTTCTTCTTCTTAGCCAC
ATATGGAGATGGTGAGCCTACCGACAATGCAGCGAGATTCTACAAATGGTTCACC
GAGGGGAATGACAGAGGAGAAATGGCTTAAGAACTTGAAGTATGGAGTGTGGAT
TAGGAAACAGACAATATGAGCATTTTAATAAGGTTGCCAAAGTTGTAGATGACAT
TCTTGTGCAACAAGGTGCACAGCGTCTTGTACAAGTTGGTCTTGGAGATGATGAC
CAGTGTATTGAAGATGACTTTACCGCTTGGCGAGAAGCATTGTGGCCCGAGCTTG
ATACAATACTGAGGGAAGAAGGGGATACAGCTGTTGCCACACCATACTGCAGC
TGTGTTAGAATACAGAGTTTTCTATTCACGACTCTGAAGATGCCAAATTCAATGAT
ATAAACATGGCAAATGGGAATGGTTACACTGTGTTTGATGCTCAACATCCTTACA
AAGCAAATGTGCTGTAAAAGGGAGCTTCATACTCCCGAGTCTGATCGTTCTTG
TATCCATTTGGAATTTGACATTGCTGGAAGTGGACTTACGTATGAAACTGGAGAT
CATGTTGGTGTACTTTGTGATAACTTAAGTGAAACTGTAGATGAAGCTCTTAGAT
TGCTGGATATGTCACCTGATACTTATTTCTCACTTACGCTGAAAAAGAAGACGG
CACACCAATCAGCAGCTCACTGCCTCCTCCCTTCCCACCTTGCAACTTGAGAACA
GCGCTTACACGATATGCATGTCTTTTGAGTTCCTCAAAGAAGTCTGCTTTAGTTG
CGTTGGCTGCTCATGCATCTGATCCTACCGAAGCAGAACGATTAAAACACCTTGC
TTCACCTGCTGGAAAGGATGAATATTCAAAGTGGGTAGTAGAGAGTCAAAGAAGT
CTACTTGAGGTGATGGCCGAGTTTCTTCAGCCAAGCCACCCTTGGTGTCTTCT
TCGCTGGAGTTGCTCCAAGGTTGCAGCCTAGGTTCTATTCGATATCATCATCGCC
CAAGATTGCTGAAACTAGAATTCACGTCACATGTGCACTGGTTTTATGAGAAAATG
CCAAGTGGCAGGATTCATAAGGGAGTGTGTTCCACTTGGATGAAGAATGCTGTGC
CTTACGAGAAGAGTGAAAACCTGTTCTCGGCGCCGATATTTGTTAGGCAATCCAA
CTTCAAGCTTCTTCTGATTCTAAGGTACCGATCATCATGATCGGTCCAGGGACT
GGATTAGCTCCATTCAGAGGATTCCTTCAGGAAAGACTAGCGTTGGTAGAATCTG
GTGTTGAACTTGGGCCATCAGTTTTGTTCTTTGGATGCAGAAACCGTAGAATGGA
TTTCATCTACGAGGAAGAGCTCCAGCGATTTGTTGAGAGTGGTGTCTCTCGCAGAG
CTAAGTGTGCGCTTCTCTCGTGAAGGACCCACCAAAGAATACGTACAGCACAAGA
TGATGGACAAGGCTTCTGATATCTGGAATATGATCTCTCAAGGAGCTTATTTATA
TGTTTGTGGTGACGCCAAAGGCATGGCAAGAGATGTTACAGATCTCTCCACACA
ATAGCTCAAGAACAGGGGTCAATGGATTCAACTAAAGCAGAGGGCTTCGTGAAGA
ATCTGCAAACGAGTGGAAGATATCTTAGAGATGTATGG
```

A2 Gene sequence used in Chapter 5 and 6

ATR2tr sequence originated from the *E. coli* expression codon optimised ATR2 gene sequence synthesised by GeneArt.

```
GGTAGCGGTAATAGCAAACGTGTTGAACCGCTGAAACCGCTGGTTATTAACCGC
GTGAAGAAGAAATTGACGACGGTTCGTA AAAAAGTGACCATTTTTTTTTGGCACCCA
GACCGGCACCGCAGAAGTTTTGCAAAAGCACTGGGTGAAGAGGCAAAAGCACGT
TATGAAAAAACCGCTTCAA AATTGTGGATCTGGATGATTATGCAGCCGATGATG
ATGAGTATGAAGAAAACTGAAAAAGAAGATGTGGCCTTTTTTTTTCTGGCAAC
CTATGGTGATGGTGAACCGACCGATAATGCAGCACGTTTTTTATAAATGGTTTACC
GAAGGTAACGATCGTGGTGAATGGCTGAAAAATCTGAAATATGGTGTGTTTGGTC
TGGGTAATCGCCAGTATGAACACTTTAATAAAGTGGCCAAAGTGGTGGATGATAT
TCTGGTTGAACAGGGTGCACAGCGTCTGGTTCAGGTTGGTCTGGGTGATGATGAT
CAGTGTATCGAAGATGATTTTTACCGCATGGCGTGAAGCACTGTGGCCTGAACTGG
ATACCATTTCTGCGTGAAGAAGGTGATACCGCAGTTGCAACCCCGTATACCGCAGC
AGTTCTGGAATATCGTGTTAGCATT CATGATAGCGAGGATGCCAAATTCACCGAT
ATTAATATGGCCAATGGCAATGGCTATACCGTTTTTTGATGCACAGCATCCGTATA
AAGCAAATGTTGCAGTTAAACGCGAACTGCATACACCGGAAAGCGATCGTAGCTG
TATTCATCTGGAATTTGATATTGCAGGTAGCGGTCTGACCTATGAAACCGGTGAT
CATGTTGGTGTCTGTGTGATAATCTGAGCGAAACCGTTGATGAAGCACTGCGTC
TGCTGGATATGAGTCCGGATACCTATTTTAGCCTGCATGCAGAAAAAGAGGATGG
CACCCCGATTAGCAGCAGCCTGCCTCCGCCTTTTTCCGCCTTGTAATCTGCGTACC
GCACTGACCCGTTATGCATGTCTGCTGAGCAGCCCGAAAAAAGCGCACTGGTTG
CACTGGCAGCACATGCAAGCGATCCGACCGAAGCAGAACGTCTGAAACATCTGGC
AAGTCCGGCAGGTAAAGTTGATGAATATAGCAAATGGGTTGTGGAAAGCCAGCGT
AGCCTGCTGGAAGTTATGGCAGAATTTCCGAGCGCAAAACCGCCTCTGGGTGTTT
TTTTTGCCGGTGTTCACCGCGTCTGCAGCCTCGTTTTTTATAGCATTAGCAGCAG
TCCGAAAATTGCAGAAACCCGTATTCATGTTACCTGTGCACTGGTGTATGAAAA
ATGCCGACCGGTCGTATTCATAAAGGTGTTTGTAGCACCTGGATGAAAAATGCAG
TGCCGTATGAAAAAAGCGAAAATTGTAGCAGCGCACCGATTTTTGTTCGTCAGAG
CAATTTTAAACTGCCGAGCGATAGCAAAGTGCCGATTATTATGATTGGTCCGGGT
ACAGGTCTGGCACCGTTTTCGTGGTTTTCTGCAAGAACGTCTGGCACTGGTTGAAA
GCGGTGTTGAACTGGGTCCGAGCGTCTGTTTTTTGGTTGTGCGTAATCGTCGCAT
GGATTTTCATCTATGAAGAAGA ACTGCAGCGTTTTGTGGAAAGCGGTGCACTGGCC
GAACTGAGCGTTGCATTTAGCCGTGAAGGTCCGACCAAAGAATATGTTTCAGCACA
AAATGATGGACAAAGCCAGCGATATTTGGAATATGATTAGCCAGGGTGCCTATCT
GTATGTTTGTGGTGTGATGCAAAGGTATGGCACGTGATGTTTCATCGTAGCCTGCAT
ACCATTGCACAAGAACAGGGTAGCATGGATAGCACCAAAGCCGAAGTTTTGTTA
AAAATCTGCAGACCAGCGGTTCGTTATCTGCGTGATGTTTGGTAA
```

Modified P450 gene sequences for P450-ATR2tr fusion platform:

IFS native gene derived from Prof. Mattheos Koffas. The first six N-terminal residues (small letters) represent the synthetic mammalian peptide (amino acid sequence: MALLLAVF). The codon of the last amino acid (Serine) was changed from TCT to TCA to make it compatible for ligation independent cloning.

```
atggctctggttatttagcagtttttCTTGGTTTGTGGTTAGCTTTGTTTCTGCACTT
GCGTCCCACACCAAGTGCAAAATCAAAAGCACTTCGCCACCTCCCAAACCCTCCA
AGCCCAAAGCCTCGTCTTCCCTTCATTGGCCACCTTCACCTCTTAAAAGATAAAC
TTCTCCACTATGCACTCATCGATCTCTCCAAAAGCATGGCCCCCTTATTCTCTCT
CTCCTTCGGCTCCATGCCAACCGTCGTTGCCCTCCACCCCTGAGTTGTTCAAGCTC
TTCCTCCAAACCCACGAGGCAACTTCCCTTCAACACAAGGTTCCAAACCTCTGCCA
TAAGACGCCTCACTTACGACAACCTCTGTGGCCATGGTTCCATTTCGGACCTTACTG
GAAGTTCGTGAGGAAGCTCATCATGAACGACCTTCTCAACGCCACCACCGTCAAC
AAGCTCAGGCCTTTGAGGACCCAACAGATCCGCAAGTTCCCTTAGGGTTATGGCCC
AAAGCGCAGAGGCCCAGAAGCCCCTTGACGTCACCGAGGAGCTTCTCAAATGGAC
CAACAGCACCATCTCCATGATGATGCTCGGCGAGGCTGAGGAGATCAGAGACATC
GCTCGCGAGGTTCTTAAGATCTTCGGCGAATACAGCCTCACTGACTTCATCTGGC
CTTTGAAGTATCTCAAGGTTGGAAAGTATGAGAAGAGGATTGATGACATCTTGAA
CAAGTTCGACCCTGTTCGTTGAAAGGGTCATCAAGAAGCGCCGTGAGATCGTCAGA
AGGAGAAAGAACGGAGAAGTTGTTGAGGGCGAGGCCAGCGGCGTCTTCCTCGACA
CTTTGCTTGAATTTCGCTGAGGACGAGACCATGGAGATCAAAATTACCAAGGAGCA
AATCAAGGGCCTTGTTGTCGACTTTTTCTCTGCAGGGACAGATTCCACAGCGGTG
GCAACAGAGTGGGCATTGGCAGAGCTCATCAACAATCCCAGGGTGTGCAAAAGG
CTCGTGAGGAGGTCTACAGTGTGTTGGGCAAAGATAGACTCGTTGACGAAGTTGA
CACTCAAAACCTTCCCTTACATTAGGGCCATTGTGAAGGAGACATTCCGAATGCAC
CCACCCTCCAGTGGTCAAAAGAAAGTGCACAGAAGAGTGTGAGATTAATGGGT
ATGTGATCCCAGAGGGAGCATTGGTTCTTTTCAATGTTTGGCAAGTAGGAAGGGA
CCCCAAATACTGGGACAGACCATCAGAATTCCGTCCCGAGAGGTTCTTAGAAACT
GGTGCTGAAGGGGAAGCAGGGCCTCTTGATCTTAGGGGCCAGCATTTCCAACTCC
TCCATTTGGGTCTGGGAGGAGAATGTGCCCTGGTGTCAATTTGGCTACTTCAGG
AATGGCAACACTTCTTGCATCTCTTATCCAATGCTTTGACCTGCAAGTGCTGGGC
CCTCAAGGACAAATATTGAAAGGTGATGATGCCAAAGTTAGCATGGAAGAGAGAG
CTGGCCTCACAGTTCCAAGGGCACATAGTCTCGTTTTGTGTTCCACTTGCAAGGAT
CGGCGTTGCATCTAAACTCCTTTCA
```

IFSopt gene was synthesised and codon optimised for the expression in *E. coli* by GeneArt. The codon of the last amino acid (Serine) was changed from AGC to TCA to make it compatible for ligation independent cloning.

```
GCCCGTCCGACCCCGAGCGCAAAAAGCAAAGCACTGCGTCATCTGCCGAATCCGC
CTAGCCCGAAACCGCGTCTGCCGTTTATTGGTCATCTGCATCTGCTGAAAGATAA
ACTGCTGCATTATGCACTGATTGATCTGAGCAAAAAACATGGTCCGCTGTTTAGC
CTGAGCTTTGGTAGCATGCCGACCGTTGTTGCAAGCACACCGGAACGTGTTTAAAC
TGTTTCTGCAGACCCATGAAGCGACCAGCTTTAATAACCGTTTTTCAGACCAGCGC
AATTCGTCGTCTGACCTATGATAATAGCGTTGCAATGGTTCCGTTTGGTCCGTAT
TGAAATTTGTGCGTAAACTGATCATGAACGATCTGCTGAATGCAACCACCGTTA
ATAAACTGCGTCCGCTGCGTACCCAGCAGATTCGTAAATTTCTGCGTGTTATGGC
ACAGAGCGCAGAAGCACAGAAACCGCTGGATGTTACCGAGGAACTGCTGAAATGG
ACCAATAGCACCATTAGCATGATGATGCTGGGTGAAGCCGAAGAAATTCGTGATA
TTGCACGTGAAGTGCTGAAAATCTTTGGTGAATATAGCCTGACCGATTTTATCTG
GCCTCTGAAATATCTGAAAGTGGGCAAATATGAAAACGCATCGATGATATTCTG
AATAAATTTGATCCGGTGGTGGAAACGCGTGATTA AAAAACGTCGTGAAATTGTTT
GCCGTGCAAAAATGGTGAAGTTGTTGAAGGTGAAGCCAGCGGTGTTTTTCTGGA
TACCCTGCTGGAATTTGCCGAAGATGAAACCATGGAAATTA AAATACCAAAGAA
CAAATTAAGGCCTGGTGGTGGATTTTTTTTAGCGCAGGCACCGATAGCACCCGAG
TTGCAACCGAATGGGCACTGGCAGAACTGATTAATAATCCGCGTGTTCTGCAGAA
AGCACGTGAAGAAGTTTATAGCGTTGTTGGTAAAGATCGTCTGGTTGATGAAGTT
GATACCCAGAATCTGCCGTATATTCGTGCCATTGTGAAAGAAACCTTTCGTATGC
ATCCGCCTCTGCCGGTTGTTAAACGTAAATGTACCGAAGAATGCGAAATCAACGG
TTATGTTATTCCGGAAGGTGCACTGGTTCTGTTTAAATGTTTGGCAGGTTGGTCGT
GATCCGAAATATTTGGGATCGTCCGAGCGAATTTTCGTCCGGAACGTTTTCTGGAAA
CCGGTGCAGAAGGTGAAGCAGGTCCGCTGGATCTGCGTGGTTCAGCATTTTTCAGCT
GCTGCCGTTTGGTAGCGGTCGTCGTATGTGTCCGGGTGTTAATCTGGCAACCAGC
GGTATGGCAACCCTGCTGGCAAGCCTGATTCAGTGTTTTTGATCTGCAGGTTCTGG
GTCCGCAGGGTCAGATTCTGAAAGGTGATGATGCAAAAAGTGAGCATGGAAGAACG
TGCAGGTCAGACCGTTCCGCGTGCACATAGCCTGGTTTTGTGTTCCGCTGGCACGT
ATTGGTGTGCAAGCAAACCTGCTGTCA
```

CYP73A5 (cinnamate-4-hydroxylase from *Arabidopsis*) was synthesised and codon optimised for the expression in *E. coli* by GeneArt. The truncated version of CYP73A5 (73A5tr) was created by deleting the hydrophobic N-terminal region and to improve the expression in *E. coli* and Alanin was added just after the start codon methionin (in bold).³²¹

The codon of the last amino acid (Cysteine) will be changed from TGC to TCA (Serine) to make it compatible for ligation independent cloning.

```
ATGGCCCTGCGTGGTAAAAAACTGAACTGCCTCCGGGTCCGATTCCGATCCCGATTTTTT
GGTAATTGGCTGCAGGTTGGTGATGATCTGAATCATCGTAATCTGGTGGACTACGCCAAA
AAATTCGGTGACCTGTTTCTGCTGCGTATGGGTGTCAGCGTAATCTGGTTGTTGTTAGCAGT
CCGGATCTGACCAAAGAAGTTCTGCATACCCAGGGTGTGTAATTTGGTAGCCGTACCCGT
AATGTTGTGTTTGGATATCTTTACAGGTAAAGGTCAGGATATGGTGTGTTACCGTTTATGGT
GAACATTGGCGTAAAATGCGTCTGATTATGACCGTTCCGTTCTTTACCAATAAAGTTGTT
CAGCAGAATCGCGAAGGCTGGGAATTTGAAGCAGCAAGCGTTGTTGAGGACGTGAAAAAA
AACCCGGATAGCGCAACCAAAGGTATTGTTCTGCGTAAACGTCTGCAGCTGATGATGTAT
AATAACATGTTCCGCATCATGTTTCGATCGTCGTTTTGAAAGCGAAGATAGTCCGCTGTTT
CTGCGTCTGAAAGCACTGAATGGTGAACGTAGCCGTCTGGCACAGAGCTTTGAATATAAC
TATGGCGATTTTTATCCCGATTCTGCGTCCGTTTCTGCGTGGTTATCTGAAAATTTGCCAG
GATGTTAAAGATCGTCGTATTGCCCTGTTCAAAAATACTTTGTGGACGAACGCAAACAA
ATTGCAAGCAGCAAACCGACCGGTAGCGAAGGTCTGAAATGTGCAATTGATCATATTCTG
GAAGCCGAACAGAAAGGCGAAATTAATGAAGATAATGTGCTGTACATTGTGAAAACATT
AACGTTGCAGCCATTGAAACCACCCTGTGGTCAATTGAATGGGGTATTGCAGAACTGGTT
AACCATCCGGAAATTCAGAGTAACTGCGTAATGAACTGGATACCGTTCTGGGTCCGGGT
GTTTCAGGTTACCGAACCGGATCTGCATAAACTGCCGTATCTGCAGGCAGTTGTTAAAGAA
ACCCTGCGTCTGCGTATGGCAATTCGCTGCTGGTTCCGCATATGAATCTGCATGATGCA
AAACTGGCAGGTTATGATATTCCGGCAGAAAGCAAATTTCTGGTTAATGCATGGTGGCTG
GCCAATAATCCGAATAGCTGGAAAAAACCGGAAGAATTTGTCGCGAACGCTTTTTTTGAA
GAAGAAAGCCACGTTGAAGCCAATGGTAATGATTTTCGTTATGTTCCGTTTGGTGTGGT
CGTCGTAGCTGTCCGGGTATTATTCTGGCACTGCCGATTCTGGGTATTACCATTGGTTCGT
ATGGTGCAGAAATTTGAACTGCTGCCTCCGCCGGTTCAGAGCAAAGTTGATACCAGCGAA
AAAGGTGGTCAGTTTAGCCTGCATATTCTGAACCATAGCATTATTGTGATGAAACCGCGT
AACTTCA
```

CYP82E4tr (N-demethylase from *Nicotiana tabacum*) derived from Prof. Ralph Dewey. The truncated version of CYP82E4 (82E4tr) was created by deleting the hydrophobic N-terminal region. The codon TAT of the last amino acid (Tyrosine) will be changed from to ACA (Threonine) to keep the electrophilic charge and to make it compatible for ligation independent cloning.

```
ACAAAAAATCTCAAAAACCTTCAAAACCCTTACCACCGAAAATCCCCGGAGGAT
GGCCGGTAATCGGCCATCTTTTCCACTTCAATGACGACGGCGACGACCGTCCATT
AGCTCGAAAACCTCGGAGACTTAGCTGACAAATACGGCCCCGTTTTCACTTTTCGG
CTAGGCCTTCCCCTTGTCTTAGTTGTAAGCAGTTACGAAGCTGTAAAAGACTGTT
TCTCTACAAATGACGCCATTTTTTCCAATCGTCCAGCTTTTCTTTACGGCGATTA
CCTTGGCTACAATAATGCCATGCTATTTTTGGCCAATTACGGACCTTACTGGCGA
AAAAATCGAAAATTAGTTATTCAGGAAGTTCCTCTCCGCTAGTCGTCTCGAAAAAT
TCAAACACGTGAGATTTGCAAGAATTCAAGCGAGCATTAAGAATTTATATACTCG
AATTGATGGAAATTCGAGTACGATAAATTTAACTGATTGGTTAGAAGAATTGAAT
TTTGGTCTGATCGTGAAGATGATCGCTGGAAAAAATTATGAATCCGGTAAAGGAG
ATGAACAAGTGGAGAGATTTAAGAAAGCGTTTAAGGATTTTATGATTTTATCAAT
GGAGTTTGTGTTATGGGATGCATTTCCAATTCCATTATTTAAATGGGTGGATTTT
CAAGGGCATGTTAAGGCTATGAAAAGGACTTTTAAAGATATAGATTCTGTTTTTC
AGAATTGGTTAGAGGAACATATTAATAAAAAGAGAAAAAATGGAGGTTAATGCAGA
AGGGAATGAACAAGATTTCAATTGATGTGGTGCTTTCAAAAATGAGTAATGAATAT
CTTGGTGAAGGTTACTCTCGTGATACTGTCATTAAGCAACGGTGTTTAGTTTGG
TCTTGGATGCAGCAGACACAGTTGCTCTTCACATAAATTGGGGAATGGCATTATT
GATAACAATCAAAGGCCTTGACGAAAGCACAAGAAGAGATAGACACAAAAGTT
GGTAAGGACAGATGGGTAGAAGAGAGTGATATTAAGGATTTGGTATACCTCCAAG
CTATTGTTAAAGAAGTGTTACGATTATATCCACCAGGACCTTTGTTAGTACCACA
CGAAAATGTAGAAGATTGTGTTGTTAGTGGATATCACATTCCTAAAGGGACAAGA
TTATTTCGCAAACGTCATGAAACTGCAACGTGATCCTAAACTCTGGTCTGATCCTG
ATACTTTTCGATCCAGAGAGATTCATTGCTACTGATATTGACTTTTCGTGGTCAGTA
CTATAAGTATATCCCGTTTGGTTCTGGAAGACGATCTTGTCAGGGATGACTTAT
GCATTGCAAGTGGAACTTAACAATGGCACATTTGATCCAAGGTTTCAATTACA
GAACTCCAATGACGAGCCCTTGGATATGAAGGAAGGTGCAGGCATAACTATACG
TAAGGTAAATCCTGTGGAACCTGATAATAGCGCCTCGCCTGGCACCTGAGCTTACA
```

CYP81D8 (from *Arabidopsis*) was isolated from plant cultivated in liquid culture. The truncated version of CYP81D8 (81D8tr) was created by deleting the hydrophobic N-terminal region. The codon GTT (Valine) was changed to GTA (Valine) to make it compatible for ligation independent cloning.

```
GGAAACTCAAGCGAAAGCCAAATCTACCTCCGAGTCCGGCATGGTCATTACCGG
TGATTGGTCATCTCCGCCTTCTCAAACCACCGATTCATCGCACATTCCCTCTCCCT
CTCTCAATCCCTAAACAATGCTCCGATCTTCTCCCTCCGACTCGGTAACCGACTC
GTTTTTCGTGAACTCGTCACACTCGATCGCCGAGGAATGTTTCACCAAAAACGACG
TCGTACTGGCGAACAGACCAAACCTTCATCCTCGCTAAACACGTTGCGTACGATTA
CACAACCATGATCGCAGCTTCCCTACGGTGACCACTGGCGTAACCTCCGCCGCATC
GGCTCCGTTCGAGATATTCTCCAATCACCGTCTCAATAGCTTTTTGTCTATTTCGTA
AAGACGAGATCCGACGACTTGTGTTTTCGTCTTTCTCGGAACTTTTCAACAAGAGTT
TGTGAAAGTGGATATGAAATCAATGTTATCTGACTTAACATTCACAACATTTTA
AGAATGGTGGCCGGAAAACGTTACTACGGAGACGGTGTGAGGATGATCCGGAGG
CTAAACGTGTCCGGCAGCTTATAGCGGATGTGGTGGCTTGTGCTGGTGTGGAAA
CGCTGTTGATTACTTACCGGTTTTGCGGTTGGTTTTAGATTACGAGACACGGGTT
AAGAAGTTGGCGGGTAGGCTCGACGAGTTCTTGCAAGGATTGGTTGATGAGAAAC
GAGAAGCTAAGGAGAAAGGAAACACTATGATCGATCACTTGCTTACTCTGCAAGA
ATCCAACCGGATTACTTCACGGATCGTATCATTAAAGGAAACATGCTCGCTTTG
ATACTAGCAGGGACCGACACATCAGCGGTTACGTTAGAATGGGCATTGTGCAACG
TGTTGAACCATCCGGATGTATTGAACAAGGCGAGAGATGAAATCGATAGAAAGAT
AGGTTTAGACAGGCTTATGGATGAATCAGATATCTCAAACCTGCCTTATCTCCAA
AACATTGTGTCTGAAACGTTGCGCCTTTATCCTGCGGCTCCCATGCTTCTTCCTC
ACGTTGCCTCGGAAGATTGTAAAGTTGCAGGATACGATATGCCGCGTGGCACGAT
ACTATTGACCAATGTGTGGGCTATACACAGAGATCCTCAGCTATGGGATGATCCA
ATGAGCTTCAAGCCAGAGAGGTTTTGAGAAAGAAGGAGAAGCTCAGAAGCTAATGC
CGTTTGGGTTAGGAAGAAGGGCGTGTCTTGGTTCTGGACTGGCTCATCGGCTTAT
AAACCTGACTCTTGATCATTGATTGAGTGTGTTGGAATGGGAGAAGATTGGAGAA
GAAGTGGATATGAGTGAAGGCAAAGGTGTTACAATGCCTAAAGCCAAGCCTTTGG
AAGCCATGTGCAGAGCACGTCCCTCTGTTGTTAAAATCTTCAACGAGTCCGTA
```

Abbreviations

½ MS	Murashige and Skoog medium half strength
2-ADNT	2-amino-4,6-dinitrotoluene
2-HADNT	2-hydroxylamino-4,6-dinitrotoluene
4-ADNT	4-amino-2,6-dinitrotoluene
4-HADNT	4-hydroxylamino-2,6-dinitrotoluene
A	adenine
aa	amino acids
Abs	optical absorbance
ADE 2d	selection marker for adenine auxotrophy
ALA	5-aminolevulinic acid
<i>ampR</i>	ampillin resistance gene
ATR1	<i>Arabidopsis thaliana</i> cytochrome P450 reductase 1
BLAST	Basic Local Alignment Search Tool
bp	base pairs
BSA	bovine serum albumine
C	cytosine
cDNA	complementary DNA
CO	carbon monoxide
CPO	chloroperoxidase
CPR	cytochrome P450 reductase
DMSO	dimethylsulfoxide
DNA	deoxyribonucleic acid
dNTP	dinucleotide triphosphate
DTT	dithiothreitol
[E]	enzyme concentration
EDTA	ethylenediaminetetraacetic acid
ER	endoplasmic reticulum
<i>et al.</i>	<i>et alii</i>
EtOH	ethanol
f1 ori	<i>f1 phage origin of replication</i>
FAD	flavin adenine dinucleotide

ABBREVIATIONS

FMN	flavin mononucleotide
g	grams
G	guanine
heme	Protoporphirin IX bound to one iron atom
HEPES	4-(2-hydroxyethyl)-1-piperazineethanesulphonic acid
His	6x histidines residues
HiTEL	High Throughput Expression Laboratory
HPLC	high performance liquid chromatography
K ₂ HPO ₄	dipotassium hydrogen phosphate
kanR	kanamycine resistance gene
kb	kilo base pairs
k _{cat}	maximum turnover rate
KCl	potassium chloride
kDa	kilodaltons
kg	kilogram
KH ₂ PO ₄	potassium dihydrogen phosphate
K _M	Michaelis-Menten constant
l	litre
LacI	repressor gene for IPTG induction
LacZ	β-galactosidase gene
LB	Lysogeny Broth
LIC	Ligation independent cloning
LiCl	lithium chloride
LIC-vector	pETYSBLIC3C vector
m	meter
M	molar
M13 ori	origin of replication of filamentous phage M13
MALDI-TOF	Matrix-Assisted Laser Desorption/Ionization - <i>Time-of-Flight</i>
MgSO ₄	magnesium phosphate
min	minute(s)
mRNA	messenger RNA
NaCl	sodium chloride
NaCl	sodium chloride

ABBREVIATIONS

NAD ⁺	nicotinamide adenine dinucleotide, oxidised form
NADH	nicotinamide adenine dinucleotide, reduced form
NADP ⁺	nicotinamide adenine dinucleotide phosphate, oxidised form
NADPH	nicotinamide adenine dinucleotide phosphate, reduced form
NaOH	sodium hydroxide
NCBI	National Center for Biotechnology Information
NDSB 201	3-(1-Pyridinio)-1-propanesulfonate
NEB	New England Biolabs
(NH ₄) ₂ SO ₄	ammonium sulphate
NOS	nitric oxide synthase
OD ₆₀₀	optical density at 600 nm
oLAC	Lac operator
PAGE	<i>polyacrylamide</i> gel electrophoresis
pBR322 ori	origin of replication of the plasmid pBR322
PBS	phosphate buffered saline
PCR	polymerase chain reaction
PEG	poly-ethylene glycol
pGAL	galactose promoter
PMSF	phenylmethanesulfonylfluoride
pT7	T7 promotor
RBS	ribosome binding site
RDX	hexahydro -1,3,5-trinitro -1,3,5-triazine, Royal Demolition Explosive
RNA	ribose nucleic acid
rpm	revolutions per minute
RT	reverse transcriptase
[S]	substrate concentration
SDS	sodium dodecyl sulfate
sec	second(s)
SGI	synthetic media for yeast
SRS	substrate recognition site
SSNMR	<i>Solid State Nuclear Magnetic Resonance</i>
STDEV	one standard deviation from the mean
T	Thymine

ABBREVIATIONS

tac	tac promoter
TCA	trichloroacetic acid
TE	Tris/EDTA
Temed	N, N, N', N'-Tetramethylethylenediamine
TFA	trifluoroacetic acid
TNT	2,4,6-trinitrotoluene
tPGK	phosphoglycerate kinase terminator
Tris	2-amino-2-hydroxymethyl-1,3-propanediol
Triton X-100	4-octylphenol polyethoxylate
tT7	T7 terminator
URA3	selection marker for uracil auxotrophy
UV	ultra violet (light)
v/v	volume to volume ratio
V_{\max}	maximal reaction velocity
w/v	weight to volume ratio
X-Gal	bromochloroindolylgalactopyranoside
YPGA	yeast medium containing yeast extract, bactopectone, glucose and adenine
YPGE	yeast medium containing yeast extract, bactopectone, glucose and ethanol
ZnCl ₂	zinc chloride

References

- 1 Frazzetto, G. White biotechnology. *EMBO Rep* **4**, 835-837 (2003).
- 2 Pazmiño, D. E. T., Winkler, M., Glieder, A. & Fraaije, N. W. Monooxygenases as biocatalysts: Classification, mechanistic aspects and biotechnological applications. *J Biotechnol* **145**, 9-24 (2010).
- 3 Dunford, H. B. *Peroxidases and Catalases: Biochemistry, Biophysics, Biotechnology and Physiology*. Vol. 2nd ed. (John Wiley and Sons, 2010).
- 4 Palfey, B. A. & McDonald, C. A. Control of catalysis in flavin-dependent monooxygenases. *Archives of Biochemistry and Biophysics* **493**, 26-36 (2010).
- 5 Webb, E. C. *Enzyme nomenclature 1992: recommendations of the Nomenclature Committee of the International Union of Biochemistry and Molecular Biology on the nomenclature and classification of enzymes*. (Academic Press, Inc., 1992).
- 6 Nelson, D. R. The cytochrome p450 homepage. *Hum Genomics* **4**, 59-65 (2009).
- 7 Estabrook, R. W. A passion for P450s (remembrances of the early history of research on cytochrome P450). *Drug Metab Dispos* **31**, 1461-1473 (2003).
- 8 Mueller, G. C. & Miller, J. A. The reductive cleavage of 4-dimethylaminoazobenzene by rat liver; the intracellular distribution of the enzyme system and its requirement for triphosphopyridine nucleotide. *J Biol Chem* **180**, 1125-1136 (1949).
- 9 Mueller, G. C. & Miller, J. A. The metabolism of methylated aminoazo dyes. II. Oxidative demethylation by rat liver homogenates. *J Biol Chem* **202**, 579-587 (1953).
- 10 Gillette, J. R. Laboratory of Chemical Pharmacology, National Heart, Lung, and Blood Institute, NIH: a short history. *Annu Rev Pharmacol Toxicol* **40**, 18-41 (2000).
- 11 Axelrod, J. The enzymatic demethylation of ephedrine. *J Pharmacol Exp Ther* **114**, 430-438 (1955).
- 12 Rubin, R. P. A brief history of great discoveries in pharmacology: in celebration of the centennial anniversary of the founding of the American Society of Pharmacology and Experimental Therapeutics. *Pharmacol Rev* **59**, 289-359 (2007).
- 13 Brodie, B. B. *et al.* Detoxication of drugs and other foreign compounds by liver microsomes. *Science* **121**, 603-604 (1955).
- 14 Ryan, K. J. & Engel, L. L. Hydroxylation of steroids at carbon 21. *J Biol Chem* **225**, 103-114 (1957).
- 15 Estabrook, R. W., Cooper, D. Y. & Rosenthal, O. The Light Reversible Carbon Monoxide Inhibition of the Steroid C21-Hydroxylase System of the Adrenal Cortex. *Biochem Z* **338**, 741-755 (1963).
- 16 Cooper, D. Y., Levin, S., Narasimhulu, S. & Rosenthal, O. Photochemical Action Spectrum of the Terminal Oxidase of Mixed Function Oxidase Systems. *Science* **147**, 400-402 (1965).

- 17 Chance, B. & Williams, G. R. Kinetics of cytochrome b5 in rat liver microsomes. *J Biol Chem* **209**, 945-951 (1954).
- 18 Klingenberg, M. Pigments of rat liver microsomes. *Arch Biochem Biophys* **75**, 376-386 (1958).
- 19 Omura, T. & Sato, R. A new cytochrome in liver microsomes. *J Biol Chem* **237**, 1375-1376 (1962).
- 20 Omura, T. & Sato, R. The Carbon Monoxide-Binding Pigment of Liver Microsomes. I. Evidence for Its Hemoprotein Nature. *J Biol Chem* **239**, 2370-2378 (1964).
- 21 Omura, T. & Sato, R. The Carbon Monoxide-Binding Pigment of Liver Microsomes. Ii. Solubilization, Purification, and Properties. *J Biol Chem* **239**, 2379-2385 (1964).
- 22 Nelson, D. R., Ming, R., Alam, M. & Schuler, M. A. Comparison of cytochrome P450 Genes from six plant genomes. *Trop Plant Biol* **1**, 216-235 (2008).
- 23 Nelson, D. & Werck-Reichhart, D. A P450-centric view of plant evolution. *Plant J* **66**, 194-211 (2011).
- 24 Omura, T. Structural diversity of cytochrome P450 enzyme system. *J Biochem* **147**, 297-306 (2010).
- 25 Nebert, D. W. *et al.* The P450 gene superfamily: recommended nomenclature. *DNA* **6**, 1-11 (1987).
- 26 Nebert, D. W. *et al.* The P450 superfamily: update on new sequences, gene mapping, and recommended nomenclature. *DNA Cell Biol* **10**, 1-14 (1991).
- 27 Chapple, C. Molecular-Genetic Analysis of Plant Cytochrome P450-Dependent Monooxygenases. *Annu Rev Plant Physiol Plant Mol Biol* **49**, 311-343 (1998).
- 28 Werck-Reichhart, D. & Feyereisen, R. Cytochromes P450: a success story. *Genome Biol* **1**, reviews3003.3001–3003.3009 (2000).
- 29 Nelson, D. R. & Strobel, H. W. On the membrane topology of vertebrate cytochrome P-450 proteins. *J Biol Chem* **263**, 6038-6050 (1988).
- 30 Sakaguchi, M., Mihara, K. & Sato, R. A short amino-terminal segment of microsomal cytochrome P-450 functions both as an insertion signal and as a stop-transfer sequence. *EMBO J* **6**, 2425-2431 (1987).
- 31 Kida, Y., Ohgiya, S., Mihara, K. & Sakaguchi, M. Membrane topology of NADPH-cytochrome P450 reductase on the endoplasmic reticulum. *Arch Biochem Biophys* **351**, 175-179 (1998).
- 32 Ruan, K. H. *et al.* Solution structure and topology of the N-terminal membrane anchor domain of a microsomal cytochrome P450: prostaglandin I2 synthase. *Biochem J* **368**, 721-728 (2002).
- 33 Churchill, P. F. & Kimura, T. Topological studies of cytochromes P-450_{scc} and P-450_{11β} in bovine adrenocortical inner mitochondrial membranes. Effects of controlled tryptic digestion. *J Biol Chem* **254**, 10443-10448 (1979).
- 34 Omura, T., Sanders, E., Estabrook, R. W., Cooper, D. Y. & Rosenthal, O. Isolation from adrenal cortex of a nonheme iron protein and a flavoprotein functional as a reduced triphosphopyridine nucleotide-cytochrome P-450 reductase. *Arch Biochem Biophys* **117**, 660-673 (1966).

- 35 Omura, T. Mitochondrial P450s. *Chem Biol Interact* **163**, 86-93 (2006).
- 36 Song, W. C., Funk, C. D. & Brash, A. R. Molecular cloning of an allene oxide synthase: a cytochrome P450 specialized for the metabolism of fatty acid hydroperoxides. *Proc Natl Acad Sci U S A* **90**, 8519-8523 (1993).
- 37 Laudert, D., Pfannschmidt, U., Lottspeich, F., Hollander-Czytko, H. & Weiler, E. W. Cloning, molecular and functional characterization of *Arabidopsis thaliana* allene oxide synthase (CYP 74), the first enzyme of the octadecanoid pathway to jasmonates. *Plant Mol Biol* **31**, 323-335 (1996).
- 38 Watson, C. J. *et al.* Localization of CYP86B1 in the outer envelope of chloroplasts. *Plant Cell Physiol* **42**, 873-878 (2001).
- 39 Helliwell, C. A. *et al.* A plastid envelope location of *Arabidopsis* entkaurene oxidase links the plastid and endoplasmic reticulum steps of the gibberellin biosynthesis pathway. *Plant J* **28**, 201-208 (2001).
- 40 van den Brink, H. M., van Gorcom, R. F., van den Hondel, C. A. & Punt, P. J. Cytochrome P450 enzyme systems in fungi. *Fungal Genet Biol* **23**, 1-17 (1998).
- 41 Guengerich, F. P. Cytochrome P450 proteins and potential utilization in biodegradation. *Environ Health Perspect* **103 Suppl 5**, 25-28 (1995).
- 42 Poulos, T. L., Finzel, B. C., Gunsalus, I. C., Wagner, G. C. & Kraut, J. The 2.6-Å crystal structure of *Pseudomonas putida* cytochrome P-450. *J Biol Chem* **260**, 16122-16130 (1985).
- 43 Poulos, T. L., Finzel, B. C. & Howard, A. J. High-resolution crystal structure of cytochrome P450cam. *J Mol Biol* **195**, 687-700 (1987).
- 44 Urlacher, V. B. & Eiben, S. Cytochrome P450 monooxygenases: perspectives for synthetic application. *Trends Biotechnol* **24**, 324-330 (2006).
- 45 Lee, D. S., Nioche, P., Hamberg, M. & Raman, C. S. Structural insights into the evolutionary paths of oxylipin biosynthetic enzymes. *Nature* **455**, 363-368 (2008).
- 46 Graham, S. E. & Peterson, J. A. How similar are P450s and what can their differences teach us? *Arch Biochem Biophys* **369**, 24-29 (1999).
- 47 Poulos, T. L. & Meharena, Y. T. in *Metal Ions in Life Science* Vol. 3 (eds A. Sigel, H. Sigel, & R. K. O. Sigel) Ch. 4, 57-96 (John Wiley & Sons, 2007).
- 48 Schlichting, I. *et al.* The catalytic pathway of cytochrome p450cam at atomic resolution. *Science* **287**, 1615-1622, doi:8325 [pii] (2000).
- 49 Hasemann, C. A., Kurumbail, R. G., Boddupalli, S. S., Peterson, J. A. & Deisenhofer, J. Structure and function of cytochromes P450: a comparative analysis of three crystal structures. *Structure* **3**, 41-62 (1995).
- 50 Munro, A. W., Girvan, H. M. & McLean, K. J. Variations on a (t)heme--novel mechanisms, redox partners and catalytic functions in the cytochrome P450 superfamily. *Nat Prod Rep* **24**, 585-609 (2007).
- 51 Poulos, T. L. & Johnson, E. F. in *Cytochromes P450: Structure, Mechanism, and Biochemistry* (ed P. R. Ortiz de Montellano) Ch. 3, 87-114 (Kluwer Academic/Plenum Publisher, 2005).

- 52 Fischmann, T. O. *et al.* Structural characterization of nitric oxide synthase isoforms reveals striking active-site conservation. *Nat Struct Biol* **6**, 233-242 (1999).
- 53 Sundaramoorthy, M., Ternner, J. & Poulos, T. L. The crystal structure of chloroperoxidase: a heme peroxidase--cytochrome P450 functional hybrid. *Structure* **3**, 1367-1377 (1995).
- 54 Gotoh, O. Substrate recognition sites in cytochrome P450 family 2 (CYP2) proteins inferred from comparative analyses of amino acid and coding nucleotide sequences. *J Biol Chem* **267**, 83-90 (1992).
- 55 Pylypenko, O. & Schlichting, I. Structural aspects of ligand binding to and electron transfer in bacterial and fungal P450s. *Annu Rev Biochem* **73**, 991-1018 (2004).
- 56 Li, Y. C. & Chiang, J. Y. The expression of a catalytically active cholesterol 7 alpha-hydroxylase cytochrome P450 in *Escherichia coli*. *J Biol Chem* **266**, 19186-19191 (1991).
- 57 Sagara, Y., Barnes, H. J. & Waterman, M. R. Expression in *Escherichia coli* of functional cytochrome P450c17 lacking its hydrophobic amino-terminal signal anchor. *Arch Biochem Biophys* **304**, 272-278 (1993).
- 58 von Wachenfeldt, C., Richardson, T. H., Cosme, J. & Johnson, E. F. Microsomal P450 2C3 is expressed as a soluble dimer in *Escherichia coli* following modification of its N-terminus. *Arch Biochem Biophys* **339**, 107-114 (1997).
- 59 Cosme, J. & Johnson, E. F. Engineering microsomal cytochrome P450 2C5 to be a soluble, monomeric enzyme. Mutations that alter aggregation, phospholipid dependence of catalysis, and membrane binding. *J Biol Chem* **275**, 2545-2553 (2000).
- 60 Møller, B. L. Plant science. Dynamic metabolons. *Science* **330**, 1328-1329 (2010).
- 61 Nielsen, K. A. & Møller, B. L. in *Cytochromes P450: Structure, Mechanism, and Biochemistry* (ed P. R. Ortiz de Montellano) Ch. 12, 553-583 (Kluwer Academic/Plenum Publisher, 2005).
- 62 Sono, M., Roach, M. P., Coulter, E. D. & Dawson, J. H. Heme-Containing Oxygenases. *Chem Rev* **96**, 2841-2888 (1996).
- 63 Guengerich, F. P. Uncommon P450-catalyzed reactions. *Curr Drug Metab* **2**, 93-115 (2001).
- 64 Coon, M. J., Vaz, A. D. & Bestervelt, L. L. Cytochrome P450 2: peroxidative reactions of diversozymes. *FASEB J* **10**, 428-434 (1996).
- 65 Mansuy, D. The great diversity of reactions catalyzed by cytochromes P450. *Comp Biochem Physiol C Pharmacol Toxicol Endocrinol* **121**, 5-14 (1998).
- 66 Makris, T. M., von Koenig, K., Schlichting, I. & Sligar, S. G. The status of high-valent metal oxo complexes in the P450 cytochromes. *J Inorg Biochem* **100**, 507-518 (2006).
- 67 Ener, M. E., Lee, Y. T., Winkler, J. R., Gray, H. B. & Cheruzel, L. Photooxidation of cytochrome P450-BM3. *Proc Natl Acad Sci U S A* **107**, 18783-18786 (2010).

- 68 Sligar, S. G. Coupling of spin, substrate, and redox equilibria in cytochrome P450. *Biochemistry* **15**, 5399-5406 (1976).
- 69 Daff, S. N. *et al.* Redox control of the catalytic cycle of flavocytochrome P-450 BM3. *Biochemistry* **36**, 13816-13823 (1997).
- 70 Rittle, J. & Green, M. T. Cytochrome P450 compound I: capture, characterization, and C-H bond activation kinetics. *Science* **330**, 933-937 (2010).
- 71 Jung, C., de Vries, S. & Schunemann, V. Spectroscopic characterization of cytochrome P450 Compound I. *Arch Biochem Biophys* **507**, 44-55 (2011).
- 72 Davydov, R., Macdonald, I. D. G., Makris, T. M., Sligar, S. G. & Hoffman, B. M. EPR and ENDOR of Catalytic Intermediates in Cryoreduced Native and Mutant Oxy-Cytochromes P450cam: Mutation-Induced Changes in the Proton Delivery System. *J Am Chem Soc* **121**, 10654-10655 (1999).
- 73 Davydov, R. *et al.* Hydroxylation of camphor by reduced oxy-cytochrome P450cam: mechanistic implications of EPR and ENDOR studies of catalytic intermediates in native and mutant enzymes. *J Am Chem Soc* **123**, 1403-1415 (2001).
- 74 Denisov, I. G., Makris, T. M., Sligar, S. G. & Schlichting, I. Structure and chemistry of cytochrome P450. *Chem Rev* **105**, 2253-2277 (2005).
- 75 Kumar, D. *et al.* New features in the catalytic cycle of cytochrome P450 during the formation of compound I from compound 0. *J Phys Chem B* **109**, 19946-19951 (2005).
- 76 Aldag, C. *et al.* Probing the role of the proximal heme ligand in cytochrome P450cam by recombinant incorporation of selenocysteine. *Proc Natl Acad Sci U S A* (2009).
- 77 Matsunaga, I. *et al.* Enzymatic reaction of hydrogen peroxide-dependent peroxygenase cytochrome P450s: kinetic deuterium isotope effects and analyses by resonance Raman spectroscopy. *Biochemistry* **41**, 1886-1892 (2002).
- 78 Lu, Y. & Mei, L. Co-expression of P450 BM3 and glucose dehydrogenase by recombinant *Escherichia coli* and its application in an NADPH-dependent indigo production system. *J Ind Microbiol Biotechnol* **34**, 247-253 (2007).
- 79 Miners, J. O. Evolution of drug metabolism: hitchhiking the technology bandwagon. *Clin Exp Pharmacol Physiol* **29**, 1040-1044 (2002).
- 80 Guengerich, F. P. Cytochrome P450 enzymes in the generation of commercial products. *Nat Rev Drug Discov* **1**, 359-366 (2002).
- 81 Nelson, D. R. Introductory remarks on human CYPs. *Drug Metab Rev* **34**, 1-5 (2002).
- 82 Guengerich, F. P., Wu, Z. L. & Bartleson, C. J. Function of human cytochrome P450s: characterization of the orphans. *Biochem Biophys Res Commun* **338**, 465-469 (2005).
- 83 Guengerich, F. P. Cytochrome P450s and other enzymes in drug metabolism and toxicity. *AAPS J* **8**, E101-111 (2006).
- 84 Gorinova, N., Nedkovska, M. & Atanassov, A. Cytochromes P450 monooxygenases as a tool for metabolizing of herbicides in plants. *Biotechnology & Biotechnological Equipment* **19** (2005).

- 85 Kahn, R. A. & Durst, F. Function and evolution of plant cytochrome P450. *Recent Adv Phytochem* **34**, 151-189 (2000).
- 86 Peterson, J. A. & Lu, J. Y. Bacterial cytochromes P450: isolation and identification. *Methods Enzymol* **206**, 612-620 (1991).
- 87 Das, N. & Chandran, P. Microbial Degradation of Petroleum Hydrocarbon Contaminants: An Overview. *Biotechnology Research International* **2011** (2011).
- 88 Robins, K. T., Osorio-Lozada, A., Avi, M. & Meyer, H. P. Lonza: Biotechnology - A Key Ingredient for Success in the Future. *Chimia* **63**, 327-330 (2009).
- 89 Miwa, G. T., West, S. B., Huang, M. T. & Lu, A. Y. Studies on the association of cytochrome P-450 and NADPH-cytochrome c reductase during catalysis in a reconstituted hydroxylating system. *J Biol Chem* **254**, 5695-5700 (1979).
- 90 French, J. S., Guengerich, F. P. & Coon, M. J. Interactions of cytochrome P-450, NADPH-cytochrome P-450 reductase, phospholipid, and substrate in the reconstituted liver microsomal enzyme system. *J Biol Chem* **255**, 4112-4119 (1980).
- 91 Bösterling, B. & Trudell, J. R. Association of cytochrome b5 and cytochrome P-450 reductase with cytochrome P-450 in the membrane of reconstituted vesicles. *J Biol Chem* **257**, 4783-4787 (1982).
- 92 Gut, J., Richter, C., Cherry, R. J., Winterhalter, K. H. & Kawato, S. Rotation of cytochrome P-450. II. Specific interactions of cytochrome P-450 with NADPH-cytochrome P-450 reductase in phospholipid vesicles. *J Biol Chem* **257**, 7030-7036 (1982).
- 93 Nisimoto, Y. *et al.* Possible association of NADPH-cytochrome P-450 reductase and cytochrome P-450 in reconstituted phospholipid vesicles. *Biochemistry* **22**, 3586-3594 (1983).
- 94 Richter, C., Winterhalter, K. H. & Cherry, R. J. Rotational diffusion of cytochrome P-450 in rat liver microsomes. *FEBS Lett* **102**, 151-154 (1979).
- 95 Miwa, G. T. & Lu, A. Y. The association of cytochrome P-450 and NADPH-cytochrome P-450 reductase in phospholipid membranes. *Arch Biochem Biophys* **234**, 161-166 (1984).
- 96 Kuznetsov, V. Y., Ivanov, Y. D. & Archakov, A. I. Atomic force microscopy revelation of molecular complexes in the multiprotein cytochrome P450 2B4-containing system. *Proteomics* **4**, 2390-2396 (2004).
- 97 Peterson, J. A. & Graham, S. E. A close family resemblance: the importance of structure in understanding cytochromes P450. *Structure* **6**, 1079-1085 (1998).
- 98 Williams, P. A., Cosme, J., Sridhar, V., Johnson, E. F. & McRee, D. E. Mammalian microsomal cytochrome P450 monooxygenase: structural adaptations for membrane binding and functional diversity. *Mol Cell* **5**, 121-131 (2000).
- 99 Murtazina, D. *et al.* Membrane-protein interactions contribute to efficient 27-hydroxylation of cholesterol by mitochondrial cytochrome P450 27A1. *J Biol Chem* **277**, 37582-37589 (2002).

- 100 Headlam, M. J., Wilce, M. C. & Tuckey, R. C. The F-G loop region of cytochrome P450_{scc} (CYP11A1) interacts with the phospholipid membrane. *Biochim Biophys Acta* **1617**, 96-108 (2003).
- 101 Mitani, F., Ishimura, Y., Izumi, S. & Watanabe, K. Immunohistochemical localization of adrenodoxin and adrenodoxin reductase in bovine adrenal cortex. *Acta Endocrinol* **90**, 317-327 (1979).
- 102 Lambeth, J. D., Geren, L. M. & Millett, F. Adrenodoxin interaction with adrenodoxin reductase and cytochrome P-450_{scc}. Cross-linking of protein complexes and effects of adrenodoxin modification by 1-ethyl-3-(3-dimethylaminopropyl)carbodiimide. *J Biol Chem* **259**, 10025-10029 (1984).
- 103 Hatano, O., Sagara, Y., Omura, T. & Takakusu, A. Immunocytochemical localization of adrenodoxin in bovine adrenal cortex by protein A-gold technique. *Histochemistry* **91**, 89-97 (1989).
- 104 Hara, T. & Kimura, T. Active complex between adrenodoxin reductase and adrenodoxin in the cytochrome P-450_{scc} reduction reaction. *J Biochem* **105**, 601-605 (1989).
- 105 Zöllner, A. *et al.* Analysis of the interaction of a hybrid system consisting of bovine adrenodoxin reductase and flavodoxin from the cyanobacterium *Anabaena* PCC 7119. *Bioelectrochemistry* **63**, 61-65 (2004).
- 106 Sakaki, T., Kominami, S., Hayashi, K., Akiyoshi-Shibata, M. & Yabusaki, Y. Molecular engineering study on electron transfer from NADPH-P450 reductase to rat mitochondrial P450_{c27} in yeast microsomes. *J Biol Chem* **271**, 26209-26213 (1996).
- 107 Lehnerer, M., Schulze, J., Bernhardt, R. & Hlavica, P. Some properties of mitochondrial adrenodoxin associated with its nonconventional electron donor function toward rabbit liver microsomal cytochrome P450 2B4. *Biochem Biophys Res Commun* **254**, 83-87 (1999).
- 108 Hrycay, E. G., Gustafsson, J. A., Ingelman-Sundberg, M. & Ernster, L. Sodium periodate, sodium chloride, organic hydroperoxides, and H₂O₂ as hydroxylating agents in steroid hydroxylation reactions catalyzed by partially purified cytochrome P-450. *Biochem Biophys Res Commun* **66**, 209-216 (1975).
- 109 Nakahara, K., Tanimoto, T., Hatano, K., Usuda, K. & Shoun, H. Cytochrome P-450 55A1 (P-450_{dNIR}) acts as nitric oxide reductase employing NADH as the direct electron donor. *J Biol Chem* **268**, 8350-8355 (1993).
- 110 Toritsuka, N. *et al.* Functional and structural comparison of nitric oxide reductases from denitrifying fungi *Cylindrocarpus tonkinense* and *Fusarium oxysporum*. *Biochim Biophys Acta* **1338**, 93-99 (1997).
- 111 Yang, Y., Zhang, D. & Cerniglia, C. E. Purification and characterization of a cytosolic cytochrome P450 from yeast *Trichosporon cutaneum*. *FEMS Microbiol Lett* **154**, 347-353 (1997).
- 112 Stündl, U. M. *et al.* Purification and characterization of cytosolic cytochrome P450 forms from yeasts belonging to the genus *Trichosporon*. *Arch Biochem Biophys* **357**, 131-136 (1998).

- 113 Nittler, M. P., Hocking-Murray, D., Foo, C. K. & Sil, A. Identification of *Histoplasma capsulatum* transcripts induced in response to reactive nitrogen species. *Mol Biol Cell* **16**, 4792-4813 (2005).
- 114 Kizawa, H. *et al.* Nucleotide sequence of the unique nitrate/nitrite-inducible cytochrome P-450 cDNA from *Fusarium oxysporum*. *J Biol Chem* **266**, 10632-10637 (1991).
- 115 Porter, T. D. & Kasper, C. B. NADPH-cytochrome P-450 oxidoreductase: flavin mononucleotide and flavin adenine dinucleotide domains evolved from different flavoproteins. *Biochemistry* **25**, 1682-1687 (1986).
- 116 Murakami, H., Yabusaki, Y., Sakaki, T., Shibata, M. & Ohkawa, H. A genetically engineered P450 monooxygenase: construction of the functional fused enzyme between rat cytochrome P450c and NADPH-cytochrome P450 reductase. *DNA* **6**, 189-197 (1987).
- 117 Tamura, S., Korzekwa, K. R., Kimura, S., Gelboin, H. V. & Gonzalez, F. J. Baculovirus-mediated expression and functional characterization of human NADPH-P450 oxidoreductase. *Arch Biochem Biophys* **293**, 219-223 (1992).
- 118 Yamano, S. *et al.* Human NADPH-P450 oxidoreductase: complementary DNA cloning, sequence and vaccinia virus-mediated expression and localization of the CYPOR gene to chromosome 7. *Mol Pharmacol* **36**, 83-88 (1989).
- 119 Narhi, L. O. & Fulco, A. J. Characterization of a catalytically self-sufficient 119,000-dalton cytochrome P-450 monooxygenase induced by barbiturates in *Bacillus megaterium*. *J Biol Chem* **261**, 7160-7169 (1986).
- 120 Noble, M. A. *et al.* Roles of key active-site residues in flavocytochrome P450 BM3. *Biochem J* **339** 371-379 (1999).
- 121 Sevrioukova, I. F., Hazzard, J. T., Tollin, G. & Poulos, T. L. The FMN to heme electron transfer in cytochrome P450BM-3. Effect of chemical modification of cysteines engineered at the FMN-heme domain interaction site. *J Biol Chem* **274**, 36097-36106 (1999).
- 122 Sevrioukova, I. F., Li, H., Zhang, H., Peterson, J. A. & Poulos, T. L. Structure of a cytochrome P450-redox partner electron-transfer complex. *Proc Natl Acad Sci U S A* **96**, 1863-1868 (1999).
- 123 Munro, A. W., Girvan, H. M. & McLean, K. J. Cytochrome P450--redox partner fusion enzymes. *Biochim Biophys Acta* **1770**, 345-359 (2007).
- 124 Neeli, R. *et al.* The dimeric form of flavocytochrome P450 BM3 is catalytically functional as a fatty acid hydroxylase. *FEBS Lett* **579**, 5582-5588 (2005).
- 125 Kitazume, T., Haines, D. C., Estabrook, R. W., Chen, B. & Peterson, J. A. Obligatory intermolecular electron-transfer from FAD to FMN in dimeric P450BM-3. *Biochemistry* **46**, 11892-11901 (2007).
- 126 Kunst, F. *et al.* The complete genome sequence of the gram-positive bacterium *Bacillus subtilis*. *Nature* **390**, 249-256 (1997).
- 127 Gustafsson, M. C. *et al.* Expression, purification, and characterization of *Bacillus subtilis* cytochromes P450 CYP102A2 and CYP102A3: flavocytochrome homologues of P450 BM3 from *Bacillus megaterium*. *Biochemistry* **43**, 5474-5487 (2004).

- 128 Lentz, O., Urlacher, V. & Schmid, R. D. Substrate specificity of native and mutated cytochrome P450 (CYP102A3) from *Bacillus subtilis*. *J Biotechnol* **108**, 41-49 (2004).
- 129 Budde, M., Maurer, S. C., Schmid, R. D. & Urlacher, V. B. Cloning, expression and characterisation of CYP102A2, a self-sufficient P450 monooxygenase from *Bacillus subtilis*. *Appl Microbiol Biotechnol* **66**, 180-186 (2005).
- 130 Ruettinger, R. T., Wen, L. P. & Fulco, A. J. Coding nucleotide, 5' regulatory, and deduced amino acid sequences of P-450BM-3, a single peptide cytochrome P-450:NADPH-P-450 reductase from *Bacillus megaterium*. *J Biol Chem* **264**, 10987-10995 (1989).
- 131 Nakayama, N., Takemae, A. & Shoun, H. Cytochrome P450foxy, a catalytically self-sufficient fatty acid hydroxylase of the fungus *Fusarium oxysporum*. *J Biochem* **119**, 435-440 (1996).
- 132 Kitazume, T., Takaya, N., Nakayama, N. & Shoun, H. *Fusarium oxysporum* fatty-acid subterminal hydroxylase (CYP505) is a membrane-bound eukaryotic counterpart of *Bacillus megaterium* cytochrome P450BM3. *J Biol Chem* **275**, 39734-39740 (2000).
- 133 Seo, J. A., Proctor, R. H. & Plattner, R. D. Characterization of four clustered and coregulated genes associated with fumonisin biosynthesis in *Fusarium verticillioides*. *Fungal Genet Biol* **34**, 155-165 (2001).
- 134 Lah, L., Krasevec, N., Trontelj, P. & Komel, R. High diversity and complex evolution of fungal cytochrome P450 reductase: cytochrome P450 systems. *Fungal Genet Biol* **45**, 446-458 (2008).
- 135 De Mot, R. & Parret, A. H. A novel class of self-sufficient cytochrome P450 monooxygenases in prokaryotes. *Trends Microbiol* **10**, 502-508 (2002).
- 136 Roberts, G. A., Grogan, G., Greter, A., Flitsch, S. L. & Turner, N. J. Identification of a new class of cytochrome P450 from a *Rhodococcus* sp. *J Bacteriol* **184**, 3898-3908 (2002).
- 137 Roberts, G. A. *et al.* A self-sufficient cytochrome p450 with a primary structural organization that includes a flavin domain and a [2Fe-2S] redox center. *J Biol Chem* **278**, 48914-48920 (2003).
- 138 Jackson, C. J. *et al.* A novel sterol 14 α -demethylase/ferredoxin fusion protein (MCCYP51FX) from *Methylococcus capsulatus* represents a new class of the cytochrome P450 superfamily. *J Biol Chem* **277**, 46959-46965 (2002).
- 139 Lamb, D. C. *et al.* Lanosterol biosynthesis in the prokaryote *Methylococcus capsulatus*: insight into the evolution of sterol biosynthesis. *Mol Biol Evol* **24**, 1714-1721 (2007).
- 140 Seth-Smith, H. M. *et al.* Cloning, sequencing, and characterization of the hexahydro-1,3,5-Trinitro-1,3,5-triazine degradation gene cluster from *Rhodococcus rhodochrous*. *Appl Environ Microbiol* **68**, 4764-4771 (2002).
- 141 Jackson, R. G., Rylott, E. L., Fournier, D., Hawari, J. & Bruce, N. C. Exploring the biochemical properties and remediation applications of the unusual explosive-degrading P450 system XplA/B. *Proc Natl Acad Sci U S A* **104**, 16822-16827 (2007).

- 142 Fisher, C. W., Shet, M. S., Caudle, D. L., Martin-Wixtrom, C. A. & Estabrook, R. W. High-level expression in *Escherichia coli* of enzymatically active fusion proteins containing the domains of mammalian cytochromes P450 and NADPH-P450 reductase flavoprotein. *Proc Natl Acad Sci U S A* **89**, 10817-10821 (1992).
- 143 Shet, M. S. *et al.* Purification and enzymatic properties of a recombinant fusion protein expressed in *Escherichia coli* containing the domains of bovine P450 17A and rat NADPH-P450 reductase. *Arch Biochem Biophys* **311**, 402-417 (1994).
- 144 Shet, M. S., Fisher, C. W., Holmans, P. L. & Estabrook, R. W. Human cytochrome P450 3A4: enzymatic properties of a purified recombinant fusion protein containing NADPH-P450 reductase. *Proc Natl Acad Sci U S A* **90**, 11748-11752 (1993).
- 145 Li, S., Podust, L. M. & Sherman, D. H. Engineering and analysis of a self-sufficient biosynthetic cytochrome P450 PikC fused to the RhFRED reductase domain. *J Am Chem Soc* **129**, 12940-12941 (2007).
- 146 Sabbadin, F. *et al.* LICRED: a versatile drop-in vector for rapid generation of redox-self-sufficient cytochrome P450s. *Chembiochem* **11**, 987-994 (2010).
- 147 Sibbesen, O., De Voss, J. J. & Montellano, P. R. Putidaredoxin reductase-putidaredoxin-cytochrome p450cam triple fusion protein. Construction of a self-sufficient *Escherichia coli* catalytic system. *J Biol Chem* **271**, 22462-22469 (1996).
- 148 Gillam, E. M. Engineering cytochrome p450 enzymes. *Chem Res Toxicol* **21**, 220-231 (2008).
- 149 Hlavica, P. Assembly of non-natural electron transfer conduits in the cytochrome P450 system: a critical assessment and update of artificial redox constructs amenable to exploitation in biotechnological areas. *Biotechnol Adv* **27**, 103-121 (2009).
- 150 Grogan, G. Cytochromes P450: exploiting diversity and enabling application as biocatalysts. *Curr Opin Chem Biol* **15**, 241-248 (2011).
- 151 O'Reilly, E., Kohler, V., Flitsch, S. L. & Turner, N. J. Cytochromes P450 as useful biocatalysts: addressing the limitations. *Chem Commun (Camb)* **47**, 2490-2501 (2011).
- 152 Carmichael, A. B. & Wong, L. L. Protein engineering of *Bacillus megaterium* CYP102. The oxidation of polycyclic aromatic hydrocarbons. *Eur J Biochem* **268**, 3117-3125 (2001).
- 153 Labinger, J. A. & Bercaw, J. E. Understanding and exploiting C-H bond activation. *Nature* **417**, 507-514 (2002).
- 154 Mas-Ballesté, R. & Que, L., Jr. Chemistry. Targeting specific C-H bonds for oxidation. *Science* **312**, 1885-1886 (2006).
- 155 Newhouse, T. & Baran, P. S. If C-H bonds could talk: selective C-H bond oxidation. *Angew Chem Int Ed Engl* **50**, 3362-3374 (2011).
- 156 Appleby, A. C. A soluble haemoprotein P 450 from nitrogen-fixing *Rhizobium* bacteroids. *Biochim Biophys Acta* **147**, 399-402 (1967).

- 157 Katagiri, M., Ganguli, B. N. & Gunsalus, I. C. A soluble cytochrome P-450 functional in methylene hydroxylation. *J Biol Chem* **243**, 3543-3546 (1968).
- 158 Grogan, G., Roberts, G. A., Parsons, S., Turner, N. J. & Flitsch, S. L. P450(camr), a cytochrome P450 catalysing the stereospecific 6-endo-hydroxylation of (1 R)-(+)-camphor. *Appl Microbiol Biotechnol* **59**, 449-454 (2002).
- 159 Hawkes, D. B., Adams, G. W., Burlingame, A. L., Ortiz de Montellano, P. R. & De Voss, J. J. Cytochrome P450(cin) (CYP176A), isolation, expression, and characterization. *J Biol Chem* **277**, 27725-27732 (2002).
- 160 Ikeda, H., Nonomiya, T., Usami, M., Ohta, T. & Omura, S. Organization of the biosynthetic gene cluster for the polyketide anthelmintic macrolide avermectin in *Streptomyces avermitilis*. *Proc Natl Acad Sci U S A* **96**, 9509-9514 (1999).
- 161 Healy, F. G., Krasnoff, S. B., Wach, M., Gibson, D. M. & Loria, R. Involvement of a cytochrome P450 monooxygenase in thaxtomin A biosynthesis by *Streptomyces acidiscabies*. *J Bacteriol* **184**, 2019-2029 (2002).
- 162 Volokhan, O., Sletta, H., Ellingsen, T. E. & Zotchev, S. B. Characterization of the P450 monooxygenase NysL, responsible for C-10 hydroxylation during biosynthesis of the polyene macrolide antibiotic nystatin in *Streptomyces noursei*. *Appl Environ Microbiol* **72**, 2514-2519 (2006).
- 163 Funhoff, E. G., Bauer, U., Garcia-Rubio, I., Witholt, B. & van Beilen, J. B. CYP153A6, a soluble P450 oxygenase catalyzing terminal-alkane hydroxylation. *J Bacteriol* **188**, 5220-5227 (2006).
- 164 van Beilen, J. B. & Funhoff, E. G. Expanding the alkane oxygenase toolbox: new enzymes and applications. *Curr Opin Biotechnol* **16**, 308-314 (2005).
- 165 Yamazaki, H. & Shimada, T. Progesterone and testosterone hydroxylation by cytochromes P450 2C19, 2C9, and 3A4 in human liver microsomes. *Arch Biochem Biophys* **346**, 161-169 (1997).
- 166 Urban, P., Mignotte, C., Kazmaier, M., Delorme, F. & Pompon, D. Cloning, yeast expression, and characterization of the coupling of two distantly related *Arabidopsis thaliana* NADPH-cytochrome P450 reductases with P450 CYP73A5. *J Biol Chem* **272**, 19176-19186 (1997).
- 167 Humphreys, J. M., Hemm, M. R. & Chapple, C. New routes for lignin biosynthesis defined by biochemical characterization of recombinant ferulate 5-hydroxylase, a multifunctional cytochrome P450-dependent monooxygenase. *Proc Natl Acad Sci U S A* **96**, 10045-10050 (1999).
- 168 Schoch, G. *et al.* CYP98A3 from *Arabidopsis thaliana* is a 3'-hydroxylase of phenolic esters, a missing link in the phenylpropanoid pathway. *J Biol Chem* **276**, 36566-36574 (2001).
- 169 Choe, S. *et al.* The DWF4 gene of *Arabidopsis* encodes a cytochrome P450 that mediates multiple 22 α -hydroxylation steps in brassinosteroid biosynthesis. *Plant Cell* **10**, 231-243 (1998).

- 170 Sekimata, K. *et al.* Brz220 interacts with DWF4, a cytochrome P450 monooxygenase in brassinosteroid biosynthesis, and exerts biological activity. *Biosci Biotechnol Biochem* **72**, 7-12 (2008).
- 171 Szekeres, M. *et al.* Brassinosteroids rescue the deficiency of CYP90, a cytochrome P450, controlling cell elongation and de-etiolation in Arabidopsis. *Cell* **85**, 171-182 (1996).
- 172 Kauschmann, A. *et al.* Genetic evidence for an essential role of brassinosteroids in plant development. *Plant J* **9**, 701-713 (1996).
- 173 Neff, M. M. *et al.* BAS1: A gene regulating brassinosteroid levels and light responsiveness in Arabidopsis. *Proc Natl Acad Sci U S A* **96**, 15316-15323 (1999).
- 174 Urlacher, V. B., Lutz-Wahl, S. & Schmid, R. D. Microbial P450 enzymes in biotechnology. *Appl Microbiol Biotechnol* **64**, 317-325 (2004).
- 175 Kiener, A. Enzymatic Oxidation of Methyl Groups on Aromatic Heterocycles: A Versatile Method for the Preparation of Heteroaromatic Carboxylic Acids. *Angew Chem Int Ed Engl* **32**, 774-775 (1992).
- 176 Gregory, J. F., 3rd. Nutritional Properties and significance of vitamin glycosides. *Annu Rev Nutr* **18**, 277-296 (1998).
- 177 Bender, D. A. *Nutritional Biochemistry of the Vitamins*. 200-229 (Cambridge University Press 2003).
- 178 Sauveplane, V. *et al.* Arabidopsis thaliana CYP77A4 is the first cytochrome P450 able to catalyze the epoxidation of free fatty acids in plants. *FEBS J* **276**, 719-735 (2009).
- 179 Thomas, J. M. & Raja, R. Designing catalysts for clean technology, green chemistry, and sustainable development. *Annu Rev Mater Res* **35**, 315-350 (2005).
- 180 Boyes, D. C. *et al.* Growth stage-based phenotypic analysis of Arabidopsis: a model for high throughput functional genomics in plants. *Plant Cell* **13**, 1499-1510 (2001).
- 181 Analysis of the genome sequence of the flowering plant Arabidopsis thaliana. *Nature* **408**, 796-815 (The Arabidopsis Genome Initiative, 2000).
- 182 Bak, S. *et al.* in *The Arabidopsis Book* Vol. 9 (ed R. Last) (The American Society of Plant Biologists, 2011).
- 183 Kushiro, M. *et al.* Obtusifoliol 14 α -demethylase (CYP51) antisense Arabidopsis shows slow growth and long life. *Biochem Biophys Res Commun* **285**, 98-104 (2001).
- 184 Kim, H. B. *et al.* Arabidopsis cyp51 mutant shows postembryonic seedling lethality associated with lack of membrane integrity. *Plant Physiol* **138**, 2033-2047 (2005).
- 185 Hayashi, E., Fuzimoto, K. & Imaishi, H. Expression of Arabidopsis thaliana cytochrome P450 monooxygenase, CYP71A12, in yeast catalyzes the metabolism of herbicide pyrazoxyfen. *Plant Biotechnol* **24**, 393-396 (2007).
- 186 Millet, Y. A. *et al.* Innate immune responses activated in Arabidopsis roots by microbe-associated molecular patterns. *Plant Cell* **22**, 973-990 (2010).

- 187 Nafisi, M. *et al.* Arabidopsis cytochrome P450 monooxygenase 71A13 catalyzes the conversion of indole-3-acetaldoxime in camalexin synthesis. *Plant Cell* **19**, 2039-2052 (2007).
- 188 Maughan, J. A., Nugent, J. H. & Hallahan, D. L. Expression of CYP71B7, a cytochrome P450 expressed sequence Tag from Arabidopsis thaliana. *Arch Biochem Biophys* **341**, 104-111 (1997).
- 189 Zhou, N., Tootle, T. L. & Glazebrook, J. Arabidopsis PAD3, a gene required for camalexin biosynthesis, encodes a putative cytochrome P450 monooxygenase. *Plant Cell* **11**, 2419-2428 (1999).
- 190 Schuhegger, R. *et al.* CYP71B15 (PAD3) catalyzes the final step in camalexin biosynthesis. *Plant Physiol* **141**, 1248-1254 (2006).
- 191 Mizutani, M., Ohta, D. & Sato, R. Isolation of a cDNA and a genomic clone encoding cinnamate 4-hydroxylase from Arabidopsis and its expression manner in planta. *Plant Physiol* **113**, 755-763 (1997).
- 192 Chen, H., Jiang, H. & Morgan, J. A. Non-natural cinnamic acid derivatives as substrates of cinnamate 4-hydroxylase. *Phytochemistry* **68**, 306-311 (2007).
- 193 Laudert, D. & Weiler, E. W. Allene oxide synthase: a major control point in Arabidopsis thaliana octadecanoid signalling. *Plant J* **15**, 675-684 (1998).
- 194 Laudert, D., Schaller, F. & Weiler, E. W. Transgenic Nicotiana tabacum and Arabidopsis thaliana plants overexpressing allene oxide synthase. *Planta* **211**, 163-165 (2000).
- 195 Park, J. H. *et al.* A knock-out mutation in allene oxide synthase results in male sterility and defective wound signal transduction in Arabidopsis due to a block in jasmonic acid biosynthesis. *Plant J* **31**, 1-12 (2002).
- 196 Cho, K. B., Lai, W., Hamberg, M., Raman, C. S. & Shaik, S. The reaction mechanism of allene oxide synthase: Interplay of theoretical QM/MM calculations and experimental investigations. *Arch Biochem Biophys* **507**, 14-25 (2011).
- 197 Bate, N. J. & Rothstein, S. J. C6-volatiles derived from the lipoxygenase pathway induce a subset of defense-related genes. *Plant J* **16**, 561-569 (1998).
- 198 Duan, H., Huang, M. Y., Palacio, K. & Schuler, M. A. Variations in CYP74B2 (hydroperoxide lyase) gene expression differentially affect hexenal signaling in the Columbia and Landsberg erecta ecotypes of Arabidopsis. *Plant Physiol* **139**, 1529-1544 (2005).
- 199 Chehab, E. W., Perea, J. V., Gopalan, B., Theg, S. & Dehesh, K. Oxylinin Pathway in Rice and Arabidopsis. *J Integr Plant Biol* **49**, 43-51 (2007).
- 200 Schoenbohm, C., Martens, S., Eder, C., Forkmann, G. & Weisshaar, B. Identification of the Arabidopsis thaliana flavonoid 3'-hydroxylase gene and functional expression of the encoded P450 enzyme. *Biol Chem* **381**, 749-753 (2000).
- 201 Ohta, D. & Mizutani, M. Plant geraniol/nerol 10-hydroxylase and DNA coding therefor. US patent (1998).

- 202 Li-Beisson, Y. *et al.* Nanoridges that characterize the surface morphology of flowers require the synthesis of cutin polyester. *Proc Natl Acad Sci U S A* **106**, 22008-22013 (2009).
- 203 Wittstock, U. & Halkier, B. A. Cytochrome P450 CYP79A2 from *Arabidopsis thaliana* L. Catalyzes the conversion of L-phenylalanine to phenylacetaldoxime in the biosynthesis of benzylglucosinolate. *J Biol Chem* **275**, 14659-14666 (2000).
- 204 Hull, A. K., Vij, R. & Celenza, J. L. *Arabidopsis* cytochrome P450s that catalyze the first step of tryptophan-dependent indole-3-acetic acid biosynthesis. *Proc Natl Acad Sci U S A* **97**, 2379-2384 (2000).
- 205 Mikkelsen, M. D., Hansen, C. H., Wittstock, U. & Halkier, B. A. Cytochrome P450 CYP79B2 from *Arabidopsis* catalyzes the conversion of tryptophan to indole-3-acetaldoxime, a precursor of indole glucosinolates and indole-3-acetic acid. *J Biol Chem* **275**, 33712-33717 (2000).
- 206 Mikkelsen, M. D. *et al.* Modulation of CYP79 genes and glucosinolate profiles in *Arabidopsis* by defense signaling pathways. *Plant Physiol* **131**, 298-308 (2003).
- 207 Glawischnig, E., Hansen, B. G., Olsen, C. E. & Halkier, B. A. Camalexin is synthesized from indole-3-acetaldoxime, a key branching point between primary and secondary metabolism in *Arabidopsis*. *Proc Natl Acad Sci U S A* **101**, 8245-8250 (2004).
- 208 Zhao, Y. *et al.* Trp-dependent auxin biosynthesis in *Arabidopsis*: involvement of cytochrome P450s CYP79B2 and CYP79B3. *Genes Dev* **16**, 3100-3112 (2002).
- 209 Ljung, K. *et al.* Sites and regulation of auxin biosynthesis in *Arabidopsis* roots. *Plant Cell* **17**, 1090-1104 (2005).
- 210 Hansen, C. H. *et al.* Cytochrome p450 CYP79F1 from *Arabidopsis* catalyzes the conversion of dihomomethionine and trihomomethionine to the corresponding aldoximes in the biosynthesis of aliphatic glucosinolates. *J Biol Chem* **276**, 11078-11085 (2001).
- 211 Reintanz, B. *et al.* Bus, a bushy *Arabidopsis* CYP79F1 knockout mutant with abolished synthesis of short-chain aliphatic glucosinolates. *Plant Cell* **13**, 351-367 (2001).
- 212 Chen, S. *et al.* CYP79F1 and CYP79F2 have distinct functions in the biosynthesis of aliphatic glucosinolates in *Arabidopsis*. *Plant J* **33**, 923-937 (2003).
- 213 Tantikanjana, T., Mikkelsen, M. D., Hussain, M., Halkier, B. A. & Sundaresan, V. Functional analysis of the tandem-duplicated P450 genes SPS/BUS/CYP79F1 and CYP79F2 in glucosinolate biosynthesis and plant development by Ds transposition-generated double mutants. *Plant Physiol* **135**, 840-848 (2004).
- 214 Clay, N. K., Adio, A. M., Denoux, C., Jander, G. & Ausubel, F. M. Glucosinolate metabolites required for an *Arabidopsis* innate immune response. *Science* **323**, 95-101 (2009).
- 215 Bednarek, P. *et al.* A glucosinolate metabolism pathway in living plant cells mediates broad-spectrum antifungal defense. *Science* **323**, 101-106 (2009).

- 216 Pfalz, M., Vogel, H. & Kroymann, J. The gene controlling the indole glucosinolate modifier1 quantitative trait locus alters indole glucosinolate structures and aphid resistance in Arabidopsis. *Plant Cell* **21**, 985-999 (2009).
- 217 Kai, K. *et al.* Metabolomic characterization of the possible involvement of a Cytochrome P450, CYP81F4, in the biosynthesis of indolic glucosinolate in Arabidopsis. *Plant Biotechnol* **28**, 379-385 (2011).
- 218 Kruse, T. *et al.* In planta biocatalysis screen of P450s identifies 8-methoxypsoralen as a substrate for the CYP82C subfamily, yielding original chemical structures. *Chem Biol* **15**, 149-156 (2008).
- 219 Liu, F. *et al.* The Arabidopsis P450 protein CYP82C2 modulates jasmonate-induced root growth inhibition, defense gene expression and indole glucosinolate biosynthesis. *Cell Res* **20**, 539-552 (2010).
- 220 Murgia, I., Tarantino, D., Soave, C. & Morandini, P. Arabidopsis CYP82C4 expression is dependent on Fe availability and circadian rhythm, and correlates with genes involved in the early Fe deficiency response. *J Plant Physiol* **168** (2011).
- 221 Lee, S. *et al.* Herbivore-induced and floral homoterpene volatiles are biosynthesized by a single P450 enzyme (CYP82G1) in Arabidopsis. *PNAS* **107**, 21205–21210 (2010).
- 222 Bak, S. & Feyereisen, R. The involvement of two p450 enzymes, CYP83B1 and CYP83A1, in auxin homeostasis and glucosinolate biosynthesis. *Plant Physiol* **127**, 108-118 (2001).
- 223 Naur, P. *et al.* CYP83A1 and CYP83B1, two nonredundant cytochrome P450 enzymes metabolizing oximes in the biosynthesis of glucosinolates in Arabidopsis. *Plant Physiol* **133**, 63-72 (2003).
- 224 Hemm, M. R., Ruegger, M. O. & Chapple, C. The Arabidopsis ref2 mutant is defective in the gene encoding CYP83A1 and shows both phenylpropanoid and glucosinolate phenotypes. *Plant Cell* **15**, 179-194 (2003).
- 225 Bak, S., Tax, F. E., Feldmann, K. A., Galbraith, D. W. & Feyereisen, R. CYP83B1, a cytochrome P450 at the metabolic branch point in auxin and indole glucosinolate biosynthesis in Arabidopsis. *Plant Cell* **13**, 101-111 (2001).
- 226 Meyer, K., Cusumano, J. C., Somerville, C. & Chapple, C. C. Ferulate-5-hydroxylase from Arabidopsis thaliana defines a new family of cytochrome P450-dependent monooxygenases. *Proc Natl Acad Sci U S A* **93**, 6869-6874 (1996).
- 227 Ruegger, M., Meyer, K., Cusumano, J. C. & Chapple, C. Regulation of ferulate-5-hydroxylase expression in Arabidopsis in the context of sinapate ester biosynthesis. *Plant Physiol* **119**, 101-110 (1999).
- 228 Raes, J., Rohde, A., Christensen, J. H., Van de Peer, Y. & Boerjan, W. Genome-wide characterization of the lignification toolbox in Arabidopsis. *Plant Physiol* **133**, 1051-1071 (2003).

- 229 Gachon, C. M., Langlois-Meurinne, M., Henry, Y. & Saindrenan, P. Transcriptional co-regulation of secondary metabolism enzymes in Arabidopsis: functional and evolutionary implications. *Plant Mol Biol* **58**, 229-245 (2005).
- 230 Shimada, Y. *et al.* Brassinosteroid-6-oxidases from Arabidopsis and tomato catalyze multiple C-6 oxidations in brassinosteroid biosynthesis. *Plant Physiol* **126**, 770-779 (2001).
- 231 Shimada, Y. *et al.* Organ-specific expression of brassinosteroid-biosynthetic genes and distribution of endogenous brassinosteroids in Arabidopsis. *Plant Physiol* **131**, 287-297 (2003).
- 232 Castle, J., Szekeres, M., Jenkins, G. & Bishop, G. J. Unique and overlapping expression patterns of Arabidopsis CYP85 genes involved in brassinosteroid C-6 oxidation. *Plant Mol Biol* **57**, 129-140 (2005).
- 233 Kwon, M. *et al.* A double mutant for the *CYP85A1* and *CYP85A2* Genes of Arabidopsis exhibits a brassinosteroid Dwarf phenotype. *J Plant Biol* **48**, 237-244 (2005).
- 234 Pérez-España, V. H., Sánchez-León, N. & Vielle-Calzada, J. P. CYP85A1 is required for the initiation of female gametogenesis in Arabidopsis thaliana. *Plant Signal Behav* **6**, 321-326 (2011).
- 235 Nomura, T. *et al.* The last reaction producing brassinolide is catalyzed by cytochrome P-450s, CYP85A3 in tomato and CYP85A2 in Arabidopsis. *J Biol Chem* **280**, 17873-17879 (2005).
- 236 Kim, T. W. *et al.* Arabidopsis CYP85A2, a cytochrome P450, mediates the Baeyer-Villiger oxidation of castasterone to brassinolide in brassinosteroid biosynthesis. *Plant Cell* **17**, 2397-2412 (2005).
- 237 Benveniste, I. *et al.* CYP86A1 from Arabidopsis thaliana encodes a cytochrome P450-dependent fatty acid omega-hydroxylase. *Biochem Biophys Res Commun* **243**, 688-693 (1998).
- 238 Duan, H. & Schuler, M. A. Differential expression and evolution of the Arabidopsis CYP86A subfamily. *Plant Physiol* **137**, 1067-1081 (2005).
- 239 Li, Y. *et al.* Identification of acyltransferases required for cutin biosynthesis and production of cutin with suberin-like monomers. *Proc Natl Acad Sci U S A* **104**, 18339-18344 (2007).
- 240 Höfer, R. *et al.* The Arabidopsis cytochrome P450 CYP86A1 encodes a fatty acid omega-hydroxylase involved in suberin monomer biosynthesis. *J Exp Bot* **59**, 2347-2360 (2008).
- 241 Xiao, F. *et al.* Arabidopsis CYP86A2 represses *Pseudomonas syringae* type III genes and is required for cuticle development. *EMBO J* **23**, 2903-2913 (2004).
- 242 Rupasinghe, S. G., Duan, H. & Schuler, M. A. Molecular Definitions of Fatty Acid Hydroxylases in Arabidopsis thaliana. *Proteins* **68**, 279-293 (2007).
- 243 Rupasinghe, S. G. *et al.* High-yield expression and purification of isotopically labeled cytochrome P450 monooxygenases for solid-state NMR spectroscopy. *Biochim Biophys Acta* **1768**, 3061-3070 (2007).

- 244 Wellesen, K. *et al.* Functional analysis of the LACERATA gene of Arabidopsis provides evidence for different roles of fatty acid omega - hydroxylation in development. *Proc Natl Acad Sci U S A* **98**, 9694-9699 (2001).
- 245 Compagnon, V. *et al.* CYP86B1 is required for very long chain omega-hydroxyacid and alpha, omega -dicarboxylic acid synthesis in root and seed suberin polyester. *Plant Physiol* **150**, 1831-1843 (2009).
- 246 Kai, K. *et al.* Metabolomics for the characterization of cytochromes P450-dependent fatty acid hydroxylation reactions in Arabidopsis. *Plant Biotechnol* **26**, 175-182 (2009).
- 247 Helliwell, C. A., Chandler, P. M., Poole, A., Dennis, E. S. & Peacock, W. J. The CYP88A cytochrome P450, ent-kaurenoic acid oxidase, catalyzes three steps of the gibberellin biosynthesis pathway. *Proc Natl Acad Sci U S A* **98**, 2065-2070 (2001).
- 248 Mathur, J. *et al.* Transcription of the Arabidopsis CPD gene, encoding a steroidgenic cytochrome P450, is negatively controlled by brassinosteroids. *Plant J* **14**, 593-602 (1998).
- 249 Bancoş, S. *et al.* Regulation of transcript levels of the Arabidopsis cytochrome p450 genes involved in brassinosteroid biosynthesis. *Plant Physiol* **130**, 504-513 (2002).
- 250 Choe, S. *et al.* Overexpression of DWARF4 in the brassinosteroid biosynthetic pathway results in increased vegetative growth and seed yield in Arabidopsis. *Plant J* **26** (2001).
- 251 Fujita, S. *et al.* Arabidopsis CYP90B1 catalyses the early C-22 hydroxylation of C27, C28 and C29 sterols. *Plant J* **45**, 765-774 (2006).
- 252 Kim, G. T., Tsukaya, H. & Uchimiya, H. The ROTUNDIFOLIA3 gene of Arabidopsis thaliana encodes a new member of the cytochrome P-450 family that is required for the regulated polar elongation of leaf cells. *Genes Dev* **12**, 2381-2391 (1998).
- 253 Kim, G. T. *et al.* CYP90C1 and CYP90D1 are involved in different steps in the brassinosteroid biosynthesis pathway in Arabidopsis thaliana. *Plant J* **41**, 710-721 (2005).
- 254 Ohnishi, T. *et al.* C-23 hydroxylation by Arabidopsis CYP90C1 and CYP90D1 reveals a novel shortcut in brassinosteroid biosynthesis. *Plant Cell* **18**, 3275-3288 (2006).
- 255 Bishop, G. J. Refining the plant steroid hormone biosynthesis pathway. *Trends Plant Sci* **12**, 377-380 (2007).
- 256 Koo, A. J., Cooke, T. F. & Howe, G. A. Cytochrome P450 CYP94B3 mediates catabolism and inactivation of the plant hormone jasmonoyl-L-isoleucine. *Proc Natl Acad Sci U S A* **108**, 9298-9303 (2011).
- 257 Kitaoka, N. *et al.* Arabidopsis CYP94B3 encodes jasmonyl-L-isoleucine 12-hydroxylase, a key enzyme in the oxidative catabolism of jasmonate. *Plant Cell Physiol* **52**, 1757-1765 (2011).
- 258 Kandel, S. *et al.* Characterization of a methyl jasmonate and wounding-responsive cytochrome P450 of Arabidopsis thaliana catalyzing dicarboxylic fatty acid formation in vitro. *FEBS J* **274**, 5116-5127 (2007).

- 259 Greer, S. *et al.* The cytochrome P450 enzyme CYP96A15 is the midchain alkane hydroxylase responsible for formation of secondary alcohols and ketones in stem cuticular wax of Arabidopsis. *Plant Physiol* **145**, 653-667 (2007).
- 260 Kim, J. & DellaPenna, D. Defining the primary route for lutein synthesis in plants: the role of Arabidopsis carotenoid beta-ring hydroxylase CYP97A3. *Proc Natl Acad Sci U S A* **103**, 3474-3479 (2006).
- 261 Fiore, A., Dall'osto, L., Fraser, P. D., Bassi, R. & Giuliano, G. Elucidation of the beta-carotene hydroxylation pathway in Arabidopsis thaliana. *FEBS Lett* **580**, 4718-4722 (2006).
- 262 Kim, J. E. *Carotenoid pathway engineering in carrot and functional characterization of cytochrome P450 carotenoid hydroxylase* PhD thesis, The University of British Columbia, (2007).
- 263 Tian, L., Musetti, V., Kim, J., Magallanes-Lundback, M. & DellaPenna, D. The Arabidopsis LUT1 locus encodes a member of the cytochrome p450 family that is required for carotenoid epsilon-ring hydroxylation activity. *Proc Natl Acad Sci U S A* **101**, 402-407 (2004).
- 264 Franke, R. *et al.* Changes in secondary metabolism and deposition of an unusual lignin in the ref8 mutant of Arabidopsis. *Plant J* **30**, 47-59 (2002).
- 265 Franke, R. *et al.* The Arabidopsis REF8 gene encodes the 3-hydroxylase of phenylpropanoid metabolism. *Plant J* **30**, 33-45 (2002).
- 266 Nair, R. B. *et al.* Arabidopsis CYP98A3 mediating aromatic 3-hydroxylation. Developmental regulation of the gene, and expression in yeast. *Plant Physiol* **130**, 210-220 (2002).
- 267 Abdulrazzak, N. *et al.* A coumaroyl-ester-3-hydroxylase insertion mutant reveals the existence of nonredundant meta-hydroxylation pathways and essential roles for phenolic precursors in cell expansion and plant growth. *Plant Physiol* **140**, 30-48 (2006).
- 268 Morant, M. *et al.* Catalytic activity, duplication and evolution of the CYP98 cytochrome P450 family in wheat. *Plant Mol Biol* **63**, 1-19 (2007).
- 269 Matsuno, M. *et al.* Evolution of a novel phenolic pathway for pollen development. *Science* **325**, 1688-1692 (2009).
- 270 Helliwell, C. A. *et al.* Cloning of the Arabidopsis ent-kaurene oxidase gene GA3. *Proc Natl Acad Sci U S A* **95**, 9019-9024 (1998).
- 271 Helliwell, C. A., Poole, A., Peacock, W. J. & Dennis, E. S. Arabidopsis ent-kaurene oxidase catalyzes three steps of gibberellin biosynthesis. *Plant Physiol* **119**, 507-510 (1999).
- 272 Swain, S. M., Singh, D. P., Helliwell, C. A. & Poole, A. T. Plants with increased expression of ent-kaurene oxidase are resistant to chemical inhibitors of this gibberellin biosynthesis enzyme. *Plant Cell Physiol* **46**, 284-291 (2005).
- 273 Morrone, D., Chen, X., Coates, R. M. & Peters, R. J. Characterization of the kaurene oxidase CYP701A3, a multifunctional cytochrome P450 from gibberellin biosynthesis. *Biochem J* **431**, 337-344 (2010).
- 274 Morant, M. *et al.* CYP703 is an ancient cytochrome P450 in land plants catalyzing in-chain hydroxylation of lauric acid to provide building blocks for sporopollenin synthesis in pollen. *Plant Cell* **19**, 1473-1487 (2007).

- 275 Dobritsa, A. A. *et al.* CYP704B1 is a long-chain fatty acid omega-hydroxylase essential for sporopollenin synthesis in pollen of Arabidopsis. *Plant Physiol* **151**, 574-589 (2009).
- 276 Yi, B. *et al.* Two duplicate CYP704B1-homologous genes BnMs1 and BnMs2 are required for pollen exine formation and tapetal development in Brassica napus. *Plant J* **63**, 925-938 (2010).
- 277 Mizutani, M. & Ohta, D. Diversification of P450 genes during land plant evolution. *Annu Rev Plant Biol* **61**, 291-315 (2010).
- 278 Saito, S. *et al.* Arabidopsis CYP707As encode (+)-abscisic acid 8'-hydroxylase, a key enzyme in the oxidative catabolism of abscisic acid. *Plant Physiol* **134**, 1439-1449 (2004).
- 279 Kushiro, T. *et al.* The Arabidopsis cytochrome P450 CYP707A encodes ABA 8'-hydroxylases: key enzymes in ABA catabolism. *EMBO J* **23**, 1647-1656 (2004).
- 280 Okamoto, M. *et al.* CYP707A1 and CYP707A2, which encode abscisic acid 8'-hydroxylases, are indispensable for proper control of seed dormancy and germination in Arabidopsis. *Plant Physiol* **141**, 97-107 (2006).
- 281 Millar, A. A. *et al.* Seed dormancy and ABA metabolism in Arabidopsis and barley: the role of ABA 8'-hydroxylase. *Plant J* **45**, 942-954 (2006).
- 282 Kitahata, N. *et al.* Chemical regulation of abscisic acid catabolism in plants by cytochrome P450 inhibitors. *Bioorg Med Chem* **13**, 4491-4498 (2005).
- 283 Ueno, K. *et al.* Differences between the structural requirements for ABA 8'-hydroxylase inhibition and for ABA activity. *Bioorg Med Chem* **13**, 3359-3370 (2005).
- 284 Araki, Y. *et al.* A new non-azole inhibitor of ABA 8'-hydroxylase: effect of the hydroxyl group substituted for geminal methyl groups in the six-membered ring. *Bioorg Med Chem Lett* **16**, 3302-3305 (2006).
- 285 Saito, S. *et al.* A plant growth retardant, uniconazole, is a potent inhibitor of ABA catabolism in Arabidopsis. *Biosci Biotechnol Biochem* **70**, 1731-1739 (2006).
- 286 Umezawa, T. *et al.* CYP707A3, a major ABA 8'-hydroxylase involved in dehydration and rehydration response in Arabidopsis thaliana. *Plant J* **46**, 171-182 (2006).
- 287 Morikawa, T. *et al.* Cytochrome P450 CYP710A encodes the sterol C-22 desaturase in Arabidopsis and tomato. *Plant Cell* **18**, 1008-1022 (2006).
- 288 Arnqvist, L., Persson, M., Jonsson, L., Dutta, P. C. & Sitbon, F. Overexpression of CYP710A1 and CYP710A4 in transgenic Arabidopsis plants increases the level of stigmaterol at the expense of sitosterol. *Planta* **227**, 309-317 (2008).
- 289 Griebel, T. & Zeier, J. A role for beta-sitosterol to stigmaterol conversion in plant-pathogen interactions. *Plant J* **63**, 254-268 (2010).
- 290 Zhang, Y. *et al.* Two Arabidopsis cytochrome P450 monooxygenases, CYP714A1 and CYP714A2, function redundantly in plant development through gibberellin deactivation. *Plant J* **67**, 342-353 (2011).

- 291 Zhang, R., Xia, X., Lindsey, K. & da Rocha, P. S. Functional complementation of *dwf4* mutants of *Arabidopsis* by overexpression of CYP724A1. *J Plant Physiol* (2011).
- 292 Turk, E. M. *et al.* CYP72B1 inactivates brassinosteroid hormones: an intersection between photomorphogenesis and plant steroid signal transduction. *Plant Physiol* **133**, 1643-1653 (2003).
- 293 Thornton, L. E., Rupasinghe, S. G., Peng, H., Schuler, M. A. & Neff, M. M. *Arabidopsis* CYP72C1 is an atypical cytochrome P450 that inactivates brassinosteroids. *Plant Mol Biol* **74**, 167-181 (2010).
- 294 Takei, K., Yamaya, T. & Sakakibara, H. *Arabidopsis* CYP735A1 and CYP735A2 encode cytokinin hydroxylases that catalyze the biosynthesis of trans-Zeatin. *J Biol Chem* **279**, 41866-41872 (2004).
- 295 Yoshida, Y. *et al.* Structural and evolutionary studies on sterol 14-demethylase P450 (CYP51), the most conserved P450 monooxygenase: II. Evolutionary analysis of protein and gene structures. *J Biochem* **122**, 1122-1128 (1997).
- 296 Trzaskos, J., Kawata, S. & Gaylor, J. L. Microsomal enzymes of cholesterol biosynthesis. Purification of lanosterol 14 alpha-methyl demethylase cytochrome P-450 from hepatic microsomes. *J Biol Chem* **261**, 14651-14657 (1986).
- 297 Ferreira, M. E. *et al.* The ergosterol biosynthesis pathway, transporter genes, and azole resistance in *Aspergillus fumigatus*. *Med Mycol* **43 Suppl 1**, S313-319 (2005).
- 298 Lepesheva, G. I. *et al.* CYP51 from *Trypanosoma cruzi*: a phyla-specific residue in the B' helix defines substrate preferences of sterol 14alpha-demethylase. *J Biol Chem* **281**, 3577-3585 (2006).
- 299 Hotze, M., Schröder, G. & Schröder, J. Cinnamate 4-hydroxylase from *Catharanthus roseus*, and a strategy for the functional expression of plant cytochrome P450 proteins as translational fusions with P450 reductase in *Escherichia coli*. *FEBS Lett* **374**, 345-350 (1995).
- 300 Kaltenbach, M., Schröder, G., Schmelzer, E., Lutz, V. & Schröder, J. Flavonoid hydroxylase from *Catharanthus roseus*: cDNA, heterologous expression, enzyme properties and cell-type specific expression in plants. *Plant J* **19**, 183-193 (1999).
- 301 Schröder, G. *et al.* Light-induced cytochrome P450-dependent enzyme in indole alkaloid biosynthesis: tabersonine 16-hydroxylase. *FEBS Lett* **458**, 97-102 (1999).
- 302 Irmeler, S. *et al.* Indole alkaloid biosynthesis in *Catharanthus roseus*: new enzyme activities and identification of cytochrome P450 CYP72A1 as secologanin synthase. *Plant J* **24**, 797-804 (2000).
- 303 St-Pierre, B. & De Luca, V. A Cytochrome P-450 Monooxygenase Catalyzes the First Step in the Conversion of Tabersonine to Vindoline in *Catharanthus roseus*. *Plant Physiol* **109**, 131-139 (1995).
- 304 Wang, L. *et al.* Three new terpenoid indole alkaloids from *Catharanthus roseus*. *Planta Med* **77**, 754-758 (2011).

- 305 Lamb, D. C., Kelly, D. E., Hanley, S. Z., Mehmood, Z. & Kelly, S. L. Glyphosate is an inhibitor of plant cytochrome P450: functional expression of *Thlaspi arvensae* cytochrome P45071B1/reductase fusion protein in *Escherichia coli*. *Biochem Biophys Res Commun* **244**, 110-114 (1998).
- 306 Leonard, E. & Koffas, M. A. Engineering of artificial plant cytochrome P450 enzymes for synthesis of isoflavones by *Escherichia coli*. *Appl Environ Microbiol* **73**, 7246-7251 (2007).
- 307 Kim, D. H., Kim, B. G., Jung, N. R. & Ahn, J. H. Production of genistein from naringenin using *Escherichia coli* containing isoflavone synthase-cytochrome P450 reductase fusion protein. *J Microbiol Biotechnol* **19**, 1612-1616 (2009).
- 308 Kochs, G. & Grisebach, H. Enzymic synthesis of isoflavones. *Eur J Biochem* **155**, 311-318 (1986).
- 309 Hashim, M. F., Hakamatsuka, T., Ebizuka, Y. & Sankawa, U. Reaction mechanism of oxidative rearrangement of flavanone in isoflavone biosynthesis. *FEBS Lett* **271**, 219-222 (1990).
- 310 Sawada, Y. & Ayabe, S. Multiple mutagenesis of P450 isoflavonoid synthase reveals a key active-site residue. *Biochem Biophys Res Commun* **330**, 907-913 (2005).
- 311 Dewick, P. M. in *The Flavonoids: Advances in Research* (eds J. B. Harborne & T.J. Mabry) Ch. 10, 535-640 (Chapman and Hall, 1982).
- 312 Akiyama, T. *et al.* Genistein, a specific inhibitor of tyrosine-specific protein kinases. *J Biol Chem* **262**, 5592-5595 (1987).
- 313 Barnes, S. Effect of genistein on in vitro and in vivo models of cancer. *J Nutr* **125**, 777S-783S (1995).
- 314 Cassidy, A., Bingham, S. & Setchell, K. Biological effects of isoflavones in young women: importance of the chemical composition of soyabean products. *Br J Nutr* **74**, 587-601 (1995).
- 315 Wei, H., Bowen, R., Cai, Q., Barnes, S. & Wang, Y. Antioxidant and antipromotional effects of the soybean isoflavone genistein. *Proc Soc Exp Biol Med* **208**, 124-130 (1995).
- 316 Humphreys, J. M. & Chapple, C. Molecular 'pharming' with plant P450s. *Trends Plant Sci* **5**, 271-272 (2000).
- 317 Barnes, S. The biochemistry, chemistry and physiology of the isoflavones in soybeans and their food products. *Lymphat Res Biol* **8**, 89-98 (2010).
- 318 Barnes, H. J., Arlotto, M. P. & Waterman, M. R. Expression and enzymatic activity of recombinant cytochrome P450 17 alpha-hydroxylase in *Escherichia coli*. *Proc Natl Acad Sci U S A* **88**, 5597-5601 (1991).
- 319 Duan, H. & Schuler, M. A. Heterologous expression and strategies for encapsulation of membrane-localized plant P450s. *Phytochem Rev* **5**, 507-523 (2006).
- 320 Gonzalez, F. J. & Korzekwa, K. R. Cytochromes P450 expression systems. *Annu Rev Pharmacol Toxicol* **35**, 369-390 (1995).
- 321 Barnes, H. J. Maximizing expression of eukaryotic cytochrome P450s in *Escherichia coli*. *Meth Enzymol* **272**, 3-14 (1996).

- 322 Pernecky, S. J., Larson, J. R., Philpot, R. M. & Coon, M. J. Expression of truncated forms of liver microsomal P450 cytochromes 2B4 and 2E1 in *Escherichia coli*: influence of NH₂-terminal region on localization in cytosol and membranes. *Proc Natl Acad Sci U S A* **90**, 2651-2655 (1993).
- 323 Yabusaki, Y., Murakami, H. & Ohkawa, H. Primary structure of *Saccharomyces cerevisiae* NADPH-cytochrome P450 reductase deduced from nucleotide sequence of its cloned gene. *J Biochem* **103**, 1004-1010 (1988).
- 324 Sakaki, T., Oeda, K., Miyoshi, M. & Ohkawa, H. Characterization of rat cytochrome P-450MC synthesized in *Saccharomyces cerevisiae*. *J Biochem* **98**, 167-175 (1985).
- 325 Oeda, K., Sakaki, T. & Ohkawa, H. Expression of rat liver cytochrome P-450MC cDNA in *Saccharomyces cerevisiae*. *DNA* **4**, 203-210 (1985).
- 326 Urban, P. *et al.* Characterization of recombinant plant cinnamate 4-hydroxylase produced in yeast. Kinetic and spectral properties of the major plant P450 of the phenylpropanoid pathway. *Eur J Biochem* **222**, 843-850 (1994).
- 327 Bozak, K. R., Yu, H., Sirevag, R. & Christoffersen, R. E. Sequence analysis of ripening-related cytochrome P-450 cDNAs from avocado fruit. *Proc Natl Acad Sci U S A* **87**, 3904-3908 (1990).
- 328 Fahrendorf, T. & Dixon, R. A. Stress responses in alfalfa (*Medicago sativa* L.). XVIII: Molecular cloning and expression of the elicitor-inducible cinnamic acid 4-hydroxylase cytochrome P450. *Arch Biochem Biophys* **305**, 509-515 (1993).
- 329 Schuler, M. A. The role of cytochrome P450 monooxygenases in plant-insect interactions. *Plant Physiol* **112**, 1411-1419 (1996).
- 330 Sakaki, T., Shibata, M., Yabusaki, Y., Murakami, H. & Ohkawa, H. Expression of bovine cytochrome P450c17 cDNA in *Saccharomyces cerevisiae*. *DNA* **8**, 409-418 (1989).
- 331 Murakami, H., Yabusaki, Y., Sakaki, T., Shibata, M. & Ohkawa, H. Expression of cloned yeast NADPH-cytochrome P450 reductase gene in *Saccharomyces cerevisiae*. *J Biochem* **108**, 859-865 (1990).
- 332 Ohkawa, H., Yabusaki, Y., Sakaki, T., Murakami, H. & Shibata, M. Hydroxylation reactions by recombinant yeast cells expressing P450 monooxygenases. *Ann N Y Acad Sci* **613**, 37-43 (1990).
- 333 Shibata, M., Sakaki, T., Yabusaki, Y., Murakami, H. & Ohkawa, H. Genetically engineered P450 monooxygenases: construction of bovine P450c17/yeast reductase fused enzymes. *DNA Cell Biol* **9**, 27-36 (1990).
- 334 Akiyoshi-Shibata, M., Sakaki, T., Yabusaki, Y., Murakami, H. & Ohkawa, H. Expression of bovine adrenodoxin and NADPH-adrenodoxin reductase cDNAs in *Saccharomyces cerevisiae*. *DNA Cell Biol* **10**, 613-621 (1991).
- 335 Sakaki, T., Akiyoshi-Shibata, M., Yabusaki, Y. & Ohkawa, H. Organella-targeted expression of rat liver cytochrome P450c27 in yeast. Genetically engineered alteration of mitochondrial P450 into a microsomal form creates a novel functional electron transport chain. *J Biol Chem* **267**, 16497-16502 (1992).

- 336 Shiota, N., Nagasawa, A., Sakaki, T., Yabusaki, Y. & Ohkawa, H. Herbicide-resistant tobacco plants expressing the fused enzyme between rat cytochrome P4501A1 (CYP1A1) and yeast NADPH-cytochrome P450 oxidoreductase. *Plant Physiol* **106**, 17-23, doi:106/1/17 [pii] (1994).
- 337 Eberle, D., Ullmann, P., Werck-Reichhart, D. & Petersen, M. cDNA cloning and functional characterisation of CYP98A14 and NADPH:cytochrome P450 reductase from *Coleus blumei* involved in rosmarinic acid biosynthesis. *Plant Mol Biol* **69**, 239-253 (2009).
- 338 Pompon, D., Louerat, B., Bronine, A. & Urban, P. Yeast expression of animal and plant P450s in optimized redox environments. *Methods Enzymol* **272**, 51-64 (1996).
- 339 Kandel, S. *et al.* Cloning, functional expression, and characterization of CYP709C1, the first sub-terminal hydroxylase of long chain fatty acid in plants. Induction by chemicals and methyl jasmonate. *J Biol Chem* **280**, 35881-35889 (2005).
- 340 Benveniste, I. *et al.* Evolutionary relationship and substrate specificity of *Arabidopsis thaliana* fatty acid omega-hydroxylase. *Plant Science* **170**, 326-338 (2006).
- 341 Olry, A., Schneider-Belhaddad, F., Heintz, D. & Werck-Reichhart, D. A medium-throughput screening assay to determine catalytic activities of oxygen-consuming enzymes: a new tool for functional characterization of cytochrome P450 and other oxygenases. *Plant J* **51**, 331-340 (2007).
- 342 Andersen, M. D., Busk, P. K., Svendsen, I. & Møller, B. L. Cytochromes P-450 from cassava (*Manihot esculenta* Crantz) catalyzing the first steps in the biosynthesis of the cyanogenic glucosides linamarin and lotaustralin. Cloning, functional expression in *Pichia pastoris*, and substrate specificity of the isolated recombinant enzymes. *J Biol Chem* **275**, 1966-1975 (2000).
- 343 Katsumata, T. *et al.* *Arabidopsis* CYP85A2 catalyzes lactonization reactions in the biosynthesis of 2-deoxy-7-oxalactone brassinosteroids. *Biosci Biotechnol Biochem* **72**, 2110-2117 (2008).
- 344 Studier, F. W. Protein production by auto-induction in high density shaking cultures. *Protein Expr Purif* **41**, 207-234 (2005).
- 345 Bonsor, D. *et al.* Ligation independent cloning (LIC) as a rapid route to families of recombinant biocatalysts from sequenced prokaryotic genomes. *Org Biomol Chem* **4**, 1252-1260 (2006).
- 346 Sakaki, T., Shibata, M., Yabusaki, Y., Murakami, H. & Ohkawa, H. Expression of bovine cytochrome P450c21 and its fused enzymes with yeast NADPH-cytochrome P450 reductase in *Saccharomyces cerevisiae*. *DNA Cell Biol* **9**, 603-614 (1990).
- 347 Lindwall, G., Chau, M., Gardner, S. R. & Kohlstaedt, L. A. A sparse matrix approach to the solubilization of overexpressed proteins. *Protein Eng* **13**, 67-71 (2000).
- 348 Laemmli, U. K. Cleavage of structural proteins during the assembly of the head of bacteriophage T4. *Nature* **227**, 680-685 (1970).
- 349 Guengerich, F. P., Martin, M. V., Sohl, C. D. & Cheng, Q. Measurement of cytochrome P450 and NADPH-cytochrome P450 reductase. *Nat Protoc* **4**, 1245-1251 (2009).

- 350 Louërat-Oriou, B., Perret, A. & Pompon, D. Differential redox and electron-transfer properties of purified yeast, plant and human NADPH-cytochrome P-450 reductases highly modulate cytochrome P-450 activities. *Eur J Biochem* **258**, 1040-1049 (1998).
- 351 Hull, A. K. & Celenza, J. L. Bacterial expression and purification of the Arabidopsis NADPH-cytochrome P450 reductase ATR2. *Protein Expr Purif* **18**, 310-315 (2000).
- 352 Sabbadin, F. *Engineering Cytochromes P450 for Biocatalysis and Bioremediation* PhD thesis, University of York, (2010).
- 353 Chen, H. & Morgan, J. A. High throughput screening of heterologous P450 whole cell activity. *Enzyme and Microbial Technology* **38**, 760–764 (2006).
- 354 Saunders, J. A. & Blume, D. E. Quantification of major tobacco alkaloids by high-performance liquid chromatography. *J Chromatogr* **205**, 147-154 (1981).
- 355 Hughes, J. B., Wang, C. Y. & Zhang, C. Anaerobic Biotransformation of 2,4-Dinitrotoluene and 2,6-Dinitrotoluene by *Clostridium acetobutylicum*: A Pathway through Dihydroxylamino Intermediates. *Environ Sci Technol* **33**, 1065-1070 (1999).
- 356 Wang, C. Y., Zheng, D. & Hughes, J. B. Stability of hydroxylamino- and amino-intermediates from reduction of 2,4,6-trinitrotoluene, 2,4-dinitrotoluene, and 2,6-dinitrotoluene. *Biotechnol Lett* **22**, 15-19 (2000).
- 357 Kim, D. H. *et al.* Generation of human metabolites of 7-ethoxycoumarin by bacterial cytochrome P450 BM3. *Drug Metab Dispos* **36**, 2166-2170 (2008).
- 358 Niraula, N. P., Kanth, B. K., Sohng, J. K. & Oh, T. J. Hydrogen peroxide-mediated dealkylation of 7-ethoxycoumarin by cytochrome P450 (CYP107AJ1) from *Streptomyces peucetius* ATCC27952. *Enzyme and Microbial Technology* **48**, 181-186 (2011).
- 359 Asami, T. *et al.* Selective interaction of triazole derivatives with DWF4, a cytochrome P450 monooxygenase of the brassinosteroid biosynthetic pathway, correlates with brassinosteroid deficiency in planta. *J Biol Chem* **276**, 25687-25691 (2001).
- 360 Schoch, G. A., Attias, R., Belghazi, M., Dansette, P. M. & Werck-Reichhart, D. Engineering of a water-soluble plant cytochrome P450, CYP73A1, and NMR-based orientation of natural and alternate substrates in the active site. *Plant Physiol* **133**, 1198-1208 (2003).
- 361 Schoch, G. A., Attias, R., Le Ret, M. & Werck-Reichhart, D. Key substrate recognition residues in the active site of a plant cytochrome P450, CYP73A1. Homology guided site-directed mutagenesis. *Eur J Biochem* **270**, 3684-3695 (2003).
- 362 Duan, H., Civjan, N. R., Sligar, S. G. & Schuler, M. A. Co-incorporation of heterologously expressed Arabidopsis cytochrome P450 and P450 reductase into soluble nanoscale lipid bilayers. *Arch Biochem Biophys* **424**, 141-153 (2004).
- 363 Lorenz, A. *Bioengineering transgenic plants to detoxify nitroaromatic explosive compounds* PhD thesis, University of York, (2007).

- 364 Gandia-Herrero, F. *et al.* Detoxification of the explosive 2,4,6-trinitrotoluene in Arabidopsis: discovery of bifunctional O- and C-glucosyltransferases. *Plant J* **56**, 963-974 (2008).
- 365 Beynon, E. R. *et al.* The role of oxophytodienoate reductases in the detoxification of the explosive 2,4,6-trinitrotoluene by Arabidopsis. *Submitted to Plant Physiology* (2009).
- 366 Brentner, L. B. *et al.* Expression of glutathione S-transferases in poplar trees (*Populus trichocarpa*) exposed to 2,4,6-trinitrotoluene (TNT). *Chemosphere* **73**, 657-662 (2008).
- 367 Haudenschild, C., Schalk, M., Karp, F. & Croteau, R. Functional expression of regiospecific cytochrome P450 limonene hydroxylases from mint (*Mentha* spp.) in *Escherichia coli* and *Saccharomyces cerevisiae*. *Arch Biochem Biophys* **379**, 127-136 (2000).
- 368 Lupien, S., Karp, F., Wildung, M. & Croteau, R. Regiospecific cytochrome P450 limonene hydroxylases from mint (*Mentha*) species: cDNA isolation, characterization, and functional expression of (-)-4S-limonene-3-hydroxylase and (-)-4S-limonene-6-hydroxylase. *Arch Biochem Biophys* **368**, 181-192 (1999).
- 369 Croteau, R. B., Davis, E. M., Ringer, K. L. & Wildung, M. R. (-)-Menthol biosynthesis and molecular genetics. *Naturwissenschaften* **92**, 562-577 (2005).
- 370 Halkier, B. A., Sibbesen, O., Koch, B. & Moller, B. L. Characterization of cytochrome P450TYR, a multifunctional haem-thiolate N-hydroxylase involved in the biosynthesis of the cyanogenic glucoside dhurrin. *Drug Metabol Drug Interact* **12**, 285-297 (1995).
- 371 Kempf, A. C., Zanger, U. M. & Meyer, U. A. Truncated human P450 2D6: expression in *Escherichia coli*, Ni(2+)-chelate affinity purification, and characterization of solubility and aggregation. *Arch Biochem Biophys* **321**, 277-288 (1995).
- 372 Schalk, M. & Croteau, R. A single amino acid substitution (F363I) converts the regiochemistry of the spearmint (-)-limonene hydroxylase from a C6- to a C3-hydroxylase. *Proc Natl Acad Sci U S A* **97**, 11948-11953 (2000).
- 373 Schiestl, R. H. & Gietz, R. D. High efficiency transformation of intact yeast cells using single stranded nucleic acids as a carrier. *Curr Genet* **16**, 339-346 (1989).
- 374 Desikan, R., S. A. H.-M., Hancock, J. T. & Neill, S. J. Regulation of the Arabidopsis transcriptome by oxidative stress. *Plant Physiol* **127**, 159-172 (2001).
- 375 Narusaka, Y. *et al.* Crosstalk in the responses to abiotic and biotic stresses in Arabidopsis: analysis of gene expression in cytochrome P450 gene superfamily by cDNA microarray. *Plant Mol Biol* **55**, 327-342 (2004).
- 376 Pickett, J. A. *et al.* Developments in aspects of ecological phytochemistry: the role of cis-jasmone in inducible defence systems in plants. *Phytochemistry* **68**, 2937-2945 (2007).

- 377 Bruce, T. J. *et al.* cis-Jasmone induces Arabidopsis genes that affect the chemical ecology of multitrophic interactions with aphids and their parasitoids. *Proc Natl Acad Sci U S A* **105**, 4553-4558 (2008).
- 378 Matthes, M., Bruce, T., Chamberlain, K., Pickett, J. & Napier, J. Emerging roles in plant defense for cis-jasmone-induced cytochrome P450 CYP81D11. *Plant Signal Behav* **6**, 563-565 (2011).
- 379 Bianchi, V. *et al.* Escherichia coli ferredoxin NADP⁺ reductase: activation of E. coli anaerobic ribonucleotide reduction, cloning of the gene (fpr), and overexpression of the protein. *J Bacteriol* **175**, 1590-1595 (1993).
- 380 Krapp, A. R. *et al.* The flavoenzyme ferredoxin (flavodoxin)-NADP(H) reductase modulates NADP(H) homeostasis during the soxRS response of Escherichia coli. *J Bacteriol* **184**, 1474-1480 (2002).
- 381 Quinlan, R. F., Jaradat, T. T. & Wurtzel, E. T. Escherichia coli as a platform for functional expression of plant P450 carotene hydroxylases. *Arch Biochem Biophys* **458**, 146-157 (2007).
- 382 Jenkins, C. M. & Waterman, M. R. NADPH-flavodoxin reductase and flavodoxin from Escherichia coli: characteristics as a soluble microsomal P450 reductase. *Biochemistry* **37**, 6106-6113 (1998).
- 383 McConkey, M. E., Gershenzon, J. & Croteau, R. B. Developmental regulation of monoterpene biosynthesis in the glandular trichomes of peppermint. *Plant Physiol* **122**, 215-224 (2000).
- 384 Robineau, T. *et al.* The chemically inducible plant cytochrome P450 CYP76B1 actively metabolizes phenylureas and other xenobiotics. *Plant Physiol* **118**, 1049-1056 (1998).
- 385 Lu, A. Y. H. in *Molecular Aspects of Monooxygenases and Bioactivation of Toxic Compounds* (ed E. Arnc) 135-147 (Plenum Press, 1989).
- 386 Gutierrez, A., Paine, M., Wolf, C. R., Scrutton, N. S. & Roberts, G. C. Relaxation kinetics of cytochrome P450 reductase: internal electron transfer is limited by conformational change and regulated by coenzyme binding. *Biochemistry* **41**, 4626-4637 (2002).
- 387 Simmons, D. L., Lalley, P. A. & Kasper, C. B. Chromosomal assignments of genes coding for components of the mixed-function oxidase system in mice. Genetic localization of the cytochrome P-450PCN and P-450PB gene families and the nadph-cytochrome P-450 oxidoreductase and epoxide hydratase genes. *J Biol Chem* **260**, 515-521 (1985).
- 388 Benveniste, I., Lesot, A., Hasenfratz, M. P., Kochs, G. & Durst, F. Multiple forms of NADPH-cytochrome P450 reductase in higher plants. *Biochem Biophys Res Commun* **177**, 105-112 (1991).
- 389 Nelson, D. R. Progress in tracing the evolutionary paths of cytochrome P450. *Biochim Biophys Acta* **1814**, 14-18 (2011).
- 390 Ro, D. K., Ehling, J. & Douglas, C. J. Cloning, functional expression, and subcellular localization of multiple NADPH-cytochrome P450 reductases from hybrid poplar. *Plant Physiol* **130**, 1837-1851 (2002).
- 391 Mizutani, M. & Ohta, D. Two isoforms of NADPH:cytochrome P450 reductase in Arabidopsis thaliana. Gene structure, heterologous expression in insect cells, and differential regulation. *Plant Physiol* **116**, 357-367 (1998).

- 392 Yang, C. Q., Lu, S., Mao, Y. B., Wang, L. J. & Chen, X. Y. Characterization of two NADPH: cytochrome P450 reductases from cotton (*Gossypium hirsutum*). *Phytochemistry* **71**, 27-35 (2010).
- 393 Paquette, S. M., Jensen, K. & Bak, S. A web-based resource for the Arabidopsis P450, cytochromes b5, NADPH-cytochrome P450 reductases, and family 1 glycosyltransferases *Phytochemistry* **70**, 1940-1947 (2009).
- 394 Rohde, A. *et al.* Molecular phenotyping of the pal1 and pal2 mutants of Arabidopsis thaliana reveals far-reaching consequences on phenylpropanoid, amino acid, and carbohydrate metabolism. *Plant Cell* **16**, 2749-2771 (2004).
- 395 Varadarajan, J. *et al.* ATR3 encodes a diflavin reductase essential for Arabidopsis embryo development. *New Phytol* **187**, 67-82 (2010).
- 396 von Heijne, G. Protein targeting signals. *Curr Opin Cell Biol* **2**, 604-608 (1990).
- 397 Massey, V. & Ganther, H. On the interpretation of the absorption spectra of flavoproteins with special reference to D-amino acid oxidase. *Biochemistry* **4**, 1161-1173 (1965).
- 398 Meijer, A. H. *et al.* Isolation and characterization of a cDNA clone from Catharanthus roseus encoding NADPH:cytochrome P-450 reductase, an enzyme essential for reactions catalysed by cytochrome P-450 monooxygenases in plants. *Plant J* **4**, 47-60 (1993).
- 399 Shet, M. S., Sathasivan, K., Arlotto, M. A., Mehdy, M. C. & Estabrook, R. W. Purification, characterization, and cDNA cloning of an NADPH-cytochrome P450 reductase from mung bean. *Proc Natl Acad Sci U S A* **90**, 2890-2894 (1993).
- 400 Theorell, H. & Åkesson, Å. Absorption Spectrum of Further Purified Cytochrome C. *Science* **90**, 67 (1939).
- 401 Barlow, G. H. & Margoliash, E. Electrophoretic behavior of mammalian-type cytochromes c. *J Biol Chem* **241**, 1473-1477 (1966).
- 402 Myer, Y. P., Srivastava, R. B., Kumar, S. & Raghavendra, K. State of Heme in Heme c systems: Cytochrome c and Heme c models. *J Protein Chem* **2**, 13-42 (1983).
- 403 Vinu, A., Streb, C., Murugesan, V. & Hartmann, M. Adsorption of Cytochrome C on New Mesoporous Carbon Molecular Sieves. *J Phys Chem B* **107**, 8297-8299 (2003).
- 404 Eisenthal, R. & Cornish-Bowden, A. The direct linear plot. A new graphical procedure for estimating enzyme kinetic parameters. *Biochem J* **139**, 715-720 (1974).
- 405 Collins, M. L. & Salton, M. R. Solubility characteristics of *Micrococcus lysodeikticus* membrane components in detergents and chaotropic salts analyzed by immunoelectrophoresis. *Biochim Biophys Acta* **553**, 40-53 (1979).
- 406 Frear, D. S., Swanson, H. R. & Tanaka, F. S. N-demethylation of substituted 3-(phenyl)-1-methylureas: isolation and characterization of a microsomal mixed function oxidase from cotton. *Phytochemistry* **8**, 2157-2169 (1969).

- 407 Ishimaru, A. & Yamazaki, I. The Carbon Monoxide-binding Hemoprotein Reducible by Hydrogen Peroxide in Microsomal Fractions of Pea Seeds. *J Biol Chem* **252**, 199-204 (1977).
- 408 Lamb, D. C., Warrilow, A. G., Venkateswarlu, K., Kelly, D. E. & Kelly, S. L. Activities and kinetic mechanisms of native and soluble NADPH-cytochrome P450 reductase. *Biochem Biophys Res Commun* **286**, 48-54 (2001).
- 409 Warrilow, A. G., Lamb, D. C., Kelly, D. E. & Kelly, S. L. Phanerochaete chrysosporium NADPH-cytochrome P450 reductase kinetic mechanism. *Biochem Biophys Res Commun* **299**, 189-195 (2002).
- 410 Murataliev, M. B., Arino, A., Guzov, V. M. & Feyereisen, R. Kinetic mechanism of cytochrome P450 reductase from the house fly (*Musca domestica*). *Insect Biochem Mol Biol* **29**, 233-242 (1999).
- 411 Madyastha, K. M. & Coscia, C. J. Detergent-solubilized NADPH-cytochrome c(P-450) reductase from the higher plant, *Catharanthus roseus*. Purification and characterization. *J Biol Chem* **254**, 2419-2427 (1979).
- 412 Menting, J. G., Cornish, E. & Scopes, R. K. Purification and partial characterization of NADPH-cytochrome c reductase from *Petunia hybrida* flowers. *Plant Physiol* **106**, 643-650 (1994).
- 413 Ponnampereuma, K. & Croteau, R. Purification and characterization of an NADPH-cytochrome P450 (cytochrome c) reductase from spearmint (*Mentha spicata*) glandular trichomes. *Arch Biochem Biophys* **329**, 9-16 (1996).
- 414 Chen, L. *et al.* Coexpression of cytochrome P4502A6 and human NADPH-P450 oxidoreductase in the baculovirus system. *Drug Metab Dispos* **25**, 399-405 (1997).
- 415 Kärger, E. *et al.* *Candida maltosa* NADPH-cytochrome P450 reductase: cloning of a full-length cDNA, heterologous expression in *Saccharomyces cerevisiae* and function of the N-terminal region for membrane anchoring and proliferation of the endoplasmic reticulum. *Yeast* **12**, 333-348 (1996).
- 416 Kraus, P. F. & Kutchan, T. M. Molecular cloning and heterologous expression of a cDNA encoding berbaminine synthase, a C--O phenol-coupling cytochrome P450 from the higher plant *Berberis stolonifera*. *Proc Natl Acad Sci U S A* **92**, 2071-2075 (1995).
- 417 Siminszky, B., Corbin, F. T., Ward, E. R., Fleischmann, T. J. & Dewey, R. E. Expression of a soybean cytochrome P450 monooxygenase cDNA in yeast and tobacco enhances the metabolism of phenylurea herbicides. *Proc Natl Acad Sci U S A* **96**, 1750-1755 (1999).
- 418 Ayabe, S. & Akashi, T. Cytochrome P450s in flavonoid metabolism. *Phytochem Rev* **5**, 271-282 (2006).
- 419 Bell-Lelong, D. A., Cusumano, J. C., Meyer, K. & Chapple, C. Cinnamate-4-hydroxylase expression in *Arabidopsis*. Regulation in response to development and the environment. *Plant Physiol* **113**, 729-738 (1997).
- 420 Emond, P. *et al.* Synthesis of tropane and nortropane analogues with phenyl substitutions as serotonin transporter ligands. *Bioorg Med Chem* **9**, 1849-1855 (2001).

- 421 Thavaneswaran, S. & Scammells, P. J. Further investigation of the N-demethylation of tertiary amine alkaloids using the non-classical Polonovski reaction. *Bioorg Med Chem Lett* **16**, 2868-2871, doi:S09 (2006).
- 422 von Braun, J. Die Einwirkung von Bromcyan auf tertiäre Amine. *Ber. Dtsch. Chem. Ges.* **33**, 1438–1452 (1900).
- 423 Csutoras, C., Zhang, A., Bidlack, J. M. & Neumeyer, J. L. An investigation of the N-demethylation of 3-deoxymorphine and the affinity of the alkylation products to mu, delta, and kappa receptors. *Bioorg Med Chem* **12**, 2687-2690 (2004).
- 424 Kraiss, G. & Nádor, K. A convenient synthesis of Nortropine from tropine or tropione. *Tetrahedron Lett.* **12**, 57-58 (1971).
- 425 Hecht, S. S. Biochemistry, biology, and carcinogenicity of tobacco-specific N-nitrosamines. *Chem Res Toxicol* **11**, 559-603 (1998).
- 426 Rylott, E. L. *et al.* Engineering plants for the phytoremediation of RDX in the presence of the co-contaminating explosive TNT. *New Phytol* (2011).
- 427 Siminszky, B., Gavilano, L., Bowen, S. W. & Dewey, R. E. Conversion of nicotine to nornicotine in *Nicotiana tabacum* is mediated by CYP82E4, a cytochrome P450 monooxygenase. *Proc Natl Acad Sci U S A* **102**, 14919-14924 (2005).
- 428 Jung, W. *et al.* Identification and expression of isoflavone synthase, the key enzyme for biosynthesis of isoflavones in legumes. *Nat Biotechnol* **18**, 208-212 (2000).
- 429 Hao, D. Y. & Yeoam, M. M. Nicotine N-demethylase in cell-free preparations from tobacco cell cultures. *Phytochemistry* **42** (1996).
- 430 Ghosheh, O., Dwoskin, L. P., Li, W. K. & Crooks, P. A. Residence times and half-lives of nicotine metabolites in rat brain after acute peripheral administration of [2'-(14)C]nicotine. *Drug Metab Dispos* **27**, 1448-1455 (1999).
- 431 Gavilano, L. B. & Siminszky, B. Isolation and characterization of the cytochrome P450 gene CYP82E5v2 that mediates nicotine to nornicotine conversion in the green leaves of tobacco. *Plant Cell Physiol* **48**, 1567-1574 (2007).
- 432 Thuan, N. T. *et al.* Elimination of caffeine interference in HPLC determination of urinary nicotine and cotinine. *Clin Chem* **35**, 1456-1459 (1989).
- 433 Hariharan, M. & VanNoord, T. Liquid-chromatographic determination of nicotine and cotinine in urine from passive smokers: comparison with gas chromatography with a nitrogen-specific detector. *Clin Chem* **37**, 1276-1280 (1991).
- 434 Demetriou, D., Rustemeier, K., Voncken, P. & Schepers, G. High-performance liquid chromatographic determination of nicotine and its urinary metabolites via their 1,3-diethyl-2-thiobarbituric acid derivatives. *Chirality* **5**, 300-302 (1993).
- 435 Yin, H., Wood, T. K. & Smets, B. F. Reductive transformation of TNT by *Escherichia coli* resting cells: kinetic analysis. *Appl Microbiol Biotechnol* **69**, 326-334 (2005).

- 436 Yin, H., Wood, T. K. & Smets, B. F. Reductive transformation of TNT by *Escherichia coli*: pathway description. *Appl Microbiol Biotechnol* **67**, 397-404 (2005).
- 437 González-Pérez, M. M., van Dillewijn, P., Wittich, R. M. & Ramos, J. L. *Escherichia coli* has multiple enzymes that attack TNT and release nitrogen for growth. *Environ Microbiol* **9**, 1535-1540 (2007).
- 438 Saito, K., Noji, M., Ohmori, S., Imai, Y. & Murakoshi, I. Integration and expression of a rabbit liver cytochrome P-450 gene in transgenic *Nicotiana tabacum*. *Proc Natl Acad Sci U S A* **88**, 7041-7045 (1991).
- 439 Nodate, M., Kubota, M. & Misawa, N. Functional expression system for cytochrome P450 genes using the reductase domain of self-sufficient P450RhF from *Rhodococcus* sp. NCIMB 9784. *Appl Microbiol Biotechnol* **71**, 455-462 (2006).
- 440 Fujita, N. *et al.* Comparison of two vectors for functional expression of a bacterial cytochrome P450 gene in *Escherichia coli* using CYP153 genes. *Biosci Biotechnol Biochem* **73**, 1825-1830 (2009).
- 441 Robin, A. *et al.* Engineering and improvement of the efficiency of a chimeric [P450cam-RhFRed reductase domain] enzyme. *Chem Commun (Camb)*, 2478-2480 (2009).
- 442 Kim, D. H. *et al.* Enhancement of isoflavone synthase activity by co-expression of P450 reductase from rice. *Biotechnol Lett* **27**, 1291-1294 (2005).
- 443 Pritchard, M. P. *et al.* A general strategy for the expression of recombinant human cytochrome P450s in *Escherichia coli* using bacterial signal peptides: expression of CYP3A4, CYP2A6, and CYP2E1. *Arch Biochem Biophys* **345**, 342-354 (1997).
- 444 Richardson, T. H. *et al.* Purification and characterization of recombinant-expressed cytochrome P450 2C3 from *Escherichia coli*: 2C3 encodes the 6 beta-hydroxylase deficient form of P450 3b. *Arch Biochem Biophys* **300**, 510-516 (1993).
- 445 Straathof, A. J., Panke, S. & Schmid, A. The production of fine chemicals by biotransformations. *Curr Opin Biotechnol* **13**, 548-556 (2002).
- 446 Breuer, M. *et al.* Industrial methods for the production of optically active intermediates. *Angew Chem Int Ed Engl* **43**, 788-824 (2004).
- 447 Graham-Lorence, S., Amarnah, B., White, R. E., Peterson, J. A. & Simpson, E. R. A three-dimensional model of aromatase cytochrome P450. *Protein Sci* **4**, 1065-1080 (1995).
- 448 Nakamura, M. *et al.* Activation of the cytochrome P450 gene, CYP72C1, reduces the levels of active brassinosteroids in vivo. *J Exp Bot* **56**, 833-840 (2005).
- 449 Takahashi, N. *et al.* shk1-D, a dwarf *Arabidopsis* mutant caused by activation of the CYP72C1 gene, has altered brassinosteroid levels. *Plant J* **42**, 13-22 (2005).
- 450 Turk, E. M. *et al.* BAS1 and SOB7 act redundantly to modulate *Arabidopsis* photomorphogenesis via unique brassinosteroid inactivation mechanisms. *Plant J* **42**, 23-34 (2005).

- 451 Godiard, L. *et al.* CYP76C2, an *Arabidopsis thaliana* cytochrome P450 gene expressed during hypersensitive and developmental cell death. *FEBS Lett* **438**, 245-249 (1998).
- 452 Ito, T. & Meyerowitz, E. M. Overexpression of a gene encoding a cytochrome P450, CYP78A9, induces large and seedless fruit in *Arabidopsis*. *Plant Cell* **12**, 1541-1550 (2000).
- 453 Chaban, C., Waller, F., Furuya, M. & Nick, P. Auxin responsiveness of a novel cytochrome p450 in rice coleoptiles. *Plant Physiol* **133**, 2000-2009 (2003).